

Univerzita Karlova v Praze

Přírodovědecká fakulta



Studium mechanismů rekombinace DNA u rostlin

Study of the DNA recombination mechanisms in plants

Mgr. Jaroslav Kozák

Dizertační práce

Vedoucí práce: RNDr. Karel J. Angelis, CSc.

Praha 2015

Prohlašuji, že tato práce byla vypracována samostatně s využitím řádně citovaných literárních zdrojů, pod vedením vedoucího práce a nebyla využita pro získání obdobného nebo jiného akademického titulu.

V Praze dne 16.12.2015

Chtěl bych tímto poděkovat zejména svému školiteli RNDr. Karlu J. Angelisovi, CSc. za odborné vedení a cenné rady. Dále můj vděk patří bývalým, ale i současným kolegům a kolegyním a všem ostatním, kteří mi pomáhali v průběhu studia. V neposlední řadě bych chtěl poděkovat rodině a přátelům za podporu a trpělivost.

Obsah

Seznam zkratk	5
Abstrakt.....	7
Abstract.....	8
1. Úvod.....	9
1.1. Vznik DSB	10
1.2. Měření opravy DSB	11
1.3. Rozeznání DSB a jeho signalizace	12
1.4. Mechanizmy opravy DSB.....	14
1.5. Proteiny udržující strukturu chromozomů v opravě DSB	21
1.6. Výběr typu rekombinace.....	23
1.7. Odolnost rostlin vůči DSB.....	25
2. Cíle práce	28
3. Materiál a metody	29
4. Prezentované publikace	30
5. Diskuze	105
5.1. Oprava DSB u <i>Arabidopsis</i> a <i>Physcomitrella</i>	105
5.2. Oprava DSB v mutantech C-NHEJ dráhy	107
5.3. AtLIG1 je určující pro rychlou opravu DSB	109
5.4. Oprava SSB v rostlinách.....	110
5.5. MRN komplex v opravě DSB u <i>Physcomitrella</i>	111
5.6. Role AtSMC6b, AtRAD21 a AtGMI1 v opravě DSB.....	115
6. Závěr	120
7. Seznam literatury	122

Seznam zkratk

A-NHEJ - alternativní nehomologní spojování konců DNA (alternative non-homologous end joining)

APT - protein (adenine phosphoribosyltransferase)

ATM - protein kináza (ataxia teleangiectasia mutated)

ATR - protein kináza (ataxia telangiectasia and Rad3 related)

BER - bázová excizní oprava DNA (base excision repair)

BIR - model homologní rekombinace (break induced replication)

BLM - Bleomycin

C-NHEJ - kanonické nehomologní spojování konců DNA (canonical non-homologous end joining)

DDR - buněčná odpověď na poškození DNA (DNA damage response)

DMS3 - protein (defective in meristem silencing 3)

DNA-PKcs - protein kináza (DNA-dependent protein kinase, catalytic subunit)

DSB - dvouvláknový zlom (double strand break)

DSBR - model homologní rekombinace (double strand break repair)

ERCC1 - protein (excision repair cross-complementation group 1)

GMI1 - protein (gama-irradiation and Mitomycin C induced 1)

Gy - jednotka absorbované dávky záření (Gray)

HR - homologní rekombinace (homologous recombination)

IR - ionizující záření (ionizing radiation)

Ku70 a Ku80 - proteiny (thyroid Ku autoantigen 70 and 80 kDa)

LIG - DNA ligáza (DNA ligase)

MIM - protein (hypersensitive to MMS, irradiation and Mitomycin C)

MMEJ - mikrohomologní spojování konců DNA (microhomology-mediated end joining)

MMC – Mitomycin C

MMS - metyl metansulfonát

MRE11 - protein (meiotic recombination 11 homolog)

MSH2 - protein (MutS protein homolog 2)

NBS1 - protein (Nijmegen breakage syndrom 1)

p53 - protein (protein 53 kDa)

PARP1 - protein (poly(ADP-ribose) polymerase 1)

PCD - autokatalycká buněčná smrt (programmed cell death)

RAD - proteiny (radiation sensitivity)

SCC1 - protein (sister chromatid cohesion protein 1)

SDSA - model homologní rekombinace (synthesis dependent strand annealing)

SMC - proteiny (structure maintenance of chromosomes)

SMCHD - proteiny (structure maintenance of chromosomes hinge domain containing)

SMCHD1 - protein (structure maintenance of chromosomes hinge domain containing 1)

SOG1 - protein (suppressor of gamma response 1)

SSA - model homologní rekombinace (single strand annealing)

SSB - jedno-vláknový zlom (single strand break)

UV - ultrafialové záření (ultraviolet radiation)

wt - divoký kmen (wild type)

XPF - protein (xeroderma pigmentosum, complementation group F)

XRCC1 - protein (X-ray repair cross-complementing protein 1)

XRCC4 - protein (X-ray repair cross-complementing protein 4)

γ -H2AX - fosforylovaná forma histonu H2AX

Abstrakt

Dvouvláknový zlom DNA (DSB) je nebezpečný typ poškození DNA, ale zároveň také slouží ke kontrolovanému zvyšování genetické variability. Za hlavní dráhy opravy DSB se považují homologní rekombinace (HR), využívající homologní sekvence, a nehomologní spojování konců DNA (C-NHEJ). Dva rostlinné modely *Arabidopsis thaliana* (*Arabidopsis*) a mech *Physcomitrella patens* (*Physcomitrella*) se liší strategií opravy DSB. *Arabidopsis* dává přednost C-NHEJ a *Physcomitrella* zase HR. Tyto modelové rostliny jsou porovnány na základě měření kinetiky opravy DSB a jednovláknových zlomů DNA (SSB) kometovým testem.

U obou rostlinných druhů je poločas první rychlé fáze opravy DSB kolem 5 minut. I když je C-NHEJ považována za hlavní dráhu opravy DSB u *Arabidopsis*, rychlá oprava není závislá na jejích faktorech AtKu80 a AtLIG4, což poukazuje na existenci efektivních záložních nehomologních drah (A-NHEJ). U *Physcomitrella* dominuje rychlá oprava DSB v mitoticky aktivních buňkách a také není závislá na PpLIG4. Naopak PpLIG4 se překvapivě účastní opravy alkylačního poškození DNA.

Esenciální ligázou rychlé opravy DSB u *Arabidopsis* je replikační AtLIG1, která je také zodpovědná za opravu alkylačního poškození DNA, a tak představuje funkční homolog LIG3. Rychlá oprava DSB je také zcela závislá na AtSMC6b, který patří do skupiny proteinů udržujících strukturu chromozomů (SMC). Menší defekt v opravě DSB je pozorován u mutantů podjednotky kohezinů AtRAD21 a AtGMI1, nově identifikovaného člena skupiny proteinů, které minimálně obsahují SMC dimerizační doménu (SMCHD). Role AtSMC6b, AtRAD21 a AtGMI1 v opravě DSB spočívá v organizaci sesterských chromatid.

Komplex proteinů MRE11, RAD50 a NBS1 (MRN), je jeden z klíčových senzorů a mediátorů opravy DSB. U *Physcomitrella* na většině funkcí MRN komplexu podílí pouze PpMRE11 a PpRAD50. Extrémní citlivost *ppmre11* a *pprad50* vůči indukci DSB sice poukazuje na značný defekt v opravě, ten však nesouvisí s rychlostí jejich opravy, ale naopak s kumulací mutací, zejména delecí. V tomto ohledu je důležitý především PpRAD50, neboť v jeho nepřítomnosti se mutabilita zvyšuje až o dva řády.

Abstract

DNA double-strand break (DSB) is a dangerous type of DNA damage, but it also serves in controlled increase of genetic variability. The two major DSB repair pathways are homologous recombination (HR) using homologous sequences and non-homologous end joining (C-NHEJ). Two model plants *Arabidopsis thaliana* (*Arabidopsis*) and the moss *Physcomitrella patens* (*Physcomitrella*) differ in DSB repair strategies. *Arabidopsis* uses C-NHEJ, however *Physcomitrella* prefers HR. These plant models are compared on the basis of measurement of DSB and single strand breaks (SSB) repair by comet assay.

The half-life of the first rapid phase of the DSB repair is about 5 minutes in both plant species. Although the C-NHEJ is considered as the main DSB repair pathway in *Arabidopsis*, rapid repair is independent of AtLIG4 and AtKu80, suggesting the existence of the effective backup non-homologous repair pathways (A-NHEJ). In *Physcomitrella*, the rapid DSB repair dominates in mitotically active cells and is also independent of PpLIG4. Conversely, PpLIG4 is surprisingly involved in the repair of the DNA alkylation damage.

An essential DNA ligase of the rapid DSB repair pathway in *Arabidopsis* is the replication ligase AtLIG1, which is also responsible for the alkylation DNA damage repair, and thus represents a functional homolog of LIG3. The rapid DSB repair is totally dependent on structural maintenance of chromosomes protein (SMC) AtSMC6b. A slight defect in the DSB repair is also observed in mutant of cohesin subunit AtRAD21 and AtGMI1, a newly identified member of a SMC-hinge domain-containing protein family (SMCHD). The role of AtSMC6b, AtRAD21 and AtGMI1 in the DSB repair lays mainly in the organisation of sister chromatids.

The complex of proteins MRE11, RAD50 and NBS1 (MRN) is one of the key sensors and mediators of the DSB repair. In *Physcomitrella*, only PpMRE11 and PpRAD50 participate on MRN complex functions. Extreme sensitivity of *ppmre11* and *pprad50* to the induction of DSB suggests extensive defect in repair, which is not related to the rate of repair, but rather to the accumulation of mutations, especially deletions. In this regard, PpRAD50 is particularly important, because in its absence the mutability increases up to two orders of magnitude.

1. Úvod

Souhrn procesů spojených s výměnou genetické informace, ať už v rámci jedné, nebo mezi dvěma molekulami DNA se nazývá rekombinace. Základní podmínkou rekombinace je existence DSB, při jehož opravě může docházet ke vzniku nových sekvencí DNA. Řízený vznik DSB a jeho následná rekombinantní oprava je součástí přirozených procesů, jako jsou meiotické dělení, formování pohlaví v kvasinkách, integrace cizorodé DNA, transpozice, zrání lymfocytů a přesmyk tříd imunoglobulinů. Rekombinací se odstraňují také všechny ostatní DSB a to jak endogenního, tak exogenního původu. DSB se považují za vysoce nebezpečný typ poškození DNA, neboť neopravený zlom může vést k nepatřičné reorganizaci genomu, ztrátě DNA, nebo indukci buněčné smrti (Bennett et al. 1996).

Oprava DSB tedy představuje křížovátku mezi genetickou variabilitou a nestabilitou. Existence DSB si vynutila vznik evolučně konzervovaných rekombinantních drah, kde se uplatňují dva základní mechanismy, HR a C-NHEJ. HR využívá při opravě DSB homologní sekvence, a to z ní dělá téměř bezchybný opravný mechanismus. Naopak C-NHEJ jednoduše spojuje konce DNA nezávisle na homologii, a tak je více náchylná ke změnám sekvence v místě opravy. Defekt v opravě DSB se u savců projevuje zvýšenou genetickou nestabilitou a s ní spojenou predispozicí vůči nádorovému bujení (Phillips a McKinnon 2007).

Rostliny vlastní homology většiny proteinů podílejících se na opravě DSB u savců. V tomto ohledu mají rostliny k savcům blíže než kvasinky (Shrivastav et al. 2008). Z hlediska opravy DNA představují rostliny velmi zajímavý systém. Přisedlý způsob života, využívání nejsilnější biologické redoxní reakce - fotolýzy vody, tvorba rostlinného těla dělením několika apikálních buněk, u některých druhů dlouhověkost a schopnost vegetativního množení poukazují na existenci efektivních drah opravy DNA. Studium rostlinné rekombinace prohlubuje porozumění odolnosti rostlin vůči stresu (Boyko a Kovalchuk 2011; Molinier et al. 2006). Zároveň otevírá cestu k cílené genetické manipulaci některých rostlin (Puchta a Fauser 2013; Qi et al. 2013). Aplikace poznatků má a v budoucnu bude mít zásadní vliv na výnos.

V nedávné době také studium rekombinace u rostlin přispělo k přehodnocení pohledu na opravu DSB a akceptování dalšího typu opravy DSB, alternativní NHEJ (A-NHEJ), nezávislého na HR, či klasickém C-NHEJ (Decottignies 2013). A-NHEJ

je spojována s nárůstem chromosomových translokací, a to ji postupně staví do středu současného výzkumu opravy DSB, neboť produkce zlomů DNA je stále běžným způsobem léčby nádorových onemocnění (Lieber 2010a). Studium A-NHEJ a obecně opravy DSB rozšíří pohled na procesy spojené s udržováním integrity genomu, a tím pomůže nejen při objasňování příčin vzniku rakoviny, ale i tvorbě nových terapeutických přístupů v její léčbě (Hühn et al. 2013).

1.1. Vznik DSB

Mimo záměrně indukované DSB se musí buňky vypořádat s řadou neplánovaných zlomů, které vznikají při zastavení replikace DNA a selhání funkce topoizomeráz. Během jednoho buněčného cyklu se savčí, či myší fibroblasty musí vypořádat přibližně s 10 DSB endogenního původu (Haber 1999). V případě rostlin a řady dalších organismů je také důležitým zdrojem DSB proces vysychání a opětovné hydratace, přičemž extrémní případ představují spóry a semena (Pitcher et al. 2007; Kranner et al. 2010).

Významným endogenním zdrojem DSB jsou kyslíkové radikály. Mitochondrie přeměňují 0,1 – 1 % zpracovávaného kyslíku na superoxid (Chance et al. 1979), který je dále konvertován na hydroxylové radikály schopné reagovat s buněčným matrix. Podobně chloroplasty produkují značné množství kyslíkových radikálů při fotolýze vody (Triantaphylidès a Havaux 2009). Protein D1, centrální část fotosystému II, je proto vůbec nejčastěji nahrazovaným proteinem (Raven 2012). Překročí-li hladina radikálů antioxidační schopnosti buněčných obranných mechanismů, dochází k peroxidaci lipidů membrán, poškození proteinů a DNA. Například savčí buňky se musí za jediný den vypořádat až s 10 000 oxidačně poškozenými bázemi (Ames et al. 1993) a až 50 000 SSB (Tice a Setlow 1985).

Oxidace bází DNA, ale také jejich alkylace například metyl metansulfonát (MMS), vede k poškození, které je opravováno bázovou excizní (BER) (Lindahl a Wood 1999). Poškozené báze jsou odstraňovány specifickými DNA glykosylázami za vzniku místa bez báze, které je dále štěpeno specifickou endonukleázou. Pokud není vzniklý SSB opraven polymerázou a ligázou, může způsobit zastavení replikace za vzniku DSB (Kuzminov 2001).

DSB lze také indukovat ultrafialovým (UV), či ionizujícím zářením (IR). Například IR při průchodu prostředím buňky ionizuje molekuly vody a dávka 1 gray (Gy) produkuje 1000 SSB a přibližně 20 až 40 DSB (Ward 1990). Dále řada

přírodních, ale i syntetických látek, zvyšuje množství reaktivních radikálů, nebo reaguje přímo s DNA. Jednou takovou skupinou látek je přírodní antibiotikum s antikancerogenním účinkem Bleomycin (BLM), které napodobují účinek IR. BLM se rutině používá při léčbě některých typů nádorů (Lewis a Nydorf 2006). BLM chelátuje kovy a po interkalaci do DNA a reakci s kyslíkem produkuje superoxid poškozující DNA. Redukcí se komplex opět aktivuje a následuje další štěpení za vzniku DSB (Strekowski et al. 1988). Jeho aktivita se vlivem interkalace omezuje především na DNA, a tak BLM ve srovnání s IR indukuje přibližně jen 10 SSB na 1 DSB (Povirk et al. 1977)

1.2. Měření opravy DSB

Opravu DSB je možné monitorovat mnoha způsoby, které však vždy postihují jen část zkoumané problematiky. Jednotlivé metody umožňují sledovat fyzické spojení DNA, kovalentní modifikace opravných proteinů, jejich časoprostorové rozdělení, či změny sekvence v místě opravy. Nejběžnější metody detekující přímo fragmentaci genomu jsou pulzní gelová elektroforéza a kometový test (Ostling a Johanson 1984; Herschleb et al. 2007). Tyto metody jsou zpravidla méně citlivé, avšak umožňují přímé měření kinetiky opravy DSB, respektive obnovení celistvosti DNA. Citlivější je nepřímá vizualizace DSB pomocí imunofluorescenční detekce kovalentních modifikací proteinů spojených s opravou DNA (Banáth et al. 2004).

Pulzní gelová elektroforéza je ve srovnání s kometovým testem instrumentálně, finančně i časově náročnější. Je limitována zdlouhavou a pracnou přípravou vzorku a možností separace fragmentů DNA o maximální velikosti 10 Mb (Herschleb et al. 2007). Kometový test je založen na elektroforéze jednotlivých buněk ukotvených v agarózovém gelu. Vzniklý útvar připomíná kometu, ve které množství DNA v ohonu komety koreluje s mírou poškození DNA v dané buňce (Ostling a Johanson 1984). Nejběžnější je neutrální, anebo alkalické provedení kometového testu, které vede k detekci DSB, anebo SSB. Případná inkubace vzorků s reparačními endonukleázami umožňuje měření poškození DNA, které se samo o sobě neprojevuje jako zlom, například alkylované a oxidované báze DNA (Angelis et al. 1999; Collins et al. 1997; Angelis et al. 2000).

Nejběžnější imunofluorescenční značkou spojovanou s opravou DSB je fosforylovaná forma histonu H2AX (γ -H2AX). Fluorescenční detekce vyžaduje fosforylaci rozsáhlých oblastí DNA, a tak v případě čistě lokální změny nemusí být

rychle opravený zlom vůbec zaznamenán. Naopak jedna detekovaná oblast může obsahovat více DSB, anebo se v konečném obrazu můžou promítnout dvě prostorově oddělené oblasti do jedné. Navíc o kinetice opravy DSB měřené prostřednictvím γ -H2AX je nutné uvažovat jako o defosforylaci (Chowdhury et al. 2005). Regulace procesů, vedoucích od momentu spojení DNA k ukončení opravy defosforylací γ -H2AX, jsou ještě méně popsány, než procesy odpovídající za jejich formaci. Například u kvasinek, při úpravě párovacího lokusu pomocí HR, dochází k defosforylaci γ -H2AX už během prodlužování vmezeřeného vlákna DNA (Keogh et al. 2006).

Kvalitu opravy DSB je možné zachytit jejich specifickou indukci v rámci reportérové sekvence. Změna ve fenotypu anebo přímo sekvenace výsledných spojů pak vypovídá o povaze opravy (Puchta 2005). Například haploidní genom *Physcomitrella* umožňuje mutační analýzu genu pro adenin fosforibosyltransferázu (APT). Jeho inaktivací mutant získává schopnost růstu na médiu obsahujícím jinak toxický 2-fluoroadenin (Trouiller et al. 2007), a tak je možné určit mutabilitu i povahu inaktivujících mutací.

1.3. Rozeznání DSB a jeho signalizace

Organizmy vlastní komplexní systém odpovědi na přítomnost poškození DNA (DDR). Rozsah poškození DNA je zaznamenán DDR, která pak spouští procesy vedoucí k zastavení buněčného cyklu, opravě DNA, senescenci a apoptóze. U rostlin se místo apoptózy spouští autokatalycká buněčná smrt (PCD) (Lukas et al. 2004; Hoeberichts a Woltering 2003; Fulcher a Sablowski 2009). DDR je tedy klíčová součást buněčné viability a genomové stability organismů, včetně rostlin (Yoshiyama et al. 2013a; Jackson a Bartek 2010; Ciccia a Elledge 2010). U savců DDR představuje významnou bariéru proti rozvoji nádorového bujení (Jackson a Bartek 2010; Wyman a Kanaar 2006).

Klíčovou roli v aktivaci DDR mají signalizační fosfokinázy ATM, ATR a DNA-PKcs (Sirbu a Cortez 2013). ATM je aktivována přítomností DSB (Bakkenist a Kastan 2003). Naopak za aktivaci ATR může řada různých typů poškození DNA, které souvisejí s replikací, například jednovláknové úseky DNA (Cimprich a Cortez 2008). Signál je dále mediován, přičemž dochází ke kumulaci transkripčního faktoru p53, který představuje klíčovou křižovátku DDR, na které se rozhoduje o zastavení

buněčného cyklu a opravy DNA, anebo apoptóze (Shieh et al. 1997; Helton a Chen 2007).

Rostliny nemají p53, klíčový mediátor opravy DSB a indukce apoptózy (Helton a Chen 2007). Nedávno byl objeven AtSOG1, první exkluzivně rostlinný transkripční DDR faktor, který je funkčně podobný p53. AtSOG1 se sice liší v sekvenci a po aktivaci ATM nedochází k jeho kumulaci, ale v rámci rostlinné DDR představuje hlavní regulátor exprese stovek genů (Yoshiyama et al. 2013b; Yoshiyama et al. 2009). AtSOG1, obdobně jako p53, rozhoduje o tom, zda poškozená buňka projde endoreduplikací k senescenci, nebo zanikne pomocí PCD (Adachi et al. 2011; Fulcher a Sablowski 2009).

U savců aktivované ATM, ATR a DNA-PKcs fosforylují řadu proteinů, mimo jiné histony H2AX na C-koncovém serinu za vzniku γ -H2AX (Warmerdam a Kanaar 2010). Tento signál se může rozprostírat až do vzdálenosti 2 Mb od místa s DSB (Rogakou et al. 1999). Souběžně dochází k acetylaci histonu H3 (Brand et al. 2001). V obou případech se vytváří vazebná místa pro množství proteinů, které dále modifikují a rozvolňují chromatin, čímž se objevují další vazebná místa pro proteiny účastníci se opravy DSB a signalizace (Stucki et al. 2005; Chapman a Jackson 2008; Osley et al. 2007). Tyto změny se postupně šíří od DSB, neboť přestavba chromatinu je nezbytná k efektivní kumulaci γ -H2AX (Park et al. 2006).

Imunologická detekce γ -H2AX se stala běžným nástrojem měření indukce DSB a jejich opravy, avšak otázkou zůstává, do jaké míry se γ -H2AX podílí na opravě DSB. V lidských buňkách se H2AX vyskytuje přibližně v 1 z 10 nukleozomů, a tak se nějaký H2AX průměrně nachází až 1 Kb od DSB (Friedberg et al. 2006). V případě prostorově méně náročných drah nehomologní rekombinace je to dost daleko na to, aby se γ -H2AX přímo podílel na opravě DSB. Ukazuje se, že aktivace ATM je nezbytná pro opravu přibližně 10 % DSB indukovaných IR, přičemž tyto zlomy se nachází především v heterochromatinu (Goodarzi et al. 2008).

Za klíčový senzor DSB se považuje MRN komplex, který je tvořen proteiny MRE11, RAD50 a NBS1 (Lamarche et al. 2010). Téměř okamžitě po indukci DSB dochází k masivní a rychlé akumulaci MRN komplexu v poškozené oblasti DNA (He et al. 2012; Polo a Jackson 2011), kde se prostřednictvím NBS1 aktivuje ATM (Girard et al. 2002; Petrini a Stracker 2003; Lamarche et al. 2010). Struktura MRN komplexu je podmíněna RAD50 a umožňuje překlenout DSB (De Jager et al. 2001).

Rychlá lokalizace a stabilizace DSB je důležitá pro zkrácení doby, po kterou jsou konce DNA vystaveny nukleázám a navzájem se od sebe vzdalují. Nukleázová aktivita MRE11 může vést k resekci konců DSB a produkci jednovláknových úseků DNA, které aktivují ATR (Jazayeri et al. 2006).

Dalším senzorem DSB je součást C-NHEJ heterodimer Ku70/Ku80, který má vysokou vazebnou afinitu vůči DSB a nachází se v chromatinu ve významném množství (Blier et al. 1993). Navázané Ku70/Ku80 heterodimery mohou být překlenuty pomocí DNA-PKcs (Meek et al. 2004). Podobně PARP1, přestože je součástí BER, má vyšší afinitu vůči DSB než SSB (D'Silva et al. 1999; Kun et al. 2002), a dokonce by mohl být odpovědný za směřování MRN komplexu do blízkosti DSB (Haince et al. 2008).

K aktivaci ATM dochází také se změnou struktury chromatinu. Rozvolnění DNA vede k vystavení jinak skrytých epitopů histonů, což dosud neznámým způsobem aktivuje ATM nezávisle na MRN komplexu. Děje se tak například po vystavení buněk hypotonickému prostředí a po inhibici topoizomeráz II a histon deacetyláz (Bakkenist a Kastan 2003; Jang et al. 2010; Siu et al. 2004).

V genomu rostlin nalezneme homology všech známých senzorů DSB (Amiard et al. 2013). Rostliny mají stejný mechanismus signalizace DSB jako jiné eukaryoty (Yoshiyama et al. 2013a; Sweeney et al. 2009). Zachována je také role MRN komplexu v aktivaci ATM (Amiard et al. 2010). Dosud však nebyl nalezen homolog DNA-PKcs, a tak se fosforylace účastní pouze ATM a ATR (Friesner et al. 2005; Culligan et al. 2006; Ricaud et al. 2007). Na rozdíl od obratlovců jsou rostlinní mutanti v ATM, ATR a H2AX za standardních podmínek nerozlišitelní od divokého kmene (wt) (Culligan et al. 2004; Culligan a Britt 2008; Lang et al. 2012). Defekt v AtH2AX vede pouze k lehké změně v opravě DSB a samotná fosforylace AtH2AX a aktivace AtATM není esenciální pro opravu DSB (Amiard et al. 2010; Lang et al. 2012). Podobně u lidských buněk oprava DSB probíhá i bez aktivace DDR, avšak DDR rozhoduje o zapojení jednotlivých typů opravných drah a koordinuje opravu s pozicí v buněčném cyklu (O'Driscoll a Jeggo 2006).

1.4. Mechanizmy opravy DSB

Selhání replikace v místě poškození DNA představuje nejběžnější zdroj endogenních DSB. HR umožňuje replikační restart, a proto se nachází u všech organismů. Nutností existence homologní sekvence je HR omezena především

do S a G₂ fáze buněčného cyklu. Naopak C-NHEJ může probíhat po celý buněčný cyklus, neboť jednoduše spojuje konce DNA nezávisle na homologii. Vlivem zpracování konců DNA, ať už syntesou, nebo resekci, je oprava pomocí C-NHEJ více náchylná ke změně sekvence DNA (Pfeiffer et al. 2004).

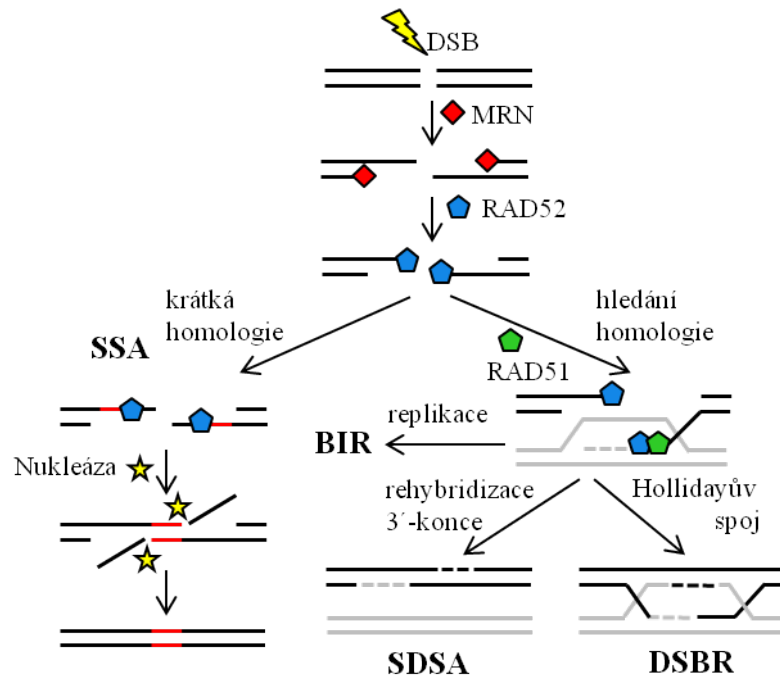
U rychle se dělících buněk je poměrně často k dispozici sesterská chromatida, a tak jim pro opravu DSB stačí HR, avšak přestane-li buňka s dělením, začíná být HR nedostatečná. Tento stav si vynutil vznik C-NHEJ. Například *Escherichia coli* nemá homology C-NHEJ, avšak bakteriální buňky podléhající sporulaci a vysychání jsou odkázány na C-NHEJ (Shuman a Glickman 2007). Zatím co kvasinky preferují HR, rostliny podobně jako většina eukaryot dává přednost C-NHEJ (Kinner et al. 2008).

C-NHEJ se původně označovala jen NHEJ a až později se začala označovat jako kanonická, či dominantní C-NHEJ, neboť se ukazuje, že na jejím pozadí operují ještě další alternativní dráhy A-NHEJ, které jsou proteinovým vybavením odlišné od C-NHEJ a HR. Zatímco C-NHEJ je rychlá a relativně bezchybná, pomalejší A-NHEJ dráhy jsou spojovány s chromozomovými translokacemi a genetickou nestabilitou (Bétermier et al. 2014; Kuhfittig-Kulle et al. 2007; Ferguson et al. 2000).

1.4.1. Homologní rekombinace

Prvním krokem všech typů HR je tvorba 3'-jednovláknových konců DNA nukleázovou aktivitou MRN komplexu. Na tyto konce se pak váže RAD52 a v závislosti na něm další opravné proteiny, které tak vytváří nukleoproteinovou filamentu (Van Dyck et al. 1999; Assenmacher a Hopfner 2004; Lok a Powell 2012). Byla popsána řada dílčích typů HR (obr.1), které se vzájemně liší především ve způsobu zpracování nukleoproteinové filamenty: hybridizace jednovláknových úseků DNA (SSA), meiotická oprava DSB (DSBR), syntézou podmíněná hybridizace vláken (SDSA) probíhající v somatických buňkách a zlomem indukovaná replikace (BIR) (Symington 2002; Li a Heyer 2008). Až na SSA model opravy DSB dochází během HR k hybridizaci dvou různých molekul DNA. Výsledkem HR, kromě SSA mechanismu, je vždy genová konverse, a tak HR probíhající v repetitivních oblastech, nebo využívající ektopické sekvence může vést k nevhodným reorganizacím genomu. Proto je HR omezena do S a G₂ fáze buněčného cyklu, kdy je k dispozici sesterská chromatida (Saleh-Gohari a Helleday 2004).

Existuje-li homologie v blízkém okolí DSB, může RAD52 katalyzovat hybridizaci 3'-jednovláknových konců DNA, a usměrnit tak opravu DSB ve prospěch SSA. SSA má přednost především v oblastech s repetitivními sekvencemi, avšak během opravy dochází ke ztrátě DNA mezi homologními sekvencemi (obr. 1). Pokud místo zlomu neobsahuje dostatečnou homologii, RAD52 povolává RAD51, který vytváří s 3'-jednovláknovým koncem DNA komplex vyhledávající homologní sekvenec v templátu (Takata et al. 2001).



Obrázek 1.: Mechanizmy HR. Formovaný 3'-jednovláknový konec DNA může být zpracován SSA, DSBR, SDSA anebo BIR mechanismem.

DSBR model se uplatňuje během meiózy a slouží ke kontrolovanému zvyšování genetické variability (Shaw a Moore 1998). Výsledkem je tvorba Hollidayovy struktury mezi paternálním a maternálním chromosomem, která může být zpracována s použitím, nebo bez použití mechanismu crossing over (obr. 1) (Schwacha a Kleckner 1995). DSBR je v somatických buňkách potlačován, neboť rekombinace mezi neadekvátními homologními oblastmi je vysoce mutabilní (Richardson et al. 1998). V somatických buňkách může HR probíhat SDSA a BIR mechanismem, které pro opravu DSB využívají sesterské chromatidy, homologního chromozómu, nebo ektopické sekvenec. U SDSA je prodloužený 3'-konec DNA rehybridizován s 3'-koncem DNA za zlomem, čímž je znemožněna formace Hollidayova spoje (obr. 1). SDSA umožňuje vysvětlit HR probíhající na substrátech

s homologií pouze na jednom konci DSB, kde druhý nehomologní konec DNA opravuje C-NHEJ (Puchta 2005). BIR se liší od SDSA pouze v tom, že syntéza DNA pokračuje na velké vzdálenosti a může principiálně dosáhnout až konce chromosomu (obr. 1). BIR je možný mechanismus odpovídající za udržování délky telomer i v nepřítomnosti telomerázy (Nabetani a Ishikawa 2011).

U většiny eukaryot není HR hlavní dráhou opravy DSB, neboť úroveň cílené integrace cizorodé DNA je až tisíckrát nižší ve srovnání s nahodilou (Fattah et al. 2008; Britt a May 2003). U *Arabidopsis* byl určen podíl jednotlivých drah na opravě DSB indukovaných pomocí sekvenčně specifické endonukleázy. Rostliny podobně jako většina eukaryot opravují DSB zejména pomocí C-NHEJ. V případě homologie blízké DSB koncům je asi jen 30 % zlomů opravováno SSA a 7 % pomocí SDSA. Frekvence alelické, či ektopické HR je ještě tisíckrát nižší (Puchta 2005). Kvasinky jsou naopak téměř zcela odkázány na HR, neboť už dva DSB mohou být pro HR mutanty letální (Krogh a Symington 2004). Vysoká úroveň cílené integrace cizorodé DNA byla například pozorována také u kuřecích DT40 buněk (Wang et al. 2001), nebo u zástupce nižších rostlin, mechu *Physcomitrella* (Kamisugi et al. 2005).

1.4.2. C-NHEJ

C-NHEJ se jeví jako dominantní dráha opravy DSB většiny eukaryot. C-NHEJ vytváří mnoho rozdílných spojů při stejné počáteční sekvenci v místě DSB. Oprava začíná rozeznáním DSB heterodimerem Ku70/Ku80, který má vysokou afinitu vůči různým typům konců DNA a zároveň se v buňce nachází ve významném množství (Blair et al. 1993; Lieber 2010b; Lieber et al. 1997). Ku70/Ku80 heterodimer téměř okamžitě asociuje s DSB, přičemž vzniklý komplex chrání konce DNA před degradací a umožňuje jejich přiblížení a překlenutí. Ku70/Ku80 heterodimer povolává další proteiny nezbytné pro opracování a spojení DSB (obr. 2), jako jsou DNA-PKcs, nukleázy Artemis a MRE11, polymerázy μ a λ a komplex XRCC4/LIG4 (Lieber 2010b).

LIG4/XRCC4 je nejflexibilnější ligáza schopná spojovat nekompatibilní konce DNA skrze mezery, či jen jedno vlákno DNA (Gu et al. 2007). DNA-PKcs fosforyluje v okolí DSB řadu proteinů, čímž stimuluje endonukleázovou aktivitu Artemis a ligační aktivitu XRCC4/LIG4 komplexu (Meek et al. 2004). Počátek existence Artemis a DNA-PKcs koliduje s počátkem V(D)J rekombinace a možná,

že se tyto proteiny vyvinuly, aby u obratlovců nahradily funkci MRN komplexu v C-NHEJ (Falck et al. 2005).

Přírozně vzniklé DSB zpravidla nejsou přímo ligovatelné a vyžadují úpravu konců DNA pomocí nukleáz a polymeráz. Oba konce DSB jsou zpracovávány nezávisle a navíc i opakovacím mechanismem, ve kterém se odbourávání DNA může střídát s jejím prodlužováním (Povirk 2012). U rostlin byla pozorována nepřímá úměrnost mezi velikostí genomu a délkou delecí, a tak se i příbuzné rostlinné druhy mohou významně lišit v obsahu DNA. Běžnou součástí opravy DSB u *Arabidopsis* je resekce konců DNA, což zřejmě vedlo v průběhu evoluce k redukci genomu (Kirik et al. 2000). Podobně v mezidruhovém srovnání lidské HeLa buněčné linie a tabáku se ukázalo, že zatímco v HeLa buňkách je až 50 % DSB opraveno bezchybně, u tabáku je to jen 20 %. Navíc u tabáku jsou delece delší a inserce naopak kratší (Pelczar et al. 2003). Avšak nejvýznamnější rozdíl mezi savci a rostlinami je diametrálně odlišná viabilita C-NHEJ mutantů. Zatímco defekt v C-NHEJ u savců často vede k embryonální letalitě, příslušní mutanti u *Arabidopsis* jsou za standardních podmínek nerozlišitelní od wt (Friesner a Britt 2003).

1.4.3. A-NHEJ

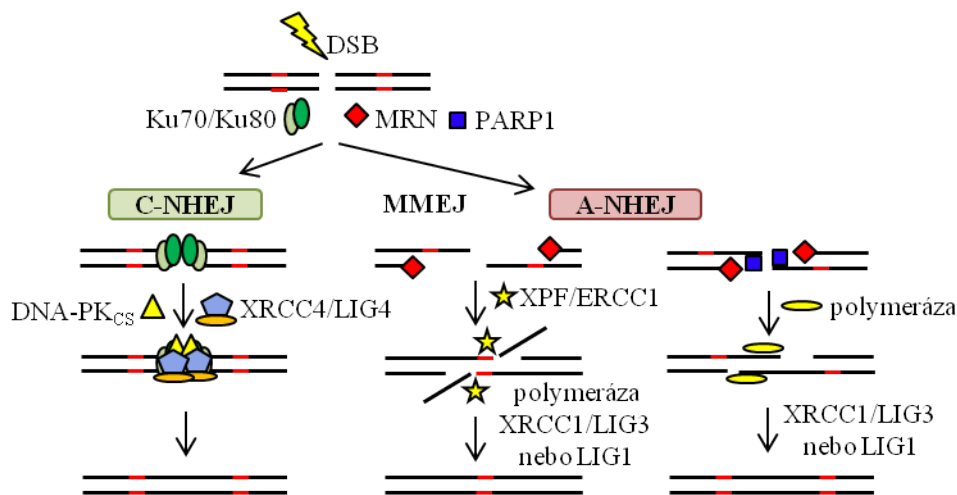
Savčí buněčné linie s defektem v C-NHEJ jsou citliví vůči DSB, ale i tak je dokážou opravovat (DiBiase et al. 2000; Kabotyanski et al. 1998). Genetické studie ukázaly, že tato C-NHEJ nezávislá oprava není mediována HR. Například kombinace defektů v C-NHEJ a HR u kuřecích DT40 buněk nevedla dále k poklesu v opravě DSB (Wang et al. 2001). Obdobně u *Arabidopsis* defekt v C-NHEJ a HR nevede ke zrušení opravy DSB (Charbonnel et al. 2011). Možnost nahrazení celé C-NHEJ se jeví jako rozumná ve srovnání s následky způsobené neopraveným DSB (Flores et al. 1998).

U buněk C-NHEJ mutantů řady organizmů byl pozorován nárůst ve využívání mikrohomologií při opravě DSB, a tak byla postulována dráha nehomologní rekombinace řízená mikrohomologií (MMEJ) (Decottignies 2013; McVey a Lee 2008). Avšak později byla u savců objevena A-NHEJ nezávislá na mikrohomologii (obr. 2) (Boboila et al. 2010; Simsek et al. 2011; Wang et al. 2008). Znalost A-NHEJ je zatím omezená a její studium komplikuje přítomnost HR a C-NHEJ. Většina dosud objevených proteinů A-NHEJ je spojována s replikací a opravou DNA, a tak je velmi složité vymezit jejich nové role. Diskutabilní je také, zda existuje

pouze MMEJ, nebo více A-NHEJ drah. U eukaryot se nachází tři ligázy LIG1, LIG3 a LIG4. LIG4 je výhradně spojována s C-NHEJ, což poukazuje na jistou roli zbývajících ligáz, LIG1 a LIG3 v A-NHEJ. Pochopení A-NHEJ tak začíná u DNA ligáz, neboť bez pomoci dalších proteinů dokážou spojovat fragmenty DNA *in vitro* (Chen et al. 2009).

Všechny tři ligázy jsou schopné ligovat tupé konce, avšak LIG1 a LIG3 jsou méně efektivní než LIG4. Efektivita se zvýší, pokud DSB obsahuje 2 až 3 komplementární báze na 3'- koncích DNA. Hybridizace mikrohomologií pak může nahradit funkci Ku70/Ku80 heterodimeru, který však mimo překlenutí DSB stimuluje aktivitu LIG4. Stejný substrát zpracovává také LIG1 a LIG3, i když s nižší efektivitou (Gu et al. 2007). Při formování genů imunoglobulinů vznikají DSB s 3'- koncovými přesahy. Pokud jsou konce komplementární, mohou být spojeny nezávisle na Ku70/Ku80 heterodimeru (Weinstock et al. 2007). Aktivita LIG4 v savcích B-buňkách je exkluzivně vyhrazena pro C-NHEJ, neboť mutant Ku70 a dvojitý mutant Ku70/LIG4 vykazují rozsáhlé delece a translokace IgH lokusu (Boboila et al. 2010). Určení role LIG1 a LIG3 podobně jako zapojení mikrohomologií v opravě DSB je komplikované. Například u myších buněk LIG1 opravuje DSB nezávisle na mikrohomologii, ale až po odstranění LIG3 (Simsek et al. 2011). U lidských buněk se naopak obě ligázy podílejí na opravě extrachromozomálního DSB obsahujícího mikrohomologi (Liang et al. 2008).

Protože většina přirozeně vzniklých DSB nemá předem připravené mikrohomologie na 3'- koncích DNA, vyvinula se C-NHEJ jako dráha opravy DSB nezávislá na mikrohomologiích (Gerstein a Lieber 1993). Nejčastější spoj neobsahuje ani jeden homologní nukleotid a s rostoucím počtem homologních nukleotidů použitých při opravě DSB četnost výsledného spoje klesá. Využívání mikrohomologie naopak výrazně roste při defektu LIG4 (Gauss a Lieber 1996; Han a Yu 2008). A-NHEJ zvyšuje úroveň chromozomových přestaveb, a tak důvodem pro evoluci C-NHEJ mohla být nutnost inhibice výrazně nebezpečnějších drah opravy DSB (Virsik-Köpp et al. 2003). Klíčovým se jeví Ku70/Ku80 heterodimer, který vazbou na konce DNA brání zpracování zlomu jinými opravnými dráhami (Mansour et al. 2010). Jeho delece obnovuje viabilitu myšího mutantu v LIG4 (Karanjwala et al. 2002). Podobně XRCC4/LIG4 u savců inhibuje A-NHEJ (Simsek a Jasin 2010).



Obrázek 2.: C-NHEJ a základní modely A-NHEJ. MMEJ je zařazena mezi A-NHEJ.

S A-NHEJ je spojována řada proteinů: histon H1, PARP1, XRCC1, MRN komplex, XPF/ERCC1 a DNA polymerázy. MRN komplex hraje určitou roli v iniciaci A-NHEJ (Grabarz et al. 2012; Rass et al. 2009). Model založený na resekcí vychází z klíčové funkce MRN komplexu, který je odpovědný za rozeznání, překlenutí a přípravu konců DNA před jejich hybridizací (Rass et al. 2009). MRN komplex je společně s nukleázou XPF/ERCC1 součástí MMEJ (obr. 2) (Ma et al. 2003). Další A-NHEJ je založena na PARP1 a XRCC1/LIG3. Přestože je PARP1 součástí BER, má vysokou afinitu vůči DSB a kompetuje s Ku70/Ku80 heterodimerem o vazbu na DSB (D’Silva et al. 1999; Kun et al. 2002; Wang et al. 2006). PARP1 mimo stabilizaci DSB také stimuluje XRCC1/LIG3 (Audebert et al. 2008; Audebert et al. 2004). Dalším proteinem schopným přemostění DSB je histon H1, který stimuluje XRCC1/LIG3 a inhibuje HR a C-NHEJ (Rosidi et al. 2008; Downs et al. 2003). Další navržený model A-NHEJ je založen na doplnění konců DSB DNA polymerázou a následném spojení ligázou (obr. 2) (Simsek et al. 2011).

U vyšších rostlin se nachází více A-NHEJ drah. Na MMEJ u *Arabidopsis* participuje kromě AtXPF/AtERCC1 také AtMRE11 (Charbonnel et al. 2011; Heacock et al. 2004). Naopak AtXRCC1 definuje další A-NHEJ odlišnou od C-NHEJ a AtXPF/AtERCC1 mediované MMEJ (Charbonnel et al. 2010; Charbonnel et al. 2011). Studie na mitotických buňkách kořenů semenáčků ukázala, že čtyřnásobný mutant s defektem ve všech dosud známých drahách opravy DSB, tedy C-NHEJ, HR, A-NHEJ a MMEJ sice vykazuje extrémně citlivý fenotyp vůči DSB, avšak DSB stále opravuje. Defekt v kinetice opravy DSB vyjádřený

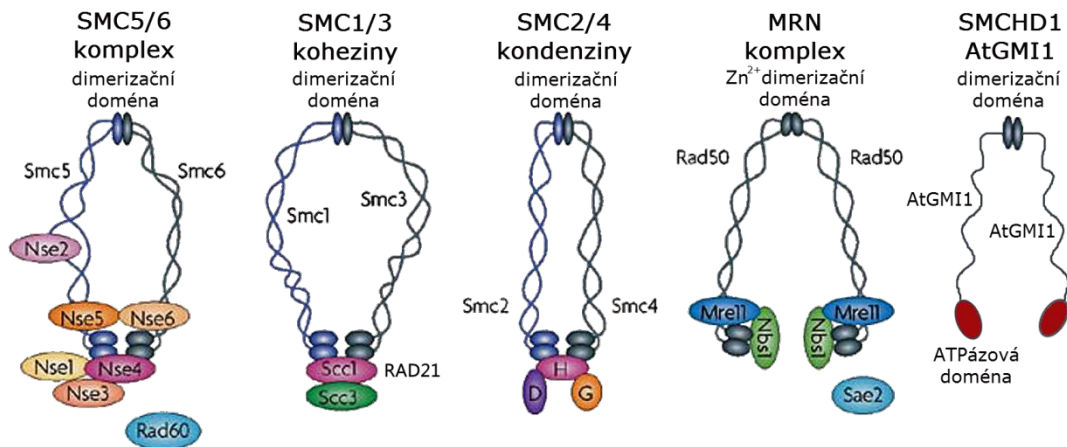
počtem γ -H2AX se projevuje hlavně v prvních 10 minutách po IR, pak už oprava probíhá stejně rychle jako wt. Tato zbytková ligační aktivita se projevuje zvýšenou frekvencí fúzí telomer (Charbonnel et al. 2011).

Rostliny postrádají *LIG3*, která je u savců součástí BER a také A-NHEJ (Cappelli et al. 1997; Simsek et al. 2011). Jistá exkluzivita *AtLIG4* v C-NHEJ nutně poukazuje na zapojení jedné, nebo obou zbývajících DNA ligáz, replikační *AtLIG1* a pro rostliny specifické *AtLIG6* (Waterworth et al. 2010). Semenáčky *atlig4* dokážou registrovat svůj defekt, neboť v odpovědi na indukci DSB reagují zvýšenou expresí zbývajících DNA ligáz (Furukawa et al. 2015). Opravdu esenciální rostlinnou DNA ligázou je jen replikační *AtLIG1*, neboť mutant v obou zbývajících ligázách *AtLIG4/AtLIG6* stále produkuje viabilní semena a za standardních podmínek je nerozlišitelný od wt (Waterworth et al. 2010). Esenciálnost *LIG1* v replikaci se odráží v tom, že u rostlin, ale ani u kvasinek a savců není její mutant viabilní (Babiychuk et al. 1998; Petrini et al. 1995; Johnston 1979).

1.5. Proteiny udržující strukturu chromozomů v opravě DSB

Veškeré procesy spojené s DNA probíhají na úrovni chromatinu. Na organizaci chromozomů se podílejí také SMC proteiny, které tvoří základ tří typů komplexů (obr. 3). Komplex *SMC1/3* odpovídá za kohezi sesterských chromatid, *SMC2/4* komplex se podílí na kondenzaci chromosomů během dělení buněk a *SMC5/6* komplex je zapojen v HR opravě DNA. Participace *SMC1/3* a *SMC5/6* komplexů na organizaci sesterských chromatid se u jejich mutantů projevuje defektem v HR (Potts et al. 2006; De Piccoli et al. 2006). Dokonce i kondenziny se podílí na opravě DNA, kondenzin I je zapojen do opravy SSB a kondenzin II se účastní HR (Wu a Yu 2012). Důležitost SMC komplexů podporuje fakt, že se během evoluce objevily dříve než histony (Nasmyth a Haering 2005).

Sbalení molekuly SMC vede k tvorbě ATPázy oddělené spojníkem od dimerizační domény, a právě dimerizace je základem jejich funkce (Haering et al. 2002; Chiu et al. 2004). Podobnou strukturu má i *RAD50*, součást MRN komplexu (obr. 3) (He et al. 2012). Spojení dvou MRN komplexů umožňuje různé způsoby podpory DNA v oblasti DSB (Lammens et al. 2011). SMC proteiny naopak vytvářejí, společně s dalšími proteiny, prstence kolem DNA duplexů (Hirano 2006).



Obrázek 3.: Struktura SMC a MRN komplexů (Murray a Carr 2008 - upraveno) a model struktury SMCHD1 a AtGMI1 (Böhmdorfer et al. 2011).

SMC1/3 komplex obepíná sesterské chromatidy, a tím usnadňují HR mezi nimi. Defekt v kohezinech vede k citlivosti vůči DSB, redukcí HR a ke kumulaci chromozomových aberací (Covo et al. 2010; Atienza et al. 2005; Sjögren a Nasmyth 2001). Mimo kohezi esenciální pro dělení buňky existuje i dodatečná koheze, která je indukována DSB specificky v S a G₂ fázi buněčného cyklu v závislosti na MRN komplexu (Kim et al. 2002; Ström et al. 2004; Heidinger-Pauli et al. 2008). SMC1/3 komplex se také zapojuje do DRR, například v savcích se podílí na aktivaci S a G₂ kontrolního bodu buněčného cyklu (Watrin a Peters 2009; Yazdi et al. 2002). Součástí SMC1/3 komplexu je také RAD21 (obr. 3), který byl poprvé identifikován u kvasinek (SCC1) skrze citlivý fenotyp vůči ultrafialovému záření (UV) a IR, a to ještě před objevem jeho role v držení sesterských chromatid (Birkenbihl a Subramani 1992). U *Arabidopsis* se nacházejí tři homology AtRAD21, které jsou exprimovány v pletivech bohatých na mitotické buňky. Po indukci DSB se zvyšuje exprese pouze u *AtRAD21.1* a jenom mutant v *AtRAD21.1* je citlivý k IR (da Costa-Nunes et al. 2006).

SMC5/6 komplex se poněkud liší v sekvenci od kohezínů a kondenzínů (Wu a Yu 2012). SMC6 byl původně objeven v kvasinkách skrze citlivost vůči IR, kde se podobně jako u jiných organismů podílí na HR mezi sesterskými chromatidami (De Piccoli et al. 2006; Lehmann et al. 1995; Potts et al. 2006; Watanabe et al. 2009). U lidských buněk je směřování kohezínů do místa DSB závislé na SMC5/6 komplexu. Společný defekt SMC1/3 a SMC5/6 komplexů se neprojevuje dalším poklesem ve výměně sesterských chromatid, a tak oba

komplexy figurují ve stejných procesech (Potts et al. 2006). U kvasinek se SMC5/6 podílí také na stabilizaci rDNA a na opravě rozpadlých replikačních komplexů (Murray a Carr 2008).

U *Arabidopsis* se nachází dva AtSMC6 proteiny, AtSMC6a a AtSMC6b (AtMIM). T-DNA inzerční mutant pro AtSMC6b, *atmim*, je citlivý vůči MMS, IR a MMC a vykazuje pokles v HR u somatických buněk (Mengiste et al. 1999). Exprese *AtSMC6b* je v semenáčcích až dvacetkrát vyšší než exprese *AtSMC6a*, a tak se AtSMC6b jeví jako hlavní jednotka AtSMC5/6 komplexu, která odpovídá za až 75 % veškerých HR událostí. U mutantů AtSMC5/AtSMC6 komplexu klesá po ozáření IR schopnost organizace chromozomů. U *atrad51* je organizace chromatid srovnatelná s wt, a to i po indukci DSB, a tak koheze spíše předchází HR (Watanabe et al. 2009).

Dimerizační doména má zásadní vliv na funkci SMC komplexů. Postupně se rozrůstá nová skupina SMCHD proteinů obsahujících minimálně SMC dimerizační doménu. Nedávno byly popsány dva proteiny, u myši SMCHD1 a u rostlin AtDMS3. Oba proteiny jsou zapojeny v metylaci DNA. SMCHD1 hraje důležitou roli v inaktivaci X-chromosomu (Blewitt et al. 2005; Kanno et al. 2008).

SMCHD1 strukturně připomíná SMC proteiny, neboť na C- a N- koncích obsahuje dimerizační doménu a ATPázu, které jsou oddělené dosud necharakterizovaným spojníkem (obr. 3). ATPáza je příbuzná s ATPázou topizomerázy IV (Blewitt et al. 2008). Naopak AtDMS3 je tvořen jen dimerizační doménu (Kanno et al. 2008). Na základě sekvence *SMCHD1* byl v genomu *Arabidopsis* nalezen dosud neidentifikovaný strukturní homolog AtGMI1. Název AtGMI1 je odvozen z pozorování indukce jeho exprese po působení IR nebo Mitomycinem C (Böhmdorfer et al. 2011).

1.6. Výběr typu rekombinace

V každém konkrétním případě opravy DSB je nutné vybrat takový typ rekombinace, který nejlépe zajistí stabilitu genomu. Zastoupení jednotlivých drah opravy DSB se může lišit mezi organizmy, v rámci různých typů buněk organismu a jejich vývojových stádií, v jednotlivých buňkách během buněčného cyklu, a dále také v závislosti na lokální struktuře chromatinu a komplexitě DSB (oblast kolem zlomu obsahuje další jiné typy poškození DNA). Řízení výběru rekombinantní dráhy

je tedy esenciální pro potlačení genetické nestability a zachování rovnováhy mezi stabilitou a diverzitou genomu (Grabarz et al. 2012).

Velikost a organizace genomu mají vliv na frekvenci používání jednotlivých typů drah opravy DSB. Eukaryoty s malým genomem a vysokým obsahem jedinečných sekvencí preferují HR. Naopak velikost savčího genomu komplikuje hledání homologie a fakt, že obsahuje obrovské množství repeticí, zvyšuje pravděpodobnost translokací (Eccles et al. 2009; Lieber et al. 1997). C-NHEJ je proto hlavní dráhou opravy DSB většiny eukaryot, avšak to nesnižuje nezbytnou roli HR rekombinantním restartu replikace a meióze.

HR vyžaduje formaci poměrně dlouhých 3'-jednovláknových DNA konců, a tak se resekce konců DSB jeví jako klíčová v řízení HR. Resekce 3'-konců DNA je rozdělena do dvou fází. V té první je DSB rozeznán MRN komplexem, který odstraní přibližně 100 nukleotidů (Mimitou a Symington 2008). V druhé a delší resekci, nezbytné pro HR, se zapojují další nukleázy (Nimonkar et al. 2011). Právě druhá fáze resekce umožňuje obnažení alespoň 250 nukleotidů kompletní homologie, která je nezbytná pro invazi 3'-konce DNA do homologního duplexu (Rubnitz a Subramani 1984). Resekce však mohou být substrátem A-NHEJ a SSA, které významně mění sekvenci v místě opravy. SSA by měla být lokalizována jen do repetitivních oblastí, kde naopak HR mezi četnými a po genomu rozptýlenými repeticemi vede k výrazným genomovým přestavbám (Guirouilh-Barbat et al. 2010). A-NHEJ je zapojena v translokacích (Boboila et al. 2010; Simsek a Jasin 2010), a proto by měla být zcela potlačována.

Resekci je nutné přísně kontrolovat a nukleázovou aktivitu MRE11 omezit především do S a G₂ fáze buněčného cyklu, kdy má HR k dispozici sesterskou chromatidu v bezprostřední blízkosti (Delacôte a Lopez 2008). Indukce p53 v G₁ fázi buněčného inhibuje resekci a vede k preferování C-NHEJ (Bertrand et al. 2004). Podobně přítomnost Ku70/Ku80 heterodimeru v místě DSB kompetičně inhibuje vazbu RAD52, MRN komplexu a PARP1, a chrání tak DSB konce před resekcí (Langerak et al. 2011; Van Dyck et al. 1999). Avšak je to MRN komplex, který v případě selhání C-NHEJ odstraňuje z DNA konců Ku70/Ku80 heterodimery (Wu et al. 2008).

U většiny eukaryot se C-NHEJ jeví jako nejlepší volba pro opravu DSB v G₁ fázi a HR v S a G₂ fázi buněčného cyklu. Toto rozdělení však ne zcela odpovídá

pozorováním u savců, kde v G₂ fázi buněčného cyklu HR opravuje DSB spojené s replikací a v heterochromatinu, ale všechny ostatní DSB jsou opravovány pomocí C-NHEJ a HR nastupuje až po jejím selhání (Shibata et al. 2011). Experimenty poukazují na rychlou výměnu proteinů C-NHEJ a HR v místě DSB, a tak se dráhy můžou střídat během opravy konkrétního DSB (Mortusewicz et al. 2008). Je však nutné také zohlednit rozsah dalšího poškození DNA v okolí DSB. Nutnost zapojení HR stoupá s rostoucí komplexitou DSB (Yajima et al. 2013; Schipler a Iliakis 2013).

Rekombinace se uskutečňuje na úrovni chromatinu, tedy komplexu DNA s histony a dalšími proteiny, které opravě DNA překáží. C-NHEJ je prostorově nenáročná, neboť minimální úsek pro vazbu Ku70/Ku80 heterodimeru představuje pouze 14 nukleotidů (Yoo et al. 1999). HR naopak vyžaduje odstranění nukleozomů a rozvolnění DNA. V okolí DSB dochází k přechodné změně v acetylaci histonů (van Attikum a Gasser 2005; Tamburini a Tyler 2005). Obecně acetylací histonů klesá jejich afinita vůči DNA. Specifická acetylace histonu H3 napomáhá resekcii DSB (Qin a Parthun 2002) a hyperacetylace histonu H4 potlačuje C-NHEJ (Jazayeri et al. 2004). Naopak deacetylace histonů usnadňuje C-NHEJ (Miller et al. 2010). Fosforylace acetyltransferáz pomocí DNA-PKcs vede k jejich inhibici, a tak pozitivně reguluje C-NHEJ (Barlev et al. 1998).

1.7. Odolnost rostlin vůči DSB

Ve srovnání s člověkem jsou rostliny schopné přežít indukci většího množství DSB. Při stejně velkých genomech přežívá kukuřice až třikrát větší dávky IR než lidské buňky (Killion a Constantin 1972). Smrtelná dávka pro člověka je 10-20 Gy, ale u rostlin je pozorována schopnost přežít dávku až 200-3000 Gy (Wada et al. 1998; Kim et al. 2009; Nagata et al. 1999). Existence efektivní opravy DSB u rostlin může souviset s nutností opravy zlomů DNA, které vznikají během vysychání a opětovné hydratace. Zvýšená resistance vůči IR je pozorována také u dalších organismů, které podléhají výkyvům v množství vody, například u bakterie *deinococcus radiodurans* anebo u bezobratlých pijavenek (Zahradka et al. 2006; Gladyshev a Meselson 2008).

Součástí životního cyklu rostlin je stádium semene, ve kterém obsah vody může klesnout pod 10 % (van Zanten et al. 2011). V tomto stádiu je embryo v klidovém stavu s potlačeným metabolismem, a takto může přečkat až stovky let bez ztráty viability (Sallon et al. 2008). S rostoucí dobou skladování však stoupá

množství zlomů DNA (Dandoy et al. 1987). Defekt v jejich opravě je spojován s chromozomovými aberacemi a poklesem klíčivosti (Abdalla a Roberts 1969; Osborne et al. 1984). V přírodě semena končí v půdě, kde se částečně rehydratují a v tomto dormantním stavu už oprava DNA probíhá. Například oves vlastní efektivní opravu DNA i po několika cyklech dehydratace a rehydratace semen (Boubriak et al. 1997).

I když je oprava DSB esenciální pro zachování klíčivosti semen, zejména po jejich dlouhodobém skladování, je dosud jen minimálně charakterizovaná. V rané fázi klíčení *Arabidopsis* je zesílená exprese proteinů opravy DNA (Waterworth et al. 2010). Oprava DSB během klíčení do jisté míry závisí na C-NHEJ, neboť ozáření mutanti této dráhy klíčí pomaleji (Friesner a Britt 2003). Pro rostliny specifická AtLIG6 se podílí na opravě DNA zejména ve starých semenech. Kumulativní efekt defektu v AtLIG4 a AtLIG6 poukazuje na minimálně dvě odlišné dráhy opravy DSB v klíčících semenech. Zároveň však viabilita dvojitého mutanta v AtLIG4/AtLIG6 ukazuje, že samotná AtLIG1 je schopná efektivně odstraňovat zlomy DNA (Waterworth et al. 2010).

Rostlinné orgány vznikají dělením apikálních meristémů. Meristém se skládá z klidového centra a centrální zóny, kde se buňky dělí pomalu. To je obklopeno buňkami, které se dělí rychleji a jsou základem budoucích rostlinných orgánů (Vernoux et al. 2000). Pomalé dělení buněk centra meristému poskytuje delší čas na opravu DNA, a tak i po akutním genotoxickém působení přežívá část buněk s kvalitním genomem, které jsou základem nových dělivých meristemických buněk. Rychle se dělicí meristemické buňky, ve srovnání s vegetativními, vykazují po indukci poškození DNA vyšší výskyt PCD, což představuje další mechanismus zachování kvality genomu kmenových buněk (Fulcher a Sablowski 2009; Ricaud et al. 2007). PCD vyžaduje *de novo* syntézu proteinů, a tak se jeví spíše jako programovaná událost než jako bezprostřední následek přítomnosti DSB (Fulcher a Sablowski 2009).

Rostliny nemají zárodečnou linii. Gamety se tvoří diferenciací somatických meristemických buněk, a tak se mutace v těchto buňkách může projevit u potomstva (Hays 2002). Například zvýšená dávka UV-B zvedá úroveň HR a vede ke změnám v genomu děděným potomstvem (Ries et al. 2000). Proto je nezbytně nutná přítomnost účinných mechanismů udržujících stabilitu genetické informace.

V tomto ohledu je zajímavé, že ani u dlouhověkých stromů nebyla zjištěna výrazně zvýšená mutační úroveň (Klekowski 1997).

Rostliny se dokážou adaptovat na přítomnost genotoxinů. Například v případě alkylačního poškození bází dochází k jisté akutní adaptaci prostřednictvím syntézy opravných proteinů. Nízká dávka genotoxinu stimuluje rostlinu, která je pak schopná se účinně vyrovnat s výrazně vyšší úrovní poškození DNA (Angelis et al. 2000). Studie prováděné na rostlinách v radiací zamořených zónách v okolí Černobylu dokumentují existenci dědičné adaptace na genetický stres, neboť potomstvo vykazuje vyšší rezistenci vůči činidlům indukujícím DSB (Kovalchuk et al. 2004; Boubriak et al. 2008). Podobně UV-C zářením zvýšená úroveň HR je pozorována i u čtvrté generace rostlin následující po působení (Molinier et al. 2006). Rostlinám je tedy vlastní výrazná schopnost adaptace na řadu biotických a abiotických stresů skrze genetické a epigenetické změny (Boyko a Kovalchuk 2011). Frekvence HR je zvýšená po řadě stresů jako zasolení půdy, kontaminace těžkými kovy, UV záření, vystavení suchu a zimě. Zvýšení intrachromozomální rekombinace může také představovat obranný mechanismus akcelerující vznik nových vlastností zvyšujících odolnost rostlin (Boyko a Kovalchuk 2011; Molinier et al. 2006).

2. Cíle práce

- Porovnání kinetiky opravy DSB a vymezení role C-NHEJ u *Arabidopsis* a *Physcomitrella*.
- Charakterizace úlohy MRN komplexu v opravě DSB u *Physcomitrella*.
- Vymezení role AtLIG1 a PpLIG4 v opravě DSB a SSB.
- Prozkoumání vlivu defektu v AtSMC6b, AtRAD21 a SMCHD proteinu AtGMI1 na opravu DSB.

3. Materiál a metody

Všichni rostlinní mutanti *Arabidopsis* a *Physcomitrella* byli pro účely experimentů pěstováni v petriho miskách na MS/2 a BCDAT mediu, v tomto pořadí. Izolaci rostlinného materiálu usnadnil celofánový disk vložený mezi rostliny a medium. Mech *Physcomitrella* je možné udržovat ve filamentárním stavu označovaném jako protonema, a tak jsou pro studium opravy DNA v závislosti na stáří definována tři stadia následující po pasáži, 1,7 a 14 dní stará protonema.

Všichni testovaní mutanti byli získáni na základě spolupráce, a tak molekulární metody vedoucí k jejich izolaci, stejně jako charakterizaci, byly prováděny jinde. Obdobně další metody uvedené v prezentovaných publikacích, jako průtoková cytometrie, RT-PCR, exprese GUS, transformace cizorodou DNA, western blot a sekvenace.

Specializace na studium opravy poškození DNA omezila metodiku především na určení toxicity MMS a BLM a hlavně kinetiky opravy SSB a DSB kometovým testem. Další důležitou metodou u *Physcomitrella* byla mutační analýza genu pro APT, která umožňuje určit kvalitu opravy DNA v mutantech opravných proteinů.

Přehled metod

Kultivace rostlin

Stanovení toxicity

Kometový test

4. Prezentované publikace

Publikace 1

Rapid repair of DNA double strand breaks in *Arabidopsis thaliana* is dependent on proteins involved in chromosome structure maintenance.

Kozák, J., West, C. E., White, C., da Costa-Nunes, J. A., Angelis, K. J.

DNA Repair (Amst.), 2009, **8**, 413–419.

IF₂₀₀₉: 4,199

Příspěvek autora: analýza kinetiky opravy DSB a podíl na přípravě manuskriptu.

Publikace 2

DNA ligase 1 deficient plants display severe growth defects and delayed repair of both DNA single and double strand breaks.

Waterworth, W. M., **Kozák, J.**, Provost, C. M., Bray, C. M., Angelis, K.J., West, C.E.

BMC Plant Biol., 2009, **9**:79

IF₂₀₀₉: 3,744

Příspěvek autora: měření a analýza kinetiky opravy DSB a SSB.

Publikace 3

GMI1, a structural-maintenance-of-chromosomes-hinge domain-containing protein, is involved in somatic homologous recombination in *Arabidopsis*.

Böhmdorfer, G., Schleiffer, A., Brunmeir, R., Ferscha, S., Nizhynska, V., **Kozák, J.**, Angelis, K. J., Kreil, D. P., Schweizer, D.

Plant J., 2011, **67**, 420–433

IF₂₀₁₁: 6,160

Příspěvek autora: měření a analýza kinetiky opravy DSB.

Publikace 4

MRE11 and RAD50, but not NBS1, are essential for gene targeting in the moss *Physcomitrella patens*.

Kamisugi, Y., Schaefer, D. G., **Kozák, J.**, Charlot, F., Vrielynck, N., Holá, M., Angelis, K. J., Cuming, A. C., Nogué, F.

Nucleic Acids Res., 2012, **40**, 3496–3510

IF₂₀₁₂: 8,278

Příspěvek autora: měření a analýza kinetiky opravy DSB.

Publikace 5

Genotoxin induced mutagenesis in the model plant *Physcomitrella patens*.

Holá, M., **Kozák, J.**, Vágnerová, R., Angelis, K. J.

Biomed Res. Int., 2013, **2013**,

IF₂₀₁₃: 2,706

Příspěvek autora: měření a analýza kinetiky opravy DSB.

Publikace 6

The AtRAD21.1 and AtRAD21.3 *Arabidopsis* cohesins play a synergistic role in somatic DNA double strand break damage repair.

da Costa-Nunes, J. A., Capitão, C., **Kozák, J.**, Costa-Nunes, P., Ducasa, G. M., Pontes, O., Angelis, K. J.

BMC Plant Biol. **14**, 353 (2014).

IF₂₀₁₄: 3,813

Příspěvek autora: měření a analýza kinetiky opravy DSB.

Publikace nesouvisející s obsahem dizertační práce:

Patent PCT/CZ2015/000052

Helquats with heteroaromatic substituents, preparation thereof, and use thereof as G-quadruplex stabilizers

Inventors: Teplý, F., Hájek, M., Kužmová, E., **Kozák, J.**, Komárková, V., Hubálková, P., Reyes-Gutiérrez, P. E., Jirásek, M., Sonawane, M. R., Joshi, V. D., Severa, L., Novotná, J.

I declare that the contribution of Jaroslav Kozák to the presented results in Waterworth et al., *BMC plant biology*, 2009, as stated in “Presented publications” chapter, is true.



Leeds, 22.6.2015

Wanda M. Waterworth

Potvrzuji, že příspěvek Jaroslava Kozáka k prezentovaným výsledkům v Waterworth et al., *BMC plant biology*, 2009, tak jak je uvedeno v kapitole “Prezentované publikace”, je pravda.



Leeds, 22.6.2015

Wanda M. Waterworth

I declare that the contribution of Jaroslav Kozák to the presented results in Böhmdorfer et al., *The Plant Journal*, 2011, as stated in “Presented publications” chapter, is true.



17.11.2015

Gudrun Böhmdorfer

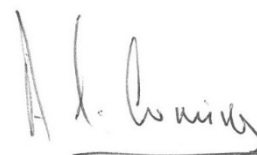
Potvrzuji, že příspěvek Jaroslava Kozáka k prezentovaným výsledkům v Böhmdorfer et al., *The Plant Journal*, 2011, tak jak je uvedeno v kapitole “Prezentované publikace”, je pravda.



17.11.2015

Gudrun Böhmdorfer

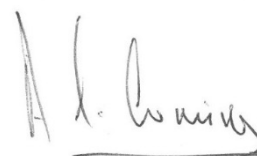
I declare that the contribution of Jaroslav Kozák to the presented results in Kamisugi et al., *Nucleic Acids Research*, 2012, as stated in “Presented publications” chapter, is true.



Leeds, 22.6.2015

Andrew C. Cuming

Potvrzuji, že příspěvek Jaroslava Kozáka k prezentovaným výsledkům v Kamisugi et al., *Nucleic Acids Research*, 2012, tak jak je uvedeno v kapitole “Prezentované publikace”, je pravda.



Leeds, 22.6.2015

Andrew C. Cuming

I declare that the contribution of Jaroslav Kozák to the presented results in Holá et al., *Biomed Res Int.*, *BMC Plant Biology*, 2013, as stated in “Presented publications” chapter, is true.



Prague, 26.11.2015

Marcela Holá

Potvrzuji, že příspěvek Jaroslava Kozáka k prezentovaným výsledkům v Holá et al., *Biomed Res Int.*, *BMC Plant Biology*, 2013, tak jak je uvedeno v kapitole “Prezentované publikace”, je pravda.



Praha, 26.11.2015

Marcela Holá

I declare that the contribution of Jaroslav Kozák to the presented results in da Costa-Nunes et al., *BMC Plant Biology*, 2014, as stated in "Presented publications" chapter, is true.

Lisbon, 23rd June 2015
Lisbon, 23.6.2015

José A da Costa-Nunes
José A da Costa-Nunes

Potvrzují, že příspěvek Jaroslava Kozáka k prezentovaným výsledkům v da Costa-Nunes et al., *BMC Plant Biology*, 2014, tak jak je uvedeno v kapitole "Prezentované publikace", je pravda.

Lisbon, 23rd June 2015
Lisabon, 23.6.2015

José A da Costa-Nunes
José A da Costa-Nunes



Contents lists available at ScienceDirect

DNA Repair

journal homepage: www.elsevier.com/locate/dnarepair

Brief report

Rapid repair of DNA double strand breaks in *Arabidopsis thaliana* is dependent on proteins involved in chromosome structure maintenanceJaroslav Kozak^a, Christopher E. West^b, Charles White^c,
José A. da Costa-Nunes^d, Karel J. Angelis^{a,*}^a Institute of Experimental Botany AS CR, Na Karlovce 1, 160 00 Praha 6, Czech Republic^b CPS, Faculty of Biological Sciences, University of Leeds, Leeds LS2 9JT, UK^c Génétique, Reproduction et Développement, UMR CNRS 6247 – Clermont Université – INSERM U931, 63177 Aubière cedex, France^d ISA, Universidade Técnica de Lisboa, 1349-017 Lisboa, Portugal

ARTICLE INFO

Article history:

Received 18 July 2008

Received in revised form 5 November 2008

Accepted 9 November 2008

Available online 31 December 2008

Keywords:

AtKU80

AtRAD21.1

AtLIG4-4

MIM

Bleomycin

Comet assay

ABSTRACT

DNA double strand breaks (DSBs) are one of the most cytotoxic forms of DNA damage and must be repaired by recombination, predominantly via non-homologous joining of DNA ends (NHEJ) in higher eukaryotes. However, analysis of DSB repair kinetics of plant NHEJ mutants *atlig4-4* and *atku80* with the neutral comet assay shows that alternative DSB repair pathways are active. Surprisingly, these kinetic measurements show that DSB repair was faster in the NHEJ mutant lines than in wild-type *Arabidopsis*.

Here we provide the first characterization of this KU-independent, rapid DSB repair pathway operating in *Arabidopsis*. The alternate pathway that rapidly removes the majority of DSBs present in nuclear DNA depends upon structural maintenance of chromosomes (SMC) complex proteins, namely MIM/AtRAD18 and AtRAD21.1. An absolute requirement for SMC proteins and kleisin for rapid repair of DSBs in *Arabidopsis* opens new insight into the mechanism of DSB removal in plants.

Crown Copyright © 2008 Published by Elsevier B.V. All rights reserved.

1. Introduction

Due to their sessile nature and need of sunlight, plants are particularly exposed to environmental genotoxins, which lead directly or indirectly via generation of reactive oxidative species (ROS) to DNA lesions including single (SSB) and double strand breaks (DSBs). DSBs are particularly critical lesions, because if unrepaired they lead to major karyotypic instability and cell death. Early studies showed that breaks induced in plant DNA by ionizing radiation are rapidly repaired in genomic DNA of seed embryos [1,2], carrot cell cultures [3], *Tradescantia* stamen hairs [4] as well as more recently in growing root meristems of *Vicia faba* [5,6]. An important role for DNA ligases was proposed in pathways for the removal of X-ray induced DNA breakage, which requires the rejoining of the phosphodiester bond of the DNA backbone in the final stage of repair [7]. The study of DNA repair kinetics has benefited greatly from the single cell gel

electrophoresis (comet) assay, which has been adapted to differentiate between SSB and DSB repair in genomic DNA [8–10]. This technique has been successfully applied in DNA repair studies of various plants such as *V. faba* [6,11], tobacco [12] and *Arabidopsis* [13].

DSB repair is mediated either by homologous recombination (HR) catalyzed by the RAD52 epistasis group or by non-homologous end-joining (NHEJ), which involves the KU heterodimer and the DNA ligase 4/XRCC4 complex. The molecular components of these pathways are highly conserved amongst eukaryotes and recent studies have revealed the requirement for both HR and NHEJ in DSB repair in plants as reviewed in Bray and West [14] and Bleuyard et al. [15]. From these studies in plants and other eukaryotes, it was assumed that NHEJ was responsible for the majority of DSB repair in higher plants. Surprisingly, here we report that the NHEJ knockout *ku80* and *lig4* *Arabidopsis* mutants repair DSBs very rapidly, with similar kinetics to wild-type plants. This demonstrates that rapid repair of the majority of DSBs in plant cells is independent of the evolutionarily conserved factors of the “classic” NHEJ (C-NHEJ) pathway. Furthermore, we have identified putative components of this rapid DSB repair pathway including the plant orthologue of structure maintenance of chromosome AtSMC6/AtRAD18 protein MIM [16] and kleisin AtRAD21.1, whose yeast homologue is part of SMC1–3 cohesion complex [17].

Abbreviations: DSB, DNA double strand break; SSB, DNA single strand break; NHEJ, non-homologous end-joining; C-NHEJ, classical-NHEJ; SMC, structural maintenance of chromosomes; ROS, reactive oxidative species; UV, ultraviolet; IR, ionizing radiation.

* Corresponding author. Tel.: +420 224322603; fax: +420 224322603.

E-mail address: angelis@ueb.cas.cz (K.J. Angelis).

1568-7864/\$ – see front matter. Crown Copyright © 2008 Published by Elsevier B.V. All rights reserved.
doi:10.1016/j.dnarep.2008.11.012

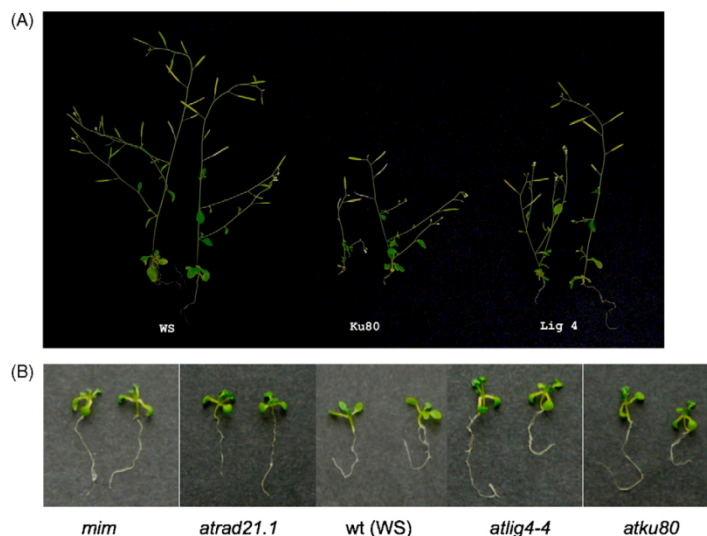


Fig. 1. Phenotype of *Arabidopsis* mutant lines. (A) Mature *atlig4-4* and *atku80* mutant lines showed minor growth defects when compared to the background *Arabidopsis* ecotype WS after four weeks growing in soil. (B) No germination or growth defects were detected in the 10-day-old seedlings used for preparation of comet slides (*atmim*, *atrad21.1*, *Arabidopsis* Ws (wild-type), *atlig4-4* and *atku80*).

2. Materials and methods

2.1. *Arabidopsis* lines

Arabidopsis insertion mutants of *atmim* [16], *atrad21.1* [17] and *atku80* [18] have been described previously. In this study we used the unpublished line *atlig4-4* (Fig. 1A) that is phenotypically indistinguishable from previously described mutants in this gene [19,20]. For details on isolation and characterization of *atlig4-4* see Supplementary information.

Interestingly none of mutant lines used in this study showed delays in germination or growth during the first 10 days after the onset of germination (Fig. 1B).

Control experiments with wild-type *Arabidopsis* were carried out using the same ecotype as the mutant: *Arabidopsis* Ws in experiments with *mim*, *atku80* and *atlig4-4* and *Arabidopsis* Col0 with *atrad21.1*. The comet data for Ws and Col0 were identical (see Supplementary information).

2.2. Bleomycin treatment

Seeds were germinated on Petri plates with MS/2 media (M0223, Duchefa, The Netherlands) solidified with 0.8% Plant Agar (P1001, Duchefa, The Netherlands) during 16/8 h day/night regime at 22 °C and 18 °C, respectively. Sensitivity and repair kinetics of *Arabidopsis* wild-type and mutant lines were measured using 10-day-old *Arabidopsis* seedlings (Fig. 1B). Prior to treatment, seedlings were gently transferred from agar to liquid medium in 5 cm Petri plates to avoid drying.

The phenotype was checked by continuous exposure of seedlings to 5, 50 and 100 µg/ml Bleomycin (Bleocin inj., Euro Nippon Kayaku GmbH, Germany) for one week in liquid MS/2 (Fig. 2A).

DSB fragmentation of nuclear DNA was measured in seedlings treated with indicated concentrations of Bleomycin for 1 h in liquid MS/2. In repair kinetic experiments, after the treatment with 50 µg/ml Bleomycin seedlings were thoroughly rinsed in H₂O, blot-

ted on filter paper and either flash-frozen in liquid N₂ ($t = 0$) or left to recover on filter discs moist with MS/2 for the indicated repair times, before being frozen in liquid N₂. Part of the treated seedlings was also let to recover in liquid MS/2 for one week to see the effect of this dose on the growth vigor (Fig. 2B).

2.3. Comet assay

DSBs were detected by a neutral comet assay [21] as described previously [10,13]. In brief, approximately 100 mg of frozen tissue were cut with a razor blade in 300 µl PBS + 10 mM EDTA on ice and tissue debris removed by filtration through 50 µm mesh funnels (Partec, Germany) into Eppendorf tubes on ice. 50 µl of nuclei suspension were dispersed in 200 µl of melted 0.7% LMT agarose (15510-027, GibcoBRL, Gaithersburg, USA) at 40 °C and four 80 µl aliquots were immediately pipetted onto each of two coated microscope slides (in duplicates per slide), covered with a 22 mm × 22 mm cover slip and then chilled on ice for 1 min to solidify the agarose. After removal of cover slips, slides were immersed in lysing solution (2.5 M NaCl, 10 mM Tris-HCl, 0.1 M EDTA, 1% N-lauroyl sarcosinate, pH 7.6) on ice for at least 1 h to dissolve cellular membranes and remove attached proteins. The whole procedure from chopping tissue to placement into lysing solution takes approximately 3 min. After lysis, slides were twice equilibrated for 5 min in TBE electrophoresis buffer to remove salts and detergents. Comet slides were then subjected to electrophoresis at 1 V/cm (app. 12 mA) for 5 min. After electrophoresis, slides were placed for 5 min in 70% EtOH, 5 min in 96% EtOH and air-dried.

Comets were viewed in epifluorescence with a Nikon Eclipse 800 microscope after staining with GelRed stain (Biotium, Hayward, USA) and evaluated by the Comet module of the LUCIA cytogenetics software suite (LIM, Praha, Czech Republic).

2.4. Data evaluation

The fraction of DNA in comet tails (% tail-DNA) was used as a measure of DNA damage. Data for *Arabidopsis* Ws and Col0 and the

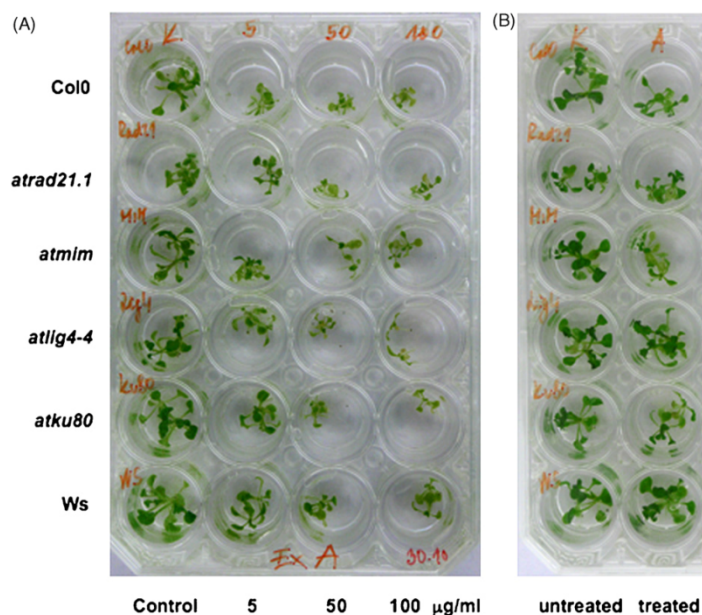


Fig. 2. Sensitivity of *Arabidopsis* lines (*Arabidopsis* Col0, *atr21.1*, *atmim*, *atlig4-4*, *atku80* and *Arabidopsis* Ws) to Bleomycin treatment. (A) 10-day-old seedlings growing for following week in the presence of 5, 50 and 100 µg Bleomycin/ml in liquid MS/2 media. (B) 10-day-old seedlings treated similarly as for measurement of repair kinetics with 50 µg Bleomycin/ml for 1 h and grown for additional week in liquid MS/2.

four lines (*atmim*, *atr21-1*, *atlig4-4* and *atku80*) analyzed in this study were measured in at least 3 independent experiments. In each experiment, the % tail-DNA was measured at 5 time points: 0, 5, 10, 20 and 60 min after treatment and in control seedlings without treatment. Measurements included 4 independent gel replicas of 25 evaluated comets totaling at least 300 comets analyzed per experimental point.

The percentage of damage remaining as plotted in Fig. 4 after a given repair time (t_x) is defined as:

$$\% \text{ damage remaining } (t_x) = \frac{\text{mean \% tail-DNA } (t_x) - \text{mean \% tail-DNA (control)}}{\text{mean \% tail-DNA } (t_0) - \text{mean \% tail-DNA (control)}} \times 100$$

3. Results and discussion

3.1. Bleomycin induction of DSBs and their detection with comet assay

The radiomimetic antibiotic Bleomycin was used to induce DNA damage, subsequently detected by the neutral comet assay. In 10-day-old *Arabidopsis* wild-type seedlings we observed a linear increase of DNA damage ($R^2 = 0.9574$) in the 0–50 µg/ml dose range (Fig. 3). When treated with 50 µg/ml Bleomycin, the fraction of DNA migrating in comet tails was approximately 50% above the background level in all mutant and wild-type *Arabidopsis* lines used in this study (Fig. 4A and B). This shows that Bleomycin is capable of inducing DSBs with equivalent efficiency regardless of the plant genotype. Bleomycin, which belongs to a family of low-molecular-weight glycometallopeptides, functions as a catalyst activated by interaction with DNA and attachment of Fe(II) to produce ROS, SSBs and DSBs [22].

The comet assay carried out under neutral conditions directly detects DSBs present in nuclear DNA [21,23] and currently represents, in comparison to other methods [24], the quickest preparation method for their detection. Preparation of comet slides from isolated nuclei takes less than 5 min, making this method particularly suitable for measurement of rapid repair processes. Speed and unbiased detection of DSBs is an advantage over non-direct methods of DSBs quantification as e.g. γ H2AX foci [25].

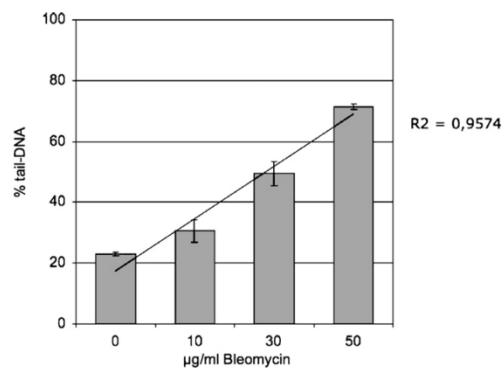


Fig. 3. Induction of DSBs by Bleomycin. 10-day-old seedlings of *Arabidopsis* Ws were treated with 10, 30 and 50 µg/ml Bleomycin for 1 h. Nuclei isolated from treated and untreated seedlings were analyzed by the neutral comet assay and evaluated for comet formation. The mean percentage of DNA in the comet tail for 300 comets for each concentration point are shown. (Error bars—standard error.) Induction of DSB is linear without any signs of saturation ($R^2 = 0.9574$) in the 0–50 µg/ml Bleomycin concentration range used.

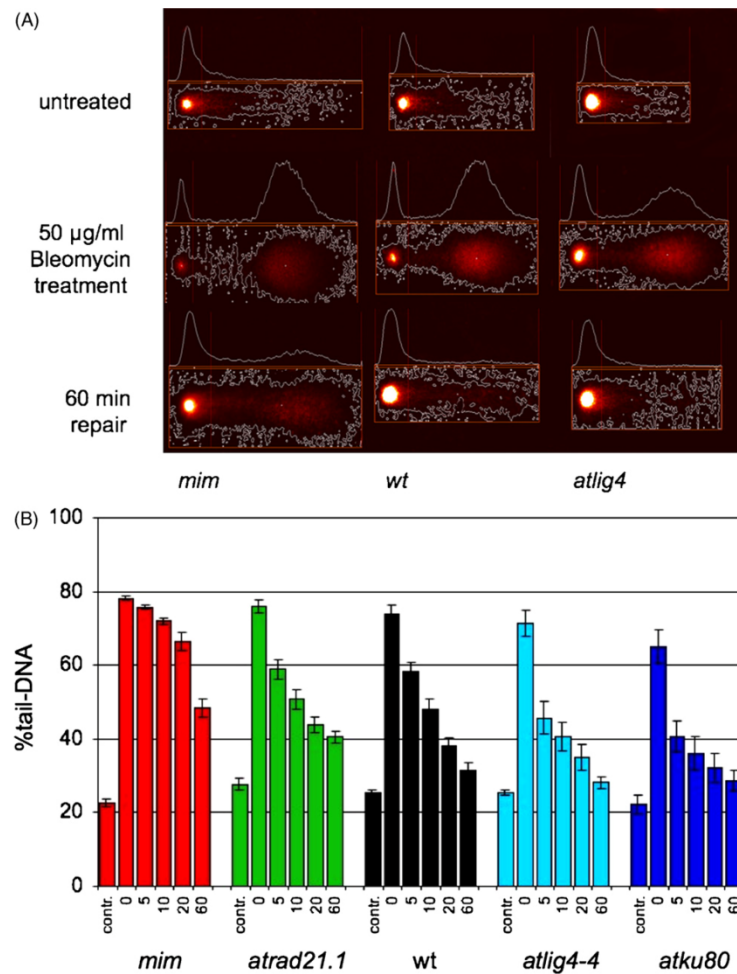


Fig. 4. Detection of DNA damage by comet assay. Comet slides were prepared from untreated and Bleomycin treated 10-day-old wild-type and mutant seedlings by the neutral comet protocol. Representative comet images (A) are shown for wild-type (Wt), *atmim* and *atlig4-4* mutants, untreated or treated and left to repair for 60 min. The extent of DSB repair is manifested by the fraction of DNA remaining in the comet tails after repair recovery (% tail-DNA) and quantified with the LIM software. Mean values of 300 comets are plotted on (B) to show time course of DSB repair in mutant lines over 1 h repair period. Background DNA damage in untreated (control) seedlings and damage after 1 h treatment with 50 µg/ml Bleomycin ($t=0$) is similar in all lines. (Error bars—standard error).

3.2. Genome integrity in untreated plants

In this study we have analyzed young seedlings in the early leaf development phase [26]. Surprisingly none of mutant lines showed a delay in germination or growth of the seedling during first 10 days after the onset of germination (Fig. 1B). However a delayed growth phenotype was manifested during later stages in all but *atrad21.1* mutated lines [16–18]; for *atlig4-4* and *atku80* see Fig. 1A.

Levels of background DNA damage were similar in all mutant and wild-type seedlings, with approximately 20% DNA migrating in the comet tail (Fig. 4A and B). This is surprising as it suggests that the mutations do not lead directly to the accumulation of DSBs in nuclear DNA, despite the hypersensitivities of the mutant lines to induced DNA damage. In contrast to young seedlings, mature leaves of all mutants and wild-type *Arabidopsis* showed such exten-

sive fragmentation of nuclear DNA (more than 90% tail-DNA) that it was not possible to measure differences between lines using this material (data not shown).

3.3. DSB repair kinetics in wild-type and mutant lines

A 1-h treatment of mutant and wild-type seedlings with 50 µg/ml Bleomycin caused a large shift in the migration of the genomic DNA. All lines displayed similar extents of fragmentation with 60–80% of DNA migrating in the comet tail (Fig. 4A and B). Nevertheless all tested lines effectively survive this dose for one week (Fig. 2B) as compared to survival of seedlings continuously exposed even to 10 times lower Bleomycin concentration for the same time (Fig. 2A). The repair kinetics of mutant and wild-type plants (Fig. 5) were determined through a time course of recovery

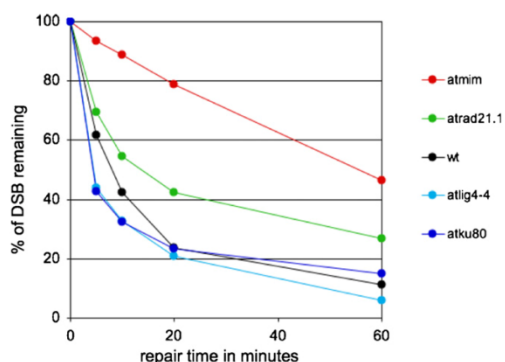


Fig. 5. Kinetics of DSB repair. Fractions of remaining DSBs were calculated for 0, 5, 10, 20 and 60 min repair time points after the treatment with 50 $\mu\text{g/ml}$ Bleomycin. Maximum damage is normalised as 100% at $t=0$ for all lines. Wild-type, *atku80* and *atlig4-4* rapidly repair induced DSBs during the first 10 min. *atku80* and *atlig4-4* have even faster repair rates than wild-type, and this is most pronounced in the first 5 min. Contrary to wild-type, *atrad21.1* and *atmim* have clearly slower initial DSB repair, with a striking repair defect in *atmim*. The rate constants k and half-lives $t_{1/2}$ were calculated by regression analysis for repair points 0, 5 and 10 min (see Table 1).

from Bleomycin treatment, with the extent of remaining DNA damage calculated from the percentage of DNA in comet tails (Fig. 4B) as defined in Section 2. Wild-type seedlings displayed very rapid repair with 80% of DSBs repaired during first 20 min (Fig. 5). Repair kinetics were biphasic with a very rapid initial phase responsible for the majority of DSB repair followed by a slower phase in which the remaining DNA damage was repaired. The later phase of slower repair represents either the repair of a subset of DSBs by an alternative pathway or, more likely, other types of DNA lesions induced by Bleomycin and detected by neutral comet assay such as close SSBs due to oxidative damage [27].

In order to determine the molecular basis for rapid DSBs repair, the parameters of repair kinetics for the initial 10 min period were determined in wild-type and mutant lines using a least-square analysis of the time course of recovery after Bleomycin treatment. A linear relationship on the semi-logarithmic scale indicates that rapid removal of DSBs from genomic DNA followed first order kinetics, suggesting involvement of single rather than two DNA molecules during the initial stage of DSB repair. The rate constant k , half-life $t_{1/2}$ and R^2 for the initial rates of repair of each mutant line are provided in Table 1.

Almost all DSBs were removed within 1 h of Bleomycin treatment in wild-type, *atku80* and *atlig4-4* plants (Fig. 5). In comparison to yeast and mammals, *Arabidopsis* DSB repair is very rapid with a $t_{1/2}$ of less than 8 min. Contrary to wild-type, *atrad21.1* and *atmim* have clearly slower initial DSB repair with a striking repair defect of *atmim*. Mutant *atmim* plants retained a significant level of DNA damage after 1 h of recovery, with around half of the original number of Bleomycin induced DSBs. However, some mutant lines did display variation in the rate of DSB repair during the first 5–10 min

Table 1
Rate constants k and half-times $t_{1/2}$ of initial rapid DSB repair in *Arabidopsis* wild-type and mutant lines were determined by least-square linear regression of fraction of DSBs remaining for 0, 5 and 10 min of repair recovery (Fig. 5).

	k (min^{-1})	$t_{1/2}$ (min)	R^2
<i>mim</i>	0.0122	56.8	0.9958
<i>atrad21.1</i>	0.0630	11.0	0.9838
wild-type	0.0881	7.9	0.9932
<i>atlig4-4</i>	0.1221	5.7	0.9168
<i>atku80</i>	0.1244	5.6	0.9058

after treatment (Fig. 5) resulting in significant differences in the kinetic data provided for the initial rapid phase of DSB repair (Table 1). Surprisingly mutants in the NHEJ pathway (*atku80* and *atlig4-4*) displayed rapid DSB repair kinetics in the initial repair phase, even faster than in wild-type seedlings ($t_{1/2}$ of 5.6, 5.7 and 7.9 min, respectively). These results provide the first evidence for a rapid pathway substituting for C-NHEJ in the repair of a majority of DSBs in plants.

In mammals the ligation of non-homologous ends during V(D)J recombination and Ig class switching also depends on Xrcc4 and DNA ligase IV (Lig4). Nevertheless two recent reports [28,29] suggest an alternative robust C-NHEJ independent DSB cut and paste recombination pathway. Yan et al. [28] described that IgH class switching in C-NHEJ deficient mouse B-cells uses a novel, non-classical, end-joining pathway. This alternative end-joining pathway also frequently joins the *IgH* locus to other chromosomes leading to translocations. Nevertheless the authors do not provide data on the extent and kinetics of this alternative pathway. However, recent studies have provided the first clues for the mechanism of alternative DSB repair pathways in plant, yeast and animals. A common feature of Ku-independent end-joining in eukaryotes is a greater dependence on microhomologies to facilitate repair, in pathways termed alternative-NHEJ, backup-NHEJ (B-NHEJ) or microhomology-mediated end-joining (MHEJ) [30–33]. While the molecular basis for this end-joining activity is poorly defined, in mammals this requires PARP-1, XRCC1 and DNA ligases 3 and/or 1, rather than LIG4 which is specific for C-NHEJ [32,33].

That other factors substitute for KU70/80, LIG4, and possibly for the entire C-NHEJ pathway in plants as in other organisms, implies the presence of a possible salvage mechanism effectively repairing one of the most critical DNA lesions by joining of DSB ends [34]. The main function of this repair pathway in plants could be the demand for rapid elimination of DSBs that accumulate during seed storage upon the onset of germination [2,7]. Nevertheless the relationship of both C-NHEJ and a substituting rapid pathway in repair of DSBs in *Arabidopsis* remain to be established.

In further analysis of this novel DSB repair pathway we studied repair capacity and kinetics in *Arabidopsis* mutant lines with impaired SMC complexes [35], which are involved in a broad spectrum of chromosome maintenance functions, including cohesion (Smc1–3), chromosome condensation (Smc2–4), and DNA recombination and repair (Smc5–6) [36]. SMCs complexes were strong candidates to offset missing KU proteins in stabilization of the DSB for repair.

Cohesins play an important role in the repair of DSBs. In yeast, mutants in the cohesin subunit SCC1/RAD21/MCD1 are hypersensitive to DNA-damaging agents [37]. It has been proposed that cohesin facilitates DNA repair by holding sister chromatids together locally at the DSB (Fig. 6A). Shortly after laser irradiation, proteins known to be involved in the repair of DSBs including both SMC and non-SMC components of cohesin complexes accumulate along the beam tracks [38].

RAD21/SCC1 is a member of the superfamily of Kleisin proteins, which interacts with N- and C-terminal domains of SMC proteins to form a ring-like structure (Fig. 6A). *Arabidopsis* has three *RAD21* gene homologues. The transcript level of *AtRAD21.1* is increased specifically after induction of DNA damage and this protein plays a critical role in recovery from DNA damage during seed imbibition, prior to germination [17]. We show here that *atrad21.1* mutant have a nearly two-fold defect on the initial rate of DSB repair when compared to wild-type plants ($t_{1/2}$ 11.0 min and 7.9 min, respectively) and after 1 h 30% of total DNA damage remained unrepaired as compared to only 15% in wild-type seedlings. The effect of *atrad21.1* on DSB repair is, however, less pronounced than that of *atmim*.

Of the several SMC mutant lines available, it was decided to test SMC6/MIM which has been shown to affect several aspects of

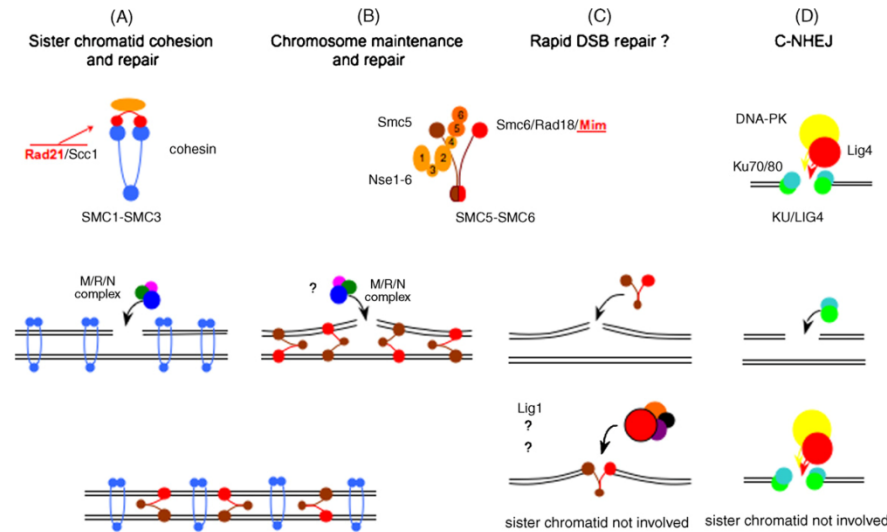


Fig. 6. Possible roles of Smc complexes in DSB repair. (A) The Smc1–3 cohesin complex stabilizes DSBs by enclosing sister chromatids in proteinaceous loops (in blue) and enables entry of the M/R/N complex for completing repair by HR. RAD21 and other kleisins are involved in circularization of Smc1–3 heterodimer (structure on top). In contrast, the Smc5–6 heterodimer forms a V-shaped complex with auxiliary proteins (structure on top), which interacts with DNA through its ends (brown). The complex can either bind together sister chromatids (B), or as suggested by Lehmann [36] stabilize DSBs by direct linking of both DNA ends (C). Stabilization of DNA ends would then parallel binding of KU70/80 heterodimer to DSB ends as a prerequisite for direct end-joining in the C-NHEJ pathway (D).

chromosome biology [16]. The Smc5–6 complex was initially identified via a radiation-sensitive mutant of *Schizosaccharomyces pombe*. The *rad18-X* mutant was isolated in a screen for radiation sensitivity and was found to be sensitive to both UV and IR [39]. Models have been proposed in which the role of the Smc5–6 complex is to hold either sister chromatids or broken DNA ends together to facilitate repair of the DSB (Fig. 6B and C). De Piccoli et al. [40] showed that Smc5–6 complex is recruited to the DSB to support repair by homologous recombination between sister chromatids, similar to cohesin functions. In addition *smc5-6* mutants suffer from high levels of gross chromosomal rearrangements. Based on the study of Pebernard et al. [41] there is no clear candidate for a RAD21/SCC1 related factor to bridge head domains. They propose that Smc5–6 may function without enclosing sister chromatids in a proteinaceous loop suggesting a dual function of the Smc5–6 complex in stabilizing DSB as depicted in Fig. 6B and C. This was first indicated by mutational analysis of *smc6*, in which the repair function was separated from the essential role in genome maintenance [42].

The *Arabidopsis* MIM protein belongs to the Smc5–6 complex and is an orthologue of Smc6. The corresponding mutant is hypersensitive to UV, IR and mitomycin C and shows a reduced frequency of intrachromosomal recombination [16]. In our studies, *atmim* mutant displayed the most severe reduction in the initial rate of DSB repair ($t_{1/2}$ 56.8 min) with first order kinetics consistent with complete abolition of the initial rapid repair, leaving only the slower repair pathway(s) (Fig. 4). This suggests that the initial rapid repair of DSBs has an absolute requirement for MIM. Interestingly, the *atmim* mutant only displayed a two-fold reduction in intrachromosomal recombination, showing that homologous recombination was still active in this line [43]. Hence, this can be taken as a further indication that even if HR is involved in the process of rapid DSBs repair, it is likely not solely responsible for removal of DSBs during early rapid stages of DSBs repair. Due to “non-ring” structure of the SMC5–6 heterodimer, the complex could provide stability by holding together sister chromatids at the sites of DSB, to facilitate

recombinational repair (Fig. 6B). This structure would also allow stabilization of DNA ends of DSB in a way the KU proteins binding to DSB in the C-NHEJ repair pathway (Fig. 6D), thereby enabling access to repair factors for direct sealing of the DSB as depicted in Fig. 6C. Our preliminary results suggest that DNA ligase 1 could be one of the factors providing final ligation of DSBs as demonstrated by two-fold reduction of initial rate of repair in siRNA/Lig1 mutant (Waterworth et al. (2009), in preparation).

Data obtained with *atmim* suggests that the Smc5–6 complex is a key player in rapid, global DSB repair in nuclear DNA, rather than Smc1–3 components of the cohesin complex to which *atrad21.1* belongs.

4. Summary

By using the neutral version of the comet assay to directly quantify DSBs in nuclear DNA we have found that a previously uncharacterised pathway is responsible for the rapid repair of the majority of Bleomycin induced DSBs in nuclear DNA of *Arabidopsis*. This novel recombination mechanism is independent of the C-NHEJ pathway, but requires the SMC protein MIM to stabilize the DSB and a DNA ligase(s) other than LIG4 for ligation. These results provide the first biochemical and molecular characterization of an alternative DSB repair pathway, responsible for the recombination previously observed in *atlig4* and *atku80* mutant lines of *Arabidopsis* [20,30].

Conflict of interest

None.

Acknowledgements

KJA would like to acknowledge financial support of Ministry of Education, Sport and Youth of the Czech Republic (project

LC06004), EU project COMICS (LSHB-CT-2006-037575) and of EU project TAGIP (LSHG-CT-2005-018785) Work done in the group of CW was supported by the Centre Nationale de la Recherche Scientifique, the Université Blaise Pascal and the EU project TAGIP (LSHG-CT-2005-018785). Support from the Royal Society, UK for KJA and CEW is gratefully acknowledged, and work in the lab of CEW is supported by the UK Biotechnology and Biological Sciences Research Council (grant number JF20608). JCN is supported by Portugal funding agency F.C.T. (fellowship SFRH/BPD/30365/2006).

Appendix A. Supplementary data

Supplementary data associated with this article can be found, in the online version, at doi:10.1016/j.dnarep.2008.11.012.

References

- [1] S. Tano, H. Yamaguchi, Repair of radiation induced single-strand breaks in DNA of barley embryos, *Mutat. Res.* 42 (1977) 71–78.
- [2] D.J. Osborne, A. Dell'Aquila, R.H. Elder, DNA repair in plant cells. An essential event of early germination in seeds, *Folia Biol. (Praha)* 30 (1984) 155–169.
- [3] G.P. Howland, R.W. Hart, M.L. Yette, Repair of DNA strand breaks after gamma-irradiation of protoplasts isolated from cultured wild carrot cells, *Mutat. Res.* 27 (1975) 81–86.
- [4] J. Velemínský, J. van't Hoff, Repair of X-ray-induced single-strand breaks in root tips of *Tradescantia* clones 02 and 4430, *Mutat. Res.* 131 (1984) 143–146.
- [5] K.J. Angelis, J. Velemínský, R. Rieger, I. Schubert, Repair of Bleomycin-induced DNA double-strand breaks in *Vicia faba*, *Mutat. Res.* 212 (1989) 155–157.
- [6] G. Koppen, K.J. Angelis, Repair of X-ray induced DNA damage measured by the comet assay in roots of *Vicia faba*, *Environ. Mol. Mutagen.* 32 (1998) 281–285.
- [7] R.H. Elder, A. Dell'Aquila, M. Mezzina, A. Sarassin, D.J. Osborn, DNA ligase in repair and replication in the embryos of rye *Secale cereale*, *Mutat. Res.* 181 (1987) 61–71.
- [8] P.L. Olive, J.P. Banath, Detection of DNA double-strand breaks through the cell cycle after exposure of X-rays, bleomycin, etoposide and 125Ird, *Int. J. Radiat. Biol.* 64 (1993) 349–358.
- [9] A. Rapp, K.O. Greulich, After double-strand break induction by UV-A, homologous recombination and nonhomologous end joining cooperate at the same DSB if both systems are available, *J. Cell. Sci.* 117 (2004) 4935–4945.
- [10] K.J. Angelis, M. Dušinská, A.R. Collins, Single cell gel electrophoresis: detection of DNA damage at different levels of sensitivity, *Electrophoresis* 20 (1999) 2133–2138.
- [11] G. Jovtchev, M. Menke, I. Schubert, The comet assay detects adaptation to MNU-induced DNA damage in barley, *Mutat. Res.* 493 (2001) 95–100.
- [12] T. Gichner, O. Ptáček, D.A. Stavreva, M. Plewa, Comparison of DNA damage in plants as measured by single cell gel electrophoresis and somatic leaf mutations induced by monofunctional alkylating agents, *Environ. Mol. Mutagen.* 33 (1999) 279–286.
- [13] M. Menke, I.-P. Cheng, K.J. Angelis, I. Schubert, DNA damage and repair in *Arabidopsis thaliana* as measured by the comet assay after treatment with different classes of genotoxins, *Mutat. Res.* 493 (2001) 87–93.
- [14] C.M. Bray, C.E. West, DNA repair mechanisms in plants: crucial sensors and effectors for the maintenance of genome integrity, *New Phytol.* 168 (2005) 511–528.
- [15] J.-Y. Bleuyard, M.E. Gallego, C.I. White, Recent advances in understanding of the DNA double-strand break repair machinery of plants, *DNA-Repair* 5 (2006) 1–12.
- [16] T. Mengiste, E. Revenkova, N. Bechtold, J. Paszkowski, SMC-like protein is required for efficient homologous recombination in *Arabidopsis*, *EMBO J.* (1999) 4505–4512.
- [17] J.A. da Costa-Nunes, A.M. Bhatt, S. O'Shea, C.E. West, C.M. Bray, U. Grossniklaus, H.G. Dickinson, Characterization of the three *Arabidopsis thaliana* RAD21 cohesins reveals differential responses to ionizing radiation, *J. Exp. Bot.* 57 (2006) 971–983.
- [18] M.E. Gallego, N. Jalut, C.I. White, Telomerase dependence of telomere lengthening in Ku80 mutant *Arabidopsis*, *Plant Cell* 15 (2003) 782–789.
- [19] J.D. Friesner, A.B. Britt, Ku80- and DNA ligase IV-deficient plants are sensitive to ionizing radiation and defective in T-DNA integration, *Plant J.* 34 (2003) 427–440.
- [20] H. van Attikum, P. Bundock, R.M. Overmeer, L.Y. Lee, S.B. Gelvin, P.J. Hooykaas, The *Arabidopsis* AtLIG4 gene is required for the repair of DNA damage, but not for the integration of *Agrobacterium* T-DNA, *Nucl. Acids Res.* 31 (2003) 4247–4255.
- [21] P.L. Olive, J.P. Banath, The comet assay: a method to measure DNA damage in individual cells, *Nat. Protocols* 1 (2006) 23–29.
- [22] R.J. Steighner, L.F. Povirk, Bleomycin-induced DNA lesions at mutational hot spots: implications for the mechanism of double-strand cleavage, *Proc. Natl. Acad. Sci. U.S.A.* 87 (1990) 8350–8354.
- [23] J.L. Fernández, F. Vázquez-Gundín, M.T. Rivero, A. Genescá, J. Gosálvez, V. Goyanes, DBD-FISH on neutral comets: simultaneous analysis of DNA single and double-strand breaks in individual cells, *Exp. Cell Res.* 270 (2001) 102–109.
- [24] G. Iliakis, D. Blöcher, L. Metzger, G. Pantelias, Comparison of DNA double-strand break rejoining as measured by pulsed field gel electrophoresis, neutral sucrose gradient centrifugation and non-unwinding filter elution in irradiated plateau-phase CHO cells, *Int. J. Radiat. Biol.* 59 (1991) 927–939.
- [25] J.D. Friesner, B. Liu, K. Culligan, A.B. Britt, Ionizing radiation-dependent gamma-H2AX focus formation requires ataxia telangiectasia mutated and ataxia telangiectasia mutated and Rad3-related, *Mol. Biol. Cell* 16 (2005) 2566–2576.
- [26] D.C. Boyes, A.M. Zayed, R. Ascenzi, A.J. McCaskill, N.E. Hoffman, K.R. Davis, Growth stage-based phenotypic analysis of arabidopsis: a model for high throughput functional genomic in plants, *Plant Cell* 13 (2001) 1499–1510.
- [27] L. Benítez-Bribiesca, P. Sánchez-Suarez, Oxidative damage, Bleomycin and gamma radiation induced different types of DNA strand breaks in normal lymphocytes and thymocytes, a comet assay study, *Ann. NY Acad. Sci.* 887 (1999) 133–149.
- [28] C.T. Yan, C. Boboila, E.K. Souza, S. Franco, T.R. Hickernell, M. Murphy, S. Gumaste, M. Geyer, A.A. Zarrin, J.P. Mains, K. Rajewsky, F.W. Alt, IgH class switching and translocation use a robust non-classical end-joining pathway, *Nature* 449 (2007) 479–483.
- [29] B. Corneo, R.L. Wendland, L. Deriano, X. Cui, I.A. Klein, S.Y. Wong, S. Arnal, A.J. Holub, G.R. Weller, B.A. Pancake, S. Shah, V.L. Brandt, K. Meek, D.B. Roth, Rag mutations reveal robust alternative end joining, *Nature* 449 (2007) 483–486.
- [30] M. Heacock, E. Spangler, K. Riha, J. Puizina, D.E. Shippen, Molecular analysis of telomere fusions in *Arabidopsis*: multiple pathways for chromosome end-joining, *EMBO J.* 23 (2004) 2304–2313.
- [31] N. Bannardo, A. Cheng, N. Huang, J.M. Stark, Alternative-NHEJ is a mechanistically distinct pathway of mammalian chromosome break repair, *PLoS Genet.* 4 (2008) e1000110.
- [32] L. Liang, L. Deng, S.C. Nguyen, X. Zhao, C.D. Maulin, C. Shao, J.A. Tischfield, Human DNA ligases I and III, but not ligase IV, are required for microhomology-mediated end joining of DNA double-strand breaks, *Nucl. Acids Res.* 36 (2008) 3297–3310.
- [33] W. Wu, M. Wang, W. Wu, S.K. Singh, T. Mussfeldt, G. Iliakis, Repair of radiation induced DNA double strand breaks by backup NHEJ is enhanced in G2, *DNA Repair* 7 (2008) 329–338.
- [34] M.J. Flores, T. Ortiz, J. Piñero, F. Cortés, Protection provided by exogenous DNA ligase in *Go* human lymphocytes treated with restriction enzyme MspI or Bleomycin as shown by the comet assay, *Environ. Mol. Mutagen.* 32 (1998) 336–343.
- [35] F. Cortés-Ledesma, G. dePicolis, J.E. Haber, L. Aragón, A. Aquilera, SMC proteins, new players in the maintenance of genomic stability, *Cell Cycle* 6 (2007) 914–918.
- [36] A.R. Lehmann, The role of SMC proteins in the responses to DNA damage, *DNA Repair* 4 (2005) 309–314.
- [37] R.P. Birkenbihl, S. Subramani, Cloning and characterization of rad21 an essential gene of *Schizosaccharomyces pombe* involved in DNA double-strand break repair, *Nucl. Acids Res.* 20 (1992) 6605–6611.
- [38] J.S. Kim, T.B. Krasieva, V. LaMorte, A.M. Taylor, K. Yokomori, Specific recruitment of human cohesin to laser-induced DNA damage, *J. Biol. Chem.* 277 (2002) 45149–45153.
- [39] J. Phipps, A. Nasim, D.R. Miller, Recovery, repair and mutagenesis in *Schizosaccharomyces pombe*, *Adv. Genet.* 23 (1985) 1–72.
- [40] G. De Piccoli, F. Cortes-Ledesma, G. Ira, J. Torres-Rosell, S. Uhle, S. farmer, J.-Y. Hwang, F. Machin, A. Ceschia, A. McAleenan, V. Cordon-Preciado, A. Clemente-Blanco, F. Viella-Mitjana, P. Ullal, A. Jarmuz, B. Leitao, D. Bressan, F. Dotiwala, A. Papusha, X. Zhao, K. Myung, J.E. Haber, A. Aquilera, L. Aragón, Smc5-Smc6 mediate DNA double-strand-break repair by promoting sister-chromatid recombination, *Nat. Cell Biol.* 8 (2006) 1032–1034.
- [41] S. Pebernard, J. Wohlschlegel, W. Hayes McDonald, J.R. Yates III, M.N. Boddy, The Nse5-Nse6 dimer mediates DNA repair roles of the Smc5-Smc6 complex, *Mol. Cell Biol.* 26b (2006) 1617–1630.
- [42] M.I. Fusteri, A.R. Lehmann, A novel SMC protein complex in *Schizosaccharomyces pombe* contains Rad18 DNA repair protein, *EMBO J.* 19 (2000) 1691–1702.
- [43] M. Hanin, T. Mengiste, A. Bogucki, J. Paszkowski, Elevated levels of intrachromosomal homologous recombination in *Arabidopsis* overexpressing the MIM gene, *Plant J.* 24 (2000) 183–189.

Research article

Open Access

DNA ligase I deficient plants display severe growth defects and delayed repair of both DNA single and double strand breaks

Wanda M Waterworth^{*1}, Jaroslav Kozak², Claire M Provost³,
Clifford M Bray³, Karel J Angelis² and Christopher E West¹

Address: ¹CPS, Faculty of Biological Sciences, University of Leeds, Leeds LS2 9JT, UK, ²Institute of Experimental Botany AS CR, Na Karlovce 1, 160 00 Praha 6, Czech Republic and ³Faculty of Life Sciences, University of Manchester, Oxford Road, Manchester M13 9PT, UK

Email: Wanda M Waterworth^{*} - fbswmw@leeds.ac.uk; Jaroslav Kozak - kozak@ueb.cas.cz;
Claire M Provost - claire.m.provost@manchester.ac.uk; Clifford M Bray - cliff.bray@manchester.ac.uk; Karel J Angelis - angelis@ueb.cas.cz;
Christopher E West - c.e.west@leeds.ac.uk

^{*} Corresponding author

Published: 26 June 2009

Received: 20 January 2009

BMC Plant Biology 2009, 9:79 doi:10.1186/1471-2229-9-79

Accepted: 26 June 2009

This article is available from: <http://www.biomedcentral.com/1471-2229/9/79>

© 2009 Waterworth et al; licensee BioMed Central Ltd.

This is an Open Access article distributed under the terms of the Creative Commons Attribution License (<http://creativecommons.org/licenses/by/2.0>), which permits unrestricted use, distribution, and reproduction in any medium, provided the original work is properly cited.

Abstract

Background: DNA ligase enzymes catalyse the joining of adjacent polynucleotides and as such play important roles in DNA replication and repair pathways. Eukaryotes possess multiple DNA ligases with distinct roles in DNA metabolism, with clear differences in the functions of DNA ligase orthologues between animals, yeast and plants. DNA ligase I, present in all eukaryotes, plays critical roles in both DNA repair and replication and is indispensable for cell viability.

Results: Knockout mutants of *atlig1* are lethal. Therefore, RNAi lines with reduced levels of AtLIG1 were generated to allow the roles and importance of *Arabidopsis* DNA ligase I in DNA metabolism to be elucidated. Viable plants were fertile but displayed a severely stunted and stressed growth phenotype. Cell size was reduced in the silenced lines, whilst flow cytometry analysis revealed an increase of cells in S-phase in *atlig1-RNAi* lines relative to wild type plants. Comet assay analysis of isolated nuclei showed *atlig1-RNAi* lines displayed slower repair of single strand breaks (SSBs) and also double strand breaks (DSBs), implicating AtLIG1 in repair of both these lesions.

Conclusion: Reduced levels of *Arabidopsis* DNA ligase I in the silenced lines are sufficient to support plant development but result in retarded growth and reduced cell size, which may reflect roles for AtLIG1 in both replication and repair. The finding that DNA ligase I plays an important role in DSB repair in addition to its known function in SSB repair, demonstrates the existence of a previously uncharacterised novel pathway, independent of the conserved NHEJ. These results indicate that DNA ligase I functions in both DNA replication and in repair of both ss and dsDNA strand breaks in higher plants.

Background

As sessile, photosynthetic organisms, plants are necessarily exposed to high levels of environmental stresses including UVB, gamma irradiation and heavy metals

which increase somatic recombination frequencies in plants and their progeny [1]. In plants, repair of DNA damage products is particularly important because somatic tissues give rise to germ cells at a relatively late

stage in development, which means that mutations accumulating in somatic cells from the effects of environmental genotoxins can be passed onto the next generation of plants [2]. Effective cellular response mechanisms have evolved to cope with DNA damage including cell cycle delay or arrest and activation of DNA repair pathways [3].

DNA ligases play essential roles in all organisms by maintaining the physical structure of DNA. These enzymes seal gaps in the sugar-phosphate backbone of DNA that arise during DNA replication, DNA damage and repair. In *Arabidopsis*, as in other eukaryotes, the ligation reaction uses ATP as a cofactor and the involvement of a covalent AMP-ligase intermediate [4]. Eukaryotes have evolved multiple DNA ligase isoforms, with both specific and overlapping roles in the replication and repair of the nuclear and organellar genomes. DNA ligase 1 (LIG1) is present in all eukaryotes where it is required for joining DNA fragments produced during DNA replication. DNA ligase 1 also plays important roles in DNA single strand break (SSB) repair pathways in mammals and yeast. These pathways are less well characterised in plants, but orthologues of several SSB repair genes are identifiable in the genomes of higher plants [5]. *LIG1* is an essential gene with lethal knockout phenotypes in yeast, mammalian cells and *Arabidopsis* [6-8]. Whilst LIG1 is essential for cell division in yeast and plants, mouse embryos are viable and develop until mid-term without LIG1, indicating that a second ligase may substitute for growth up to this point [9]. Similarly, mouse cell lines deficient in LIG1 are also viable, indicating that other DNA ligase activities can substitute for LIG1 in DNA replication [10]. Interestingly, although plants deficient in AtLIG1 are null, cell division in gametophytes prior to fertilisation appeared unaffected, suggesting that either that a second ligase can partially substitute for DNA ligase 1, or that ligase 1 levels in haploid cells are sufficient to support gametogenesis [8].

DNA ligase 4 (LIG4) is also present in all eukaryotes and mediates the final step in the non-homologous end joining (NHEJ) pathway of DSB repair. However, there are clear differences between eukaryotes regarding the presence of other forms of DNA ligase. Plants lack a DNA ligase III (LIG3) orthologue, which in mammals participates in base excision repair of the nuclear genome and also functions in the maintenance of the mitochondrial genome [11]. Whilst yeast has two DNA ligases (LIG1 and LIG4), there are three DNA ligase genes in *Arabidopsis thaliana*, two of which (LIG1 and LIG4) have been functionally characterised [12]. An additional third DNA ligase unique to plants, termed ligase VI, has been cloned from rice and *Arabidopsis* [13,14] although the *in planta* function of this DNA ligase remains to be determined.

In addition to the nuclear genome plants possess chloroplast and mitochondrial genomes. AtLIG1 has been shown to be targeted to both the nucleus and the mitochondria [15]. This dual targeting is controlled via an evolutionarily conserved posttranscriptional mechanism that involves the use of alternative start codons to translate distinct ligase proteins from a single transcript.

Whilst a role for *Arabidopsis* LIG4 in NHEJ is well established, the role of the other DNA ligases in *Arabidopsis* DNA repair remains unclear. Previous studies have demonstrated that LIG1 is an essential gene in plants, consistent with a non-redundant role in nuclear DNA replication [8]. However, the lethality of AtLIG1 mutations prevents analysis of the potential roles of this enzyme in DNA repair processes in plants. To address this question, we created *Arabidopsis* lines with reduced AtLIG1 levels which were sufficient to allow growth and development, but which produced plants which were potentially compromised in DNA repair. Analysis of these plants identified lines which exhibited growth defects and a reduced capacity for the repair of both SSBs and DSBs, providing evidence that AtLIG1 is involved in recombination pathways in higher plants. This has provided the first report of a role for AtLIG1 in DSB repair and identification of a novel DNA DSB repair pathway in plants.

Results

Phenotypic analyses of DNA ligase I deficient plants

In the absence of viable knockout lines, *Arabidopsis* plants with reduced levels of LIG1 were generated using an RNAi approach to gain further insight into gene function (Figure 1A). Both *Arabidopsis* DNA LIGASE 1 (*AtLIG1*) transcript and protein levels in the silenced lines were determined by semi-quantitative RT-PCR and Western blotting respectively (Figures 1B and 1C). Two lines with reduced levels of AtLIG1 protein were selected for further analysis and designated *atlig1-RNAiA* and *atlig1-RNAiB*. These plants displayed an approximate four-fold reduction in AtLIG1 protein (Figure 1B), which although resulting in severe growth defects, was sufficient for propagation of these lines through to seed production.

LIG1-deficient plants displayed a stunted and stressed phenotype (Figure 2A-D) which became more pronounced with age. Leaf and root growth were measured to quantify growth differences between AtLIG1-silenced lines and wild type plants. Interestingly the lines with reduced AtLIG1 protein did not display any delay in germination (data not shown). During the first one to two weeks growth roots were significantly smaller in the *atlig1-RNAiA* compared to wild type or *atlig1-RNAiB* plants ($p < 0.01$ t-Test, Figure 3A-C).

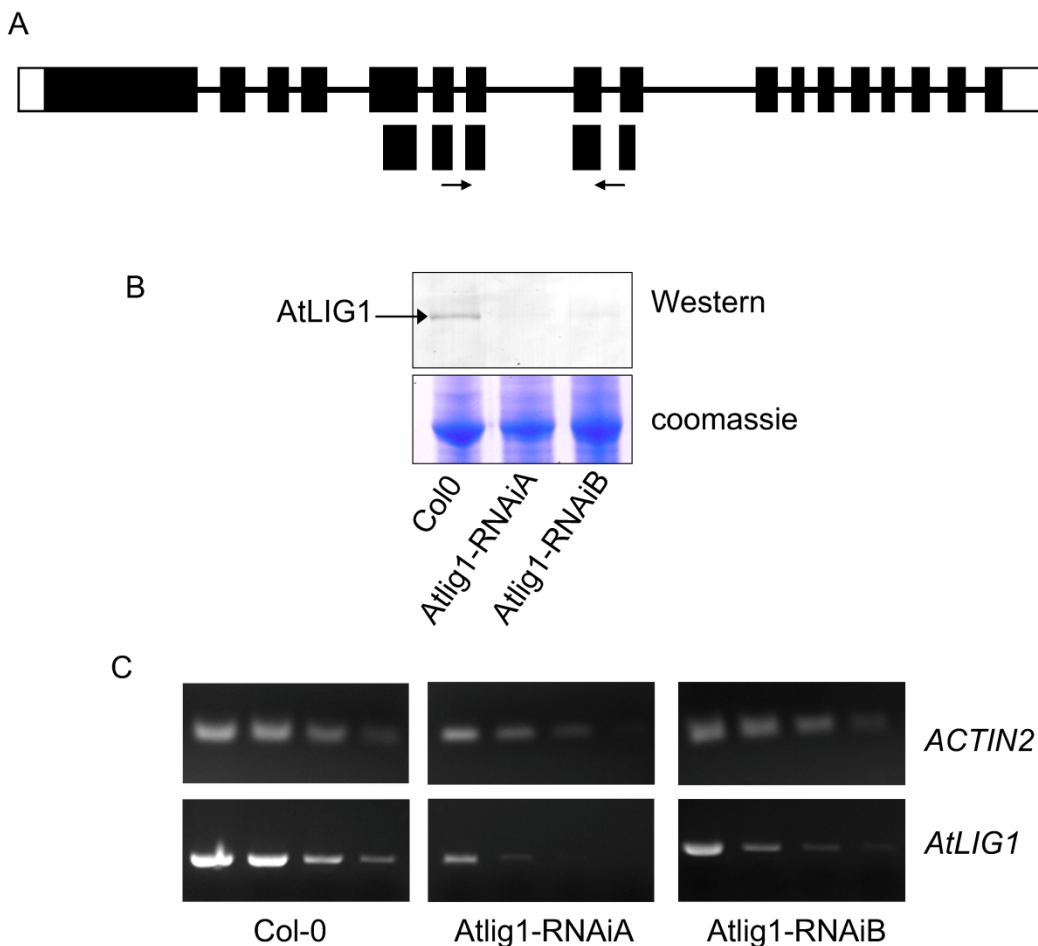


Figure 1
Silencing DNA ligase I expression in *Arabidopsis thaliana*. a) organisation of the *AtLIG1* region used for silencing b) Western analysis showing AtLIG1 protein levels in wild type and silenced lines c) RT-PCR analysis of *AtLIG1* transcript levels in wild type and silenced lines

A reduction in length and width of the third and fourth leaves became more pronounced with plant age in both silenced lines relative to wild type controls (Figure 3B, C). By 30 days the average length of the third leaves was 4.2 mm in *atlig1-RNAi* lines as compared to a wild-type value of 15 mm ($p < 0.01$ t-Test). Corresponding leaf widths were 10.4 mm for the wild-type and significantly less for the RNAi lines at 3.8–4.6 mm ($p < 0.01$ t-Test). The daily growth rate was 1.25 ± 0.14 mm for wild-type, 0.37 ± 0.10 mm for *atlig1-RNAiA* and 0.35 ± 0.14 mm for *atlig1-*

RNAiB line. The final size of mature *Arabidopsis* leaves is a function of both cell division and cell expansion [16]. Therefore, further investigation of the reduced organ size in the *atlig1-RNAi* lines analysed cell size in protoplasts isolated from rosette leaves of wild type and silenced lines after four weeks growth. Cell size was significantly reduced in the *atlig1-RNAi* lines (Figure 3D) with mean cell diameters of 22.9 ± 0.5 μ m and 29.6 ± 0.8 μ m in the *atlig1-RNAiA* and *atlig1-RNAiB* lines respectively, compared to 40.5 ± 0.8 μ m in wild type plants. This 43% and

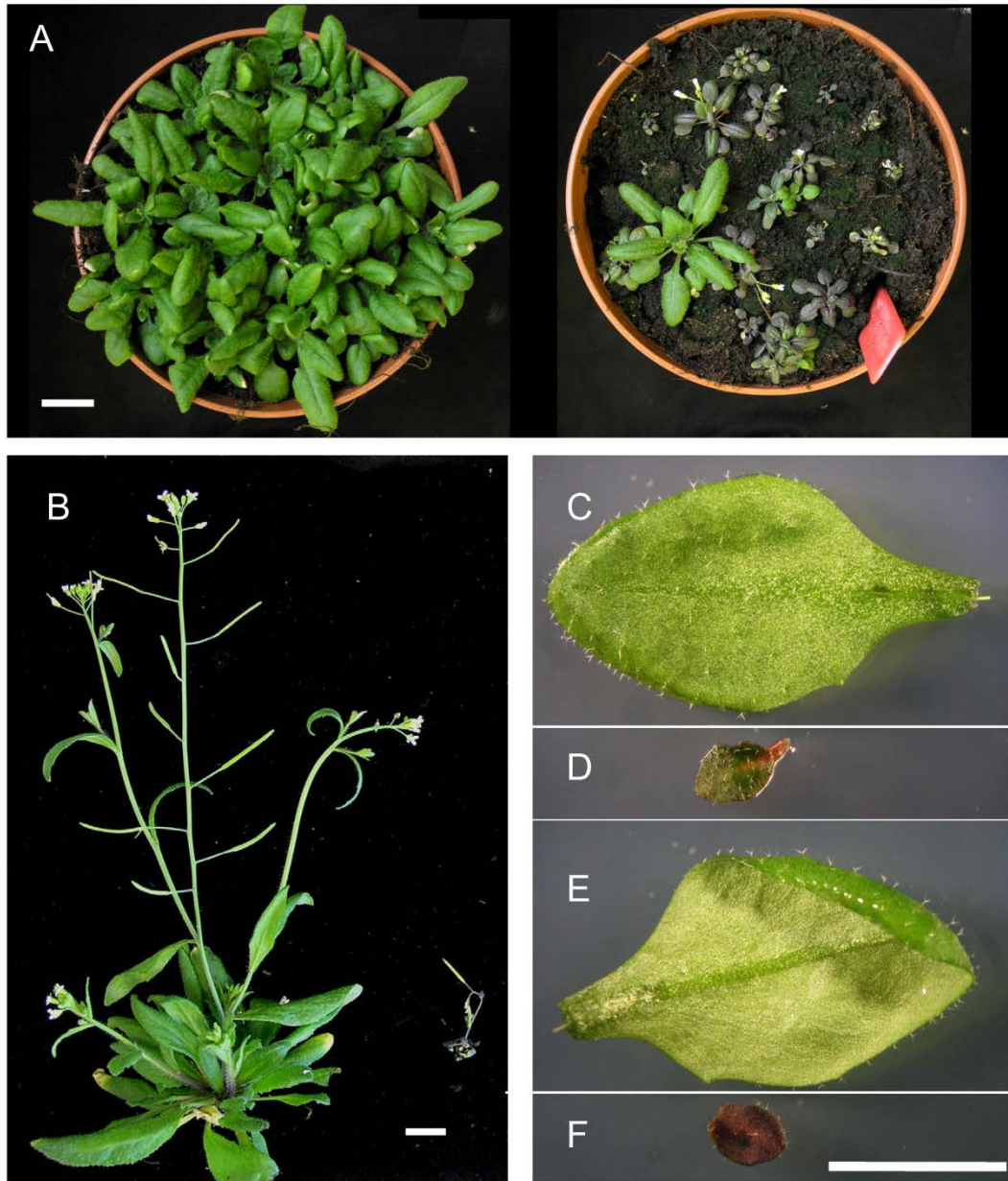


Figure 2
Phenotypic analyses of AtLIG1 deficient plants. A) Comparison of wild-type and *atlig1-RNAi* lines. B) WT and *atlig1-RNAi* plants photographed 6 weeks after germination. Adaxial leaf from WT (C) and *atlig1-RNAi* lines (D) Abaxial surface of WT (E) and *atlig1-RNAi* lines (F). Bar = 1 cm

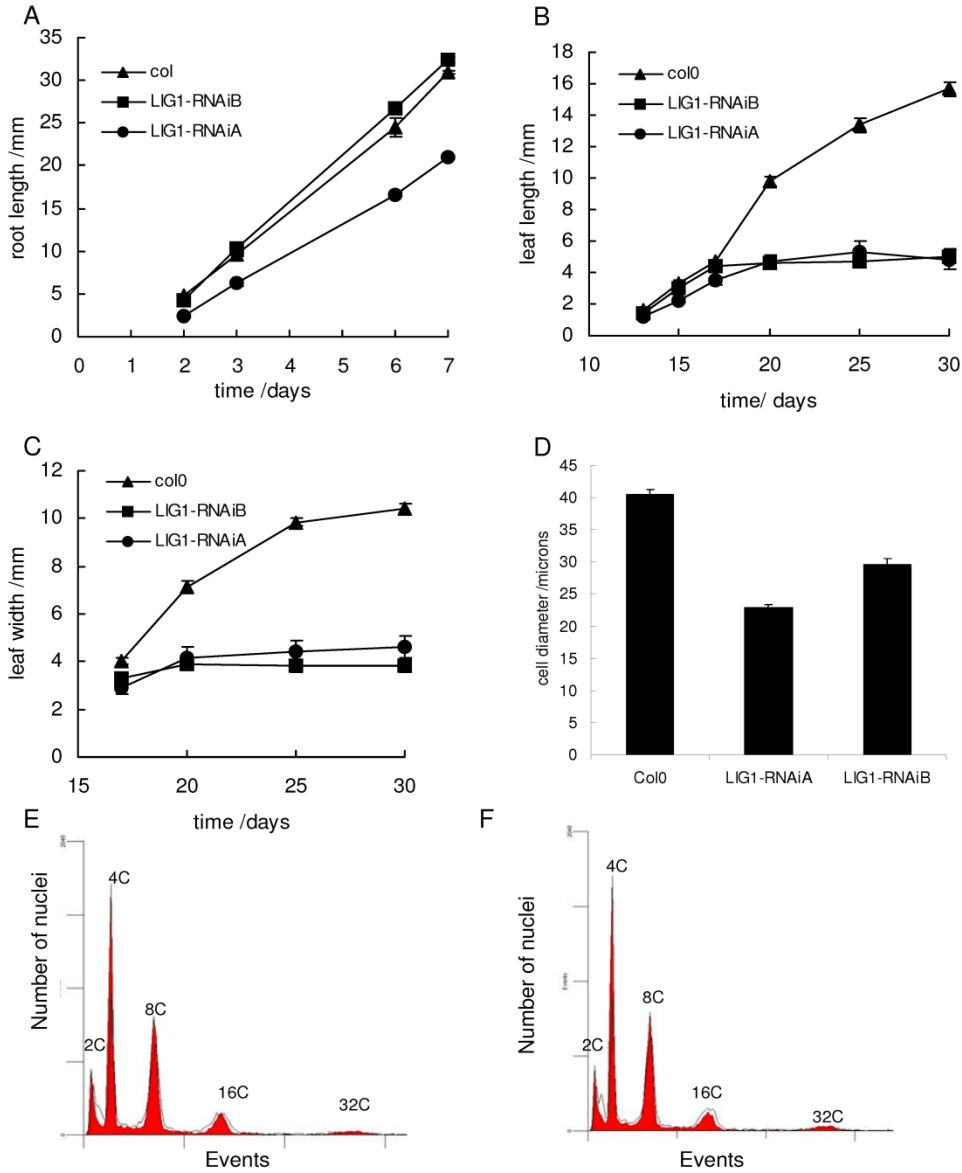


Figure 3
***AtLIG1* silencing results in reduced tissue and cell size, but endoreduplication is not affected.** A) Root growth in wild-type compared to *atlig1-RNAi* silenced plants B) Leaf length in wild-type compared to *atlig1-RNAi* silenced plants C) Leaf width of the third leaves was measured. D) Protoplast cell size from rosette leaves from plants at first bolting. Error bars indicate SE. E) Flow cytometry of wild type 2 week seedlings with Col-0 (red coloured plot) and *atlig1-RNAiA* (black line). F) Flow cytometry of wild type 2 week seedlings with Col-0 (red coloured plot) and *atlig1-RNAiB* (black line). Error bars indicate SE.

27% reduction in cell size of *atlig1-RNAiA* and *atlig1-RNAiB* plants respectively was not sufficient to explain the approximate 70% reduction in leaf length and 60% reduction in leaf width observed relative to wild type plants. This indicated that reduced cell number was also responsible for the decreased organ size in the *atlig1-RNAi* lines.

The extent to which cells have undergone endoreduplication is an important factor in the determination of plant cell size [17]. Flow cytometry was performed on the silenced and wild type plants to determine the ploidy levels of leaf cells. Distinct peaks were observed with wild type and the *atlig1-RNAi* lines, corresponding to 2C, 4C, 8C, 16C and 32C, with no significant difference between the wild type and LIG1 depleted lines in terms of peak height (Figure 3E, F). However, the *atlig1-RNAi* lines both displayed an increase in cells between 2C and 4C indicative of slowed progression or arrest in S-phase. This is consistent with a requirement for AtLIG1 not only in DNA replication and may also reflect impairment in DNA repair pathways leading to compromised S-phase. Normal endoreduplication in the *atlig1-RNAi* lines was confirmed by the development of typical trichomes and a wild type-like etiolation response, both of which are compromised in mutants affecting the endocycle [18] (data not shown).

Analysis of *atlig1-RNAi* single strand break repair kinetics

Single cell electrophoresis (Comet) assay under strictly neutral (N/N) or neutral with alkaline unwinding step (A/N) conditions quantifies the repair kinetics of double or single strand DNA breaks respectively [19,20]. The Comet assay was used here to investigate the kinetics of DNA repair in *atlig1-RNAi* lines compared to wild-type plants. DNA single strand breaks were induced by MMS treatment in ten-day old seedlings of wild type and AtLIG1 depleted lines, with a linear dose response curve up to 2 mM MMS (Figure 4A). Background DNA damage contributed around 20% DNA comet tails in untreated (control) seedlings and 60% of comet tail DNA after 1 hour treatment with 2 mM MMS ($t = 0$). The effects seen were similar in wild type and *atlig1A* lines (Figure 4B). Seedlings treated with 2 mM MMS were analysed using the comet assay and the *atlig1-RNAi* lines displayed reduced repair rates of induced DNA SSB damage in comparison to wild-type with around 50% of damage remaining after 360 min in controls compared to 85% in *atlig1-RNAi* plants (Figure 4C). Notably, *atlig1-RNAi* plants, but not wild type controls, demonstrated an initial increase in SSB accumulation in the first 60 min of recovery following MMS treatment (Figure 4C). This may be attributable to the accumulation of SSBs arising from unrestricted removal of alkylated bases induced by MMS in genomic DNA and a delayed ligation step arising from the limited availability

of DNA ligase activity during base excision repair in the RNAi line.

Reduced rates of DNA double strand break repair in *atlig1-RNAi* lines

Single cell electrophoresis under neutral conditions was used to analyse the repair of DNA double strand breaks in the wild type and silenced lines. This analysis revealed similar levels of background (non-induced) DNA damage in all mutant and wild-type seedlings, with approximately 25% of DNA migrating in the comet tail (Figure 5A, B). This indicated there was no significant accumulation of DSBs in 10 day old seedlings deficient in AtLIG1 in the absence of genotoxin treatment. As differences in growth between WT and AtLIG1 deficient lines become more pronounced at around 20 days onwards, the effect of diminished levels of AtLIG1 on the long term growth and development of the plants may well be attributable to the accumulation of unrepaired damage.

The radiomimetic bleomycin [21] causes DNA double strand breaks in DNA. A one hour treatment of the ten-day seedlings with the bleomycin (30 $\mu\text{g/ml}$) resulted in a large shift in the migration of the genomic DNA with 60–80% migrating in the comet tail, indicative of extensive fragmentation, with AtLIG1 deficient and wild type plants displaying similar responses (Figure 5A). Most DSBs were removed within one hour of bleomycin treatment in wild type lines (Figure 5). The kinetics of DSB repair in mutant and wild type plants were then determined by the comet assay over a time course of recovery from bleomycin treatment, with the extent of DNA damage remaining being calculated from the percentage of DNA in the tail (as defined in the Methods). Wild type seedlings displayed very rapid repair of DSBs. The repair was biphasic, with a very rapid initial phase followed by a slower phase in which the small remainder of DNA damage was repaired. The initial rapid removal of the majority of DSBs from genomic DNA followed first order kinetics. Analysis of the first ten minutes following bleomycin treatment found significantly slower DSB repair in the RNAi lines compared to wild type plants with a $t_{1/2}$ of 6.7 and 9.1 min for two independent RNAi lines compared to 4.9 min for wild type plants (Figure 5B). These differences led to the presence of a residual 10–20% of DSBs remaining in the RNAi lines at 60 min as compared to hardly detectable levels in wild type plants, equating to the level of DSBs seen in wild type lines at 20 min. This contrasts with the repair kinetics of *atlig4* mutant plants, which do not display a reduction in the initial rapid repair observed in the *atlig1-RNAi* lines [22]. These results were consistent with a role for AtLIG1 in a novel pathway for the rapid repair of DSBs in plants, although the essential roles of this ligase in plant cells makes it difficult to determine the full extent of the role of AtLIG1 in this pathway.

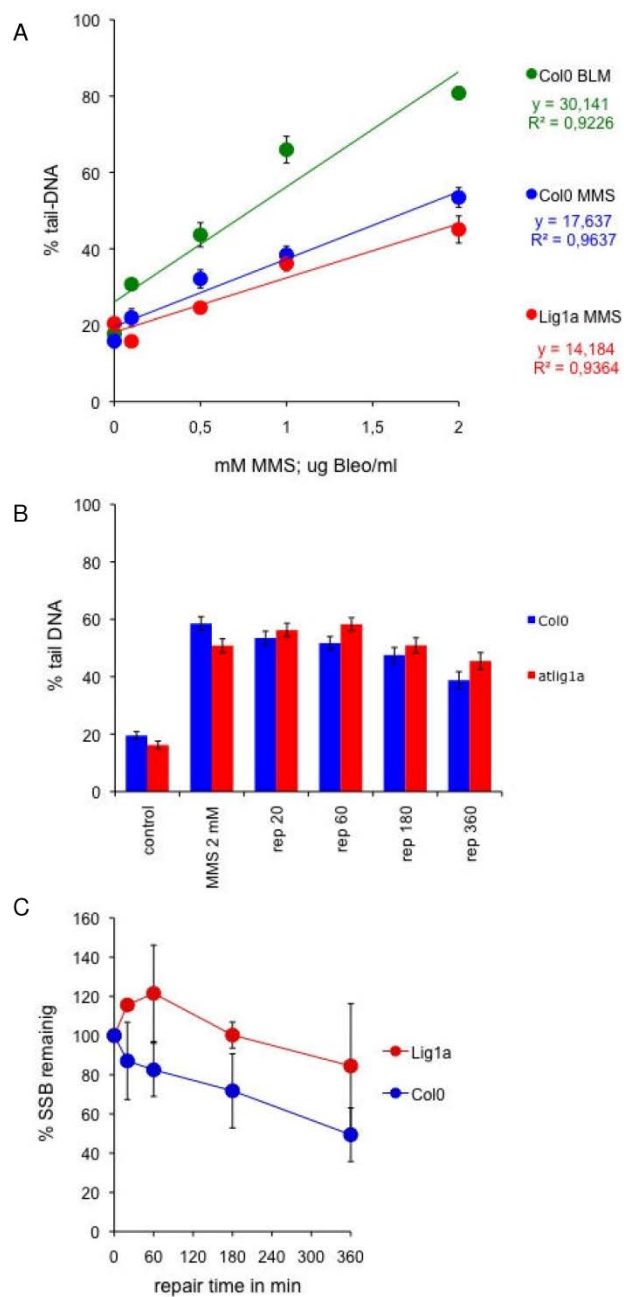


Figure 4 (see legend on next page)

Figure 4 (see previous page)

Kinetics of single strand break repair is altered in the *atlig1*-RNAi lines. (A) Induction of SSBs by methyl methanesulfonate (MMS). Ten day old seedlings of *Arabidopsis* Col0 were treated with for 1 hour. Nuclei isolated from treated and untreated seedlings were analysed by the alkali/neutral version of comet assay and evaluated for comet formation. The mean percentage of DNA in the comet tail for 300 comets for each concentration of MMS are shown. Induction of SSBs is linear in the 0–2 mM MMS concentrations range ($R^2 = 0.9638$ Col0 and $R^2 = 0.9365$ *atlig1*-RNAi respectively). (B) Time course of SSB repair in Col0 and *atlig1*-RNAi lines over 6 hour repair period. Background DNA damage in untreated (control) seedlings and damage after 1 hour treatment with 2mM MMS ($t = 0$) is similar in both lines. Contrary to wild type plants, the number of SSBs in *atlig1*-RNAi increases for 60 minutes after the end of treatment suggesting delayed ligation during repair. (C) Kinetics of SSB repair. The percentage of SSBs remaining were calculated for 0, 20, 60, 180 and 360 minute repair time points after the treatment with 2 mM MMS. Maximum damage is normalised as 100% at $t = 0$ for all lines.

Discussion

DNA ligases play essential cellular roles in sealing the phosphodiester backbone during DNA repair and replication. Although a role for *Arabidopsis* LIG4 in NHEJ is well established, the role of the other ligases in *Arabidopsis* DNA repair processes remains unclear. In the present study, the effects of reduced AtLIG1 levels on plant growth and DNA repair kinetics were investigated by analysis of RNAi silenced plant lines.

AtLIG1 silenced lines displayed a number of growth defects associated with reduced organ size and activation of stress responses. The slowed leaf growth of *AtLIG1* deficient lines as compared to wild-type became increasingly evident with age. This is consistent with a gradual increased accumulation of DNA damage products with leaf age due to reduced levels of *AtLIG1* resulting in compromised repair capacity. *AtLIG1* silenced lines displayed a number of growth defects including reduced organ size and activation of stress responses. The lack of normal *AtLIG1* levels resulted in reduced cell size and an increase in cells in S-phase, which over the plant's life span was manifested phenotypically as retarded leaf growth. This becomes increasingly evident with plant age and is consistent with a requirement for *AtLIG1* for normal growth and development. The oldest leaves of *AtLIG1* deficient plants began to develop a dark green and eventually purple colouration, especially marked on the abaxial leaf surface (Figure 2A–D). The development of this stressed phenotype is similar to previous accounts of the *Arabidopsis* stress response, where the changes in colouration were due to elevated levels of anthocyanin production [2,23]. The oldest leaves eventually bleached, similar to plants exposed to a wide range of treatments including high UVC irradiation [24]. This finding demonstrates that reduction in normal *AtLIG1* levels produces phenotypic changes associated with environmental stresses, consistent with the accumulation of DNA damage in the RNAi lines with age. Environmental stresses often induce reactive oxygen species resulting in forms of DNA damage are predominantly repaired via base and nucleotide excision repair pathways. Chronic exposure to these stresses may also

result in accumulation of DSBs in the plant genome with time as a consequence of unrepaired single strand breaks being converted into more cytotoxic DSBs [25,26]. The stress response exhibited by the *atlig1*-RNAi lines may be activated by the presence of DNA strand breaks usually associated with oxidative DNA damage. The *AtLIG1* deficient plants displayed reduced growth but interestingly the RNAi lines bolted and flowered significantly earlier than wild-type lines (data not shown) in common with previous studies that reported precocious flowering in plants stressed by exposure to low levels of gamma-radiation [25] or UVC [27].

Further analysis investigated the repair kinetics of single and double strand DNA breaks induced in wild type and silenced lines. Of the different forms of DNA damage, DSBs are one of the most cytotoxic and, if left unrepaired, can result in chromosome fragmentation and loss of genetic information. In eukaryotes, DSBs are repaired by homologous recombination or NHEJ pathways. In *Arabidopsis* the NHEJ pathway components KU70, KU80 and LIG4 are all required for survival of gamma irradiated plants [28]. However, several lines of evidence strongly support the existence of end joining pathways which are independent of KU and LIG4 in higher plants. Knockout mutants of classical NHEJ (C-NHEJ) pathway components in higher plants such as *atku80* and *atlig4* are able to integrate T-DNA at random sites in the genome with frequencies of between 10–100% of that found in wild type plants [29–31]. Consistent with these observations, illegitimate end-joining is still active in non-homologous end joining mutants, observed by chromosomal fusions and plasmid re-joining assays *in planta* [32,33]. Recent studies revealed that *atlig4* mutants display rapid rates of DSB repair, similar to those of wild type plants, indicating either that a second ligase activity or an independent pathway can effectively substitute for loss of LIG4 [22]. Analysis of the RNAi lines indicated that *AtLIG1* was required for the initial rapid phase of repair, with reduced *AtLIG1* levels resulting in an increase in the half life of a DSB. This was not attributable to increased background levels of DSBs in the untreated *atlig1*-RNAi lines, as these basal lev-

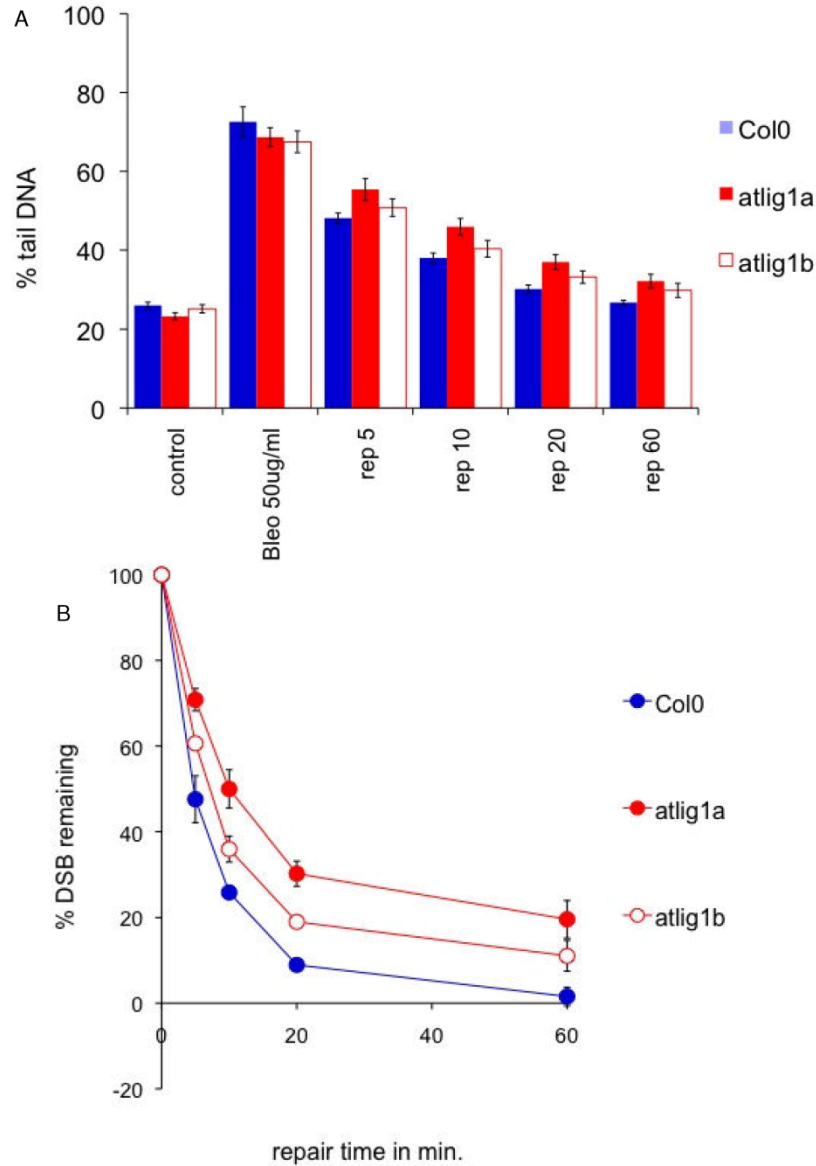


Figure 5
DSB repair in *Arabidopsis* Col0 and *atlig1-RNAiA* and *atlig1-RNAiB* lines determined by neutral comet assay. (A) Time course of DSB repair during 1-hour repair period. Background DNA damage in untreated (control) seedlings and damage after 1 hour treatment with 30 μ g/ml bleomycin ($t = 0$) is similar in all lines. Defects in DSB repair is manifested by DNA remaining in comet tails (% tail DNA). (B) Kinetics of DSB repair measured over the first 60 min show biphasic kinetics. Percents of DSB remaining were calculated from % tail DNA as described in Comet data evaluation.

els of genome fragmentation were similar to wild type lines. The decreased rates of DSB repair in the silenced plants suggests that AtLIG1 does not simply substitute for AtLIG4 in C-NHEJ, as *atlig4* mutants do not display a reduction in this initial rapid phase of DSB repair. Rather, these results indicate that AtLIG1 is required for the fast rejoining of the majority of DSBs within 10 min after the removal of bleomycin. While AtLIG4 is not required for the rapid initial phase of DSB repair, *atlig4* mutants are hypersensitive to genotoxic agents. This suggests that a subset of DSBs may persist in *atlig4* mutants that cannot be repaired by the rapid, AtLIG1 dependent mechanism. The repair of these DSBs requires the KU and LIG4 mediated slower repair pathway, and failure to eliminate these lesions from the genome results in the IR hypersensitivity of NHEJ mutants. Parallel pathways for end joining have also been identified in mammals, where a LIG4 and KU independent pathway has been characterised [34,35]. The molecular mechanisms of these pathways are beginning to be determined, with one pathway mediated by PARP1 and LIG3 displaying greatest activity in the G2 phase of the cell cycle [35]. *In vitro* studies using human cell extracts showed that both LIG1 and LIG3 can function in microhomology mediated end joining, whereas LIG4 was not required [34]. A significant difference between DSB repair in plants and mammals is the requirement for LIG4 for the rapid repair of DSBs [35] in contrast to the rapid DSB repair observed in *Arabidopsis lig4* mutant lines [22]. This rapid repair pathway is dependent on the structural maintenance of chromosome (SMC)-like proteins MIM and RAD21.1 and analysis of the RNAi lines suggest a role for LIG1 in this DNA repair pathway. Future studies will further delineate the molecular mechanism of this repair pathway in plants.

Conclusion

While *atlig1* null mutants are non-viable, plants with reduced AtLIG1 levels display growth defects, reduced cell size and a greater proportion of cells in S-phase, consistent with roles for *Arabidopsis* DNA ligase 1 in both DNA repair and DNA replication pathways. Additionally *atlig1-RNAi* plants show reduced rates of DNA repair, including a significant delay in the initial rapid phase of DSB repair. These results indicate that AtLIG1 is required for the rapid KU/LIG4 independent repair of DSBs in plants.

Methods

Generation and characterisation of AtLIG1 – RNAi silenced lines

Vector pFGC5941 (TAIR) was used for generation of the silencing constructs [36]. This has a CaMV 35S promoter to drive the expression of the inverted repeat target sequence separated by a 1,352-bp ChsA intron from the petunia Chalcone synthase A gene to stabilize the inverted repeat of the target gene fragment. A 458 bp region of

AtLIG1 was amplified by PCR with primers incorporating XbaI and SmaI sites for the forward primer: 5'-GGTCTAGAGGCGCGCCGATACTGAATAAATTCAGGACATC-3' (LIG1if) and AscI and BamHI sites for the reverse primer: 5'-GGTGGGATCCATTAAATCATCGATATCGTTAGATGTTACAG-3' (LIG1ir). The PCR product was cloned into pFGC5941 in a two-step cloning procedure that integrates the fragment in opposite orientations on either side of the ChsA intron. The RNAi construct was then used to transform *Arabidopsis* allowing plant selection by basta resistance. The extent of AtLIG1 silencing in plants was determined by Western analysis of AtLIG1 protein levels (Fig 1A). Polyclonal antiserum was raised to full length AtLIG1 overexpressed in *E. coli*. AtLIG1 cDNA [36] was cloned into the plasmid pCal-c (Stratagene) and expressed with a C-terminal calmodulin binding protein (CBP) tag. Expression was induced by the addition of isopropylthiogalactoside (1 mM) for 3 h in *E. coli* strain BL21 (DE3) pLysS (Promega). Bacteria were recovered by centrifugation, resuspended in RS buffer (50 mM Tris-Cl pH 7.5, 50 mM NaCl, 2 mM CaCl₂, 5% (v/v) glycerol, 0.1% (v/v) Triton X100) and lysed by freeze thawing and sonication. The extract was cleared by centrifugation at 13 000 g for 10 min, applied to a calmodulin affinity resin (Stratagene) and washed with RS buffer. Purified AtLIG1 protein was eluted in 50 mM Tris-Cl pH 7.5, 50 mM NaCl, 2 mM EGTA, 5% (v/v) glycerol, 0.1% (v/v) Triton X100. Further purification was achieved by preparative SDS-PAGE and coomassie stained bands were electroeluted (BioRad) and used for immunisation. In Western analysis of *Arabidopsis* cell extracts, antiserum to AtLIG1 (but not preimmune) identified a band of the expected molecular weight, detected using alkaline phosphatase coupled anti-sheep IgG secondary antiserum and visualised by incubation with nitroretazolium blue chloride/5-bromo-4-chloro-3-indolyl phosphate (Sigma).

Comet assay

DSBs were detected by a neutral comet assay [37] and SSB by A/N version of comet assay as described previously [20,38]. In brief, approximately 100 mg of frozen tissue was cut with a razor blade in 500 µl PBS+10 mM EDTA on ice and tissue debris removed by filtration through 50 µm mesh funnels (Partec, Germany) into Eppendorf tubes on ice. 30 – 50 µl of nuclei suspension was dispersed in 300 µl of melted 0.5% agarose (GibcoBRL, Gaithersburg, USA) at 40°C. Four 80 µl aliquots were immediately pipetted onto each of two coated microscope slides (in duplicates per slide) on a 40°C heat block, covered with a 22 × 22 mm cover slip and then chilled on ice for 1 min to solidify the agarose. After removal of cover slips, slides were dipped in lysing solution (2.5 M NaCl, 10 mM Tris-HCl, 0.1 M EDTA, 1% N-lauroyl sarcosinate, pH 10) on ice for at least 1 hour to dissolve cellular membranes and remove attached proteins. The whole procedure from

chopping tissue to dipping into lysing solution takes approximately 3 minutes. After lysis, slides were twice equilibrated for 5 minutes in TBE electrophoresis buffer to remove salts and detergents and then electrophoresed at 1 V/cm (app. 20 mA) for 5 minutes. After electrophoresis, slides were dipped for 5 min in 70% EtOH, 5 min in 96% EtOH and air-dried. Comets were viewed in epifluorescence Nikon Eclipse 800 microscope after staining with GelRed stain (Biotium, Hayward, USA) and evaluated by Comet module of Lucia cytogenetics software suite (LIM, Praha, Czech Republic). Wild-type Col0 were used as controls for experiments with *atlig1-RNAiA* and *atlig1-RNAiB*.

Comet data evaluation

The comet slides were coded and blind evaluated. The fraction of DNA in comet tails (% tail-DNA) was used as a measure of DNA damage. Data in this study were measured in at least 3 independent experiments, each starting with newly grown *Arabidopsis* seedlings. In each experiment, the % tail-DNA was measured at 5 time points: 0, 20, 60, 180 and 360 minutes after treatment and in control seedlings without treatment. Measurements included 4 independent gel replicas of 25 evaluated comets totalling at least 300 comets analyzed per experimental point [38]. The percentage of damage remaining as plotted in Figure 4 and 5 after a given repair time (t_x) is defined as:

$$\% \text{ damage remaining } (t_x) = \frac{\text{mean \%T DNA } (t_x) - \text{mean \%T DNA (control)}}{\text{mean \%T DNA } (t_0) - \text{mean \%T DNA (control)}} \times 100$$

Preparation of polyclonal antiserum to Arabidopsis ligase I protein

The ORF of the cloned *Arabidopsis thaliana* ligase 1 cDNA in the pCR2.1 vector (Invitrogen, Leek, The Netherlands) was amplified with primers containing BglII (AGCAAGATCTTAAACAATAGTTATCTTGGGATCA) and NheI (TGCAACATATGGCGTCGACAGTCTCAG) sites at the 5' and 3' ends of the ORF respectively using the proof-reading DNA polymerase *Pfu* (Stratagene, UK). The DNA fragment was introduced at the NdeI site of the pET-11b vector (Calbiochem-Novabiochem, Nottingham, UK) in frame with a 6×His tag coding region, yielding 6×His-ligase 1 *E. coli* BL21(DE3)pLysS was transformed with 6×His-*PHR1* and cultured in LB medium supplemented with 50 mg.l⁻¹ ampicillin until an OD 600 nm of 0.6–1.0 was reached. Expression of 6×His-ligase 1 was induced by the addition of 1 mM isothioisopropylgalactoside and growth continued for 3 h. Bacterial cell extracts were prepared by sonication of 36 ml cells suspended in 50 mM Tris-HCl, pH 7.5, 2 mM EDTA, 0.1% Triton X-100 (1:10 buffer: culture media ratio used) and incubated with 100 µg.ml⁻¹ lysozyme at 30°C for 15 min. The resultant suspension was centrifuged at 10 000 g for 30 min at 4°C. The pelleted proteins were purified by preparative SDS-PAGE using 10% acrylamide gels. The 6×His-AtLIG1 band was excised from the Coomassie-blue stained gel and

destained using several changes of 100 mM Tris-HCl pH 7.0. Protein was electroeluted from the gel slices, mixed with Freud's adjuvant and used to raise antiserum in sheep (Scottish Antibody Production Unit, Carlisle, Scotland).

Western blotting

Proteins were extracted from wheat tissue as described by Pang and Hays (1991). Protein concentrations were determined by the Bio-Rad protein assay (Bio-Rad Laboratories, Hemel Hempstead, UK) using bovine serum albumin (BSA) as a standard. Protein samples were separated by SDS-PAGE (10% gel) and transferred to PVDF membrane (Bio-Rad) for 3 h at 100 V. The blots were probed with anti-ligase 1 antiserum. The immune complexes were detected by alkaline-phosphatase conjugated antisheep IgG (Sigma-Aldrich, Poole, UK) and developed using premixed BCIP/NBT solution (Sigma). Primary and secondary antisera were used at 1/10000 and 1/30000 dilutions respectively.

Flow cytometry

Ploidy analysis was performed using the Cystain absolute P kit (Partec) according to the manufacturer's instructions. Plant nuclei were isolated by chopping fresh leaf material in extraction buffer (Partec) before filtering through a 50 µm membrane. RNase digestion and staining with propidium iodide was followed by analysis using a Becton Dickinson FACSCalibur cytometer.

Cell size

Cell size was determined by brightfield microscopy (Zeiss LSM 510 META Axiovert 200 M inverted confocal microscope) and image analysis using LSM Image browser software (Zeiss).

Abbreviations

NHEJ: non-homologous end joining; SSB: Single strand break; DSB: Double strand break; AtLIG1: *Arabidopsis* DNA ligase I; MMS: Methyl methanesulfonate

Authors' contributions

WMW, JK, CMP and CEW performed the experiments. CEW, CMB and KJA designed the experiments and WMW, KJA, CMB and CEW wrote the manuscript. All authors read and approved the final version of the manuscript.

Acknowledgements

Support from the Royal Society, UK for KJA and CEW is gratefully acknowledged, and work in the labs of CMB and CEW is supported by the UK Biotechnology and Biological Sciences Research Council and the Leverhulme Trust. KJA would like to acknowledge financial support of Ministry of Education, Sport and Youth of the Czech Republic (project IM0505 and LC06004), EU 6FP project COMICS (LSHB-CT-2006-037575). We thank Dr. Georgina Drury for critical reading of the manuscript.

References

- Molinier J, Ries G, Zipfel C, Hohn B: **Transgenerational memory of stress in plants.** *Nature* 2006, **442(7106)**:1046-1049.
- Ries G, Heller W, Puchta H, Sandermann H, Seidlitz HK, Hohn B: **Elevated UV-B radiation reduces genome stability in plants.** *Nature* 2000, **406(6791)**:98-101.
- Zhou BB, Elledge SJ: **The DNA damage response: putting checkpoints in perspective.** *Nature* 2000, **408(6811)**:433-439.
- Wu YQ, Hohn B, Ziemienowicz A: **Characterization of an ATP-dependent type I DNA ligase from Arabidopsis thaliana.** *Plant Mol Biol* 2001, **46(2)**:161-170.
- Kunz BA, Anderson HJ, Osmond MJ, Vonarx EJ: **Components of nucleotide excision repair and DNA damage tolerance in Arabidopsis thaliana.** *Environ Mol Mutagen* 2005, **45(2)**:115-127.
- Johnston LH, Nasmyth KA: **Saccharomyces cerevisiae cell cycle mutant cdc9 is defective in DNA ligase.** *Nature* 1978, **274(5674)**:891-893.
- Petrini JH, Xiao Y, Weaver DT: **DNA ligase I mediates essential functions in mammalian cells.** *Mol Cell Biol* 1995, **15(8)**:4303-4308.
- Babychuk E, Cottrill PB, Storozhenko S, Fuangthong M, Chen Y, O'Farrell MK, Van Montagu M, Inze D, Kushnir S: **Higher plants possess two structurally different poly(ADP-ribose) polymerases.** *Plant J* 1998, **15(5)**:635-645.
- Bentley D, Selfridge J, Millar JK, Samuel K, Hole N, Ansell JD, Melton DW: **DNA ligase I is required for fetal liver erythropoiesis but is not essential for mammalian cell viability.** *Nat Genet* 1996, **13(4)**:489-491.
- Bentley DJ, Harrison C, Ketchen AM, Redhead NJ, Samuel K, Waterfall M, Ansell JD, Melton DW: **DNA ligase I null mouse cells show normal DNA repair activity but altered DNA replication and reduced genome stability.** *J Cell Sci* 2002, **115(Pt 7)**:1551-1561.
- Lakshminpathy U, Campbell C: **Mitochondrial DNA ligase III function is independent of Xrcc1.** *Nucleic Acids Res* 2000, **28(20)**:3880-3886.
- Bray CM, Sunderland PA, Waterworth WM, West CE: **DNA ligase - a means to an end joining.** *SEB Exp Biol Ser* 2008, **59**:203-217.
- Bonatto D, Revers LF, Brendel M, Henriques JA: **The eukaryotic Pso2/Snm1/Artemis proteins and their function as genomic and cellular caretakers.** *Braz J Med Biol Res* 2005, **38(3)**:321-334.
- West CE, Waterworth WM, Jiang Q, Bray CM: **Arabidopsis DNA ligase IV is induced by gamma-irradiation and interacts with an Arabidopsis homologue of the double strand break repair protein XRCC4.** *Plant J* 2000, **24(1)**:67-78.
- Sunderland PA, West CE, Waterworth WM, Bray CM: **An evolutionarily conserved translation initiation mechanism regulates nuclear or mitochondrial targeting of DNA ligase I in Arabidopsis thaliana.** *The Plant Journal* 2006, **47(3)**:356-367.
- De Veylder L, Beeckman T, Beemster GTS, Krools L, Terras F, Landrieu I, Schueren E Van Der, Maes S, Naudts M, Inze D: **Functional Analysis of Cyclin-Dependent Kinase Inhibitors of Arabidopsis.** *Plant Cell* 2001, **13(7)**:1653-1668.
- Sugimoto-Shirasu K, Roberts K: **"Big it up": endoreduplication and cell-size control in plants.** *Current Opinion in Plant Biology* 2003, **6(6)**:544.
- Sugimoto-Shirasu K, Stacey NJ, Corsar J, Roberts K, McCann MC: **DNA Topoisomerase VI Is Essential for Endoreduplication in Arabidopsis.** *Current Biology* 2002, **12(20)**:1782.
- Angelis KJ, Dusinska M, Collins AR: **Single cell gel electrophoresis: detection of DNA damage at different levels of sensitivity.** *Electrophoresis* 1999, **20(10)**:2133-2138.
- Menke M, Chen I, Angelis KJ, Schubert I: **DNA damage and repair in Arabidopsis thaliana as measured by the comet assay after treatment with different classes of genotoxins.** *Mutat Res* 2001, **493(1-2)**:87-93.
- Charles K, Povirk LF: **Action of bleomycin on structural mimics of intermediates in DNA double-strand cleavage.** *Chem Res Toxicol* 1998, **11(12)**:1580-1585.
- Kozak J, West CE, White C, da Costa-Nunes JA, Angelis KJ: **Rapid repair of DNA double strand breaks in Arabidopsis thaliana is dependent on proteins involved in chromosome structure maintenance.** *DNA Repair (Amst)* 2008, **8**:413-419.
- Wade HK, Bibikova TN, Valentine WJ, Jenkins GI: **Interactions within a network of phytochrome, cryptochrome and UV-B phototransduction pathways regulate chalcone synthase gene expression in Arabidopsis leaf tissue.** *The Plant Journal* 2001, **25(6)**:675-685.
- Jiang CZ, Yen CN, Cronin K, Mitchell D, Britt AB: **UV- and gamma-radiation sensitive mutants of Arabidopsis thaliana.** *Genetics* 1997, **147(3)**:1401-1409.
- Kovalchuk I, Molinier J, Yao Y, Arkhipov A, Kovalchuk O: **Transcriptome analysis reveals fundamental differences in plant response to acute and chronic exposure to ionizing radiation.** *Mutat Res* 2007, **624(1-2)**:101-113.
- Kovalchuk I, Titov V, Hohn B, Kovalchuk O: **Transcriptome profiling reveals similarities and differences in plant responses to cadmium and lead.** *Mutat Res* 2005, **570(2)**:149-161.
- Martinez C, Pons E, Prats G, Leon J: **Salicylic acid regulates flowering time and links defence responses and reproductive development.** *Plant J* 2004, **37(2)**:209-217.
- Bleuyard J-Y, Gallego ME, White CI: **Recent advances in understanding of the DNA double-strand break repair machinery of plants.** *DNA Repair* 2006, **5(1)**:1.
- Friesner J, Britt AB: **Ku80- and DNA ligase IV-deficient plants are sensitive to ionizing radiation and defective in T-DNA integration.** *Plant J* 2003, **34(4)**:427-440.
- Li J, Vaidya M, White C, Vainstein A, Citovsky V, Tzfira T: **Involvement of KU80 in T-DNA integration in plant cells.** *PNAS* 2005, **102(52)**:19231-19236.
- van Attikum H, Bundock P, Overmeer RM, Lee LY, Gelvin SB, Hooykaas PJ: **The Arabidopsis AtLIG4 gene is required for the repair of DNA damage, but not for the integration of Agrobacterium T-DNA.** *Nucleic Acids Res* 2003, **31(14)**:4247-4255.
- Heacock M, Spangler E, Riha K, Puizina J, Shippen DE: **Molecular analysis of telomere fusions in Arabidopsis: multiple pathways for chromosome end-joining.** *Embo J* 2004, **23(11)**:2304-2313.
- Gallego ME, Bleuyard JY, Daoudal-Cotterell S, Jallut N, White CI: **Ku80 plays a role in non-homologous recombination but is not required for T-DNA integration in Arabidopsis.** *Plant J* 2003, **35(5)**:557-565.
- Liang L, Deng L, Nguyen SC, Zhao X, Maulion CD, Shao C, Tischfield JA: **Human DNA ligases I and III, but not ligase IV, are required for microhomology-mediated end joining of DNA double-strand breaks.** *Nucl Acids Res* 2008, **36(10)**:3297-3310.
- Wu W, Wang M, Wu W, Singh SK, Mussfeldt T, Iliakis G: **Repair of radiation induced DNA double strand breaks by backup NHEJ is enhanced in G2.** *DNA Repair (Amst)* 2008, **7(2)**:329-338.
- Taylor RM, Hamer MJ, Rosamond J, Bray CM: **Molecular cloning and functional analysis of the Arabidopsis thaliana DNA ligase I homologue.** *Plant J* 1998, **14(1)**:75-81.
- Olive PL, Banath JP: **The comet assay: a method to measure DNA damage in individual cells.** *Nat Protoc* 2006, **1(1)**:23-29.
- Lovell DP, Omori T: **Statistical issues in the use of the comet assay.** *Mutagenesis* 2008, **23(3)**:171-182.

Publish with **BioMed Central** and every scientist can read your work free of charge

"BioMed Central will be the most significant development for disseminating the results of biomedical research in our lifetime."

Sir Paul Nurse, Cancer Research UK

Your research papers will be:

- available free of charge to the entire biomedical community
- peer reviewed and published immediately upon acceptance
- cited in PubMed and archived on PubMed Central
- yours — you keep the copyright

Submit your manuscript here:
http://www.biomedcentral.com/info/publishing_adv.asp



Publikace 3

GMI1, a structural-maintenance-of-chromosomes-hinge domain-containing protein, is involved in somatic homologous recombination in Arabidopsis

Gudrun Böhmendorfer^{1,2,*}, Alexander Schleiffer³, Reinhard Brunmeir^{1,4}, Stefan Ferscha¹, Viktoria Nizhynska¹, Jaroslav Kozák⁵, Karel J. Angelis⁵, David P. Kreil⁶ and Dieter Schweizer¹

¹Gregor Mendel Institute of Molecular Plant Biology, Austrian Academy of Sciences, Dr. Bohr-Gasse 3, 1030 Vienna, Austria,

²Max F. Perutz Laboratories, Center for Molecular Biology, Department of Biochemistry and Cell Biology, University of Vienna, Dr. Bohr Gasse 9, 1030 Vienna, Austria,

³IMP/IMBA Bioinformatics Department, Dr. Bohr-Gasse 7, 1030 Vienna, Austria,

⁴Singapore Institute for Clinical Sciences, A-STAR, 30 Medical Drive, 117609 Singapore,

⁵Institute of Experimental Botany AS CR, Na Karlovce 1, 160 00 Praha 6, Czech Republic, and

⁶Chair of Bioinformatics, Boku University Vienna, 1190 Muthgasse 18, Austria

Received 28 December 2010; revised 3 April 2011; accepted 6 April 2011; published online 20 May 2011.

*For correspondence (fax +43 1 4277 9748; e-mail gudrun.boehmendorfer@gmi.oeaw.ac.at or gudrun.boehmendorfer@univie.ac.at).

SUMMARY

DNA double-strand breaks (DSBs) pose one of the most severe threats to genome integrity, potentially leading to cell death. After detection of a DSB, the DNA damage and repair response is initiated and the DSB is repaired by non-homologous end joining and/or homologous recombination. Many components of these processes are still unknown in *Arabidopsis thaliana*. In this work, we characterized γ -irradiation and mitomycin C induced 1 (GMI1), a member of the SMC-hinge domain-containing protein family. RT-PCR analysis and promoter-GUS fusion studies showed that γ -irradiation, the radio-mimetic drug bleocin, and the DNA cross-linking agent mitomycin C strongly enhance *GMI1* expression particularly in meristematic tissues. The induction of *GMI1* by γ -irradiation depends on the signalling kinase Ataxia telangiectasia-mutated (ATM) but not on ATM and Rad3-related (ATR). Epistasis analysis of single and double mutants demonstrated that ATM acts upstream of *GMI1* while the *atr gmi1-2* double mutant was more sensitive than the respective single mutants. Comet assay revealed a reduced rate of DNA double-strand break repair in *gmi1* mutants during the early recovery phase after exposure to bleocin. Moreover, the rate of homologous recombination of a reporter construct was strongly reduced in *gmi1* mutant plants upon exposure to bleocin or mitomycin C. GMI1 is the first member of its protein family known to be involved in DNA repair.

Keywords: structural maintenance of chromosomes, DNA repair, somatic homologous recombination, meristem, ATPase, genotoxic stress.

INTRODUCTION

Plant genomes are constantly exposed to various kinds of threats. Exogenous stresses can include genotoxic compounds polluting the environment, high energy radiation, or naturally occurring excessive amounts of UV-B radiation. Additionally, intrinsic factors increase the risk of DNA damage. DNA replication is an error-prone process and can lead to change or erosion of genetic information. Photosynthesis and pathogen defence produce reactive oxygen species that can potentially induce oxidative damage of the DNA leading to single- and double-strand breaks (DSBs) (Jackson, 2002;

Shrivastav *et al.*, 2008). DSBs are very dangerous as one unrepaired DSB can be lethal for the cell (Bennett *et al.*, 1993).

Non-homologous end joining (NHEJ) and homologous recombination (HR) are the two main DSB repair mechanisms. NHEJ rejoins the loose ends of a DSB after processing of the damaged site and can, therefore, result in loss of genetic information (Bleuyard *et al.*, 2006). In contrast, HR repairs DSBs using an intact homologous sequence, provided for instance by the undamaged sister chromatid as a

template and is, thereby, less error-prone. The nature of the DNA damage and the current cell cycle stage greatly influence the choice between repair pathways (Barlow *et al.*, 2008; Shrivastav *et al.*, 2008). In S or G2 phase, the presence of sister chromatids can facilitate repair via HR. In contrast, NHEJ may occur during any cell cycle stage, which might be the reason why the rate of HR is low in somatic cells (Puchta, 1999). Deletion or insertions caused by NHEJ in no longer proliferating cells are not detrimental to the viability of an entire plant. It may be more important to quickly repair any damage. In contrast, it is absolutely vital to keep the genetic information in meristems intact, as they are the progenitor cells of all tissues, including the germ line. Meristem cells have the potential to enter the mitotic cycle and thereby to pass stages in which sister chromatids are available as templates for HR. In fact, components of HR are often upregulated in meristematic tissue such as the shoot apex (Lafarge and Montane, 2003; Akutsu *et al.*, 2007; Fulcher and Sablowski, 2009; Yadav *et al.*, 2009).

Structural maintenance of chromosomes (SMC) proteins are very important for DNA repair (Lehmann, 2005; De Piccoli *et al.*, 2006; Kozak *et al.*, 2009; Schubert, 2009). They are conserved chromosomal ATPases and essential in prokaryotes and eukaryotes. While prokaryotes have only one copy of the gene, eukaryotes usually have at least six copies. Their products form three major complexes: SMC1 and SMC3 are the core components of the cohesin complex, which is important for sister chromatid cohesion, chromosome alignment, and segregation in mitosis and meiosis. SMC2 and SMC4 are part of the condensin complex, which is primarily responsible for compaction of the genetic information during cell division (Losada and Hirano, 2005). The SMC5 and SMC6 complex is involved in HR. It is thought to interact with the damaged and the intact sister chromatids during HR, holding them closely together and facilitating repair (De Piccoli *et al.*, 2006; Watanabe *et al.*, 2009). SMC proteins share a canonical structure. Long stretches of intramolecular coiled coils bring the N- and the C-terminus of the molecule together to form an ABC-type ATPase. At the other end of the back-folded protein, the SMC hinge domain resides between the coiled coils (Figure 1). The hinge domain is important for dimerisation (SMC homodimerisation in prokaryotes, and SMC1/SMC3, SMC2/SMC4, SMC5/SMC6 heterodimerisation in eukaryotes). All SMC proteins function in multi-component complexes (Lehmann, 2005).

Recently, two additional proteins containing an SMC hinge domain were described: the murine structural maintenance of chromosomes hinge domain containing 1 (SmcHD1) and Defective in meristem silencing 3 (DMS3) from *Arabidopsis thaliana*. They are members of the structural-maintenance-of-chromosomes-hinge domain-containing (SMCHD) family and are involved in DNA methylation (Blewitt *et al.*, 2005; Kanno *et al.*, 2008). In this work, we characterize γ -irradiation and mitomycin C induced 1 (GMI1),

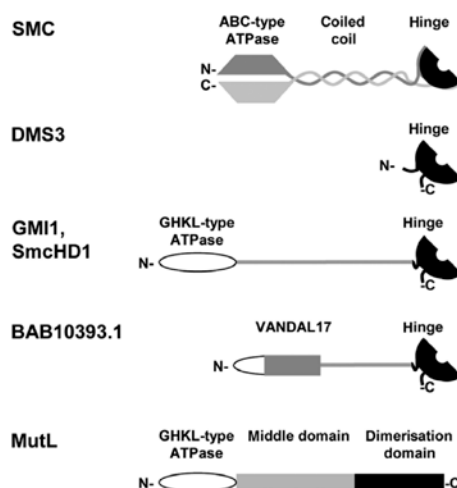


Figure 1. Protein domain architecture of GMI1 and related proteins. GMI1 has the same domain architecture as mammalian SmcHD1. They are related to SMC and DMS3 proteins, as they contain an SMC hinge domain. GMI1 and SmcHD1 contain a GHKL-ATPase domain that is present in for instance MutL. In the theoretical protein BAB10393.1 (encoded by *MOP9.9*) a transposon (VANDAL17) is inserted in the putative GHKL-ATPase. Schemes not drawn to scale.

a so far unidentified member of the SMCHD family in *Arabidopsis thaliana*. We demonstrate that *GMI1* expression is induced by the radio-mimetic drug bleocin and the cross-linking agent mitomycin C, especially in meristematic tissues. Its expression depends on the signalling kinase Ataxia telangiectasia-mutated (ATM) after γ -irradiation. GMI1 contributes to DSB repair and is involved in HR. GMI1 is the first member of the SMCHD protein family implicated in a process other than DNA methylation.

RESULTS

GMI1 is related to SMC and to GHKL-ATPase proteins

The domain arrangement of SMCHD proteins differs from that of canonical SMC proteins. DMS3 consists of a hinge domain flanked by short coiled coil regions (Figure 1; Kanno *et al.*, 2008). The murine SmcHD1 has an N-terminal ATPase domain connected via a structurally undefined linker to the C-terminal SMC-like hinge domain (Figure 1; Blewitt *et al.*, 2008). Aravind and colleagues (Iyer *et al.*, 2008) classified the ATPase domain of SmcHD1 to be a member of the MORC family of Gyrase, Hsp90, histidine kinase, and MutL (GHKL)-ATPases, structurally related to MutL (Figure 1) and topoisomerase VI.

To characterize SMCHD proteins in *Arabidopsis thaliana*, we performed iterative NCBI-BLAST searches with the murine SmcHD1 within the non-redundant protein database. In addition to At3g49250 (=DMS3), we identified two genes:

(i) *GMI1*, which has the same domain architecture as the murine SmcHD1 (GHKL-ATPase, linker, SMC-like hinge; Figure 1); and (ii) a putative pseudogene, *MOP9.9* (putative protein BAB10393.1) in head-to-tail orientation to the *GMI1* locus. A DNA transposon (VANDAL17) is inserted in the locus, disrupting the putative GHKL-ATPase domain of BAB10393.1 (Figure 1; see Data S1 for details).

GMI1 is expressed in the region of the shoot/floral meristems and young flowers

To elucidate in which organs and tissues *GMI1* is required, we analyzed the expression profile of *GMI1* by RT-PCR. The amplified cDNA was detected by Southern blotting to achieve higher sensitivity (Figure 2a). *GMI1* was strongly expressed in seedling suspension culture, closed buds, and

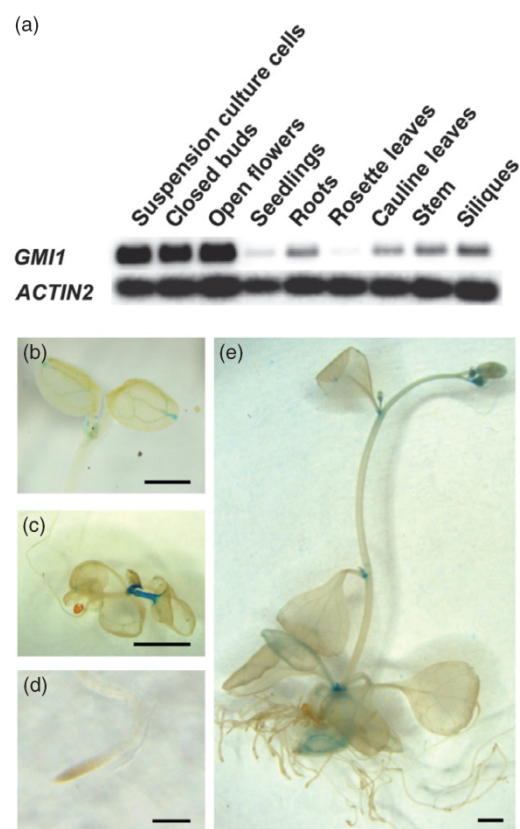


Figure 2. Spatial expression of *GMI1*. (a) Blotted and radio-actively detected RT-PCR products of *GMI1* and *ACTIN2* with RNA from various tissues. (b–e) Histochemical detection of *GMI1*_{pro}:GUS. (b) Young seedling in two-cotyledon stage (bar size = 1 mm). (c) Older seedling with true leaves (bar size = 5 mm). (d) Primary root of a young seedling (bar size = 1 mm). (e) Flowering plantlet (size bar = 1 mm).

open flowers. In all other tissues, *GMI1* mRNA was only detected at low levels. Our data fit the publicly available expression profiles showing low overall expression of *GMI1* under non-stress conditions (Hruz *et al.*, 2008). Additionally, we analyzed the expression of *GMI1*_{pro}:GUS, a fusion of the *GMI1* promoter (–1699 to –3 bp upstream of the ATG) to the β -glucuronidase (GUS) reporter gene *gusA* by histochemical staining (Figure 2b–e). In young seedlings grown on plates, hydrathodes and the vascular system of cotyledons were stained, and occasionally spots in the shoot apical meristem were present (Figure 2b). In older seedlings, the vascular staining was decreased/absent, whereas the basal area of the rosette (broader region of the shoot/floral meristem) gave a strong GUS signal (Figure 2c). In both cases, the root apical meristem was not stained (Figure 2d). In flowering plants, the basal area of the rosette, the shoot/floral meristems, lateral shoot/floral primordia, and young flowers (Figure 2e) were stained. Similar GUS staining patterns were obtained in several independent *GMI1*_{pro}:GUS plant lines.

Genotoxic drugs or γ -irradiation induce the expression of *GMI1*, especially in the shoot and root apical meristems

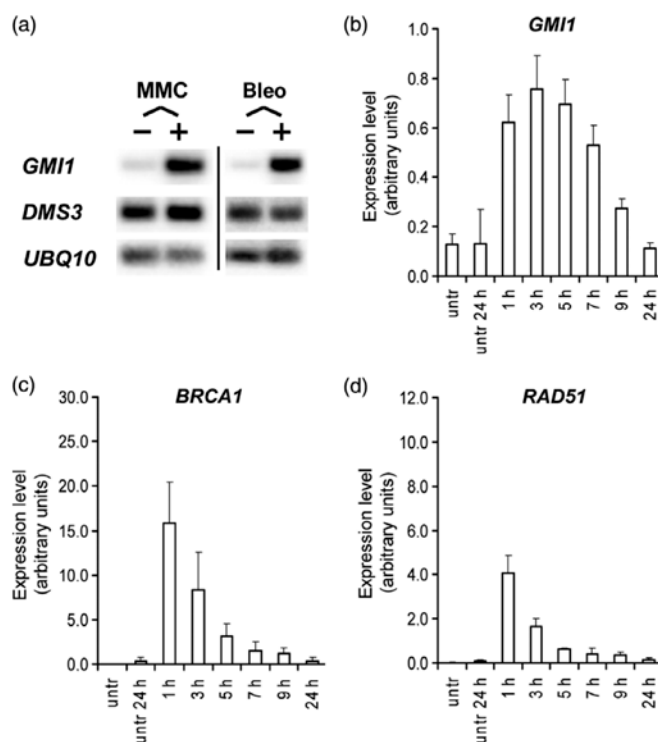
Publicly available expression profiles (Hruz *et al.*, 2008) suggested that *GMI1* is strongly induced after treatment with DNA damaging agents and γ -irradiation. To compare the response of the two SMCHD genes *DMS3* and *GMI1*, we exposed seedlings to mitomycin C for 24 h in liquid medium. Control plants were left untreated. Mitomycin C cross-links DNA strands and induces an S-phase arrest in HeLa cells (Mladenov *et al.*, 2007). We tested the expression of *GMI1*, *DMS3*, and, as an input control, *Ubiquitin 10* (*UBQ10*) by RT-PCR. PCR products were detected by radioactive probes to increase sensitivity. While the expression of *DMS3* remained unaffected, mitomycin C strongly induced the expression of *GMI1* (Figure 3a). To study the effect of the radio-mimetic drug bleocin (a member of the bleomycin family; the drug was reported to cleave double-stranded DNA and to inhibit DNA synthesis (Kandasamy *et al.*, 2009)), seedlings were cultivated with or without bleocin for 3 weeks. Again, *DMS3* mRNA levels were unaltered, whereas *GMI1* was strongly induced (Figure 3a). In short, we observed a distinct response of *DMS3* and *GMI1* to genotoxic stress on the transcriptional level.

Drugs allow a long-term exposure to a DNA damaging agent, while γ -irradiation permits to expose plants to a controlled pulse of genotoxic activity and to study their response. Therefore, we treated plants with γ -irradiation that induces oxidative stress causing DNA single and double-strand breaks as well as damaged bases. We compared the transcriptional profiles of *GMI1* and of two repair genes known to be induced by γ -irradiation (Garcia *et al.*, 2003; Akutsu *et al.*, 2007), namely Breast cancer susceptibility 1 (*BRCA1*; At4G21070) and Ras associated with diabetes protein 51 (*RAD51*; At5G20850). Wild-type plants were

Figure 3. *GMI1* is induced by mitomycin C, bleocin, and γ -irradiation.

(a) Blotted and radio-actively detected RT-PCR with RNA from seedlings treated with mitomycin C (40 μ M) for 24 h or from plantlets exposed to bleocin (100 ng/ml) for 3 weeks. Controls were left untreated.

(b–d) Real-time RT-PCR with RNA from wild-type seedlings at the indicated time-points after irradiation (100 Gy). Control plants were left untreated. Expression levels of (b) *GMI1*, (c) *BRCA1*, and (d) *RAD51* were normalized to *ROC3* expression and are relative. Error bars represent the standard deviation of two biological replicates. Bleo bleocin, MMC mitomycin C.



irradiated with 100 Gy, while control plants were left untreated (0 Gy). RNA was isolated from all samples 1, 3, 5, 7, 9, and 24 h after the pulse and analyzed by real-time RT-PCR. γ -irradiation induced all genes tested including *GMI1* within the first hour after irradiation (Figures 3b–d). The expression of *RAD51* started to decrease within the first 3 h (Figure 3d), confirming published data (Garcia *et al.*, 2003). *BRCA1* showed a similar response profile (Figure 3c). In contrast, *GMI1* mRNA continued to accumulate and began to decline approximately 5 h after the irradiation (Figure 3b). The mRNA concentration of all three genes tested returned to pre-irradiation levels within 24 h.

To visualize where *GMI1* is expressed, we analyzed plants containing the *GMI1_{pro}:GUS* construct after short and chronic treatment with bleocin and mitomycin C and after γ -irradiation (Figure 4). For chronic exposure, seedlings were grown on $\frac{1}{2}$ MS plates with or without the genotoxic drug for 1 week and then stained for GUS-activity. For short treatments, seedlings were grown on $\frac{1}{2}$ MS media for 1 week and then transferred to liquid $\frac{1}{2}$ MS media without (control) or with bleocin or mitomycin C. After incubation for 1.5 and 24 h, plantlets were GUS-stained. In both experimental setups, untreated plants showed no staining except for occasional spot-like GUS signals in developing true

leaves, while bleocin and mitomycin C induced GUS-staining in true leaves and in the regions of the shoot and root apical meristem (Figure 4a). Bleocin-treated plants also showed a GUS-signal in the vasculature close to the root tip which maybe was caused by diffusion of the strong GUS-activity from the root apical meristem. The GUS-signal was strongly induced in developing leaves, the shoot apical meristem, and lateral root primordia 2 h after γ -irradiation, while meristem cells in the primary root were stained 2 h later (Figure 4b).

GMI1 expression was strongly enhanced mainly in proliferating tissues after exposure to genotoxic compounds or γ -irradiation suggesting a role of *GMI1* in these parts of the plant.

The characterized T-DNA insertions should lead to truncated *GMI1* protein lacking the SMC hinge domain

To study the function of *GMI1* and MOP9.9, we characterized T-DNA insertions in both genes (Figure 5). We sequenced the genomic DNA flanking the insertions and isolated homozygous mutants by genotyping (Figures S1 and S2). In *gmi1-1* (SALK_036931) a T-DNA insertion ends with a left T-DNA border in intron 20 of *GMI1* and with another left T-DNA border in intron 21, thereby deleting exon 21 and parts of

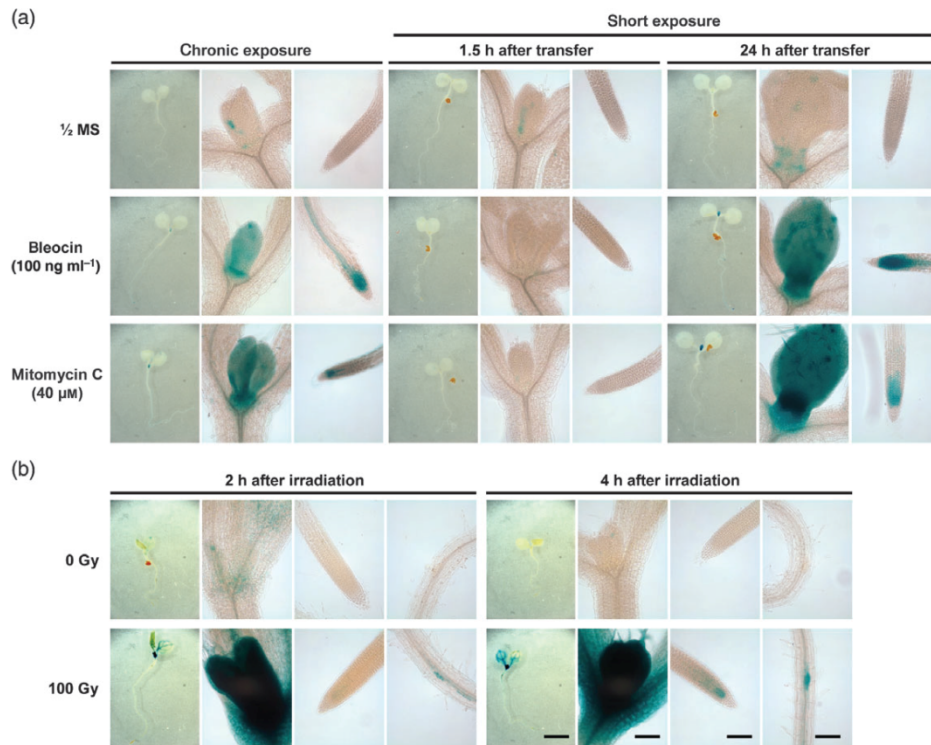


Figure 4. Expression of *GMI1* is induced by bleocin, mitomycin C, and γ -irradiation in meristem-containing tissues. (a, b) Histochemical detection of *GMI1_{pro}::GUS*.

(a) Control plants were grown on media without genotoxins. For chronic exposure, seedlings were grown on media with genotoxic compounds for a week. For time-course experiments, plantlets were transferred from 1/2 MS plates to liquid media with or without supplements. GUS-staining was performed after 1.5 h and 24 h of exposure. (b) Five-day-old seedlings were irradiated (100 Gy). Control plants were not irradiated (0 Gy). Samples were stained 2 and 4 h after irradiation. Size bar = 2.5 mm (whole plant) or 125 μ m (shoot apex, primary and lateral root tip).

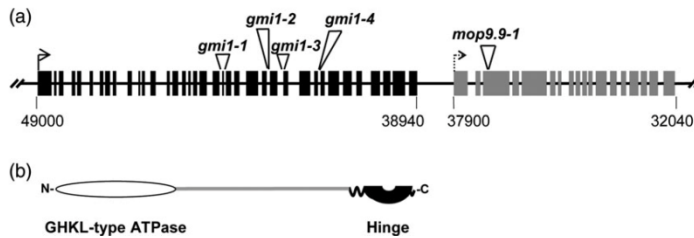


Figure 5. Molecular characterization of *GMI1* and *MOP9.9*.

(a) Genomic organization of *GMI1* (exons are black boxes), *MOP9.9* (putative exons are grey boxes), and T-DNA insertions. Numbers indicate the nucleotide positions on the BAC clone *MOP9*. (b) *GMI1* protein domains are drawn underneath their corresponding exons (irrespective of the introns).

introns 20 and 21 and resulting in a frame-shift. Lines *gmi1-2* (SALK_075103) terminates with two left borders in intron 25 and adds 25 bp of filler DNA. In *gmi1-3* (SALK_091367), the T-DNA deletes the junction between intron 26 and exon 27, while the left and right borders of *gmi1-4* (SAIL_628_B01) are in intron 29. To ensure that the T-DNA insertions are not spliced out, we performed RT-PCR with primers flanking or binding upstream, or downstream of the insertions. We only detected PCR signals with the primers binding upstream of

the T-DNA inserts (Figure S3). In all studied lines, the T-DNA is located in the linker region upstream of the SMC hinge domain, therefore maybe allowing translation of a truncated protein lacking the hinge domain. The hinge domain serves as a dimerisation domain in SMC proteins (Chiu *et al.*, 2004). As GHKL-ATPases and SMC proteins function as dimers (Bilwes *et al.*, 1999; Young *et al.*, 2001; Saecker and Record, 2002), lack of the dimerisation domain most likely renders *GMI1* non functional.

Under standard growth conditions, we did not observe any obvious phenotype in the mutant lines. Though *GMI1* expression was strong in young buds (suggesting a putative role in meiosis), pollen fertility appeared to be normal when analyzed by Alexander staining (data not shown; Alexander, 1969).

The gene *MOP9.9* seems to be a duplication of *GMI1* and is located at a distance of approximately 1 kb to *GMI1* (Figure 5a). We analyzed a T-DNA insertion in *MOP9.9* (*mop9.9-1*; SAIL_831_G04). The T-DNA is inserted in the third exon of *MOP9.9*, thereby disrupting the putative ATPase domain. We were unable to test *mop9.9-1* by RT-PCR as we failed to detect *MOP9.9* expression in all tissues analyzed. Moreover, a transposon replaces part of the putative ATPase domain of *MOP9.9*, therefore *MOP9.9* is most likely a pseudogene.

GMI1 is not a master-regulator of the transcriptional response to γ -irradiation

Members of the SMC and the SMCHD families are involved in transcriptional regulation (Blewitt *et al.*, 2008; Kanno *et al.*, 2008; Wendt *et al.*, 2008; Wierzbicki *et al.*, 2009). To determine whether GMI1 regulates the transcriptional response to γ -irradiation, we used Affymetrix ATH1 microarrays to study the gene expression profiles of *gmi1-1* mutant and wild-type plants both under normal growth conditions and after γ -irradiation. Both the wild-type and the mutant displayed a strong transcriptional response, with hundreds of genes reacting to the radiation (Tables S1 and S2). A comparative screen of the transcriptional responses of *gmi1* and wild-type (Table S3) identified 39 genes with a positive log-odds ratio for showing a different radiation response, i.e. with a different response more likely than not (Table 1). Of these, only two genes were significant at a 5% false discovery rate threshold (*cf.* Methods). One of the two genes was *GMI1* (At5g24280) itself, which was strongly up-regulated in the wild-type but was not expressed in the *gmi1* mutant. The role of the second identified gene, *PDF1.1/LCR67/AFP1* (At1g75830), is not yet understood. It did not respond to radiation in the wild-type but was found down-regulated in the irradiated mutant (from an increased level in the non-irradiated mutant). It is known to be involved in the response to biotic stress (De Coninck *et al.*, 2010). In the remaining candidates, no known DNA repair/DNA damage response genes were identified. Considering the robust transcriptional response of both, wild-type and *gmi1* mutants to γ -irradiation as well as the small number of genes showing a significantly different response, it is unlikely that GMI1 plays a key regulatory role such as has been suggested for SOG1 (*cf.* Supplement and Yoshiyama *et al.*, 2009).

In conclusion, our results do not suggest that GMI1 is a master regulator of the transcriptional response to DNA damage.

GMI1 is induced by γ -irradiation in an ATM-dependent manner

Signalling kinases coordinate the DNA damage response (Cools and De Veylder, 2009). ATM and, to a minor extent, ATR regulate the transcriptional response after γ -irradiation (Culligan *et al.*, 2006; Ricaud *et al.*, 2007), while WEE1 is important for the DNA damage checkpoint (De Schutter *et al.*, 2007). To determine if the induction of *GMI1* depends on any of these three signalling kinases, we performed real-time RT-PCR analysis with RNA isolated from wild-type (Col-0) and mutant (*atm*, *atr*, *wee1*, or *gmi1-1*) plants after γ -irradiation. *GMI1* was not induced in *atm* and not detected in *gmi1-1* plants, as the primers were flanking the T-DNA insertion site in *GMI1* (Figure 6). Hence, the expression of *GMI1* upon γ -irradiation is ATM-dependent and GMI1 acts downstream of ATM.

***atr gmi1-2* double mutants show an increased sensitivity to γ -irradiation**

Our data demonstrated an ATM-dependent induction of *GMI1*, therefore *atm gmi1* double mutants should be as sensitive to γ -irradiation as *atm* single mutants. If GMI1 played a prominent role in the ATM-dependent pathway, mutation of GMI1 should, at least partially, compromise the ATM-dependent response. Hence, *atr gmi1* double mutants should be more sensitive to γ -irradiation than the respective single mutants. To test this hypothesis, we scored the recovery of Col-0 wild-type, *gmi1-1*, *gmi1-2*, *atm*, or *atr* single, and *atm gmi1-2* or *atr gmi1-2* double mutants after γ -irradiation (100 Gy). Three weeks after irradiation, *gmi1* single mutants were only marginally more sensitive to γ -irradiation than the fully recovered wild-type plants (Figure 7 and Figures S4 and S5). *atm gmi1-2* double mutants were recovering to a similar extent as *atm* single mutants (around 10%). Approximately 2/3 of the *atr* plants recovered, while only 1/3 of the *atr gmi1-2* double mutants survived the γ -irradiation (Figure 7 and Figure S4).

Our sensitivity experiment supports the hypothesis that GMI1 acts downstream of ATM. *gmi1-2* disrupts part of the ATM-dependent network enhancing the sensitivity of *atr gmi1-2* double mutants to γ -irradiation compared with the respective single mutants.

GMI1 is important for the repair of DSBs presumably by homologous recombination

To elucidate if GMI1 plays a role in DNA repair, we determined the repair kinetics of DSBs induced by a 1-h pulse of 30 $\mu\text{g ml}^{-1}$ bleocin with neutral comet assay. Wild-type Arabidopsis had nearly repaired all DSBs after 20 min, while *gmi1* mutant plants and the α -kleisin mutant *syn2/rad21.1* still showed a decreased repair capacity at this time-point (Figure 8 and Figure S6). All the DSBs were repaired in every line 3 h after the pulse. As these results indicated that GMI1

Table 1 Differential response of Col-0 wild-type and *gmi1-1* to γ -irradiation

ID	WT, 0 Gy	WT, 100 Gy	<i>gmi1</i> , 0 Gy	<i>gmi1</i> , 100 Gy	q	B	A	M	Short description (see Supporting Information for more details)
AT5G24280	2.5, 1.9, 2.3	10.0, 10.9, 10.5	1.7, 1.3, 1.2	1.4, 1.6, 1.3	0.0002%	7.9	3.9	-8.1	gamma-irradiation and mitomycin c induced 1 (GMI1)
AT1G75830	2.1, 1.8, 1.6	3.5, 1.7, 2.1	5.4, 5.2, 5.9	2.4, 2.2, 3.0	1	2.8	3.0	-3.2	Low-molecular-weight cysteine-rich 67 (LCR67)/Plant defensin 1.1 (PDF1.1)/Cysteine-rich antifungal protein 1 (AFP1)
AT3G56250	1.8, 1.7, 1.9	4.6, 4.6, 4.6	3.7, 1.6, 1.7	3.5, 3.3, 3.5	1	2.1	2.9	-1.1	Unknown protein
AT2G36480	6.2, 6.2, 6.3	6.8, 6.9, 6.7	6.0, 6.4, 6.5	6.3, 6.0, 5.5	1	1.6	6.4	-1.0	Zinc finger (C2H2-type) family protein, similar to PCF11P-similar protein 4 (PCFS4) AT4G04885
AT4G19600	6.4, 6.3, 6.4	6.3, 7.1, 7.1	6.1, 6.2, 6.1	7.3, 5.6, 5.7	1	1.7	6.3	-1.1	Cyclin-T1-4 (CYCT14)
AT2G20020	7.7, 7.6, 7.6	7.9, 7.9, 7.6	7.6, 7.1, 7.5	7.8, 6.4, 6.3	1	1.6	7.3	-1.2	CRS2-associated factor 1 (CAF1; RNA splicing factor)
AT1G20800	1.6, 1.6, 1.7	2.0, 1.5, 1.5	1.3, 1.4, 1.4	1.1, 2.2, 2.2	1	1.5	1.7	0.9	Pseudogene of F-box family protein, similar to F-box family protein AT1G20795
AT1G22060	6.2, 6.3, 6.1	7.3, 8.3, 7.6	6.2, 6.4, 6.2	6.4, 5.9, 6.8	1	1.4	6.6	-1.2	Hypothetical protein similar to F-box family protein AT1G22000
AT4G17030	6.0, 5.6, 5.5	4.9, 3.7, 3.3	5.3, 5.6, 5.3	5.1, 4.5, 5.5	1	1.5	5.0	1.8	Arabidopsis thaliana expansin-like B1 (ATEXLB1)
AT3G57540	3.6, 3.9, 3.5	6.2, 6.4, 6.4	5.3, 3.9, 3.9	4.8, 6.4, 5.2	1	1.4	4.8	-1.5	Remorin family protein, similar to remorin family protein AT2G41870
AT2G40475	7.7, 7.6, 7.6	8.0, 8.1, 7.9	7.7, 7.8, 7.8	7.3, 8.2, 7.2	1	1.3	7.7	-0.8	Unknown protein
AT4G26660	2.4, 2.7, 2.5	1.2, 1.2, 1.1	1.9, 2.0, 2.5	2.1, 1.4, 1.9	1	1.3	1.9	1.2	Unknown protein similar to unknown protein AT5G55520, contains a kinesin-related region
AT2G40610	5.9, 5.9, 6.1	4.2, 4.2, 4.3	4.8, 8.3, 7.8	4.8, 5.1, 4.9	1	0.9	5.7	-1.1	Arabidopsis thaliana expansin A8 (ATEXPA8)
AT5G01740	7.8, 7.7, 7.6	8.1, 8.0, 7.9	7.7, 7.9, 8.1	7.0, 8.3, 6.9	1	1.0	7.6	-1.1	Unknown protein, similar to Arabidopsis thaliana wound-induced protein 12 (ATWI-12)/Senescence associated gene 20 (SAG20, AT3G10985)
AT4G33620	2.8, 2.5, 2.7	4.7, 5.0, 3.7	2.8, 2.7, 3.1	3.5, 3.3, 3.6	1	1.0	3.4	-1.4	Ulp1 protease family protein, similar to Ulp1 protease family protein AT1G09730
AT5G55700	4.5, 4.6, 4.7	5.6, 6.3, 5.2	5.0, 5.0, 4.4	4.9, 5.0, 5.0	1	0.8	5.0	-1.0	beta-amylase 4 (BAM4)/beta-amylase 6 (BMY6)
AT5G47810	5.3, 5.5, 5.4	6.1, 6.1, 6.1	5.5, 5.7, 5.6	5.5, 5.9, 5.4	1	0.8	5.7	-0.8	Phosphofructokinase 2 (PFK2)
AT1G18950	4.6, 4.7, 4.6	4.6, 5.8, 5.3	4.3, 4.2, 4.3	5.0, 4.1, 3.5	1	0.4	4.6	-0.9	Aminoacyl-tRNA synthetase family, similar to unknown protein AT5G25580
AT1G51140	3.1, 5.0, 5.3	2.9, 2.7, 2.9	3.0, 3.7, 5.2	2.8, 3.3, 2.9	1	0.7	3.6	1.5	Basic helix-loop-helix (bHLH) family protein, similar to basic helix-loop-helix (bHLH) family protein AT2G42280
AT1G47940	1.8, 1.8, 1.9	1.7, 1.4, 1.7	1.5, 1.5, 1.7	1.5, 2.2, 2.5	1	0.6	1.8	0.9	Hypothetical protein, similar to oxidoreductase, 2OG-FelI) oxygenase family protein AT3G18210
AT4G22050	1.1, 0.9, 0.9	0.5, 0.8, 0.9	1.1, 0.8, 0.9	1.8, 1.3, 2.1	1	0.7	1.1	1.1	Aspartyl protease family protein, similar to aspartic-type endopeptidase AT1G69100
AT5G49580	6.4, 6.7, 6.7	6.4, 7.5, 7.5	6.3, 6.7, 6.2	6.2, 6.2, 6.3	1	0.7	6.7	-1.0	DNAJ heat shock N-terminal domain-containing protein, similar to DNAJ heat shock N-terminal domain-containing protein AT1G16880
AT1G20120	1.5, 1.5, 1.7	2.5, 4.0, 3.9	1.9, 1.6, 1.8	1.7, 2.9, 2.6	1	0.6	2.4	-1.4	Family II extracellular lipase, putative, similar to hydrolase, acting on ester bonds/lipase AT1G20132
AT3G14980	4.9, 4.1, 3.9	5.4, 6.0, 4.4	4.4, 4.7, 4.3	4.4, 4.5, 4.4	1	0.4	4.6	-1.2	PHD finger transcription factor, putative, similar to DNA binding AT1G05380
AT2G34920	3.9, 3.9, 4.0	6.6, 6.7, 6.8	5.1, 3.2, 3.9	4.6, 6.2, 5.7	1	0.3	5.1	-1.0	Embryo sac development arrest 18 (EDA18)
AT4G02730	5.3, 5.6, 5.3	6.0, 5.6, 5.4	5.4, 5.7, 5.6	4.4, 5.5, 3.9	1	0.4	5.3	-1.4	Transducin family protein/WD-40 repeat family protein (similar to transducin family protein/WD-40 repeat family protein AT3G49660)
AT4G22610	2.4, 2.7, 2.8	2.1, 2.1, 2.3	2.4, 2.5, 2.6	3.1, 2.9, 2.4	1	0.4	2.6	0.9	Protease inhibitor/seed storage/lipid transfer protein (LTP) family protein, similar to LTP family protein AT4G22520

Table 1 (Continued)

ID	WT, 0 Gy	WT, 100 Gy	<i>gmi1</i> , 0 Gy	<i>gmi1</i> , 100 Gy	<i>q</i>	<i>B</i>	<i>A</i>	<i>M</i>	Short description (see Supporting Information for more details)
AT2G18920	2.8, 2.4, 2.3	1.8, 1.9, 1.8	2.1, 1.9, 2.3	2.2, 2.5, 3.0	1	0.4	2.2	1.1	Hypothetical protein
AT2G34740	3.2, 2.9, 3.0	2.4, 2.6, 2.4	3.4, 2.4, 2.4	3.2, 3.1, 2.9	1	0.4	2.8	1.1	Catalytic/protein serine/threonine phosphatase, similar to putative protein phosphatase 2C AT4G28400
AT1G75050	1.7, 1.8, 1.8	1.5, 1.4, 1.5	1.8, 1.6, 1.7	2.1, 2.1, 2.1	1	0.4	1.8	0.7	Hypothetical protein, similar to Arabidopsis thaumatin-like protein 3 (ATLP-3) AT1G75030
AT3G49210	5.6, 5.9, 5.7	6.1, 7.2, 6.4	6.0, 6.1, 5.3	5.5, 5.5, 5.6	1	0.2	5.9	-1.1	Hypothetical protein similar to unknown protein AT3G49200
AT2G45910	4.2, 4.4, 4.1	5.2, 5.8, 5.7	4.3, 4.4, 4.3	4.6, 5.0, 4.7	1	0.3	4.8	-1.0	Protein kinase family protein/U-box domain-containing protein (similar to protein kinase family protein/U-box domain-containing protein AT3G49060)
AT1G04790	5.6, 5.4, 5.5	5.9, 6.4, 5.6	5.7, 5.6, 5.9	5.7, 5.0, 5.0	1	0.2	5.6	-1.0	Zinc finger (C3HC4-type RING finger) family protein (similar to SDIR1 AT3G55530)
AT1G19340	1.9, 2.9, 3.0	2.2, 2.1, 2.0	2.3, 2.7, 2.3	2.7, 2.5, 2.5	1	0.2	2.5	0.9	Methyltransferase MT-A70 family protein
AT4G22970	2.6, 2.6, 2.6	3.5, 3.8, 3.1	2.9, 2.7, 2.1	2.7, 2.7, 2.9	1	0.1	2.9	-0.8	Arabidopsis homolog of separase ESP (AESP)/Radially swollen 4 (RSW4)/separase
AT2G01870	8.8, 8.7, 8.6	8.4, 7.5, 8.3	8.8, 8.5, 8.5	8.6, 7.0, 7.3	1	0.1	8.2	-0.9	Hypothetical protein
AT5G66850	4.1, 4.3, 4.1	5.5, 5.7, 4.8	3.9, 4.1, 4.1	4.3, 4.2, 4.8	1	0.1	4.5	-1.0	replace: Mitogen-activated protein kinase kinase kinase 5 (MAPKKK5)
AT4G01460	2.7, 3.1, 3.6	4.7, 5.7, 5.2	3.6, 3.2, 3.5	3.9, 4.2, 4.2	1	0.1	3.9	-1.4	Basic helix-loop-helix (bHLH) family protein, similar to bHLH family protein AT3G61950
AT5G23390	7.3, 7.2, 7.4	8.2, 9.2, 8.4	7.5, 7.6, 7.3	7.6, 7.9, 7.4	1	0.04	7.7	-1.0	Hypothetical protein (similar to unknown protein AT1G48840)
AT2G19650	6.5, 6.6, 6.4	6.8, 7.5, 7.1	6.4, 6.6, 6.4	6.1, 6.4, 5.8	1	-0.1	6.5	-0.9	DC1 domain-containing protein, similar to DC1 domain-containing protein AT2G04680
AT2G29770	1.5, 1.3, 1.5	1.7, 1.0, 1.3	1.1, 1.2, 1.2	1.7, 2.0, 2.0	1	-0.1	1.5	0.8	F-box/LRR-repeat/kelch-repeat protein, similar to kelch repeat-containing F-box family protein AT2G29780
AT4G14820	3.1, 3.3, 3.3	3.2, 2.7, 2.9	2.7, 2.7, 2.8	3.2, 3.6, 3.0	1	-0.1	3.0	0.8	Pentatricopeptide (PPR) repeat-containing protein, similar to PPR-containing protein AT2G29760
AT1G65280	7.2, 7.1, 6.8	7.2, 8.0, 7.5	7.0, 7.0, 7.0	7.0, 6.2, 6.4	1	-0.2	7.0	-1.0	Heat shock protein binding, similar to DNAJ heat shock N-terminal domain-containing protein AT5G22080
AT4G21390	2.3, 2.5, 2.2	3.0, 3.6, 3.2	2.5, 2.6, 2.5	2.4, 2.5, 4.3	1	-0.2	2.7	-0.9	B120 (protein kinase, serine/threonine kinase activity)

For our screen comparing the radiation response of wild-type and *gmi1-1* mutant, this table lists the 44 top-ranked genes most likely to show a different response. We display the response difference *M* and the average expression *A* next to the normalized signals for three independent replicates. We provide two measures of evidence strength: a *q*-value giving the false discovery rate for the list of genes up to a particular row, and a log-odds ratio *B*. Taking the list of genes with *q* < 5%, for example, guarantees a false discovery rate < 5% for that list. Genes with a positive log-odds ratio are more likely to have a different radiation response than not. The 39 such candidates with *B* > 0 are shown in bold in this table together with the next 5 genes just not making the threshold. See Experimental Procedures for analysis details. Table S3 provides a version of this table that includes all profiled genes. Tables S1 and S2 give full tables of the radiation responses of wild-type and *gmi1-1* plants. Microarray data have been deposited at GEO (acc. no. GSE23892).

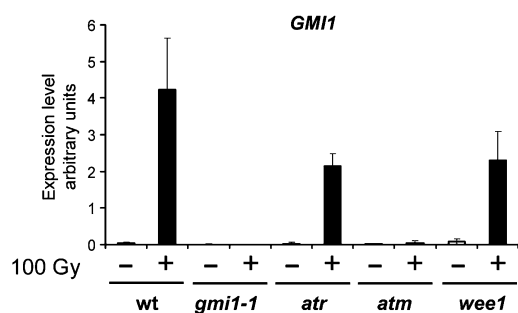


Figure 6. *GMI1* is induced in an ATM-dependent manner 1.5 h after γ -irradiation.

Real-time RT-PCR wild-type and mutant plants. Control plants (white bars) were left untreated. Irradiated plants (black bars) were harvested 1.5 h after γ -irradiation (100 Gy). Signals were normalized to *ROC3* expression and are relative. The standard deviation was obtained from two biological replicates.

is important for DSB repair, we analyzed the behaviour of the recombination reporter line 1445 Col (Tinland *et al.*, 1994; Lucht *et al.*, 2002; Fritsch *et al.*, 2004) in mutant and wild-type backgrounds. The Arabidopsis line 1445 Col contains two partially overlapping *GUS* fragments in inverted orientation separated by a linker. The overlap of several hundred base pairs between *GUS* fragments allows the reconstitution of a functional 35S_{pro}:*GUS* reporter gene by HR. Expression of the 35S_{pro}:*GUS* reporter results in blue spots in the plant tissue after GUS-staining. Hence, each blue spot represents one independent HR event. We crossed the reporter line with *gmi1-1*, *gmi1-4*, and *mop9.9-1*. All T-DNA insertions and the reporter construct were in Col-0 background. Without genotoxic treatment, the recombination rates were not significantly different among all four lines ($P > 0.1$; Table 2), while bleocin or mitomycin C treatment significantly increased the number of recombination events in each line ($P < 0.01$). For both treatments, the number of GUS-spots was not significantly different between *mop9.9-1* and wild-type ($P > 0.1$), while it was different when we compared the two *gmi1* mutants to either *mop9.9-1* or wild-type ($P < 0.01$). As the bleocin and mitomycin C experiments were not done in parallel, different media batches could contribute to the observed variation in the baseline recombination rate of plants not exposed to stress. The seed stock was identical in both experiments. Theoretically, storage conditions could contribute to an altered homologous recombination rate. To minimize potential variation contributed by the media, we used the same media batch for plates with or without genotoxin and did the replicates of each experiment in parallel. For both treatments, the fold induction observed in *gmi1* mutants was about half compared with *mop9.9-1* mutants and wild-type. These data demonstrate that *GMI1* is required for HR stimulated by bleocin or mitomycin C.

DISCUSSION

GMI1 is important for homologous recombination

Cells have complex protein networks to repair DNA damage. First, the damage is perceived by detector proteins. Next, this information is passed on by transmitter proteins to activate and coordinate the action of effector proteins. They are responsible for a transient arrest of the cell cycle and repair of the DNA damage. The activity of repair genes is often regulated on the transcriptional level (Lafarge and Montane, 2003; Culligan *et al.*, 2006). According to publicly available databases (Winter *et al.*, 2007) UV-B does not stimulate *GMI1* expression, while our data demonstrates that *GMI1* expression is induced by DSBs and oxidative damage-causing agents such as bleocin, the DNA-cross-linking compound mitomycin C, and γ -irradiation. These results indicate that *GMI1* might be important for the repair of DSBs.

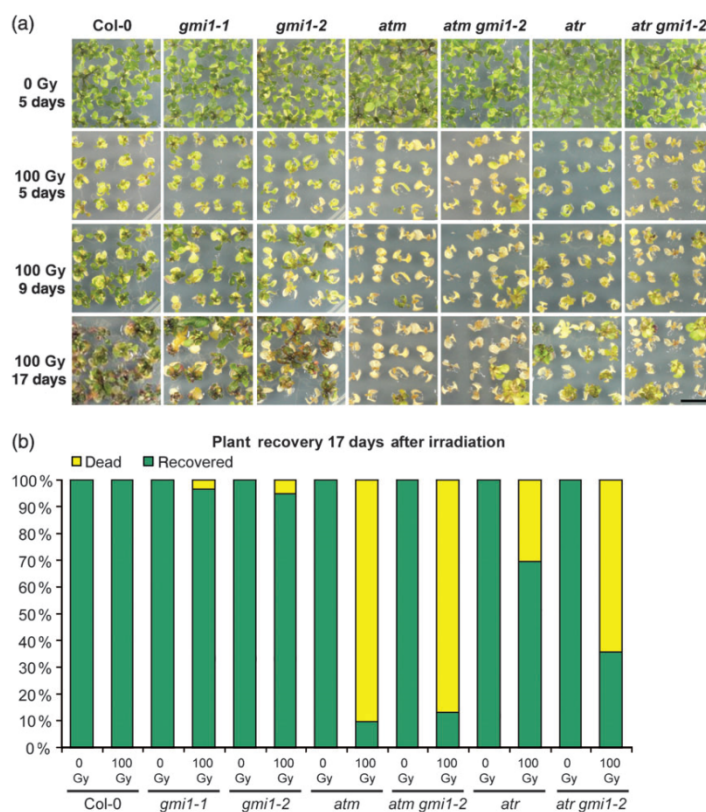
The activity of the signalling kinases ATM and ATR mainly regulates the complex DNA damage and repair response to γ -irradiation (Garcia *et al.*, 2003; Culligan *et al.*, 2004). Our work and the work of others (Culligan *et al.*, 2006) demonstrate that the expression of *GMI1* is ATM-dependent. Furthermore, *atm gmi1-2* double mutants are similarly sensitive to γ -irradiation as *atm* single mutants. The enhanced sensitivity of *atr gmi1-2* double mutants to γ -irradiation supports the hypothesis that functional *GMI1* is important in the ATM-dependent pathway of the DNA damage response. *GMI1* transcripts (detected by real-time RT-PCR) persist over a longer time-period after γ -irradiation than the transcripts of the two repair genes *BRCA1* and *RAD51*. As most DSBs were reported to be repaired within the first hour after damage (Kozak *et al.*, 2009; Takahashi *et al.*, 2010), *GMI1* activity might also be required at later stages of the DNA damage response.

The transcriptional response to γ -irradiation is mainly regulated by ATM and not ATR (Culligan *et al.*, 2006; Ricaud *et al.*, 2007). Moreover, the transcription factor SOG1 has been reported to induce transcription of repair and DNA damage response genes including *GMI1* (Yoshiyama *et al.*, 2009). Considering the robust transcriptional response of wild-type and *gmi1-1* plants to γ -irradiation as well as the small number of genes showing a significantly different response in our comparative screen, it is unlikely that *GMI1* plays a key regulatory role such as has been suggested for SOG1. *GMI1* most likely acts as an effector protein important for HR.

In principle, DSBs are repaired by NHEJ or HR. NHEJ seems to be the predominant repair mechanism in plants, consisting mainly of differentiated, no longer dividing cells (Puchta, 1999). The consequences inflicted by potential loss of genetic information seem to be less severe in these cells, as their genetic information will not be passed on to progeny cells. NHEJ compensating for a decreased efficiency of HR

Figure 7. *atr gmi1-2* double mutants show enhanced sensitivity to γ -irradiation.

(a) Pictures were taken 5, 9 and 17 days after γ -irradiation (100 Gy). Control plants were not irradiated. *atr gmi1-2* double mutants are more sensitive to γ -irradiation than the respective single mutants while *atr gmi1-2* mutants are as sensitive as *atr* mutants. All pictures are the same magnification (size bar = 1 cm). (b) Percentage of recovered and dead plants 17 days after γ -irradiation. On average 60 plants were counted per sample.



in *gmi1* mutants could explain why *gmi1* plants have no obvious phenotype under normal growth conditions and a rather mild sensitivity to γ -irradiation. Many components of somatic HR have an additional role in meiosis. Plants deficient in these factors are often (at least partially) sterile (Gallego *et al.*, 2001; Bundock and Hooykaas, 2002; Schuermann *et al.*, 2005). Even though we detected *GMI1* expression in young flowers by RT-PCR and in *GMI1_{pro}:GUS* plants by staining, we did not observe any obvious reduction in fertility in *gmi1* mutants suggesting that *GMI1* is either not involved in meiosis or an unknown factor compensates for the loss of *GMI1*.

In meristematic cells, maintaining sequence integrity is vital and HR via sister chromatids seems to be the repair mechanism of choice. Our data show that *GMI1* is most strongly expressed in young dividing tissues and, to a lesser degree, in the entire plant body. Genotoxic treatment induced *GMI1* expression in primary and lateral root meristems and intensified the signal in the shoot apical meristem. The comet assay demonstrated that *GMI1* is important for rapid DSB repair which is thought to mainly depend on SMC proteins and the activity of Ligase 1 (LIG1;

Kozak *et al.*, 2009; Waterworth *et al.*, 2009)). The GUS-spot reporter assay assigns *GMI1* a role in HR upon exposure to bleccin or mitomycin C, as the recombination rate decreased by at least half compared with the wild-type. This reduction is not as pronounced as reported for *rad51c* mutants, a component important for strand exchange in HR (Abe *et al.*, 2005) and is comparable with the value observed for *mim* (*smc6b*) mutants using a similar assay (Mengiste *et al.*, 1999).

Recent publications demonstrate the importance of the SMC1/SMC3 and the SMC5/SMC6 complexes in DNA repair (Kozak *et al.*, 2009; Watanabe *et al.*, 2009; Takahashi *et al.*, 2010), as they could facilitate HR by keeping the damaged and the correct sister chromatids closely together (De Piccoli *et al.*, 2006; Heidinger-Pauli *et al.*, 2008). According to its protein domains (an ATPase combined with an SMC hinge domain separated by a linker), *GMI1* resembles SMC proteins. Hence, *GMI1* might act in a similar way as SMC proteins in HR. The reduced recombination rate in *gmi1* mutants (lacking the SMC hinge) suggests that this domain is important for *GMI1* function. As the hinge serves as a dimerisation domain in SMC proteins (Chiu *et al.*, 2004),

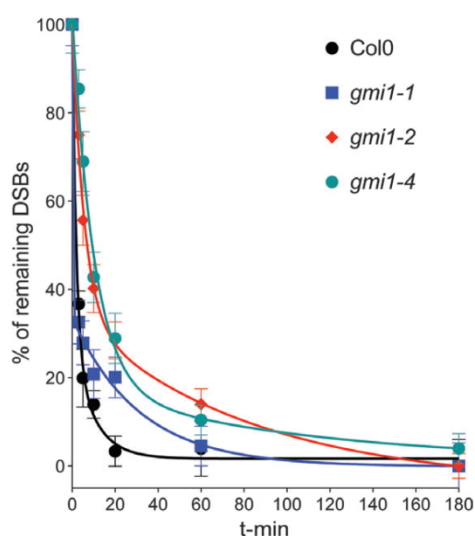


Figure 8. Repair kinetics of bleocin induced DNA double strand breaks in Col-0, *gmi1-1*, *gmi1-2*, and *gmi1-4*. Fractions of remaining DSBs were calculated for 0, 3, 5, 10, 20, 60 and 180 min repair time points after treatment with $30 \mu\text{g ml}^{-1}$ bleocin for 1 h. The maximum damage was normalized as 100% at $t = 0$ for all lines. The repair kinetic parameters were calculated with the Prism five program. The mean percentage of DNA in the comet tail for 300 comets for each concentration point is shown (error bars—standard error). All used *gmi1* lines show a defect in DSB repair. The repair kinetics of *gmi1-2* is similar to that of *atrad21.1* (Figure S6).

we propose a working hypothesis in which GMI1 acts as a dimer, presumably as part of a higher molecular complex. ATP-binding and hydrolysis are essential in ABC-ATPases such as SMC proteins (Hirano, 2002; Losada and Hirano,

2005) and in GHKL-ATPases such as gyrases (Stock, 1999) for conformational changes. Future biochemical studies and protein interaction experiments might help to unravel the putative interaction network of GMI1. Moreover, it would be interesting if the mammalian homologue of GMI1, SmcHD1, plays a role in DNA repair/DNA damage response besides the already reported function in X-inactivation.

EXPERIMENTAL PROCEDURES

Plant material and growth conditions

Plants were grown on soil or on $\frac{1}{2}$ MS media (2.21 g Murashige & Skoog medium including B5 vitamins (Duchefa, <http://www.duchefa.com/>), 10 g L^{-1} D-sucrose (Applichem, <http://www.applichem.com/>); pH 5.8; 6 g L^{-1} Plant Agar (Duchefa) for solid media) in 16 h light (approximately $90 \mu\text{mol m}^{-2} \text{ sec}^{-1}$) and 8 h darkness. Seeds were sterilized in 3% Calcium-hypochlorite (Roth, <http://www.lactan.at/>) and washed in dH_2O . Information on plant material and genotyping conditions is listed in the Data S1.

Cloning of GMI1_{pro}:GUS

The putative *GMI1* promoter was amplified by PCR (KOD Hifi DNA polymerase, Novagen) from Col-0 DNA using the primers SF_54 (CTGCAGATGTCTTATCTTTCCGAATG) and SF_55 (CCCGGGAACTGATTAACCTTTTGAATTAC). Purified PCR products (Nucleo-Spin extract kit II; Macherey-Nagel, <http://www.mn-net.com/>) were subcloned (pCR2.1; Invitrogen, <http://www.invitrogen.com/>) after poly-A-adding. A *SmaI*-*PstI* fragment was introduced in the *SmaI*-*PstI* digested pCBK04 vector (provided by Karel Riha), replacing the 35S promoter with the putative *GMI1* promoter.

RT-PCR

For spatial and temporal analysis of *GMI1* expression by blotted RT-PCRs, $3 \mu\text{g}$ of RNA (SV Total RNA Isolation System; Promega, <http://www.promega.com/>) were reverse-transcribed (primer GAC-CACGCGTATCGATGTCGACT(16)V; Revertaid, Fermentas, <http://www.fermentas.com/>). The diluted cDNA was amplified by PCR (see Data S1) and blotted on a nylon membrane (Hybond-N; Amersham

Table 2 The rate of somatic homologous recombination of line 1445 Col in *gmi1* mutants is reduced compared with wild-type and *mop9.9-1* plants

	GUS-spots per plant (avg. \pm st dev.)			
	Col-0	<i>gmi1-1</i> (–/–)	<i>gmi1-4</i> (–/–)	<i>mop9.9-1</i> (–/–)
0 ng ml^{-1} bleocin	0.76 ± 0.21	0.75 ± 0.04	0.56 ± 0.12	0.67 ± 0.12
100 ng ml^{-1} bleocin	14.54 ± 0.65	5.42 ± 1.52	4.47 ± 0.67	16.5 ± 2.18
Fold induction	approximately 19-fold	approximately 7-fold	approximately 7-fold	approximately 24-fold
0 μM MMC	0.09 ± 0.05	0.11 ± 0.06	0.07 ± 0.02	0.11 ± 0.06
40 μM MMC	2.58 ± 0.68	1.40 ± 1.02	1.06 ± 0.52	3.43 ± 0.94
Fold induction	approximately 29-fold	approximately 13-fold	approximately 15-fold	approximately 30-fold

Line 1445 Col contains two partially overlapping *GUS* fragments in inverted orientation separated by a linker. Somatic homologous recombination reconstitutes a functional *GUS*-gene manifesting as a blue spot by GUS-staining. After growth on medium with or without genotoxic compounds plants were GUS-stained and the number of GUS-spots per plant was determined. On $\frac{1}{2}$ MS, the number of GUS-spots was comparable in mutant and wild-type lines (P -value > 0.1). In every plant line, genotoxic treatment induced the number of GUS-spots significantly compared with the untreated controls (P -value < 0.01). The difference in the number of GUS-spots between wild-type and *mop9.9-1* was not significant (P -value > 0.1), while it was significant for both *gmi1* mutant lines compared with either wild-type or *mop9.9-1* (P -value < 0.01). The average (avg.) and the standard deviation (stdev.) were calculated from two technical replicates for the bleocin-experiment and three biological replicates for the mitomycin C (MMC) experiment. We applied Student's t -test (Microsoft Excel™) for the calculation of the P -values.

Biosciences; Ausubel, 2001). Hybridization was performed at 65°C with ^{32}P labelled probes (Hexanucleotide Mix, Roche; Ausubel, 2001). Data were gained by phospho-imaging (Molecular Imager FX, Bio-Rad and Quantity One, Bio-Rad, <http://www.bio-rad.com/>). For chronic bleocin treatment, seedlings were cultivated on $\frac{1}{2}$ MS media with 100 ng ml^{-1} bleocin (Calbiochem, <http://www.calbiochem.com/>) for 3 weeks. To expose plantlets to mitomycin C, plants were grown on $\frac{1}{2}$ MS media for 2 weeks and transferred to liquid $\frac{1}{2}$ MS media with $40\text{ }\mu\text{M}$ mitomycin C (Duchefa) for 24 h.

To determine *GMI1* induction after γ -irradiation by real-time RT-PCR, wild-type, *atm-2*, *atr-2*, *wee1-1* and *gmi1-1* seeds were grown on $\frac{1}{2}$ MS plates in continuous light ($100\text{ }\mu\text{mol m}^{-2}\text{ sec}^{-1}$; Percival CU-36/L4, USA) for 5 days and then irradiated (100 Gy; Co-60-gamma source Gamma-cell 220, Nordion International, Canada; Department of Nutritional Sciences, University of Vienna, Althanstrasse 14, 1090 Vienna, Austria). The dose rate was $27\text{--}34\text{ Gy min}^{-1}$. RNA was isolated from plants frozen in liquid nitrogen (SV Total RNA Isolation System; Promega) and $1\text{ }\mu\text{g}$ of total RNA reverse transcribed (iScript cDNA Synthesis Kit; Bio-Rad). Quantitative PCRs ($2 \times$ SensiMix Plus SYBR Kit & Fluorescein (PEQLAB); IQ5 iCycler Bio-Rad) were analyzed with the IQ5 optical system software (Bio-Rad). Experiments were performed in triplicates. For primers and PCR conditions see Data S1.

To test if *gmi1-1*, *gmi1-2*, *gmi1-3*, and *gmi1-4* fail to produce full-length *GMI1* mRNA, 100 ng RNA (SV Total RNA Isolation System; Promega) from mutant and wild-type plantlets either exposure to 100 ng ml^{-1} bleocin for 2 weeks or to 100 Gy γ -irradiation were reverse-transcribed (iScript cDNA Synthesis Kit; Bio-Rad; 90 min extension at 42°C) and amplified by PCR (see Data S1 for details). Genomic Col-0 DNA served as a positive control in the PCR assays.

Microarray analysis

Sample preparation and expression profiling. Approximately 50 *gmi1-1* and wild-type seeds were grown on $\frac{1}{2}$ MS plates in continuous light for 5 days and harvested 1.5 h after irradiation (100 Gy; as described for the RT-PCR experiments). RNA was isolated with TriReagent (Sigma, <https://www.sigmaaldrich.com/>) from plantlets, DNase treated (TurboDNase, Ambion, <http://www.ambion.com/>), and purified via PCI extraction and EtOH precipitation. RNA was labelled after quality assessment (Agilent Bioanalyzer 2100, Agilent, <http://www.genomics.agilent.com/>) and ATH1 microarray hybridizations were performed by NASCarray using the manufacturer recommended protocols (<http://affymetrix.arabidopsis.info/>). Three independent biological replicates were grown on separate $\frac{1}{2}$ MS plates. Microarray data were deposited at GEO (acc. no. GSE23892).

Microarray low-level data analysis and transforms. Low-level CEL-file analysis included re-assignment of probes to the TAIR genome annotation to achieve specific signals, removal of probe-sequence dependent effects, consideration of alternative chip-to-chip normalization options, and a robust expression signal summary of probe sets using a multi-chip probe-level model to down-weight random outlier probes (Huber *et al.*, 2002; Bolstad, 2004; Wu *et al.*, 2004; Dai *et al.*, 2005). See Data S1 for details.

Analysis of differential expression. For every gene, linear models were fit to obtain a contrast between radiated samples and the respective matched non-irradiated plants, as well as a contrast reflecting the differences in radiation response between the mutant and the wild-type plants. The significance of differences was adjusted for multiple testing according to Benjamini and Yekutieli

(2001) to provide strong control of the false discovery rate $< 5\%$. Few differences were observed between the mutant and wild-type radiation responses, and more aggressive quantile-quantile normalization together with the more liberal Benjamini-Hochberg multiple-testing correction yielded similar results, with just one additional gene identified (At1g75830, $q = 4.5\%$, data not shown). We consequently also determined the larger number of genes having a positive log-odds ratio for showing a different response, i.e. for which a different response was more likely than not. Setting an appropriate prior is non-trivial and we chose the more conservative estimate (1.2%) of two independent approaches: a prior of 1.2% gave self-consistent results, whereas a prior of 6.4% was obtained using a convex decreasing density estimate (Langaas *et al.*, 2005).

Histochemical GUS-staining

Plantlets were vacuum-infiltrated with GUS-staining solution (100 mM phosphate buffer pH 7.0 (Merck; Applichem), 10 mM EDTA (Roth), 0.1% Triton X-100 (Applichem), 2 mM potassium hexacyanoferrate (II) trihydrate (Fluka, <http://www.sigmaaldrich.com/>), $100\text{ }\mu\text{g ml}^{-1}$ chloramphenicol (Roth), 2 mM potassium hexacyanoferrate (III) (Applichem), 0.5 mg ml^{-1} X-GlcA (Duchefa)) and stained at 37°C over-night. After fixation (EtOH:acetic acid 3:1; Merck, Applichem) at room-temperature for 4 h and storage at 4°C in 70% EtOH (Merck, <http://www.merck-chemicals.com/>) seedlings were mounted in 30% glycerol/1 \times PBS (glycerol for microscopy; Merck) and visualized under a stereomicroscope (Leica MZ 16 FA, Leica, <http://www.leica.com>) or a microscope (Zeiss Axio Imager M1, Zeiss, <http://www.zeiss.com/>).

For chronic stress treatments, sterile seeds of two independent *GMI1_{pro}:GUS* lines were grown on $\frac{1}{2}$ MS media with $40\text{ }\mu\text{M}$ mitomycin C (Duchefa) or 100 ng ml^{-1} bleocin (Calbiochem) for 1 week. Control plants were left untreated. Seedlings were stained and analyzed as described above.

For short stress treatments, seedlings were grown on $\frac{1}{2}$ MS media for 5 days and transferred to liquid $\frac{1}{2}$ MS with or without $40\text{ }\mu\text{M}$ mitomycin C (Duchefa) or 100 ng ml^{-1} bleocin (Calbiochem). Samples were stained 1.5 and 24 h after transfer and visualized as mentioned above.

HR assay

Sterile seeds of 1445 Col (Tinland *et al.*, 1994; Lucht *et al.*, 2002; Fritsch *et al.*, 2004) in Col-0, *gmi1-1*, *gmi1-4*, or *mop9.9-1* background were grown on $\frac{1}{2}$ MS plates $\pm 100\text{ ng ml}^{-1}$ bleocin (Calbiochem) or $\pm 40\text{ }\mu\text{M}$ mitomycin C (Duchefa) under long day conditions for 3 weeks. Plants were stained in GUS staining solution (see above) at 37°C overnight and cleared in 70% EtOH (Merck) at room temperature. The number of GUS-spots per seedling was counted under a stereomicroscope (Leica MZ6). Table 2 lists average values of two technical replicates (each consisting of 22–45 plants grown on the same $\frac{1}{2}$ MS plate) in case of the bleocin experiment and 3 biological replicates (50 plants grown on separate $\frac{1}{2}$ MS plates per replicate) in case of the mitomycin C experiment. Standard deviation was calculated using the mean values of each replicate. The significance of differences was calculated using a Student's *t*-test (Excel, Microsoft).

Sensitivity assay

Sterile Col-0, *gmi1-1*, *gmi1-2*, *gmi1-4*, *atm-2*, *atr-2*, *atm-2 gmi1-2*, and *atr-2 gmi1-2* seeds were grown on $\frac{1}{2}$ MS plates in continuous light ($100\text{ }\mu\text{mol m}^{-2}\text{ sec}^{-1}$; Percival CU-36/L4, USA) for 5 days, irradiated (100 Gy), and then continued to let grow. Control plants were left untreated. Pictures were taken 5, 9 and 17 days after

γ -irradiation. The ratio of dead to recovered plants was determined 17 days after irradiation.

Comet assay

Seeds were germinated on Petri plates on ½MS media (Duchefa) solidified with 0.8% Plant Agar (Duchefa) and overlaid with cellophane to ease collection of seedlings at 16 h/8 h day/night regime at 22°C and 18°C, respectively. Sensitivity (Figure S7) and repair kinetics of Arabidopsis wild-type and mutant lines were measured using 10-day-old seedlings. Prior to treatment, seedlings were gently transferred from agar to liquid media to avoid drying. DSB fragmentation of nuclear DNA was measured in seedlings treated with 0, 10, 30, and 50 $\mu\text{g ml}^{-1}$ bleocin (inj., Euro Nippon Kayaku GmbH, <http://www.nipponkayaku.co.jp/english/>) for 1 h in liquid ½MS.

For repair kinetics, seedlings were rinsed in H₂O after bleocin treatment (30 $\mu\text{g ml}^{-1}$), blotted on filter paper and either frozen in liquid N₂ ($t = 0$) or left to recover in ½MS for the indicated repair times, before being frozen in liquid N₂. DSBs were detected by a neutral comet assay (Angelis *et al.*, 1999; Menke *et al.*, 2001; Olive and Banath, 2006) as described in the Data S1.

ACCESSION NUMBERS

The AGI locus identifiers and/or GenBank/EMBL sequences for genes in this article are: GMI1 (At5g24280; MOP9.10 of AB006701; coding sequence: NM_122334.2; protein NP_197816.2), MOP9.9 (MOP9.9 of AB006701; putative protein BAB10393.1), ATM (At3g48190), ATR (At5g40820), WEE1 (At1g02970), BRCA1 (At4g21070), RAD51 (At5g20850), DMS3 (At3g49250), ACTIN2 (At5g09810), PEROXIN4 (At5g25760), SYN2/RAD21.1 (At5g40840), ROC3 (At2g16600), and UBQ10 (At4g05320).

Microarray data and probe set description files were deposited at GEO, accession number GSE23892 (<http://www.ncbi.nlm.nih.gov/geo/query/acc.cgi?acc=GSE23892>). The author responsible for distribution of materials integral to the findings presented in this article is: Stefan Ferscha (stefan.ferscha@gmi.oew.ac.at).

ACKNOWLEDGEMENT

We would like to thank Karel Riha, Ortrun Mittelsten Scheid, Peter Schlögelhofer, Marisa Rosa, Andreas Bachmair, Maria Siomos, Max Rössler, and Ruth Quint for seeds, reagents, and helpful discussions. We would like to thank Neil Brockdorff for communicating results prior to publication and Kim Nasmyth for suggesting characterizing SMCHD proteins in plants. KJA would like to acknowledge financial support from Ministry of Education, Youth and Sports of the Czech Republic projects 1M0505, LC06004, and EU project COMICS (LSHB-CT-2006-037575). DPK gratefully acknowledges support by the Vienna Science and Technology Fund (WWTF), Baxter AG, Austrian Research Centres Seibersdorf, and the Austrian Centre of Biopharmaceutical Technology.

SUPPORTING INFORMATION

Additional Supporting Information may be found in the online version of this article:

Figure S1. Sequenced junctions of T-DNA insertions in *GMI1* and *MOP9*.

Figure S2. Genotyping-PCR of wild-type and mutant plants.

Figure S3. RT-PCR of *GMI1*.

Figure S4. *atr gmi1-2* display enhanced sensitivity.

Figure S5. *gmi1* single mutants are only mildly sensitive to γ -irradiation.

Figure S6. Repair kinetics of bleocin induced DNA double strand breaks in Col-0 wild-type, *gmi1-2*, and *rad21.1*.

Figure S7. Sensitivity assay of Col-0 wild-type, *gmi1-1*, *gmi1-2*, *gmi1-4*, and *rad21.1* to bleocin.

Table S1. Response of Col-0 wild-type to γ -irradiation, full table.

Table S2. Response of *gmi1-1* to γ -irradiation, full table.

Table S3. Differential response of wild-type and *gmi1-1* to γ -irradiation, full table.

Table S4. Primer combinations and PCR conditions for genotyping of the plant lines.

Table S5. Primers for the amplification of the genomic sequences flanking the T-DNA insertions.

Table S6. Primer combinations and PCR conditions for the *GMI1* mRNA analysis in *gmi1* mutant and Col-0 wild-type background.

Table S7. Primer combinations and PCR conditions for the expression analysis of *SMCHD* genes.

Table S8. Primer combinations and PCR conditions for real-time PCR after γ -irradiation.

Data S1. Experimental procedures.

Please note: As a service to our authors and readers, this journal provides supporting information supplied by the authors. Such materials are peer-reviewed and may be re-organized for online delivery, but are not copy-edited or typeset. Technical support issues arising from supporting information (other than missing files) should be addressed to the authors.

REFERENCES

- Abe, K., Osakabe, K., Nakayama, S., Endo, M., Tagiri, A., Todoriki, S., Ichikawa, H. and Toki, S. (2005) *Arabidopsis* RAD51C gene is important for homologous recombination in meiosis and mitosis. *Plant Physiol.* **139**, 896–908.
- Akutsu, N., Iijima, K., Hinata, T. and Tauchi, H. (2007) Characterization of the plant homolog of Nijmegen breakage syndrome 1: involvement in DNA repair and recombination. *Biochem. Biophys. Res. Commun.* **353**, 394–398.
- Alexander, M.P. (1969) Differential staining of aborted and nonaborted pollen. *Stain Technol.* **44**, 117–122.
- Angelis, K.J., Dusinska, M. and Collins, A.R. (1999) Single cell gel electrophoresis: detection of DNA damage at different levels of sensitivity. *Electrophoresis*, **20**, 2133–2138.
- Ausubel, F.M. (2001) *Current Protocols in Molecular Biology*. New York: J. Wiley.
- Barlow, J.H., Lisby, M. and Rothstein, R. (2008) Differential regulation of the cellular response to DNA double-strand breaks in G1. *Mol. Cell*, **30**, 73–85.
- Benjamini, Y. and Yekutieli, D. (2001) The control of the false discovery rate in multiple testing under dependency. *Ann. Statist.* **29**, 1165–1188.
- Bennett, C.B., Lewis, A.L., Baldwin, K.K. and Resnick, M.A. (1993) Lethality induced by a single site-specific double-strand break in a dispensable yeast plasmid. *Proc. Natl Acad. Sci. USA*, **90**, 5613–5617.
- Bilwes, A.M., Alex, L.A., Crane, B.R. and Simon, M.I. (1999) Structure of CheA, a signal-transducing histidine kinase. *Cell*, **96**, 131–141.
- Bleuyard, J.Y., Gallego, M.E. and White, C.I. (2006) Recent advances in understanding of the DNA double-strand break repair machinery of plants. *DNA Repair (Amst.)*, **5**, 1–12.
- Blewitt, M.E., Vickaryous, N.K., Hemley, S.J., Ashe, A., Bruxner, T.J., Preis, J.I., Arkell, R. and Whitelaw, E. (2005) An *N*-ethyl-*N*-nitrosourea screen for genes involved in variegation in the mouse. *Proc. Natl Acad. Sci. USA*, **102**, 7629–7634.
- Blewitt, M.E., Gendrel, A.V., Pang, Z. *et al.* (2008) SmcHD1, containing a structural-maintenance-of-chromosomes hinge domain, has a critical role in X inactivation. *Nat. Genet.* **40**, 663–669.
- Bolstad, B. (2004) *Low Level Analysis of High-density Oligonucleotide Array Data: Background, Normalization and Summarization*. Dissertation [Dissertation]. Berkeley: University of California. <http://www.bmbolstad.com/publications.html>.
- Bundock, P. and Hooykaas, P. (2002) Severe developmental defects, hypersensitivity to DNA-damaging agents, and lengthened telomeres in Arabidopsis MRE11 mutants. *Plant Cell*, **14**, 2451–2462.

- Chiu, A., Revenkova, E. and Jessberger, R. (2004) DNA interaction and dimerization of eukaryotic SMC hinge domains. *J. Biol. Chem.* **279**, 26233–26242.
- Cools, T. and De Veylder, L. (2009) DNA stress checkpoint control and plant development. *Curr. Opin. Plant Biol.* **12**, 23–28.
- Culligan, K., Tissier, A. and Britt, A. (2004) ATR regulates a G2-phase cell-cycle checkpoint in *Arabidopsis thaliana*. *Plant Cell*, **16**, 1091–1104.
- Culligan, K.M., Robertson, C.E., Foreman, J., Doerner, P. and Britt, A.B. (2006) ATR and ATM play both distinct and additive roles in response to ionizing radiation. *Plant J.* **48**, 947–961.
- Dai, M., Wang, P., Boyd, A.D. et al. (2005) Evolving gene/transcript definitions significantly alter the interpretation of GeneChip data. *Nucleic Acids Res.* **33**, e175.
- De Coninck, B.M., Sels, J., Venmans, E. et al. (2010) *Arabidopsis thaliana* plant defensin AtPDF1.1 is involved in the plant response to biotic stress. *New Phytol.* **187**, 1075–1088.
- De Piccoli, G., Cortes-Ledesma, F., Ira, G. et al. (2006) Smc5-Smc6 mediate DNA double-strand-break repair by promoting sister-chromatid recombination. *Nat. Cell Biol.* **8**, 1032–1034.
- De Schutter, K., Joubes, J., Cools, T. et al. (2007) *Arabidopsis* WEE1 kinase controls cell cycle arrest in response to activation of the DNA integrity checkpoint. *Plant Cell*, **19**, 211–225.
- Fritsch, O., Benvenuto, G., Bowler, C., Molinier, J. and Hohn, B. (2004) The INO80 protein controls homologous recombination in *Arabidopsis thaliana*. *Mol. Cell*, **16**, 479–485.
- Fulcher, N. and Sablowski, R. (2009) Hypersensitivity to DNA damage in plant stem cell niches. *Proc. Natl Acad. Sci. USA*, **106**, 20984–20988.
- Gallego, M.E., Jeanneau, M., Granier, F., Bouchez, D., Bechtold, N. and White, C.I. (2001) Disruption of the *Arabidopsis* RAD50 gene leads to plant sterility and MMS sensitivity. *Plant J.* **25**, 31–41.
- Garcia, V., Bruchet, H., Camescasse, D., Granier, F., Bouchez, D. and Tissier, A. (2003) AtATM is essential for meiosis and the somatic response to DNA damage in plants. *Plant Cell*, **15**, 119–132.
- Heidinger-Pauli, J.M., Unal, E., Guacci, V. and Koshland, D. (2008) The kleisin subunit of cohesin dictates damage-induced cohesion. *Mol. Cell*, **31**, 47–56.
- Hirano, T. (2002) The ABCs of SMC proteins: two-armed ATPases for chromosome condensation, cohesion, and repair. *Genes Dev.* **16**, 399–414.
- Hruz, T., Laule, O., Szabo, G., Wessendorp, F., Bleuler, S., Oertle, L., Widmayer, P., Gruissem, W. and Zimmermann, P. (2008) Genevestigator v3: a reference expression database for the meta-analysis of transcriptomes. *Adv. Bioinformatics*, **2008**, 420747.
- Huber, W., von Heydebreck, A., Sultmann, H., Poustka, A. and Vingron, M. (2002) Variance stabilization applied to microarray data calibration and to the quantification of differential expression. *Bioinformatics*, **18**(Suppl 1), S96–S104.
- Iyer, L.M., Abhiman, S. and Aravind, L. (2008) MutL homologs in restriction-modification systems and the origin of eukaryotic MRC ATPases. *Biol. Direct*, **3**, 8.
- Jackson, S.P. (2002) Sensing and repairing DNA double-strand breaks. *Carcinogenesis*, **23**, 687–696.
- Kandasamy, M.K., McKinney, E.C., Deal, R.B., Smith, A.P. and Meagher, R.B. (2009) *Arabidopsis* actin-related protein ARP5 in multicellular development and DNA repair. *Dev. Biol.* **335**, 22–32.
- Kanno, T., Bucher, E., Daxinger, L., Huettel, B., Böhmendorfer, G., Gregor, W., Kreil, D.P., Matzke, M. and Matzke, A.J. (2008) A structural-maintenance-of-chromosomes hinge domain-containing protein is required for RNA-directed DNA methylation. *Nat. Genet.* **40**, 670–675.
- Kozak, J., West, C.E., White, C., da Costa-Nunes, J.A. and Angelis, K.J. (2009) Rapid repair of DNA double strand breaks in *Arabidopsis thaliana* is dependent on proteins involved in chromosome structure maintenance. *DNA Repair (Amst)*, **8**, 413–419.
- Lafarge, S. and Montane, M.H. (2003) Characterization of *Arabidopsis thaliana* ortholog of the human breast cancer susceptibility gene 1: AtBRCA1, strongly induced by gamma rays. *Nucleic Acids Res.* **31**, 1148–1155.
- Langaas, M., Lindqvist, B.H. and Ferkingstad, E. (2005) Estimating the proportion of true null hypotheses, with application to DNA microarray data. *J. R. Stat. Soc. Ser. B-Stat. Methodol.* **67**, 555–572.
- Lehmann, A.R. (2005) The role of SMC proteins in the responses to DNA damage. *DNA Repair (Amst)*, **4**, 309–314.
- Losada, A. and Hirano, T. (2005) Dynamic molecular linkers of the genome: the first decade of SMC proteins. *Genes Dev.* **19**, 1269–1287.
- Lucht, J.M., Mauch-Mani, B., Steiner, H.Y., Mettraux, J.P., Ryals, J. and Hohn, B. (2002) Pathogen stress increases somatic recombination frequency in *Arabidopsis*. *Nat. Genet.* **30**, 311–314.
- Mengiste, T., Revenkova, E., Bechtold, N. and Paszkowski, J. (1999) An SMC-like protein is required for efficient homologous recombination in *Arabidopsis*. *EMBO J.* **18**, 4505–4512.
- Menke, M., Chen, I., Angelis, K.J. and Schubert, I. (2001) DNA damage and repair in *Arabidopsis thaliana* as measured by the comet assay after treatment with different classes of genotoxins. *Mutat. Res.* **493**, 87–93.
- Mladenov, E., Tsaneva, I. and Anachkova, B. (2007) Activation of the S phase DNA damage checkpoint by mitomycin C. *J. Cell. Physiol.* **211**, 468–476.
- Olive, P.L. and Banath, J.P. (2006) The comet assay: a method to measure DNA damage in individual cells. *Nat. Protoc.* **1**, 23–29.
- Puchta, H. (1999) Double-strand break-induced recombination between ectopic homologous sequences in somatic plant cells. *Genetics*, **152**, 1173–1181.
- Ricaud, L., Proux, C., Renou, J.P., Pichon, O., Fochesato, S., Ortet, P. and Montane, M.H. (2007) ATM-mediated transcriptional and developmental responses to gamma-rays in *Arabidopsis*. *PLoS ONE*, **2**, e430.
- Saecker, R.M. and Record, M.T. Jr (2002) Protein surface salt bridges and paths for DNA wrapping. *Curr. Opin. Struct. Biol.* **12**, 311–319.
- Schubert, V. (2009) SMC proteins and their multiple functions in higher plants. *Cytogenet. Genome Res.* **124**, 202–214.
- Schurmann, D., Molinier, J., Fritsch, O. and Hohn, B. (2005) The dual nature of homologous recombination in plants. *Trends Genet.* **21**, 172–181.
- Shrivastav, M., De Haro, L.P. and Nickoloff, J.A. (2008) Regulation of DNA double-strand break repair pathway choice. *Cell Res.* **18**, 134–147.
- Stock, J. (1999) Signal transduction: Gyrate protein kinases. *Curr. Biol.* **9**, R364–R367.
- Takahashi, N., Quimbaya, M., Schubert, V., Lammens, T., Vandepoele, K., Schubert, I., Matsui, M., Inze, D., Bex, G. and De Veylder, L. (2010) The MCM-binding protein ETG1 aids sister chromatid cohesion required for postreplicative homologous recombination repair. *PLoS Genet.* **6**, e1000817.
- Tinland, B., Hohn, B. and Puchta, H. (1994) *Agrobacterium tumefaciens* transfers single-stranded transferred DNA (T-DNA) into the plant cell nucleus. *Proc. Natl Acad. Sci. USA*, **91**, 8000–8004.
- Watanabe, K., Pacher, M., Dukowicz, S., Schubert, V., Puchta, H. and Schubert, I. (2009) The structural maintenance of chromosomes 5/6 complex promotes sister chromatid alignment and homologous recombination after DNA damage in *Arabidopsis thaliana*. *Plant Cell*, **21**, 2688–2699.
- Waterworth, W.M., Kozak, J., Provost, C.M., Bray, C.M., Angelis, K.J. and West, C.E. (2009) DNA ligase 1 deficient plants display severe growth defects and delayed repair of both DNA single and double strand breaks. *BMC Plant Biol.* **9**, 79.
- Wendt, K.S., Yoshida, K., Itoh, T. et al. (2008) Cohesin mediates transcriptional insulation by CCCTC-binding factor. *Nature*, **451**, 796–801.
- Wierzbicki, A.T., Ream, T.S., Haag, J.R. and Pikaard, C.S. (2009) RNA polymerase V transcription guides ARGONAUTE4 to chromatin. *Nat. Genet.* **41**, 630–634.
- Winter, D., Vinegar, B., Nahal, H., Ammar, R., Wilson, G.V. and Provart, N.J. (2007) An “electronic fluorescent pictograph” browser for exploring and analyzing large-scale biological data sets. *PLoS ONE*, **2**, e718.
- Wu, Z., Irizarry, R.A., Gentleman, R., Martinez-Murillo, F. and Spencer, F. (2004) A Model-based background adjustment for oligonucleotide expression arrays. *J. Am. Stat. Ass.* **99**, 909–917.
- Yadav, R.K., Girke, T., Pasala, S., Xie, M. and Reddy, G.V. (2009) Gene expression map of the *Arabidopsis* shoot apical meristem stem cell niche. *Proc. Natl Acad. Sci. USA*, **106**, 4941–4946.
- Yoshiyama, K., Conklin, P.A., Huefner, N.D. and Britt, A.B. (2009) Suppressor of gamma response 1 (SOG1) encodes a putative transcription factor governing multiple responses to DNA damage. *Proc. Natl Acad. Sci. USA*, **106**, 12843–12848.
- Young, J.C., Moarefi, I. and Hartl, F.U. (2001) Hsp90: a specialized but essential protein-folding tool. *J. Cell Biol.* **154**, 267–273.

MRE11 and RAD50, but not NBS1, are essential for gene targeting in the moss *Physcomitrella patens*

Yasuko Kamisugi¹, Didier G. Schaefer^{2,3}, Jaroslav Kozak⁴, Florence Charlot², Nathalie Vrielynck², Marcela Holá⁴, Karel J. Angelis⁴, Andrew C. Cuming^{1,*} and Fabien Nogue^{2,*}

¹Centre for Plant Sciences, Faculty of Biological Sciences, Leeds University, Leeds LS2 9JT, UK, ²INRA AgroParisTech, IJPB, UMR 1318, INRA centre de Versailles, route de Saint Cyr, 78026 Versailles CEDEX, France, ³Laboratoire de Biologie Moléculaire et Cellulaire, Institut de Biologie, Université de Neuchâtel, rue Emile-Argand 11, CH-2007 Neuchâtel, Switzerland and ⁴Institute of Experimental Botany, Czech Academy of Sciences, Na Karlovce 1a, 160 00 Praha 6, Czech Republic

Received November 3, 2011; Revised December 7, 2011; Accepted December 8, 2011

ABSTRACT

The moss *Physcomitrella patens* is unique among plant models for the high frequency with which targeted transgene insertion occurs via homologous recombination. Transgene integration is believed to utilize existing machinery for the detection and repair of DNA double-strand breaks (DSBs). We undertook targeted knockout of the *Physcomitrella* genes encoding components of the principal sensor of DNA DSBs, the MRN complex. Loss of function of *PpMRE11* or *PpRAD50* strongly and specifically inhibited gene targeting, whilst rates of untargeted transgene integration were relatively unaffected. In contrast, disruption of the *PpNBS1* gene retained the wild-type capacity to integrate transforming DNA efficiently at homologous loci. Analysis of the kinetics of DNA-DSB repair in wild-type and mutant plants by single-nucleus agarose gel electrophoresis revealed that bleomycin-induced fragmentation of genomic DNA was repaired at approximately equal rates in each genotype, although both the *PpMRE11* and *PpRAD50* mutants exhibited severely restricted growth and development and enhanced sensitivity to UV-B and bleomycin-induced DNA damage, compared with wild-type and *PpNBS1* plants. This implies that while extensive DNA repair can occur in the absence of a functional MRN complex; this is unsupervised in nature and results in the accumulation of deleterious

mutations incompatible with normal growth and development.

INTRODUCTION

DNA double-strand breaks (DSBs) represent one of the most cytotoxic forms of damage an organism can acquire (1). Such events occur with high frequency resulting from cellular metabolism (such as reactive radicals or stalled replication forks during S phase) and through the action of exogenous agents (such as ionizing radiation or chemical mutagens). Failure to repair such damage can lead to the irrecoverable loss of genetic material, with both immediate and long-term consequences: the onset of cancerous transformation in animal cells, or the failure to transmit genetic information in gametes (especially in plants, where there is no early developmental partitioning of germ-line and somatic cell lineages).

Unsurprisingly, all living organisms have evolved efficient mechanisms that can be deployed to sense DNA DSBs, activate DNA repair, cell-cycle arrest and sometimes apoptosis. Such is the importance of these mechanisms, that the genes encoding many of the essential components of the DNA repair machinery are highly conserved in evolution (2). In particular, this is true of the mechanism by which the broken ends of DNA molecules are recognized and recruited into DNA repair complexes. In eukaryotes, the MRN/MRX complex undertakes this task (3,4). This conserved complex is composed of three proteins, Meiotic recombination 11 (MRE11), Radiation sensitive 50 (RAD50), and

*To whom correspondence should be addressed. Tel: +33 01 30 83 30 09; Fax: +33 01 30 83 33 19; Email: fabien.nogue@versailles.inra.fr
Correspondence may also be addressed to Andrew C. Cuming. Tel: +44 113 343 3094; Fax: +44 113 343 3144; Email: a.c.cuming@leeds.ac.uk

The authors wish it to be known that, in their opinion, the first two authors should be regarded as joint First Authors.

© The Author(s) 2011. Published by Oxford University Press.
This is an Open Access article distributed under the terms of the Creative Commons Attribution Non-Commercial License (<http://creativecommons.org/licenses/by-nc/3.0>), which permits unrestricted non-commercial use, distribution, and reproduction in any medium, provided the original work is properly cited.

Nijmegen Breakage Syndrome 1 (NBS1) (X-ray sensitive 2, XRS2 in the yeast, *Saccharomyces cerevisiae*). Together, the MRE11, RAD50 and NBS1 proteins form a multisubunit complex (M₂R₂N₁) that binds the ends of broken DNA molecules, and can tether the broken ends through dimerization between adjacent MRN complexes mediated by an association between the RAD50 components (3,5). The formation of MRN–DNA complexes also initiates a cell-cycle checkpoint through interaction with the phosphoinositide 3-kinase-related protein kinases (PIKKs) ATM and ATR (for ‘Ataxia Telangiectasia Mutated’ and ‘Ataxia Telangiectasia mutated-like and Rad 3 related’) and the DNA Protein Kinase catalytic subunit (DNA-PKcs) (6). These proteins phosphorylate multiple targets to initiate a cascade of downstream events leading to DNA DSB repair either by non-homologous end joining (NHEJ), a rapid but occasionally inaccurate mechanism, or through homologous recombination (HR), a conservative mechanism that uses an homologous sequence (e.g. a sister chromatid) as a template to restore the original sequence at the DSB site. In this latter pathway, an Mre11-specific nuclease activity is required (with other components) for the resection of DNA ends necessary for strand invasion (7).

Transgene integration into flowering plant genomes occurs through the agency of endogenous mechanisms that have evolved for the repair of DNA DSBs. In flowering plants, the integration of exogenous DNA whether directly delivered via microprojectile bombardment or protoplast transfection, or delivered by *Agrobacterium*-mediated transformation occurs predominantly at random positions throughout the genome, whereas gene targeting frequencies remain extremely low (8). Random integration of transgenes requires enzymes from the NHEJ pathway, and the inefficiency of GT probably reflects the prevalence of the NHEJ pathway in repairing DNA DSBs in angiosperms (9–11). In contrast with flowering plants, transformation of the moss, *Physcomitrella patens*, with DNA containing homology with genomic sequences results in preferential incorporation of the transforming DNA at these homologous sequences (12). This facility for ‘gene targeting’ is similar to that seen in *Saccharomyces* (13) and suggests a preference for the use of the HR-dependent pathway as the primary means of undertaking DSB repair, although molecular analyses of gene targeting events provide clear evidence for modification of the transforming DNA by both NHEJ and HR reactions upon integration (14,15). *Physcomitrella* thus represents an excellent model in which to analyse DNA-DSB repair pathways in plants, particularly in regard to its outstanding gene targeting efficiency (12). Previous studies have shown that PpRAD51, the protein at the core of the HR reaction, was required to preserve genome integrity and essential to achieve gene targeting (16,17). The mismatch repair PpMSH2 gene was also shown to be essential to preserve genome integrity and to prevent homeologous gene targeting (18).

We have characterized the role of the *Physcomitrella* MRN complex in DNA DSB-repair and gene targeting. We find that in moss the major loss of function phenotypes of the MRN complex depends on PpRAD50 or

PpMRE11, but not PpNBS1. Inactivation of either PpRAD50 or PpMRE11 reduced GT ~11-fold in both Pprad50 and Ppmre11 mutants, while illegitimate integration rates only slightly affected. Gene expression studies further show that Ppmre11 and Pprad50 strains display constitutively high expression of the DNA damage response, implying the activation of alternative pathways to minimize endogenous DNA damage in the mutant strains. The mutants exhibit a severe developmental phenotype, possibly associated with early senescence processes, and hypersensitivity to UV-B and bleomycin-induced DNA damage.

MATERIALS AND METHODS

Plant material

Physcomitrella patens (Hedw.) B.S.G. ‘Gransden2004’ was vegetatively propagated as previously described (19). Individual plants were cultured as ‘spot inocula’ on BCD agar medium supplemented with 1 mM CaCl₂ and 5 mM ammonium tartrate (BCDAT medium), or as lawns of protonemal filaments by subculture of homogenized tissue on BCDAT agar medium overlain with cellophane for the isolation of protoplasts. Transformation experiments were performed as previously described (20) using linear fragments of DNA generated either by digestion of transforming vectors with restriction enzymes (19) or by polymerase chain reaction (PCR) amplification (14). Growth conditions for the generation of deletion strains were as described previously (17).

Gene identification and isolation

Genomic DNA and total RNA were isolated from *Physcomitrella* as previously described (19). For verification of gene models, RNA was extracted from a polyribosome-enriched fraction: 7-day subcultured protonemal tissue (~5 g squeeze-dried chloronemal tissue) was homogenized in 30 ml extraction buffer [200 mM sucrose 40 mM Tris–HCl, pH 8.5, 60 mM KCl, 30 mM MgCl₂, 1% (v/v) Triton X-100, 2 mM dithiothreitol] and the extract was clarified at 25 000g for 20 min (Sorvall SS34 rotor). The supernatant was layered over a cushion comprising 1 M sucrose, 40 mM Tris–HCl, pH 8.5, 20 mM KCl, 10 mM MgCl₂ and centrifuged for 3 h at 141 000g (Beckman SW28 rotor). The pellet was drained and resuspended in 0.5 ml RNA extraction buffer for aqueous phenol extraction (19). RNA used for RT-PCR was first digested with RQ DNase I (Promega) to remove residual DNA. *Physcomitrella* genomic sequences encoding the MRE11, RAD50 and NBS1 genes were identified by BLAST search (http://genome.jgi-psf.org/Phypa1_1/Phypa1_1.home.html). The available gene models were used for the design of PCR primers to amplify cognate genomic sequences, which were cloned in the plasmid pBluescript KS⁺. PCR primers used are listed in Supplementary Table S1. In order to obtain a correct gene model for each sequence, full-length complementary DNA (cDNA) sequences were amplified from *Physcomitrella* polyribosome-derived RNA by RT-PCR. Total RNA (1 µg) was reverse

transcribed using an oligo-dT₁₂₋₁₅ primer and AMV reverse transcriptase as supplied in the Promega Reverse Transcription system in a 20- μ l reaction. Following cDNA synthesis, the reaction mixture was diluted by the addition of 80 μ l water, and 1 μ l aliquots were used for PCR amplification using primers predicted to anneal with 5'- and 3'-untranslated region (UTR) sequences (Supplementary Table S1). PCR products were cloned by blunt-end ligation into the EcoRV site of pBluescript KS⁺ for sequence analysis (ABI3130) in the DNA sequencing facility of the Leeds University Faculty of Biological Sciences. Predicted polypeptide sequences were aligned with the orthologous genes from *Arabidopsis thaliana*, *Homo sapiens* and *Saccharomyces cerevisiae* using CLUSTALW.

Targeted gene knockout

Gene disruption cassettes were constructed by ligating a selection cassette comprising a neomycin phosphotransferase gene driven by the Cauliflower Mosaic Virus 35S promoter and terminated with the CaMV gene 6 termination sequence (35S-*nptII*-g6ter) derived from the vector pMBL6 (14) into convenient restriction sites within the cloned *PpMRE11*, *PpRAD50* and *PpNBS1* genes to replace endogenous coding sequences. For the *PpMRE11* gene, the selection cassette was placed between residues 1763501 (in exon 4) and 1764332 (in exon 8) in JGI Phypa1_1/scaffold 18. For the *PpRAD50* gene the selection cassette was placed between residues 1431738 (in intron 13) and 1433260 (in intron 16) in JGI Phypa1_1/scaffold 51. For the *PpNBS1* gene, the selection cassette was placed between residues 276622 (in intron 4) and 277547 (in intron 7) in JGI Phypa1_1/scaffold 219. For targeted knockout of the moss genes, fragments of DNA containing these cassettes and flanked by ~1 kb of 5'- and 3'-flanking genomic sequence were PCR amplified. These linear fragments were used to transform *Physcomitrella* protoplasts, and stable transformants were selected following regeneration in medium containing 50 μ g ml⁻¹ G418 for 2 weeks, followed by subculture onto medium lacking antibiotic for 2 weeks, and a final subculture on selective medium. Targeted replacement of the native genes by the disruption cassette was confirmed by PCR reactions using external, gene-specific primers in combination with 'outward-pointing' selection cassette-specific primers (Supplementary Table S1). Single-copy allele replacements were identified by PCR using the external primer pairs, and the absence of additional transgene insertion in the genome was confirmed by Southern blot analysis. Conditions for PCR analysis were as previously described (14) and Southern blot analysis of genomic DNA was carried out as previously described (21), using the 35S-*nptII*-g6ter cassette as a hybridization probe.

For generation of deletion mutants *mre11A* and *rad50A*, the 5'- and 3'-targeting fragments were amplified from *P. patens* genomic DNA and cloned upstream (5') and downstream (3') of the loxP sites flanking the resistance cassette in plasmid pBNRF (17) to create the plasmids pMRE11delta and pRAD50delta, respectively. For the

PpMRE11 gene, a 1009-bp 5'-targeting fragment (coordinates 1763137-1764146 in JGI Phypa1_1/scaffold 18) and an 803-bp 3'-targeting fragment (coordinates 1765334-1766184) were PCR-amplified. For *PpRad50*, an 831-bp 5' targeting fragment (coordinates 1426648-1427479 in JGI Phypa1_1/scaffold 51) and an 819-bp 3'-targeting fragment (coordinates 1435197-1436016) were PCR-amplified.

Moss protoplasts were transformed with pMRE11delta digested with BstXI and AseI, or with pRAD50delta digested with XbaI and NsiI. Stable disruptants were selected by successive subculture on selective and non-selective medium and PCR analysis as described above. Clean deletions in the *PpMRE11* (encompassing exons 7-10) and *PpRAD50* genes (exons 4-20) were obtained by transient Cre recombinase expression (18). Deletions in the recombinant loci were confirmed by PCR amplification using gene-specific external primers MRE11#1 and MRE11#2, and RAD50#1 and RAD50#2, respectively. Primers APT#14 and APT#19 were used as positive controls (Supplementary Table S1).

For gene targeting studies the vectors PpAPT-KO2 (17) and PpAPT-KO3 have been used. To obtain PpAPT-KO3, an internal 1631-bp Sall/BglII fragment containing the 35S:Hyg^R-LoxP marker was deleted in PpAPT-KO2 and replaced by an XhoI/BglII fragment from pBNRF (17) containing the 35S:Neo^R-LoxP marker.

Analysis of gene expression in mutants

Transcript abundance in selected knockout lines was determined by RT-PCR of cDNA. Total RNA was isolated from protonemal tissue (19) and 1 μ g was reverse-transcribed using a Promega reverse transcription system. The 20- μ l reaction mixture was diluted 25-fold and 5 μ l aliquots were used for PCR. Detection of *Mre11*, *Rad50* and *Nbs1* mRNA in mutant lines was by RT-PCR using primers indicated in Supplementary Table 1.

For quantitative determination of the relative abundances of transcripts encoding DNA repair genes in wild-type and mutant strains, quantitative real-time PCR was carried out using a Qiagen Rotor-Gene Q instrument and Qiagen SYBR-Green PCR kit. RNA was isolated from 7-day subcultured protonemal tissue from each of three independent lines (wild-type, *Ppmre11KO*, *Pprad50KO* and *Ppnbs1KO*, respectively), with two replicates for each sample. Transcript abundance was estimated by reference to both internal and external reference sequences. As an external reference, *Physcomitrella* RNA samples were 'spiked' with tenfold serial dilutions (10^{-1} - 10^{-4}) of an *in vitro* transcript from a full-length wheat 'Em' cDNA (22) prior to reverse transcription. These were used to test a number of candidate internal reference sequences, corresponding to *Physcomitrella* gene models Phypa1_1:227826 (SAND family endocytosis protein), Phypa1_1:209451 (Clathrin adapter complex subunit), Phypa1_1:224488 (Acyltransferase) and Phypa1_1:163153 (Ribosomal protein S4) for stability of expression in response to bleomycin treatment. Phypa1_1:227826 was subsequently selected as the

internal reference standard for the determination of the abundances of PpRad51-1 (Phypal_1:206066), PpRad51-2 ((Phypal_1:207856), PpPARP-1 (Phypal_1:150949), PpPARP-2 (Phypal_1:188096) PpKu70 (Phypal_1:60909), PpKu80 (Phypal_6:23553) and PpCtIP (Phypal_6:453490) transcripts. Relative transcript abundance was calculated using the $\Delta\Delta Ct$ method and normalized to the wild-type value.

Bleomycin and UV-B sensitivity assays

Physcomitrella explants were inoculated as 'spot inocula' onto BCDAT-agar plates supplemented with bleomycin (Bleocin inj., Euro Nippon Kayaku GmbH, Germany) at concentrations indicated in the text, to determine sensitivity to chronic exposure to the drug. Plant growth was assessed by measurement of the surface area of each plant at intervals following inoculation by digital photography of the plates. The image analysis software 'ImageJ' (23) was used to convert the digital images to binary format and determine the colony area based on counting the number of pixels corresponding to each colony. Colony area determinations based on different photographs were normalized for each colony using the estimated area of the plate.

For acute toxicity testing, protoplast viability and protonemal growth were analysed. Viability was tested when protoplasts of wild-type and *mre11*, *rad50* and *nbs1* mutants in BCD liquid medium supplemented with mannitol were treated with bleomycin at concentrations indicated in the text for 1 h. Protoplasts were washed two times and then resuspended in liquid mannitol medium. After 20 h in the dark, the protoplasts were spread on BCD agar medium supplemented with mannitol ($\sim 10^5$ protoplasts per Petri dish). After 6 days regeneration, the number of survivors was counted. We repeated these experiments three times.

Protoplasts of wild-type, *mre11* and *rad50* mutants were spread ($\sim 50\,000$ /plate) on protoplast agar medium (PpNH4 + 0.5% glucose + 8.5% mannitol). Plates were immediately irradiated with UV-B light (308 nm) in a Stratagene Stratalink. The intensity of the irradiation was controlled using the internal probe of the Stratalink and one plate of each strain was treated simultaneously. The experiment was repeated three times. Plates were immediately transferred to darkness for 24 h after treatment then to standard growth conditions for protoplast regeneration. Survival was determined after 1 week by microscopic observation.

Protonemal growth was tested by incubating 7-day-old protonemal tissue in BCDAT liquid medium containing bleomycin at concentrations indicated in the text for 1 h. The tissue was washed three times with medium lacking bleomycin and homogenized. Explants were inoculated onto BCDAT agar medium and recovery following treatment was determined by measuring the increase in plant surface area over a 3-week period.

Evaluation of spontaneous mutation frequency

Mutations in the *PpAPT* gene confer resistance to 2-Fluoroadenine (2-FA), a toxic compound for cells.

The number of 2-FA resistant colonies that grow following protoplast regeneration reflects the frequency of spontaneous mutations. Protoplasts of wild-type, *mre11*, *rad50*, *nbs1* and *msh2* (18) mutants were regenerated for 6 days on BCD agar medium supplemented with mannitol ($\sim 10^5$ protoplasts per Petri dish) and then transferred on to BCD agar medium supplemented with 5 μM 2-FA (Fluorochem). After 2 weeks, the number of resistant clones was counted. Experiments were repeated three times and statistically analysed using Fisher's exact test.

Isolation of *apt* mutants after bleomycin treatments

One-day-old protonemata prepared from 10 plates of 7-day-old tissue (around $25 \cdot 10^6$ dividing cells) of wild-type and the *Pprad50KO* mutants were exposed to sublethal acute doses of bleomycin: 50 $\mu g/ml$ for 2 h for wild-type and 0.1 $\mu g/ml$ for 1 h for the *Pprad50KO* mutant, before being transferred onto cellophane-overlaid BCDAT agar medium supplemented with 2–3 μM 2-FA. After 3 weeks, resistant foci were clearly visible. Cellophane discs bearing resistant colonies were transferred to plates without 2-FA. This process was repeated three times until stable *Ppapt* clones were established. The results of selection are summarized in Supplementary Table S2. Genomic DNA was isolated as previously described (19) and the mutant *Ppapt* genes were amplified by PCR and sequenced using the primers listed in Supplementary Table S1 and indicated in Supplementary Figure S4.

Gene targeting assays

Transformation efficiency and *APT* targeting frequency were measured as previously described (17). Moss protoplasts (4.8×10^5) were transformed with the nonhomologous pBHRF or pBNRF plasmids (17) digested respectively with HindIII or XmaI to produce a linear fragment containing the 35S::hygR or 35S::neoR markers, or with PpAPT-KO2 or PpAPT-KO3 plasmids digested respectively with BsaAI/HindIII or PvuI/BsrGI to produce the targeting *APT* fragment containing the 35S::hygR cassette (from pBHRF) or the 35S::neoR cassette (from pBNRF) flanked by genomic *PpAPT* sequences. Targeted integration of PpAPT-KO2 or PpAPT-KO3 at the *APT* genomic locus confers resistance to 2-FA. We selected primary transformants (unstable + stable) with 25 $mg\ l^{-1}$ hygromycin B (Duchefa) for PpAPT-KO2 or with 50 $mg\ l^{-1}$ G418 (Duchefa) for PpAPT-KO3. Integrative transformants were isolated following a second round of selection. Protonemal explants from these transformants were then transferred onto medium containing 5 μM of 2-FA to detect *APT* gene targeting events. Experiments were repeated three times.

DNA-DSB repair assays

Protonemal lawns of wild-type and mutant strains subcultured for 1 week were used to generate protonemal tissue for DNA repair assays by shearing tissue collected from single 9-cm plates with an IKA T2T Digital Ultra Turrax homogenizer at maximum speed (24 krpm) for

1 min in 5 ml of liquid BCD medium. This was spread on BCD-agar medium overlaid with cellophane and grown for 1, 7 or 14 days prior to harvesting for bleomycin treatment.

Protonemata were gently transferred from cellophane to liquid BCD medium in 4-cm wells of a six-well microtitre plate to avoid drying. DSBs were induced by addition of bleomycin to 10, 20, 30 and 50 $\mu\text{g ml}^{-1}$ for 1 h. Following treatment, the tissue was thoroughly rinsed in H_2O in disposable 22- μm mesh funnels (Partec GmbH, Germany), blotted on filter paper and either flash-frozen in liquid N_2 ($t = 0$) or left to recover on BCD-agar plates overlaid with cellophane for the indicated repair times, before being frozen in liquid N_2 . All handling and transfer of protonemata was with tweezers.

DNA-DSBs were detected by a neutral comet assay (24) as described previously (25,26). Approximately 100 mg of frozen tissue was cut with a razor blade in 300 μl phosphate-buffered saline (PBS)+10 mM ethylenediaminetetraacetic acid (EDTA) on ice and the tissue debris removed by filtration through 50- μm mesh funnels (Partec GmbH, Germany) into Eppendorf tubes on ice. Fifty microlitres of nuclear suspension was dispersed in 200 μl of melted 0.7% LMT agarose (15510-027, GibcoBRL, Gaithersburg, USA) at 40° C and four 80- μl aliquots were immediately pipetted onto each of two agarose coated microscope slides (two duplicates per slide), covered with a 22 \times 22-mm cover slip and then chilled on ice for 1 min to solidify the agarose. After removal of cover slips, slides were dipped in lysis solution (2.5 M NaCl, 10 mM Tris-HCl, 0.1 M EDTA, 1% N-lauroyl sarcosinate, pH 7.6) on ice for at least 1 h to dissolve cellular membranes and remove attached proteins. The whole procedure from chopping tissue to dipping into lysis solution takes \sim 3 min. After lysis, slides were twice equilibrated for 5 min in Tris-borate-EDTA (TBE) electrophoresis buffer to remove salts and detergents. Comet slides were then subjected to electrophoresis at 1 V/cm (\sim 12 mA) for 5 min. After electrophoresis, slides were dipped for 5 min in 70 % EtOH, 5 min in 96% EtOH and air-dried.

DNA 'comets' were viewed in epifluorescence with a Nikon Eclipse 800 microscope after staining with SybrGold stain (Molecular-Probes Invitrogen, USA) and evaluated by the Comet module of the LUCIA cytogenetics software suite (LIM, Praha, Czech Republic).

Comet assay data analysis

The fraction of DNA in comet tails (% tail-DNA) was used as a measure of DNA damage. Data for the wild-type strain and the three mutant lines (*Pprad50*, *Ppmre11* and *Ppnbs1*) analysed in this study were obtained in at least three independent experiments. In each experiment, the % tail-DNA was measured at seven time points: 0, 5, 10, 20, 60, 180 and 360 min after treatment and in control tissue without treatment. Measurements included four independent gel replicas of 25 evaluated comets totalling at least 300 comets analysed per experimental point.

The percentage of damage remaining as plotted on figures after given repair time (t_x) is defined as:

$$\% \text{ damage remaining } (t_x) = \frac{\left\{ \begin{array}{l} \text{mean \%T DNA damage } (t_x) \\ - \text{mean \%T DNA damage (control)} \end{array} \right\}}{\left\{ \begin{array}{l} \text{mean \%T DNA damage } (t_0) \\ - \text{mean \%T DNA damage (control)} \end{array} \right\}} \times 100$$

Repair kinetics following two-phase decay kinetics defined as:

$$\begin{aligned} \text{SpanFast} &= (Y_0 - \text{Plateau}) * \text{PercentFast} * 0.01 \\ \text{SpanSlow} &= (Y_0 - \text{Plateau}) * (100 - \text{PercentFast}) * 0.01 \\ Y &= \text{Plateau} + \text{SpanFast} * \exp(-K_{\text{Fast}} * X) + \text{SpanSlow} * \\ &\quad \exp(-K_{\text{Slow}} * X) \end{aligned}$$

was analysed by linear regression of experimental data with the Prism v.5 program (GrafPad Software Inc., USA). Goodness of fit characterized by R-squared was better than 0.99.

RESULTS

Identification of MRN complex genes

Sequence homology searches of the draft *Physcomitrella* genome identified single putative homologues of the *MRE11*, *RAD50*, and *NBS1* genes on sequence scaffolds 18, 51 and 219, respectively. Whilst EST sequences were available to provide partial support for predicted gene models for the *PpMRE11* and *PpNBS1* genes, no corroborative evidence was available for the *PpRAD50* gene, and the automated gene prediction software had not generated a gene model. We therefore generated gene models for all three genes based on BLASTX similarity to flowering plant proteins (*Arabidopsis*, rice and maize) to identify putative full-length protein coding sequences, and used these models to design PCR primers for the amplification of full-length protein coding sequences by reverse transcription-PCR of moss polyribosome-derived RNA. The resulting cDNA sequences and genomic models have been deposited in GenBank (Accession Nos: JF820817 and JF820820 for *PpMRE11*; JF82018 and JF82021 for *PpRAD50*; JF82019 and JF82022 for *PpNBS1*) and the curated and structurally annotated gene models entered in the JGI *Physcomitrella* genome browser in which they were assigned the Protein ID numbers Phypa1_1:235701 (*PpMRE11*), Phypa1_1:235526 (*PpRAD50*) and Phypa1_1:235702 (*PpNBS1*).

The deduced polypeptide sequences were compared with the corresponding human, yeast and flowering plant sequences (Supplementary Figure S1). Like both the *Arabidopsis* and human genes, the *PpMRE11* gene comprises 22 protein-coding exons. There is extensive similarity among all the *MRE11* polypeptides (Supplementary Figure S1a) especially within the N-terminal two-thirds of the protein. The *Physcomitrella* *MRE11* protein contains the characteristic phosphoesterase motifs within the nuclease domain, the capping domain and amino acids

(N123 and W225) shown to be essential for the MRE11–NBS1 interaction (4).

The RAD50 sequences (Supplementary Figure S1b) are also well conserved at the amino-acid sequence level, and show good conservation of functionally important domains. The *Physcomitrella* protein contains the characteristic Walker A and Walker B adenosine triphosphatase (ATPase) motifs at either end of the sequence that associate to form a crucially important ATP-binding cassette (27) and that typify the RAD50 protein. These are separated by a long coiled-coil domain with a central CXXC zinc-hook (CPCC in both *Physcomitrella* and *Arabidopsis*) by which pairs of RAD50 proteins interact in the tethering of broken chromosome ends by the MRN/MRX complex (28).

The *Physcomitrella* NBS1 protein (Supplementary Figure S1c) has an N-terminal fork-head associated domain, a partial BRCT domain, and putative SQ-dipeptide phosphorylation sites and conserved MRE11-interacting motifs in the C-terminal region, as identified in all previously identified NBS1 orthologs (4).

Generation of targeted knockouts of the MRN complex genes

We used gene targeting to generate mutant alleles of the *PpMRE11*, *PpRAD50* and *PpNBS1* genes. For the *PpMRE11* and *PpRAD50* genes, two types of mutant were generated: disruption mutants, designated *mre11KO* and *rad50KO*, in which several exons were replaced by an antibiotic selection cassette and deletion mutants, designated *mre11Δ* and *rad50Δ*, in which a number of exons were replaced by a selection cassette that was subsequently removed by *cre-lox* recombination (Figure 1A). For the *PpNBS1* gene, we generated a disruption mutant (*nbs1KO*) and a deletion mutant in which the complete coding sequence was deleted (*nbs1Δ*). Gene targeting events were identified by PCR and Southern blot analyses to identify lines in which precise modification of the target genes had occurred without additional insertion of the targeting constructs at adventitious loci. For the deletion mutants we confirmed by PCR that a portion of the coding regions was removed using primers that flanked the deletion (Supplementary Figure S2). RT-PCR analysis established that the full-length transcripts were no longer produced in the mutants (Figure 1B). For all further experiments, we used two independent disruption or two independent deletion strains which displayed similar phenotypes.

Gene targeting is strongly decreased in *mre11* and *rad50* mutants

The MRN complex is one of the earliest respondents to DNA-DSBs and plays a central role in controlling repair pathway choice between NHEJ and HR (5). The importance of the MRN complex for DSB repair by HR has been shown in *mre11*-deficient chicken DT40 cells in which gene targeting efficiency is strongly reduced (29). In contrast, a somatic hyper-recombination phenotype has been described in the *Arabidopsis rad50* mutant (30). In

order to examine the involvement of the MRN complex in genetic transformation of *Physcomitrella* we determined transformation and gene targeting rates in wild-type, *mre11Δ*, *rad50Δ* and *nbs1KO* cells after transformation with either an homologous vector designed to inactivate the *PpAPT* gene (*PpAPT-KO2* or *PpAPT-KO3*) or a vector sharing no homology with the moss genome (*pBHRF* or *pBNRF*) to determine the rate of untargeted transgene integration. Relative transformation frequency (RTF) was reduced to approximately one-third of the wild-type level in *mre11* and *rad50* mutants, but gene targeting (GT) was reduced by at least an order of magnitude in both *Ppmre11Δ* and *Pprad50Δ* strains compared to WT, while untargeted integration frequencies were approximately double that observed in WT (Table 1). These data demonstrate that an active MRN complex is required to achieve high GT efficiencies in *Physcomitrella*, but that a low level of GT is possible in its absence. They also indicate that the untargeted integration of DNA is still supported following the loss of MRN function but that this pathway is not significantly up-regulated as has been observed to occur in *Pprad51* mutants (17). Noticeably, RTF, GT and untargeted integration rates were unaffected in the *nbs1KO* mutant. These observations suggest that both *PpRAD50* and *PpMRE11*, but not *PpNBS1*, are directly involved in DNA DSB recognition and the targeted integration of transgenes following transformation.

PpMRE11 and *PpRAD50* but not *PpNBS1* are essential for normal growth and development

All the plants containing disruptions or deletions in the *PpMRE11* and *PpRAD50* genes exhibited a severe developmental phenotype (Figure 2). On minimal BCD medium, protonemal growth was strongly reduced and eventually ceased after a month (Figure 2A, C and G). At this stage, colonies comprised both chloronemal and caulonemal cells and carried only a few abortive gametophore initials, whereas WT colonies carried numerous fully differentiated leafy shoots (Figure 2A, C and G). In both mutants, the proportion of chloronemata was enhanced on ammonium tartrate-supplemented medium (BCDAT), which improved protonemal growth (Figure 2B, D and H) and enabled the isolation of numerous protoplasts. The rate of protoplast regeneration was approximately half that of WT (data not shown). Gametophore differentiation was also slightly improved on BCDAT medium, with numerous leafy shoot initials observed in 2-month-old colonies of both mutants (Figure 2E, F, I and J). However, further development into fully expanded leafy shoots was arrested in both strains, although at an earlier stage in *rad50* mutants than in *mre11* mutants (compare Figure 2F and J) and both mutants were thus unable to differentiate reproductive organs. In contrast, all of the *Ppnbs1KO* disruptant lines were indistinguishable from wild-type in both growth rate and developmental progression, producing normal gametophores and viable spores, demonstrating that the disruption of *PpNBS1* was neither detrimental to development nor to meiosis. These data show that a functional MRN complex is essential for normal

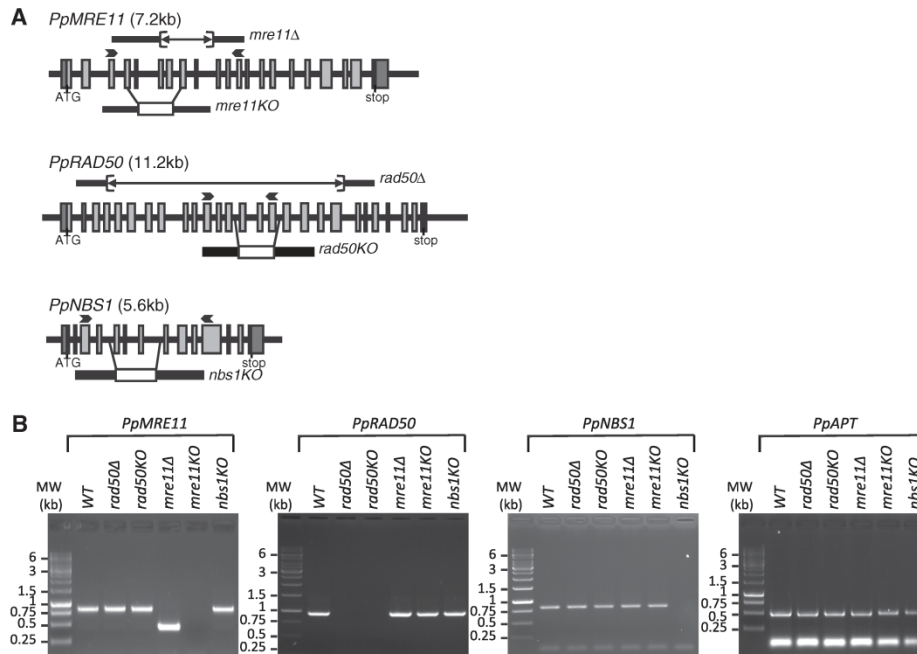


Figure 1. Targeted disruption of *Physcomitrella* MRN genes. (A) Structure of the *PpMRE11*, *PpRAD50* and *PpNBS1* genes. Exons are represented by shaded boxes, with 5'- and 3'-UTR sequences in darker grey. The region deleted by cre-lox excision of a selection cassette is shown as a line above each gene. For the replacement constructs (below each gene) the extent of targeting sequence homology is indicated by the line, and the P35S-*nptII-g6ter* selection cassette is shown as a white box, replacing the genomic region indicated by the lines joining the gene structure diagram and the replacement cassette. Arrows indicate position of primers used for RT-PCR analysis. (B) RT-PCR analysis of MRN transcripts in wild-type and mutant plants. RNA was isolated from protonemal tissue of wild-type and mutant lines for cDNA synthesis and PCR amplification using gene-specific primers (PpMRE11#1+PpMRE11#2 for *MRE11*, PpRAD50#1+PpRAD50#2 for *RAD50*, PpNBS1#1+PpNBS1#2 for *NBS1*). The *PpAPT* transcript has been used as control (primers: PpAPT#14+PpAPT#19). Primers are listed in Supplementary Figure S4.

Table 1. Comparison of transformation and gene targeting efficiencies

Genotypes	PpAPT-KO				pBHRF or pBNRF	
	RTF ^a	Antib ^R	2FA ^R	GT ^b	RTF ^a	Antib ^R
Wild type	1 ± 0.1 ^c	287 (95.7 ± 10.8 ^c)	212 (70.7 ± 11.2 ^c)	73.9 ± 3.3 ^c	0.09 ± 0.04 ^d	14 (7 ± 2.8 ^c)
<i>mre11Δ</i>	0.37 ± 0.1 ^c	81 (27 ± 4 ^c)	6 (2 ± 0.5 ^c)	7.4 ± 1 ^c	0.2 ± 0.01 ^d	34 (17.7 ± 2.8 ^c)
<i>rad50Δ</i>	0.35 ± 0.1 ^c	76 (25.3 ± 4.5 ^c)	4 (1.3 ± 0.6 ^c)	5.3 ± 2.1 ^c	0.17 ± 0.01 ^d	31 (15.5 ± 2.5 ^c)
<i>nbs1Δ</i>	0.94 ± 0.1 ^c	261 (87 ± 5.6 ^c)	178 (59.3 ± 4.5 ^c)	68.2 ± 1.4 ^c	0.17 ± 0.03 ^d	24 (12 ± 1.4 ^c)

^aRelative transformation frequencies (RTF in ^{0/100}) express the frequency of antibiotic-resistant transgenic strains in the whole regenerated population.

^bGT efficiencies (in percentage) express the frequency of 2-FA resistant among the population of antibiotic-resistant transgenic strains.

^cAverage and standard deviation was determined from three independent experiments, each of them performed in duplicates.

^dAverage and standard deviation was determined from two independent experiments, each of them performed in duplicates.

completion of processes involved in development. Noticeably, *PpNBS1* is not required to complete these processes. The similar phenotype displayed by both *rad50* and *mre11* mutants argues for the involvement of the whole MRN complex in these processes. Our data indicate that this complex is involved in the coordination between developmental programme and DNA damage repair and/or cell-cycle control, and future experiments

will assess the molecular mechanisms underlying these MRN functions.

The *mre11* and *rad50* mutants display increased sensitivity to DNA damage but no significant mutator phenotype

Wild-type and *mre11* and *rad50* mutant plants were also analysed for their sensitivity to DNA damaging agents.

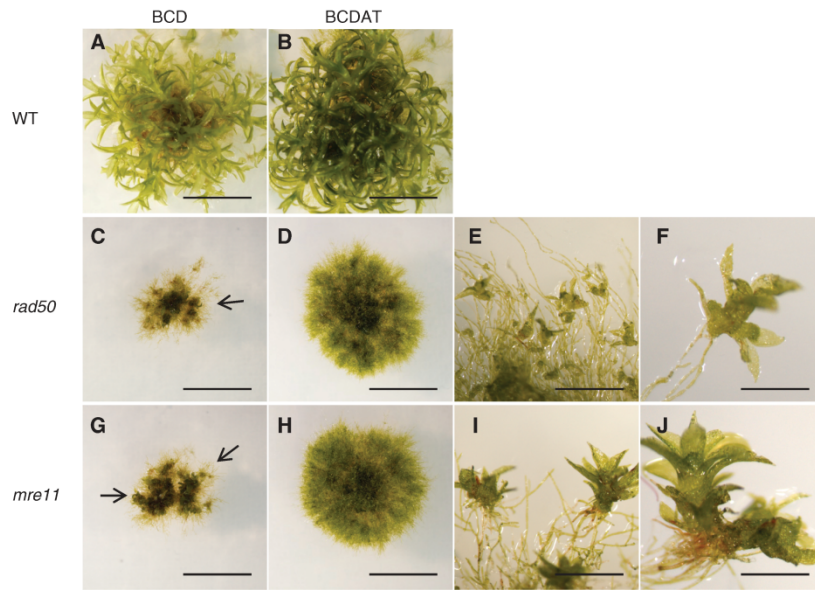


Figure 2. Vegetative developmental phenotypes of *mre11* and *rad50* mutants. WT (A and B), Rad50 7-20 (C–F) and Mre11 1-195 (G–J) 30-day-old colonies grown on BCD (A, C and G) or BCDAT (B, D and H) medium, scale 1 cm. (E, F, I and J) aborted gametophores observed at the edge of 2-month-old colonies grown on BCDAT, scale bar 500 mm in E and I, 200 mm in F and J.

Sensitivity of mutants and WT strains to UV-B (308 nm) was investigated using a protoplast survival assay (17). Both strains displayed increased sensitivity to UV-B compared to the WT (Figure 3). We further investigated sensitivity of the mutants to the DSB inducing agent bleomycin. We first monitored the growth of WT and mutant explants submitted to chronic exposure to different concentrations of bleomycin over a 3-week period. In WT and *nbs1KO* strains, growth was impaired at low doses (1–40 ng/ml), whilst higher concentrations (200 ng/ml–1 µg/ml) were lethal (Figure 4A and Supplementary Figure S3). In contrast, *Ppmre11* and *Pprad50* disruption and deletion mutants displayed hypersensitivity to bleomycin. At concentrations below 8 ng/ml, little or no growth took place, although the tissue remained green. At or above this concentration, all *mre11* and *rad50* mutant lines were killed (Figure 4A, Supplementary Figure S3A and B).

We tested the acute toxicity of bleomycin in wild type and of the different mutants at the cellular level. Following incubation for 1 h with increasing concentrations of bleomycin, the ability of protoplasts to divide and regenerate into colonies was assessed by subculture on drug-free medium. Survival was calculated as the ratio of protoplasts surviving after 15 days regeneration following treatment to the number of protoplasts undergoing normal regeneration without treatment. The LD50 for the wild type and *nbs1* mutant was about 500 ng/ml bleomycin, whereas the *mre11* and

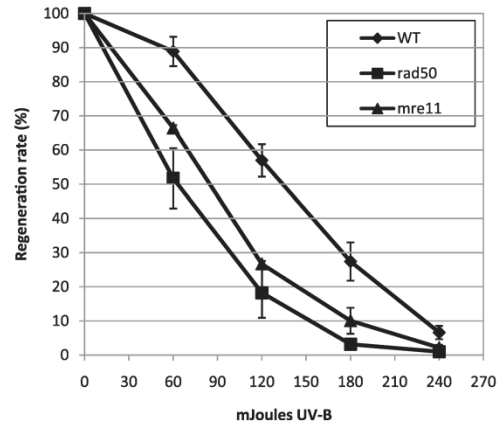


Figure 3. Hypersensitivity of the *rad50* and *mre11* mutants to UV-B treatment. Survival curves of wild type and *rad50* and *mre11* mutant protoplasts regenerating after exposure to UV-B treatment. Wild-type survival is represented with diamonds, *rad50* mutant survival is represented with squares and *mre11* mutant survival is represented with triangles. Error bars indicate SDs based on at least two independent experiments in all cases.

rad50 cells were more sensitive, with an LD50 of ~50 ng/ml (Figure 4B). The *mre11* and *rad50* cells were even more sensitive than the *rad51-1-2* double mutant, already described as hypersensitive to bleomycin (16).

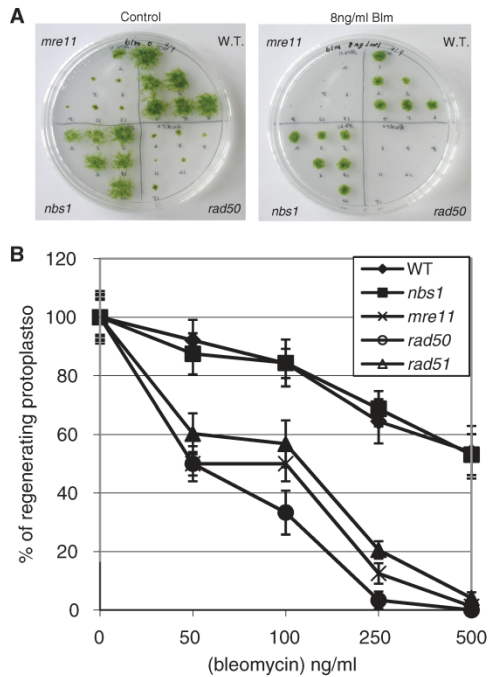


Figure 4. Hypersensitivity of the *rad50* and *mre11* mutants to bleomycin. (A) Wild-type and mutant plants were inoculated as six explants into quadrants of plates containing standard growth medium with or without bleomycin at 8 ng ml^{-1} . For the mutant strains, each inoculum represents an independent disruption line. The photograph illustrates the extent of growth 10 days following inoculation of the explants. (B) Survival curves of wild type and *nbs1*, *mre11*, *rad50* and *rad51* mutant protoplasts regenerating after exposure to bleomycin treatment. Error bars indicate SD based on at least two independent experiments in all cases.

Acute treatment of intact protonemal tissue also adversely affected the subsequent growth rate of the recovering protonemata, with the *mre11* and *rad50* mutants being more sensitive to bleomycin than the wild type (Supplementary Figure S3C).

Mutator phenotypes in the absence of proteins essential for HR have been described in *S. cerevisiae* or *A. nidulans* (31,32). We therefore evaluated the mutator phenotype of the moss MRN mutants to assess their ability to repair endogenous DNA damage, using as reporter loss of function of the adenine phosphoribosyl transferase gene (*PpAPT*) as previously described (18). The frequencies of *apt* mutations were lower than 3×10^{-7} in wild type, *rad50* and *nbs1* mutants, was 4×10^{-7} for *mre11* but was ~ 100 -fold higher (3.3×10^{-5}) in *msh2* mutants (Supplementary Table S3), which is in good accordance with previous results obtained with this mutant (18). These results indicate that loss of proteins of the MRN complex does not lead to a significant mutator phenotype in *P. patens*. It is most likely that DNA-DSB repair defects in the *mre11* and *rad50* mutants cause genomic damage so much more severe than

the point mutations seen in the *msh2* mutant that cell death results.

DNA-DSB repair is not affected in *mre11* and *rad50* mutants

Gene targeting in the *mre11* and *rad50* mutants was severely impaired, while untargeted integration frequencies were 2-fold higher than those observed in WT. Since the *rad50* and *mre11* mutants were clearly impaired in growth and hypersensitive to DNA damage, we reasoned that the mutants remained capable of ligating broken ends of DNA molecules, but in an 'unsupervised', and therefore inaccurate manner. We tested this by directly estimating the ability of wild-type and mutant strains to repair DNA damage following acute exposure to bleomycin using single nucleus gel electrophoresis (the 'comet assay'). Treatment with bleomycin for 1 h resulted in a linear, dose-dependent fragmentation of genomic DNA in both wild-type and mutant lines, with the *rad50* and *mre11* lines exhibiting a greater susceptibility to DNA damage than the wild-type and *Ppnbs1* lines, respectively (Figure 5A). The rate of repair of DSBs was determined by measuring the proportion of fragmented DNA at intervals during a recovery period.

Both wild-type and mutant lines exhibited similarly high rates of DNA repair with a characteristic biphasic profile: an initial rapid phase ($t_{1/2}$ 1–4 min) accounting for $\sim 60\%$ of the fragmented DNA, followed by a slower phase ($t_{1/2}$ 7–90 min) accounting for the remainder (Figure 5B, Table 2). The rate of DNA repair was closely correlated with the age of the protonemal tissue following subculture. Tissue that was homogenized and subcultured for only 1 day comprised largely short protonemal fragments, four to seven cells in length. This tissue exhibited the most rapid repair kinetics (Figure 5B, Table 2). Tissue that was subcultured for 1 week comprised longer filaments 15–20 cells in length, whilst after subculture for 2 weeks, the filaments were over 30 cells long. These tissues were progressively slower in their DNA repair kinetics (Figure 5C, Table 2) with an increasing proportion of the DNA-DSBs being repaired with slow-phase kinetics. We ascribe these age-related differences to the relative representation of apical cells within the protonemal population. *Physcomitrella* protonemata grow by serial division of the apical cells, so that in a 1d-subcultured homogenate, we estimate the proportion of mitotically active apical cells to comprise 30–50% of the total cell population. This proportion will be 10–15% in 7d-subcultured tissue, and $\sim 3\%$ in 14d-subcultured protonemata. Thus, the initial rapid phase of DNA repair can be accounted for by processes undertaken in the mitotically competent apical cells, whilst the slow-phase repair kinetics is likely due to processes carried out in mitotically inactive subapical cells.

Although differences can be seen in the rates of DNA repair between mutant and wild-type strains, these are not dramatic. Clearly, the extensive fragmentation of DNA that occurs during the initial bleomycin treatment is being rapidly reversed, even in mutants in which

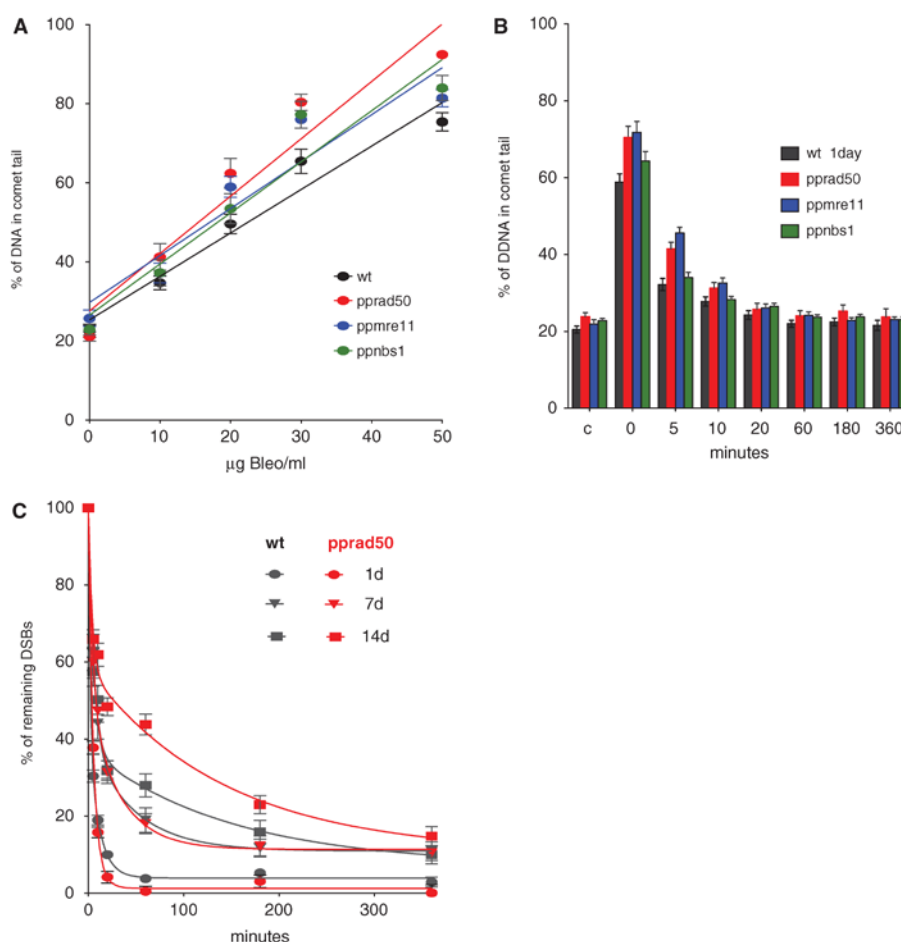


Figure 5. Kinetics of DNA repair in wild-type and mutant plants. (A) Bleomycin dose-response. Protonemal tissue from wild-type and mutant lines was treated with bleomycin for 1 h at the indicated concentrations, prior to nuclear extraction and the analysis of DNA damage by single-cell electrophoresis (the 'comet assay'). The extent of DNA damage is indicated by the proportion of DNA detected in the fragmented fraction (the 'comet tail'). The background level of genomic DNA damage in all lines is similar, at between 20 and 30%, indicating that the mutations have no significant effect on natural levels of DNA fragmentation. (B) Repair kinetics in 1-day regenerated protonemata. In both wild-type and mutant lines, the fragmentation of DNA induced by bleomycin is repaired with rapid kinetics ($t_{1/2}$ between 1 and 4 min). (C) Repair kinetics in relation to protonemal age. As protonemata are regenerated for longer periods (resulting in a concomitant reduction in the proportion of mitotically active apical cells), so the proportion of the rapid phase DNA repair declines. This occurs in both the wild-type and the *rad50KO* mutant lines.

Table 2. Kinetics of DNA repair in wild-type and mutant strains

Genotypes	Tissue age	$t_{1/2}$ fast (min)	% fast	$t_{1/2}$ slow (min)
wild-type	1d	1.2	61.4	7.6
wild-type	7d	4.0	67.6	32.9
wild-type	14d	3.8	67.7	103.4
<i>mre11KO</i>	1d	4.1	96.5	84.1
<i>nbs1KO</i>	1d	1.9	84.1	17.0
<i>rad50KO</i>	1d	2.9	71.4	5.6
<i>rad50KO</i>	7d	2.9	52.6	18.2
<i>rad50KO</i>	14d	2.7	46.8	100.0

components of the principal DNA surveillance and repair system for both HR and NHEJ-mediated repair (PpMRE11 and PpRAD50) have been eliminated.

MRN mutants exhibit enhanced repair gene expression

One possibility is that in the absence of a viable MRN complex, DNA-DSBs are repaired, but in an 'unsupervised' manner. In the absence of the tethering function to hold broken ends in close proximity, repair may be

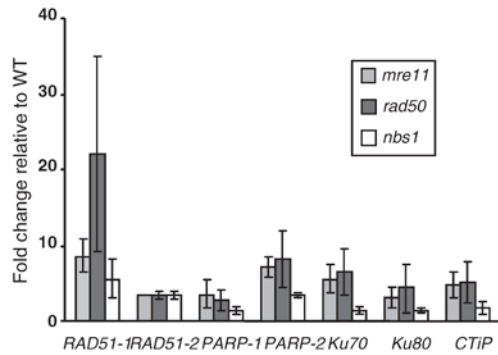


Figure 6. Gene expression analysis of DNA repair genes in the MRN mutants. Quantitative determination of the relative abundances of transcripts encoding DNA repair genes (*PpRad51-1*, *PpRad51-2*, *PpPARP-1*, *PpPARP-2*, *PpKu70*, *PpKu80* and *PpCtIP*) in 7-day-old wild-type, *Ppmre11KO*, *Pprad50KO* and *Ppnbs1KO* strains was done by quantitative real-time PCR. Relative transcript abundance was calculated using the $\Delta\Delta C_t$ method and normalized to the wild-type value. Error bars indicate SD based on at least three independent experiments with two replicates for each sample in all cases.

inaccurate, generating increased numbers of deletions and promoting end joining between inappropriate ends, resulting in increased disruption of essential genes and consequent loss of viability and cell death. Analysis of the expression of a selection of DNA repair genes, implicated in HR, NHEJ and alternative end-joining processes, showed a significantly enhanced accumulation of repair gene transcripts in MRN mutants relative to wild-type, and this was most marked in the *Ppmre11KO* and *Pprad50KO* mutants (Figure 6). This suggests that in the absence of a functional MRN complex, the cell initiates an emergency response by the rest of the DNA repair machinery. The levels of induction of the repair genes observed in the mutant lines are comparable to those seen in wild-type protonemal tissue in response to DNA-DSB induction by bleomycin (Whitaker, J., personal communication).

We then directly tested the nature of DNA repair in an MRN mutant line, by screening a series of *apt* mutants generated by bleomycin treatment of both wild-type and the *Pprad50KO* mutant. Sublethal doses of bleomycin, determined by growth tests of bleomycin-treated protonemal tissue (Supplementary Figure S3C), were used to generate mutants selected on the basis of resistance to 2-FA. The mutability of the *PpAPT* gene in the *Pprad50KO* line was observed to be at least an order of magnitude greater than that in the wild type (Supplementary Table S2). The nature of the induced mutations was examined by PCR-amplification and sequencing of the *APT* gene from a number of lines. For wild-type, each mutant analysed contained only point mutations within the *APT* coding sequence and introns (Table 3). In contrast, three of the seven mutants analysed in the *Pprad50KO* background contained deletions, varying in length between 10 and 747 bp (Table 3). This supports our working hypothesis that

MRN-supervised repair generates more severe forms of genomic damage.

DISCUSSION

GT Efficiency is reduced in the *Physcomitrella rad50* and *mre11* mutants

In *Physcomitrella* the protein at the heart of the HR pathway, PpRAD51, is required simultaneously to enable targeted integration by HR, and to repress untargeted integration by an as yet unidentified molecular mechanism (17). The unique GT efficiency of *Physcomitrella* suggests that DNA DSBs are predominantly repaired by HR in moss cells. Our analysis of mutants in the principal sensor of DNA DSBs, the MRN complex, further shows that although a fully active MRN complex clearly appears to be necessary for high-efficiency targeted transgene integration, a background level of HR with gene targeting reduced to ~8.6% of wt is still maintained in the absence of either a functional PpMRE11 or PpRAD50 protein. This contrasts with the complete abolition of gene targeting seen in *rad51* null mutants, a component specific to the HR pathway (17). Noticeably the overall frequency of untargeted transgene integration is not reduced in the *mre11* and *rad50* mutants relative to wild type (Table 1), implying that whatever mechanisms undertake random transgene integration, these are relatively unimpaired in the absence of PpMRE11 or PpRAD50. Together with the observation that a number of DNA repair genes show enhanced expression levels in *mre11* and *rad50* mutants, our results suggest that while some HR-mediated repair may still operate in *mre11* and *rad50* mutants, the HR pathway is unlikely to account for the majority of the DNA-DSBs that are rapidly religated in these mutants.

NBS1 is not required for growth and development or for HR in *Physcomitrella*

Phenotypic analyses of mutants in the MRN complex in moss failed to identify a detectable difference between wild-type and *Ppnbs1* knock-outs. In eukaryotes, the MRN-complex proteins act as the 'gatekeepers' of the DNA-DSB response, directing the repair of DSBs into either the NHEJ or HR pathways through the activation of the ATM or ATR kinases that (in mammalian cells) are recruited to sites of DNA damage through analogous mechanisms involving conserved interaction motifs (6). The NBS1 protein is involved in the recruitment of ATM to DNA-DSBs and ATRIP is involved in the recruitment of ATR to single-stranded DNA (ssDNA). The recruitment of ATM is mediated by its direct interaction with NBS1 which becomes phosphorylated at residues conserved between the *Arabidopsis* and *Physcomitrella* NBS1 sequences (6,33). In *A. thaliana*, *nbs1/atm* double mutants appear additive in their negative consequences for growth and fertility relative to the wild-type and single mutants (34). ATM is necessary for the imposition of a cell-cycle checkpoint, and for the induction of DNA-damage-responsive gene expression in *Arabidopsis*, in which the principal DNA repair pathway is through NHEJ (33,35). DNA repair in *Physcomitrella* is believed

Table 3. Mutations identified in the *APT* genomic sequence in wild-type and *Pprad50-KO* 2-FA resistant clones

Clone#	Genotype	Mutations in CDS		Mutations in introns	
		Point mutations	Deletions ^a	Point mutations	Deletions ^a
1	<i>rad50 apt</i>	+ T (2095) ^a		+ T (1683) ^a Δ T (2517) ^a	–
2	<i>rad50 apt</i>	Δ T (1706) ^a	1450–1455	+ T (1683) ^a	–
3	<i>rad50 apt</i>	A to T (1461) ^a G to C (1534) ^a	1466–1521	+ T (1683) ^a	–
4	<i>rad50 apt</i>	T to C (1291) ^a C to G (1752) ^a Δ T (1730) ^a Δ G (1524) ^a		Δ G (1524) ^a + T (1683) ^a + T (2517) ^a + T (1683) ^a	–
5	<i>rad50 apt</i>		–		–
7	<i>rad50 apt</i>	–	1050–1797	–	–
11	<i>RAD50 apt</i>	A to G (1491) ^a A to C (1498) ^a	–	Δ A (1052) ^a T to C (2330) ^a G to C (2327) ^a + GT (2328) ^a Δ A (1052) ^a T to G (1376) ^a C to A (1569) ^a + G (2328) ^a	–
12	<i>RAD50 apt</i>	–	–	+ G (2328) ^a Δ A (1052) ^a T to G (1376) ^a C to A (1569) ^a + G (2328) ^a	–
13	<i>RAD50 apt</i>	A to C (2475) ^a Δ T (2499) ^a	–	A to T (1591) ^a	–

^aPosition 1 corresponds to the first nucleotide in the genomic *PpAPT* sequence DQ117987.

to operate primarily via the HR pathway, which in mammalian cells, at least, depends principally on the activity of the ATR kinase. Thus, impairment of ATM-related signalling in the *Ppnbs1KO* mutant may have relatively little impact on growth and fertility, if NHEJ is subordinate to HR. This conclusion is also supported by the observation that HR-dependent gene targeting is unaffected in the *Ppnbs1KO* mutant. In contrast, NBS1 has been shown to be essential to HR in chicken DT40 cells, possibly by processing recombination intermediates (36) and in human cells recruitment of ATR to sites of DNA damage is dependent on ATM (37). This implies that in *Physcomitrella* NBS1 may not be involved in the production of single-stranded tails that are the substrates for HR and that induction of the HR pathway, potentially by the ATR signalling, is independent of ATM. In this respect *Physcomitrella* would more resemble budding yeast than mammals, as Tel1, the yeast equivalent of ATM, has only minor effects on end-processing and is not required for focus formation by Mec1, the yeast homolog of ATR (38,39). Alternatively, despite the conservation of the ATM interaction domain in the PpNBS1 protein, ATM activation might be independent of NBS1 in *Physcomitrella*. In this context, it would be of interest to study the exact roles of ATM and ATR in *Physcomitrella*.

RAD50 and MRE11 are essential for growth and development in *Physcomitrella*

Null mutants in any components of the MRN complex are lethal in vertebrates (5) and are severely compromised in both budding (40) and fission yeast (41). This is not the case in plants: in *Arabidopsis*, *AtRad50* and *AtMre11* mutants are impaired in growth, fertility and in their ability to recover from genotoxic stress (42,43), whereas *Atnbs1* mutant plants grow normally and are fully fertile

but are sensitive to the DNA cross-linking agent, mitomycin C (34).

Our analyses show that defects in the MRN complex can adversely affect moss development. While the *Ppnbs1KO* mutant completed its life cycle normally and displayed wild-type levels of susceptibility to DNA damage, the *Ppmre11* and *Pprad50* strains displayed a strong and similar developmental phenotype. This included defects in cell viability (reduced protoplast regeneration rates), in cell-cycle progression and cell growth (reduced colony growth) and in the completion of a complex developmental programme (abortive leafy shoot development). Precocious arrest of colony growth was also observed on minimal medium, which most likely reflects early senescence. This pleiotropic phenotype is much stronger than that observed in the HR-deficient *Pprad51* mutants (16,17) and implies that genome integrity is more severely impaired by loss of function of the MRN complex than by the inactivation of the HR pathway. The phenotype of *Ppmre11* and *Pprad50* mutants also differs from that previously reported for *Ppmsh2* mutants which do not display a strong juvenile phenotype but accumulate mutations and phenotypic alterations during development (18). Noticeably both *Pprad51* and *Ppmsh2* mutants also displayed a detectable mutator phenotype that is absent in *Ppmre11* and *Pprad50*, probably because MRN mutants accumulate a more extensive and harmful type of DNA damage that accelerates senescence.

Induced DSBs in *Physcomitrella* can be repaired via a mechanism independent of the MRN complex

Direct analysis of DNA-DSB repair by single-cell electrophoresis showed little difference in the rate of repair of DNA-DSBs in the *mre11* and *rad50* mutants compared to

wild type. Whilst some HR-mediated transgene integration still occurs in *mre11* and *rad50* mutants, it is unlikely that single-strand annealing (SSA) or homologous strand exchange (HR), which require end-processing, account for this rapid religation. Therefore, the repair of DSBs in the *mre11* and *rad50* mutants probably occurs via a pathway related to NHEJ. However, the reduced growth and survival of these mutants indicate that such a pathway reduces the genetic stability characteristic of MRN-supervised DNA repair.

Two different NHEJ pathways have been already described, the highly efficient canonical Ku- and DNA ligase IV-mediated NHEJ pathway (C-NHEJ) in which most ends are successfully rejoined without alteration of DNA sequence information (44) and an evolutionarily conserved alternative end-joining pathway (A-NHEJ) (45) thought to proceed via microhomology-mediated end joining (MMEJ), even if the relationship between A-NHEJ and MMEJ is still unclear (45). A-NHEJ represents a major source of DSB-induced genome rearrangements (translocations, deletions and inversions) (46–48) and appears to utilize binding of DNA ends by PARP-1 (polyADP ribose polymerase) and ligation by DNA Ligase III in a Ku-independent process (49,50) and involve the interaction between the MRN complex and DNA ligase III α /XRCC1 (51). The function of DNA ligase III is absent in plants, being substituted by DNA ligase I in base-excision repair (52). It may therefore be significant that the *Ppmre11* and *Pprad50* mutants show substantially elevated levels of expression of PARP and other DNA-repair associated genes, relative to the wild type, and this elevated gene expression may be responsible for the activity of an A-NHEJ repair pathway in the absence of an active MRN complex. Existence of A-NHEJ in plants has been inferred from observations that although the frequency of transgene insertion was reduced in mutants deficient in NHEJ components such as *Atku80* and *AtligIV*, it was not abolished (53–55), from the observation of illegitimate fusions between chromosome arms in telomerase-deficient *Arabidopsis*, even in an *Atku80/Atmre11* mutant background (56), from the recent demonstration of rapid ligation of bleomycin-induced DNA-DSBs in the NHEJ-deficient *Atku80* and *Atlig4* mutants (57) and from kinetic measurements of assembly and processing of DSB-specific γ -H2AX complexes in *Arabidopsis* mutants deficient in core components of the C-NHEJ and A-NHEJ pathways (58). In budding yeast both C-NHEJ and A-NHEJ are MRX-dependent processes, with the exonuclease activity of Mre11 playing an important role (59–62), whilst in vertebrates varying roles for MRN complex components have been reported (63–66). Whatever the role of the MRN complex in C-NHEJ or A-NHEJ in plants, it is likely that an NHEJ-like pathway mediates the rapid DSB repair observed in *Physcomitrella mre11* and *rad50* mutants. However, because these mutants are clearly hypersensitive to DNA damage yet do not show a mutator phenotype, it would appear that whatever rejoining of DNA ends is occurring, it is 'unsupervised' and results in genomic perturbations so severe that cells suffering bleomycin-induced breakage soon die.

The rapid interaction of the MRN complex with DNA-DSBs is essential for their stabilization, through the tethering of the adjacent free ends by the Rad50 coiled-coil/zinc hook domains (5). By retaining broken ends in close proximity, the MRN complex thereby supervises the DNA repair process, ensuring that the correct ends are rejoined, and recruiting additional factors required for either NHEJ or HR-based repair. In the absence of such tethering, unsupervised end-joining by backup pathways might occur between unrelated DNA sequences, with the concomitant accumulation of cytotoxic mutations accounting for the reduced rates of growth and enhanced sensitivity to DNA-damaging agents observed in the *Ppmre11* and *Pprad50* mutants. Combinations of mutations affecting C- or A-NHEJ (58) with *mre11* or *rad50* mutations should give us insight into the mechanism behind this DSB DNA repair.

ACCESSION NUMBERS

JF820817, JF820820, JF82018, JF82021, JF82019, JF82022.

SUPPLEMENTARY DATA

Supplementary Data are available at NAR Online: Supplementary Tables 1–3, Supplementary Figures 1–4.

FUNDING

Institut National de la Recherche Agronomique, Agence Nationale de la Recherche (Grant number ANR GNP05008G to F.N.); the UK Biotechnology and Biological Sciences Research Council (Grant number BB/I006710/1 to A.C.C. and Y.K.); the Swiss National Science Foundation (Grant number 31003A_127572 to D.S.); and the Ministry of Education, Youth and Sports of the Czech Republic (projects LC06004 and 1M0505; EU 6FP projects TAGIP LSH-2004_1.1.0-1 and COMICS LSHB-CT-2006-037575 to K.J.A., J.K. and M.H.). Funding for open access charge: Agence Nationale de la Recherche (Grant number ANR GNP05008G).

Conflict of interest statement. None declared.

REFERENCES

- San Filippo, J., Sung, P. and Klein, H. (2008) Mechanism of eukaryotic homologous recombination. *Annu. Rev. Biochem.*, **77**, 229–257.
- Aravind, L., Walker, D.R. and Koonin, E.V. (1999) Conserved domains in DNA repair proteins and evolution of repair systems. *Nucleic Acids Res.*, **27**, 1223–1242.
- Mimitou, E.P. and Symington, L.S. (2009) DNA end resection: many nucleases make light work. *DNA Repair*, **8**, 983–995.
- Rupnik, A., Lowndes, N.F. and Grenon, M. (2010) MRN and the race to the break. *Chromosoma*, **119**, 115–135.
- Stracker, T.H., Theunissen, J.W., Morales, M. and Petrini, J.H. (2004) The Mre11 complex and the metabolism of chromosome breaks: the importance of communicating and holding things together. *DNA Repair*, **3**, 845–854.

6. Falck, J., Coates, J. and Jackson, S.P. (2005) Conserved modes of recruitment of ATM, ATR and DNA-PKcs to sites of DNA damage. *Nature*, **434**, 605–611.
7. Lamarche, B.J., Orazio, N.I. and Weitzman, M.D. (2010) The MRN complex in double-strand break repair and telomere maintenance. *FEBS Lett.*, **584**, 3682–3695.
8. Hanin, M. and Paszkowski, J. (2003) Plant genome modification by homologous recombination. *Curr. Opin. Plant Biol.*, **6**, 157–162.
9. Britt, A.B. and May, G.D. (2003) Re-engineering plant gene targeting. *Trends Plant Sci.*, **8**, 90–95.
10. Ray, A. and Langer, M. (2002) Homologous recombination: ends as the means. *Trends Plant Sci.*, **7**, 435–440.
11. Tzfira, T., Li, J., Lacroix, B. and Citovsky, V. (2004) Agrobacterium T-DNA integration: molecules and models. *Trends Genet.*, **20**, 375–383.
12. Schaefer, D.G. and Zryd, J.P. (1997) Efficient gene targeting in the moss *Physcomitrella patens*. *Plant J.*, **11**, 1195–1206.
13. Schaefer, D.G. (2001) Gene targeting in *Physcomitrella patens*. *Curr. Opin. Plant Biol.*, **4**, 143–150.
14. Kamisugi, Y., Cuming, A.C. and Cove, D.J. (2005) Parameters determining the efficiency of gene targeting in the moss *Physcomitrella patens*. *Nucleic Acids Res.*, **33**, e173.
15. Kamisugi, Y., Schlink, K., Rensing, S.A., Schween, G., von Stackelberg, M., Cuming, A.C., Reski, R. and Cove, D.J. (2006) The mechanism of gene targeting in *Physcomitrella patens*: homologous recombination, concatenation and multiple integration. *Nucleic Acids Res.*, **34**, 6205–6214.
16. Markmann-Mulisch, U., Wendeler, E., Zobell, O., Schween, G., Steinbiss, H.H. and Reiss, B. (2007) Differential requirements for RAD51 in *Physcomitrella patens* and *Arabidopsis thaliana* development and DNA damage repair. *Plant Cell*, **19**, 3080–3089.
17. Schaefer, D.G., Delacote, F., Charlot, F., Vrielynck, N., Guyon-Debast, A., Le Guin, S., Neuhaus, J.M., Doutriaux, M.P. and Nogue, F. (2010) RAD51 loss of function abolishes gene targeting and de-represses illegitimate integration in the moss *Physcomitrella patens*. *DNA Repair*, **9**, 526–533.
18. Trouiller, B., Schaefer, D.G., Charlot, F. and Nogue, F. (2006) MSH2 is essential for the preservation of genome integrity and prevents homeologous recombination in the moss *Physcomitrella patens*. *Nucleic Acids Res.*, **34**, 232–242.
19. Knight, C.D., Cove, D.J., Cuming, A.C. and Quatrano, R.S. (2002) *Molecular Plant Biology*, Vol. 2. Oxford University Press, Oxford, pp. 285–299.
20. Schaefer, D., Zryd, J.P., Knight, C.D. and Cove, D.J. (1991) Stable transformation of the moss *Physcomitrella patens*. *Mol. Gen. Genet.*, **226**, 418–424.
21. Kamisugi, Y. and Cuming, A.C. (2005) The evolution of the abscisic acid-response in land plants: comparative analysis of group I LEA gene expression in moss and cereals. *Plant Mol. Biol.*, **59**, 723–737.
22. Futers, T.S., Onde, S., Turet, M. and Cuming, A.C. (1993) Sequence analysis of two tandemly linked Em genes from wheat. *Plant Mol. Biol.*, **23**, 1067–1072.
23. Abramoff, M.D., Magalhaes, P.J. and Ram, S.J. (2004) Image Processing with ImageJ. *Biophotonics Int.*, **11**, 36–42.
24. Olive, P.L. and Banath, J.P. (2006) The comet assay: a method to measure DNA damage in individual cells. *Nat. Protoc.*, **1**, 23–29.
25. Angelis, K.J., Dusinska, M. and Collins, A.R. (1999) Single cell gel electrophoresis: detection of DNA damage at different levels of sensitivity. *Electrophoresis*, **20**, 2133–2138.
26. Menke, M., Chen, I., Angelis, K.J. and Schubert, I. (2001) DNA damage and repair in *Arabidopsis thaliana* as measured by the comet assay after treatment with different classes of genotoxins. *Mutat. Res.*, **493**, 87–93.
27. Moncalian, G., Lengsfeld, B., Bhaskara, V., Hopfner, K.P., Karcher, A., Alden, E., Tainer, J.A. and Paull, T.T. (2004) The rad50 signature motif: essential to ATP binding and biological function. *J. Mol. Biol.*, **335**, 937–951.
28. Hopfner, K.P., Craig, L., Moncalian, G., Zinkel, R.A., Usui, T., Owen, B.A., Karcher, A., Henderson, B., Bodmer, J.L., McMurray, C.T. et al. (2002) The Rad50 zinc-hook is a structure joining Mre11 complexes in DNA recombination and repair. *Nature*, **418**, 562–566.
29. Yamaguchi-Iwai, Y., Sonoda, E., Sasaki, M.S., Morrison, C., Haraguchi, T., Hiraoka, Y., Yamashita, Y.M., Yagi, T., Takata, M., Price, C. et al. (1999) Mre11 is essential for the maintenance of chromosomal DNA in vertebrate cells. *EMBO J.*, **18**, 6619–6629.
30. Gherbi, H., Gallego, M.E., Jalut, N., Lucht, J.M., Hohn, B. and White, C.I. (2001) Homologous recombination in planta is stimulated in the absence of Rad50. *EMBO Rep.*, **2**, 287–291.
31. Prakash, L. (1976) The relation between repair of DNA and radiation and chemical mutagenesis in *Saccharomyces cerevisiae*. *Mutat. Res.*, **41**, 241–248.
32. Seong, K.Y., Chae, S.K. and Kang, H.S. (1997) Cloning of an *E. coli* RecA and yeast RAD51 homolog, radA, an allele of the uvsC in *Aspergillus nidulans* and its mutator effects. *Mol. Cells*, **7**, 284–289.
33. Garcia, V., Bruchet, H., Camescasse, D., Granier, F., Bouchez, D. and Tissier, A. (2003) AtATM is essential for meiosis and the somatic response to DNA damage in plants. *Plant Cell*, **15**, 119–132.
34. Waterworth, W.M., Altun, C., Armstrong, S.J., Roberts, N., Dean, P.J., Young, K., Weil, C.F., Bray, C.M. and West, C.E. (2007) NBS1 is involved in DNA repair and plays a synergistic role with ATM in mediating meiotic homologous recombination in plants. *Plant J.*, **52**, 41–52.
35. Culligan, K.M., Robertson, C.E., Foreman, J., Doerner, P. and Britt, A.B. (2006) ATR and ATM play both distinct and additive roles in response to ionizing radiation. *Plant J.*, **48**, 947–961.
36. Tauchi, H., Kobayashi, J., Morishima, K., van Gent, D.C., Shiraishi, T., Verkaik, N.S., van Heems, D., Ito, E., Nakamura, A., Sonoda, E. et al. (2002) Nbs1 is essential for DNA repair by homologous recombination in higher vertebrate cells. *Nature*, **420**, 93–98.
37. Adams, K.E., Medhurst, A.L., Dart, D.A. and Lakin, N.D. (2006) Recruitment of ATR to sites of ionising radiation-induced DNA damage requires ATM and components of the MRN protein complex. *Oncogene*, **25**, 3894–3904.
38. Dubrana, K., van Attikum, H., Hediger, F. and Gasser, S.M. (2007) The processing of double-strand breaks and binding of single-strand-binding proteins RPA and Rad51 modulate the formation of ATR-kinase foci in yeast. *J. Cell. Sci.*, **120**, 4209–4220.
39. Mantiero, D., Clerici, M., Lucchini, G. and Longhese, M.P. (2007) Dual role for *Saccharomyces cerevisiae* Tel1 in the checkpoint response to double-strand breaks. *EMBO Rep.*, **8**, 380–387.
40. Wasko, B.M., Holland, C.L., Resnick, M.A. and Lewis, L.K. (2009) Inhibition of DNA double-strand break repair by the Ku heterodimer in mrx mutants of *Saccharomyces cerevisiae*. *DNA Repair*, **8**, 162–169.
41. Raji, H. and Hartsuiker, E. (2006) Double-strand break repair and homologous recombination in *Schizosaccharomyces pombe*. *Yeast*, **23**, 963–976.
42. Bundock, P. and Hooykaas, P. (2002) Severe developmental defects, hypersensitivity to DNA-damaging agents, and lengthened telomeres in *Arabidopsis* MRE11 mutants. *Plant Cell*, **14**, 2451–2462.
43. Gallego, M.E., Jeanneau, M., Granier, F., Bouchez, D., Bechtold, N. and White, C.I. (2001) Disruption of the *Arabidopsis* RAD50 gene leads to plant sterility and MMS sensitivity. *Plant J.*, **25**, 31–41.
44. Boulton, S.J. and Jackson, S.P. (1996) *Saccharomyces cerevisiae* Ku70 potentiates illegitimate DNA double-strand break repair and serves as a barrier to error-prone DNA repair pathways. *EMBO J.*, **15**, 5093–5103.
45. McVey, M. and Lee, S.E. (2008) MMEJ repair of double-strand breaks (director's cut): deleted sequences and alternative endings. *Trends Genet.*, **24**, 529–538.
46. Gao, Y., Ferguson, D.O., Xie, W., Manis, J.P., Sekiguchi, J., Frank, K.M., Chaudhuri, J., Horner, J., DePinho, R.A. and Alt, F.W. (2000) Interplay of p53 and DNA-repair protein XRCC4 in tumorigenesis, genomic stability and development. *Nature*, **404**, 897–900.
47. Guirouilh-Barbat, J., Rass, E., Plo, J., Bertrand, P. and Lopez, B.S. (2007) Defects in XRCC4 and KU80 differentially affect the joining of distal nonhomologous ends. *Proc. Natl Acad. Sci. USA*, **104**, 20902–20907.

48. Weinstock,D.M., Brunet,E. and Jasin,M. (2007) Formation of NHEJ-derived reciprocal chromosomal translocations does not require Ku70. *Nat. Cell. Biol.*, **9**, 978–981.
49. Audebert,M., Salles,B. and Calsou,P. (2004) Involvement of poly(ADP-ribose) polymerase-1 and XRCC1/DNA ligase III in an alternative route for DNA double-strand breaks rejoining. *J. Biol. Chem.*, **279**, 55117–55126.
50. Haber,J.E. (2008) Alternative endings. *Proc. Natl Acad. Sci. USA*, **105**, 405–406.
51. Della-Maria,J., Zhou,Y., Tsai,M.S., Kuhnlein,J., Carney,J.P., Paull,T.T. and Tomkinson,A.E. (2011) Human Mre11/human Rad50/Nbs1 and DNA ligase IIIalpha/XRCC1 protein complexes act together in an alternative nonhomologous end joining pathway. *J. Biol. Chem.*, **286**, 33845–33853.
52. Waterworth,W.M., Kozak,J., Provost,C.M., Bray,C.M., Angelis,K.J. and West,C.E. (2009) DNA ligase I deficient plants display severe growth defects and delayed repair of both DNA single and double strand breaks. *BMC Plant Biol.*, **9**, 79.
53. Friesner,J. and Britt,A.B. (2003) Ku80- and DNA ligase IV-deficient plants are sensitive to ionizing radiation and defective in T-DNA integration. *Plant J.*, **34**, 427–440.
54. Li,J., Vaidya,M., White,C., Vainstein,A., Citovsky,V. and Tzfira,T. (2005) Involvement of KU80 in T-DNA integration in plant cells. *Proc. Natl Acad. Sci. USA*, **102**, 19231–19236.
55. van Attikum,H., Bundock,P. and Hooykaas,P.J. (2001) Non-homologous end-joining proteins are required for Agrobacterium T-DNA integration. *EMBO J.*, **20**, 6550–6558.
56. Heacock,M., Spangler,E., Riha,K., Puizina,J. and Shippen,D.E. (2004) Molecular analysis of telomere fusions in Arabidopsis: multiple pathways for chromosome end-joining. *EMBO J.*, **23**, 2304–2313.
57. Kozak,J., West,C.E., White,C., da Costa-Nunes,J.A. and Angelis,K.J. (2009) Rapid repair of DNA double strand breaks in Arabidopsis thaliana is dependent on proteins involved in chromosome structure maintenance. *DNA Repair (Amst)*, **8**, 413–419.
58. Charbonnel,C., Allain,E., Gallego,M.E. and White,C.I. (2011) Kinetic analysis of DNA double-strand break repair pathways in Arabidopsis. *DNA Repair*, **10**, 611–619.
59. Chen,L., Trujillo,K., Ramos,W., Sung,P. and Tomkinson,A.E. (2001) Promotion of Dnl4-catalyzed DNA end-joining by the Rad50/Mre11/Xrs2 and Hdf1/Hdf2 complexes. *Mol. Cell*, **8**, 1105–1115.
60. Ma,J.L., Kim,E.M., Haber,J.E. and Lee,S.E. (2003) Yeast Mre11 and Rad1 proteins define a Ku-independent mechanism to repair double-strand breaks lacking overlapping end sequences. *Mol. Cell. Biol.*, **23**, 8820–8828.
61. Moore,J.K. and Haber,J.E. (1996) Cell cycle and genetic requirements of two pathways of nonhomologous end-joining repair of double-strand breaks in *Saccharomyces cerevisiae*. *Mol. Cell. Biol.*, **16**, 2164–2173.
62. Zhang,X. and Paull,T.T. (2005) The Mre11/Rad50/Xrs2 complex and non-homologous end-joining of incompatible ends in *S. cerevisiae*. *DNA Repair*, **4**, 1281–1294.
63. Deriano,L., Stracker,T.H., Baker,A., Petrini,J.H. and Roth,D.B. (2009) Roles for NBS1 in alternative nonhomologous end-joining of V(D)J recombination intermediates. *Mol. Cell*, **34**, 13–25.
64. Huang,J. and Dynan,W.S. (2002) Reconstitution of the mammalian DNA double-strand break end-joining reaction reveals a requirement for an Mre11/Rad50/NBS1-containing fraction. *Nucleic Acids Res.*, **30**, 667–674.
65. Rass,E., Grabarz,A., Plo,I., Gautier,J., Bertrand,P. and Lopez,B.S. (2009) Role of Mre11 in chromosomal nonhomologous end joining in mammalian cells. *Nat. Struct. Mol. Biol.*, **16**, 819–824.
66. Taylor,E.M., Ceillon,S.M., Bonis,A., Chapman,J.R., Povirk,L.F. and Lindsay,H.D. (2010) The Mre11/Rad50/Nbs1 complex functions in resection-based DNA end joining in *Xenopus laevis*. *Nucleic Acids Res.*, **38**, 441–454.

Research Article

Genotoxin Induced Mutagenesis in the Model Plant *Physcomitrella patens*

Marcela Holá,¹ Jaroslav Kozák,² Radka Vágnerová,¹ and Karel J. Angelis¹

¹Institute of Experimental Botany ASCR, Na Karlovce 1, 160 00 Praha 6, Czech Republic

²Institute of Organic Chemistry and Biochemistry ASCR, Flemingovo nám. 2, 1600 00 Praha 6, Czech Republic

Correspondence should be addressed to Karel J. Angelis; karel.angelis@gmail.com

Received 4 October 2013; Accepted 14 November 2013

Academic Editor: Alma Balestrazzi

Copyright © 2013 Marcela Holá et al. This is an open access article distributed under the Creative Commons Attribution License, which permits unrestricted use, distribution, and reproduction in any medium, provided the original work is properly cited.

The moss *Physcomitrella patens* is unique for the high frequency of homologous recombination, haploid state, and filamentous growth during early stages of the vegetative growth, which makes it an excellent model plant to study DNA damage responses. We used single cell gel electrophoresis (comet) assay to determine kinetics of response to Bleomycin induced DNA oxidative damage and single and double strand breaks in wild type and mutant *lig4* *Physcomitrella* lines. Moreover, *APT* gene when inactivated by induced mutations was used as selectable marker to ascertain mutational background at nucleotide level by sequencing of the *APT* locus. We show that extensive repair of DSBs occurs also in the absence of the functional LIG4, whereas repair of SSBs is seriously compromised. From analysis of induced mutations we conclude that their accumulation rather than remaining lesions in DNA and blocking progression through cell cycle is incompatible with normal plant growth and development and leads to sensitive phenotype.

1. Introduction

Plants developed several strategies to protect integrity of their genome against various environmental stresses. Common denominator of most of them is oxidative stress mediated by reactive oxygen species (ROS). The origin of ROS within the cell could be a consequence of physical or chemical genotoxic treatment, as well as byproduct of internal oxygen metabolism often triggered by external stimuli as drought and salinity. To be able to cope with oxidative stress we have to assess all faces of this challenge for plants; in particular, how it affects genetic material of the cells and how eventual changes are temporarily or permanently expressed in plant phenotype. This is why we need a flexible and robust model system, which experimentally enables the use of reverse genetics for genotoxic and biochemical studies. In this paper we describe a novel system to be considered for genotoxicity testing in plants.

The moss *Physcomitrella patens* is an emerging model plant [1] with the following differences/advantages as compared to other plant test systems: efficient homologous recombination (enabling reverse genetics of virtually any

gene), dominant haploid phase (enabling assessment of mutation phenotype), small size plantlets colonies with a quick and during early vegetative stage also filamentous growth, easy cultivation in inorganic media and several options of long term storage. Here we describe and validate a system of small protonemata fragments with high fraction of apical cells primarily developed for the purpose of genotoxicity testing. However, these one-day-old protonemata could be used as a substitute of protoplasts for other purposes, for example, for moss transformation [2].

APT (adenine phosphoribosyltransferase) is an enzyme of the purine salvage pathway that converts adenine into AMP and its loss of function generates plants resistant to adenine analogues, for example, 2-FA (2-Fluoroadenine) [3]. Mutational inactivation can be used as selectable marker for mutator genotyping as well as analysis of mutations in *APT* locus on nucleotide level [4–6].

This paper is an extension of our previous study of *Physcomitrella* knockout mutants of a key MRN (MRE11, RAD50, and NBS1) complex [6] with a pleiotropic effect on DSB repair in whole. We explore and validate the above outlined moss model system for genotoxicity testing in

plants. We describe a parallel use of SCGE (single cell gel electrophoresis, comet) assay for detection of DNA damage and its repair and of APT assay with sequencing analysis of mutants. On example of *lig4*, mutated in a key component of nonhomologous DSB-end joining pathway (C-NHEJ), we show consequences of mis repair. For strengthening the model concept we also present preliminary results of *pprad51AB* sensitivity to genotoxin treatment and on *ppku70* mutation rate.

2. Material and Methods

2.1. Plant Material. *Physcomitrella patens* (Hedw.) B.S.G. "Gransden 2004" wild type and *pplig4* were vegetatively propagated as previously described [7]. The *lig4* and *ku70* mutants of C-NHEJ were generated by D. G. Schaefer, Neuchatel University, Switzerland, and F. Nogue, INRA, Paris, France, and kindly provided by F. Nogue. Detailed characteristic of this mutant will be published elsewhere. Mutant in both alleles of *Physcomitrella RAD51* gene (*pprad51AB*, clone 721) is described elsewhere [8] and was kindly provided by B. Reiss, MPIZ, Cologne, Germany.

Individual plants were cultured as "spot inocula" on BCD agar medium supplemented with 1 mM CaCl₂ and 5 mM ammonium tartrate (BCDAT medium) or as lawns of protonemal filaments by subculture of homogenized tissue on BCDAT agar medium overlaid with cellophane in growth chambers with 18/6 hours day/night cycle at 22/18°C.

One-day-old protonemal tissue for repair and mutation experiments were prepared from one-week-old tissue scraped from plates, suspended in 8 mL of BCD medium, and sheared by a T25 homogenizer (IKA, Germany) at 10 000 rpm for two 1-minute cycles and let 24 hours to recover in cultivation chamber with gentle shaking at 100 rpm. This treatment yielded suspension of 3–5 cell protonemata filaments, which readily settle for recovery. Settled protonemata could be handled without excessive losses by tweezers on glass Petri plates.

2.2. Bleomycin Treatment and Sensitivity Assay. For treatments was used Bleomycin sulphate supplied as Bleomedac inj. (Medac, Hamburg, Germany). All solutions were prepared fresh prior treatment from weighted substance in BCDAT medium.

Protonemal growth was tested by inoculating explants of wild type and 5 mutant lines onto 6 × 4 multiwell plates organized to allow in line comparison of the effect of increasing Bleomycin concentrations. The wells were filled with 2 mL of standard growth BCDAT agar medium without or with 0.01, 0.1, and 1 μg mL⁻¹ Bleomycin. The experiment was carried in 3 independent replicas and monitored up to 3 weeks for growth of "spot inocula."

Treatment of one-day-old protonemata was performed on glass 5 cm Petri plates with the aid of bent tweezers to handle tissue and pipettes to remove excess liquids. Opening of yellow tips is generally small enough to avoid suction of moss filaments when drawing majority of liquid from tissue

prior blotting of collected tissue on filter paper to remove the rest.

In dose-response and repair kinetic experiments, one-day-old protonemata were after the Bleomycin treatment thoroughly rinsed in water, blotted on filter paper, and either flash-frozen in liquid N₂ (dose response and repair $t = 0$) or left to recover on plates in liquid BCDAT medium for the indicated repair times, before being frozen in liquid N₂.

For induction and regeneration of *apt* mutants one-day-old protonemata were after Bleomycin treatment thoroughly rinsed with H₂O, suspended in 2 mL of BCDAT medium, and spread on cellophane overlaid BCDAT agar plates, which were for selection supplemented with 2-FA (2-Fluoroadenine, Sigma-Aldrich, cat. Nr. 535087) and further incubated in growth chamber.

2.3. Detection of DNA Lesions. DNA single and double strand breaks were detected by a SCGE assay using either alkaline unwinding step A/N [9, 10] or fully neutral N/N protocol [11, 12] as previously described. In brief, approximately 100 mg of frozen tissue was cut with a razor blade in 300 μL PBS + 10 mM EDTA on ice and released nuclei transferred into Eppendorf tubes on ice. 70 μL of nuclear suspension was dispersed in 280 μL of melted 0.7% LMT agarose (GibcoBRL, cat. Nr. 15510-027) at 40°C and four 80 μL aliquots were immediately pipetted onto each of two coated microscope slides (in duplicate per slide), covered with a 22 × 22 mm cover slip and then chilled on ice for 1 min to solidify the agarose. After removal of cover slips, slides were immersed in lysing solution (2.5 M NaCl, 10 mM Tris-HCl, 0.1 M EDTA, and 1% N-lauroyl sarcosinate, pH 7.6) on ice for at least 1 hour to dissolve cellular membranes and remove attached proteins. The whole procedure from chopping tissue to placement into lysing solution takes approximately 3 minutes. After lysis, slides were either first incubated 10 minutes in 0.3 M NaOH, 5 mM EDTA, pH 13.5 solution to allow partially unwind DNA double helix to reveal SSBs (A/N protocol) or without unwinding step (N/N protocol) directly equilibrated twice for 5 minutes in TBE electrophoresis buffer to remove salts and detergents. Comet slides were then subjected to electrophoresis at 1 V cm⁻¹ (app. 12 mA) for 3 minutes. After electrophoresis, slides were placed for 5 min in 70% EtOH, 5 min in 96% EtOH, and air-dried.

Comets were viewed in epifluorescence with a Nikon Eclipse 800 microscope stained with SYBR Gold (Molecular Probes/Invitrogen, cat. Nr. S11494) according to manufacture recommendation and evaluated by the LUCIA Comet cytogenetic software (LIM Inc., Czech Republic).

2.4. SCGE Assay Data Analysis. The fraction of DNA in comet tails (% tail-DNA, % T DNA) was used as a measure of DNA damage. Data for the wild type and the mutant *pplig4* line analysed in this study were obtained in at least three independent experiments. In each experiment, the % T DNA was measured at seven time points: 0, 5, 10, 20, 60, 180, and 360 min after the treatment and in control tissue without treatment. Measurements included four independent gel replicas of 25 evaluated comets totalled in at least 300

comets analysed per experimental point. The percentage of damage remaining as plotted on Figure 2(b) after given repair time (t_x) is defined as

$$\begin{aligned} & \% \text{ damage remaining } (t_x) \\ &= \frac{\text{mean \% tail-DNA } (t_x) - \text{mean \% tail-DNA (control)}}{\text{mean \% tail-DNA } (t_0) - \text{mean \% tail-DNA (control)}} \\ & \quad * 100. \end{aligned} \quad (1)$$

Time-course repair data were analysed for one- or two-phase decay kinetic by Prism v.5 program (GrafPad Software Inc., USA).

2.5. Isolation and Analysis of *apt* Mutants after Bleomycin Treatment. Mutation rates were measured as the number of *apt* mutants that appeared as green foci of regenerating clones resistant to 2-FA (Figure 3). Treated protonemata were first incubated approximately 3 weeks on plates with 2 or 3 mM 2-FA until first green foci start to emerge. Then whole cellophane overlay was transferred to a new plate with 8 mM 2-FA and emerging clones were allowed to form colonies. Stable clones were then counted.

Some clones were further propagated on plates with 8 mM 2-FA and their *APT* locus was subsequently PCR amplified and sequenced to identify the mutation(s) responsible for the resistance. Approximately 100 mg of tissue was used to isolate genomic DNA with DNeasy Plant Mini Kit (Qiagen, cat. Nr. 69104) using “ball” mill Retsch MM301 to homogenize the tissue in 2 mL round bottom Eppendorf tubes. *APT* locus was amplified from isolated genomic DNA with KOD Hot Start DNA Polymerase (Millipore/Novagen, cat. Nr. 71086), purified with the QIAquick PCR Purification Kit (Qiagen, cat. Nr. 28104) and used as a template for sequencing with BigDye Terminator v3.1 Cycle Sequencing Kit (Applied Biosystems, cat. Nr. 4337455). Locations of PCR primers used for *APT* amplification and sequencing are depicted on Supplementary Figure 2 and their sequences are listed in Supplementary Table 1 (see Supplementary Material available online at <http://dx.doi.org/10.1155/2013/535049>). To keep sequencing cost down only half volume of the BigDye Ready Reaction Mix was used in a standard sequencing reaction and combined with the same volume of Half-Term-Dye-Termination mixture (Sigma-Aldrich, cat. Nr. H1282).

2.6. Analysis of Sequencing Data. Sequences of each clone obtained on genetic analyser Prism 3130x1 (Applied Biosystems, USA) were stitched together with MacVector program Assembler 12.7.5 (MacVector, USA) into contigs and aligned to the latest annotated *APT* sequence Pp1s114_124V6.1 in the COSMOSS—the *Physcomitrella patens* resource database (<https://www.cosmoss.org/>).

3. Results and Discussion

In all experiments a model *Physcomitrella patens* has been used as one day recovered fragments of 3–5 cell size derived from the lawn of growing protonema filaments by extensive

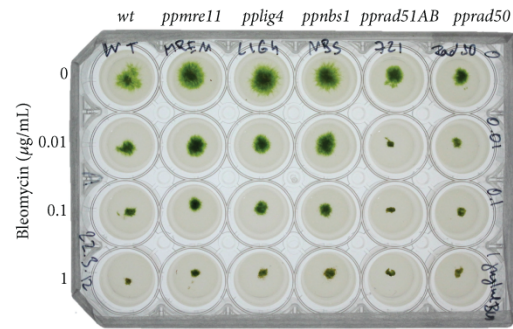


FIGURE 1: Sensitivity of the *Physcomitrella patens* repair mutants *mre11*, *lig4*, *nbs1*, *rad51AB*, and *rad50* to chronic exposure of Bleomycin. *Physcomitrella* explants were inoculated as “spot inocula” onto BCDAT-agar plates supplemented with 0, 0.01, 0.1, and 1 $\mu\text{g mL}^{-1}$ Bleomycin and photographed 10 days after inoculation.

shearing. Such one-day-old protonemata represent a unique system among plants to study plant tissue with up to 50% of apical dividing cells. Convenient mechanical handling enables quick processing of tissue after the treatment to address short repair times and with fine tip tweezers also for uniform spotting to test sensitivity. In this respect one-day-old protonemata are preferred system to so far widely used protoplasts, which could be collected only by centrifugation. Another reason for using protonemata is possibility their mechanical disintegration by razor blade chopping for rapid release of nuclei for SCGE assay. In this way direct use of protoplasts for comet assay is obstructed by nearly instant regeneration of the cell wall within 4 hours after the release from cellulase treatment (unpublished observation), because cell wall prevents DNA movement from nuclei during electrophoresis.

3.1. Sensitivity to Bleomycin Treatment. Moss wild type and *pplig4*, *mre11*, *nbs1*, *rad51AB*, and *rad50* [6, 8] mutant lines were analysed for their sensitivity to radiomimetic Bleomycin in chronic “survival” assay when test plates with various concentrations of Bleomycin were inoculated with equal tissue “spots” of one-day-old protonemata and incubated up to 3 weeks (Figure 1). Only *rad51AB* and *rad50* strains displayed one order of a magnitude higher sensitivity in comparison to other tested lines. The survival growth of *ppmre11* is somehow in contradiction with previous results of Kamisugi et al. [6], but one has to realize different assay conditions, for example, acute versus chronic exposure and protoplast cells versus protonemata. In protonema tissue under permanent genotoxic stress *mre11* express phenotype similar to wild type, *nbs1*, and also *lig4*. One can speculate that 3' to 5' exonuclease and endonuclease activity associated with MRE11 is dispensable for tissue survival, but proteins RAD50 and RAD51 supporting DNA structure are not. Kozak et al. [12] previously showed crucial role of structural maintenance

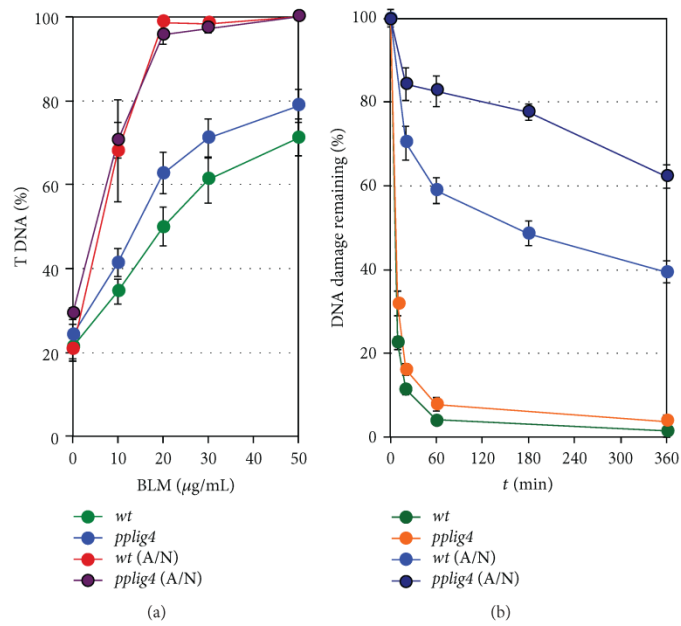


FIGURE 2: SSB and DSB repair kinetics determined by SCGE. One-day regenerated protonemal tissue from wild type and *pplig4* lines was treated with Bleomycin for 1 h prior to nuclear extraction and the analysis. (a) Dose-response as the percentage of the free DNA moved by electrophoresis into comet tail (% T DNA) at the indicated Bleomycin concentrations. DSBs were determined by N/N protocol: green: wild type, blue: *pplig4*, whereas SSBs were determined by A/N protocol: red: wild type, dark purple: *pplig4*. (b) Repair kinetics is plotted as % of DSBs remaining over the 0, 5, 10, 20, 60, 180, and 360 min period of repair recovery. Maximum damage is normalised as 100% at $t = 0$ for all lines. SSBs were induced by 1-hour treatment with $2 \mu\text{g mL}^{-1}$ Bleomycin; bright blue: wild type, dark blue: *pplig4*, and determined by A/N protocol. DSBs were induced by 1-hour treatment with $30 \mu\text{g mL}^{-1}$ Bleomycin, green: wild type, orange: *pplig4*, and determined by N/N protocol. (Error bars-standard error).

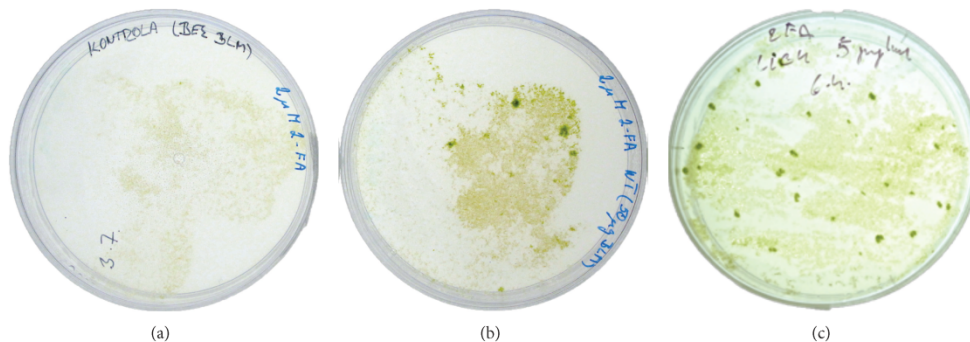


FIGURE 3: Plates with 2-FA resistant foci of wild type *Physcomitrella* (a and b) and *pplig4* (c) after 3 weeks of selection. (a) Untreated *Physcomitrella* wild type, (b) $50 \mu\text{g mL}^{-1}$ Bleomycin treated wild type protonemata for 2 hours, and (c) $5 \mu\text{g mL}^{-1}$ Bleomycin treated *pplig4* protonemata for 1 hour prior being spread on plates with BCDAT medium supplemented with $2 \mu\text{M}$ 2-FA and cultivated for 3 weeks.

of chromosome complex SMC5/6 in the repair of Bleomycin induced DSBs. In this context RAD50s have similar structural role in MRN complex as SMCs in the structure of the SMC5/6 complex [13]. Both these complexes can function in tethering of broken ends in close proximity.

3.2. Induction of DNA Lesions and Their Repair. Bleomycin, an ionizing radiation mimicking agent, functions as a catalyst activated by interaction with DNA and attachment of Fe^{2+} to produce oxygen radicals leading to lesions as SSBs, DSBs, AP-sites, and damaged bases [14, 15], which all could be

readily detected by SCGE [16]. DNA breaks and other lesions converted to breaks lead to DNA fragmentation and nucleoid unwinding allowing relaxed DNA to move in electric field from nuclei out to form a “comet” like object in which increased quantity of fragmented DNA in comet tail (% T DNA) is proportional to breakage. DSBs are detected by an N/N assay when pH of lysing and electrophoretic solutions is kept under pH 10, whilst for the detection of SSBs DNA after the lysis is allowed to unwind DNA double-helix in alkali [17] to separate individual strands and expose their fragmentation (A/N protocol [9]).

Bleomycin fragmentation of genomic DNA by induction of SSBs and DSBs is documented on Figure 2(a). Ten times higher efficiency to induce SSBs than DSBs is in agreement with generally accepted ratio of 1:10, DSBs versus SSBs, induced by ionizing radiation. Evidently this also applies for Bleomycin treatment of *Physcomitrella*. The background level of genomic DNA damage in wild type and *pplig4* is similar, between 20 and 25% T DNA, indicating that the repair defect has no significant effect on natural levels of genomic DNA fragmentation. Nevertheless, in comparison with wild type, *pplig4* is vulnerable to Bleomycin induction of DSBs and SSBs.

In both wild type and *pplig4* lines, the Bleomycin induced DSBs are repaired with a rapid, biphasic kinetics (Figure 2(b)). Half-lives of DSB survival $\tau_{1/2}$ 1.5 min for wild type and 2.5 min for *pplig4* are similar to $\tau_{1/2}$ 2.9 min for *pprad50*, $\tau_{1/2}$ 4.1 min for *ppmre11*, and $\tau_{1/2}$ 1.9 min for *ppnbs1* previously reported in [6].

Contrary to DSBs, SSBs are repaired far less efficiently. Slow SSB repair might be common feature of plants since Donà et al. [18] recently observed similar phenomenon in *Medicago truncata* cell culture irradiated with different doses of γ -ray. The SSB repair kinetic in wild type *Physcomitrella* is clearly biphasic and in this respect parallels repair of MMS induced SSBs in *Arabidopsis* [19]. In comparison to DSBs, substantially smaller fraction of SSBs is repaired with fast kinetics; the defect even more manifested in *pplig4*. It suggests an important role for LIG4 in the repair of DNA lesions like modified basis, AP sites that are usually detected as SSBs and are repaired via BER (base excision repair). It is noteworthy that LIG3, the ligase finishing BER pathway, is not represented in plants. We showed earlier that principal substitute for LIG3 in *Arabidopsis* is LIG1 [19]. The repair kinetic of MMS induced SSBs in *atlig1* posed an exceptional route. After the treatment the number of breaks continues to increase during the first hour of repair and after 3 hours returns to the level at the end of treatment. Then repair continues similarly as in the wild type (see Figure 4 in [19]). Because *atlig1* is an RNAi line with only 40% of remaining LIG1 activity, such repair course is a consequence of unbalanced BER due to attenuated ligation step. Evidently the knockout mutation in *pplig4* does not have such severe effect on repair of SSBs; nevertheless, the defect clearly shows that LIG4 is also involved in the repair of SSBs in plants.

3.3. Induction and Analysis of apt Mutants. The mutator phenotype was assessed as the loss of function of the *APT* gene [4] due to presence or error prone repair of endogenous

DNA damage in the wild-type moss and *lig4*, *mre11*, and *rad50* repair mutant lines.

We found dramatic, over two orders of magnitude, variation of mutator phenotype in response to mutagenic treatment. While wild type *Physcomitrella* with low mutator phenotype needed 2 hours and $50 \mu\text{g mL}^{-1}$ Bleomycin treatment to induce any *apt* clone, in *pprad50* with high mutator phenotype 1 hour treatment with only $0.1 \mu\text{g mL}^{-1}$ Bleomycin was enough for massive induction of *apt* clones. Other lines, *pplig4* and *ppmre11*, assumed as having “moderate” mutator phenotype, were mutagenized either with 5 or, respectively, $1 \mu\text{g mL}^{-1}$ Bleomycin for 1 hour. Mutagenesis and clone selection in *Physcomitrella* wild type and *pplig4* is depicted on Figure 3. For comparison we normalised the yield of 2-FA resistant clones to $1 \mu\text{g mL}^{-1}$ Bleomycin treatment per 1g dry tissue weight in each line as “relative number of *ppapts*.” The values of these normalised yields range from 9 in wild type to 875 for *pprad50* (see Supplementary Figure 1 where are plotted summarized results of Bleomycin mutagenesis in *Physcomitrella* wild type and *lig4*, *ku70*, *rad50*, *mre11*, and *nbs1* mutants).

Randomly picked *apt* clones from selection plates were further propagated on 2-FA media to provide enough material for isolation of genomic DNA and sequencing analysis of *APT* locus. Results of sequencing analysis are pictured in Figure 4 and detailed annotations of identified mutations are summarized in Supplementary Table 2. In total were analysed 5 clones of *Physcomitrella* wild type, 4 clones of *pplig4*, 3 clones of *ppmre11*, and 6 clones of *pprad50* and identified 48 mutations. Mutations were according to assumed mechanism of formation classified as reversions, single base insertion or deletion, and insertions or deletions larger than 2 bases either in coding (exons) or noncoding regions of *APT* locus.

Most of the identified mutations are as expected localised within CDS, in particular within exon 4 that is annotated as coding for adenine salvage activity (see Figure 4). Nevertheless, in *wt:1*, *lig4:1*, *lig4:2*, and *mre11:6 apt* clones, mutations were identified only in the noncoding region and their contribution to mutated *APT* phenotype has to be established. Majority of mutations in CDS are point mutations (base substitution, single base insertions, and deletions) and it is difficult to dissect the route of their formation. Some of single base deletions could come from classical or altered NHEJ repair of DSBs [20], but more likely they represent along with other point mutations outcome of processing base oxidative damage. Interesting point is that only single base insertions were identified in *APT* CDS of *pplig4*. Insertion of extra base might imply defect in BER repair of oxidative damage in the absence of LIG4 and could be associated with defective repair of SSBs in *pplig4*.

Long deletions are clearly associated with NHEJ repair of DSBs, because, besides one rather short (8 bp) deletion in *wt:3* clone, all appear in clones derived from *mre11* and *rad50* background. This supports our working hypothesis that MRN-unsupervised repair generates more severe forms of genomic damage [6].

Only one 4 base insertion was identified in noncoding region of *wt:2*.

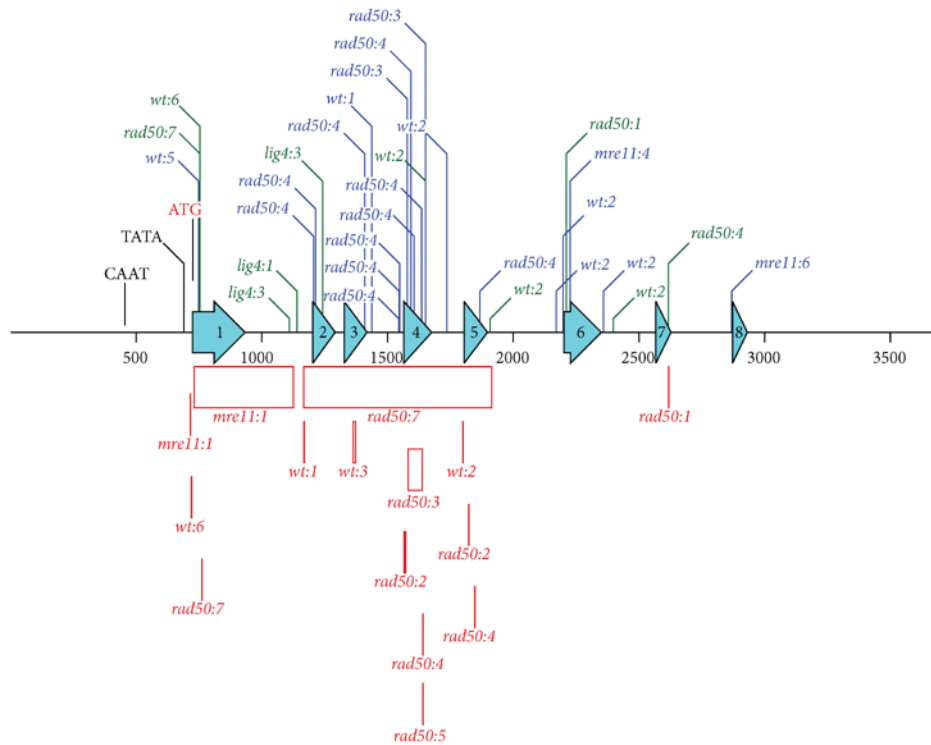


FIGURE 4: Map of identified mutations within *APT* locus. Bleomycin induced mutations are identified by color (blue: substitutions, green: insertions, and red: deletions) and tagged according to background as *wt*, *lig4*, *mre11*, and *rad50* and the number of line in which mutation was detected. Deletions are shown as boxes of size proportional to their length. On the locus map are depicted 500 nucleotide size markers and eight turquoise hollow arrows representing exons of *APT* CDS. Detailed description of each mutation is provided in Supplementary Table 2.

4. Conclusions

We validated the use of regenerating one-day-old protonemal tissue of *Physcomitrella patens* for complex analysis of genotoxic stress by parallel study of DNA damage, its repair, and mutagenic consequences in wild type and *lig4* mutant plants. From experimental point of view we developed a novel model system where 3–5 cell protonemata filaments with up to 50% of apical cells can substitute and surplus protoplasts use. Bleomycin was used to model DNA oxidative genotoxic stress with all its consequences as SSBs and DSBs, which can be followed by SCGE. We confirmed in *Physcomitrella* as previously in *Arabidopsis* rapid DSB repair even in the absence of LIG4, the key ligase of major DSB repair pathway by NHEJ mechanism [12]. Moreover, we showed crucial role of LIG4 in the repair of SSBs by BER mechanism, where it can substitute along with LIG1 [19] in plants missing LIG3. We selected and analysed by sequencing 2-FA resistant clones with Bleomycin mutated *APT* locus and found out that mutation spectra of *lig4* mutant reflects rather the defect of SSB than DSB repair. Nevertheless, as previously described [6], we interpret that mutations due to the error prone

repair in *pplig4* rather than unrepaired lesions within DNA and interfering with progression through the cell cycle are responsible for *pplig4* sensitive phenotype.

Abbreviations

A/N:	Comet assay with alkaline unwinding step
AP:	Apurinic/aprimidinic (site)
APT:	Adenine phosphoribosyltransferase
BER:	Base excision repair
CDS:	Coding DNA sequence
DSB(s):	DNA double-strand break(s)
2-FA:	2-Fluoroadenine
HR:	Homologous recombination
MMS:	Methyl methanesulfonate
NHEJ:	Nonhomologous end joining
N/N:	Neutral comet assay
ROS:	Reactive oxygen species
SCGE:	Comet assay
SSB(s):	DNA single-strand break(s)
$\tau_{1/2}$:	Half-life.

Conflict of Interests

The authors declare that they have no conflict of interests.

Acknowledgments

Czech Science Foundation (13-06595S) and Ministry of Education, Youth, and Sport CR (LD13006) supported this work. The authors appreciate Dr. Andrew Cuming's help with sequences and mutations analysis.

References

- [1] D. J. Cove, C. D. Knight, and T. Lamparter, "Mosses as model systems," *Trends in Plant Science*, vol. 2, no. 3, pp. 99–105, 1997.
- [2] M. Šmídková, M. Holá, and K. J. Angelis, "Efficient biolistic transformation of the moss *Physcomitrella patens*," *Biologia Plantarum*, vol. 54, no. 4, pp. 777–780, 2010.
- [3] C. Gaillard, B. A. Moffatt, M. Blacker, and M. Laloue, "Male sterility associated with APRT deficiency in *Arabidopsis thaliana* results from a mutation in the gene APT1," *Molecular & General Genetics*, vol. 257, no. 3, pp. 348–353, 1998.
- [4] B. Trouiller, D. G. Schaefer, F. Charlot, and F. Nogué, "MSH2 is essential for the preservation of genome integrity and prevents homeologous recombination in the moss *Physcomitrella patens*," *Nucleic Acids Research*, vol. 34, no. 1, pp. 232–242, 2006.
- [5] B. Trouiller, F. Charlot, S. Choinard, D. G. Schaefer, and F. Nogué, "Comparison of gene targeting efficiencies in two mosses suggests that it is a conserved feature of Bryophyte transformation," *Biotechnology Letters*, vol. 29, no. 10, pp. 1591–1598, 2007.
- [6] Y. Kamisugi, D. G. Schaefer, J. Kozak et al., "MRE11 and RAD50, but not NBS1, are essential for gene targeting in the moss *Physcomitrella patens*," *Nucleic Acids Research*, vol. 40, no. 8, pp. 3496–3510, 2012.
- [7] C. D. Knight, A. C. Cuming, and R. S. Quatrano, "Moss gene technology," in *Molecular Plant Biology Volume 2*, P. M. Gilmartin and C. Bowler, Eds., vol. 2, pp. 285–299, Oxford University Press, Oxford, UK, 2002.
- [8] U. Markmann-Mulisch, E. Wendeler, O. Zobell, G. Schween, H.-H. Steinbiss, and B. Reiss, "Differential requirements for RAD51 in *Physcomitrella patens* and *Arabidopsis thaliana* development and DNA damage repair," *Plant Cell*, vol. 19, no. 10, pp. 3080–3089, 2007.
- [9] K. J. Angelis, M. Dusinska, and A. R. Collins, "Single cell gel electrophoresis: detection of DNA damage at different levels of sensitivity," *Electrophoresis*, vol. 20, no. 10, pp. 2133–2138, 1999.
- [10] M. Menke, I.-P. Chen, K. J. Angelis, and I. Schubert, "DNA damage and repair in *Arabidopsis thaliana* as measured by the comet assay after treatment with different classes of genotoxins," *Mutation Research*, vol. 493, no. 1-2, pp. 87–93, 2001.
- [11] P. L. Olive and J. P. Banáth, "The comet assay: a method to measure DNA damage in individual cells," *Nature Protocols*, vol. 1, no. 1, pp. 23–29, 2006.
- [12] J. Kozak, C. E. West, C. White, J. A. da Costa-Nunes, and K. J. Angelis, "Rapid repair of DNA double strand breaks in *Arabidopsis thaliana* is dependent on proteins involved in chromosome structure maintenance," *DNA Repair*, vol. 8, no. 3, pp. 413–419, 2009.
- [13] J. M. Murray and A. M. Carr, "Smc5/6: a link between DNA repair and unidirectional replication?" *Nature Reviews Molecular Cell Biology*, vol. 9, no. 2, pp. 177–182, 2008.
- [14] R. J. Steighner and L. F. Povirk, "Bleomycin-induced DNA lesions at mutational hot spots: implications for the mechanism of double-strand cleavage," *Proceedings of the National Academy of Sciences of the United States of America*, vol. 87, no. 21, pp. 8350–8354, 1990.
- [15] A. G. Georgakilas, "Processing of DNA damage clusters in human cells: current status of knowledge," *Molecular Biosystems*, vol. 4, no. 1, pp. 30–35, 2007.
- [16] A. G. Georgakilas, S. M. Holt, J. M. Hair, and C. W. Loftin, "Measurement of oxidatively-induced clustered DNA lesions using a novel adaptation of single cell gel electrophoresis (comet assay)," in *Current Protocols in Cell Biology*, S. J. Bonifacino et al., Ed., chapter 6, p. 6.11, John Wiley & Sons, 2010.
- [17] G. Ahnström and K. Erixon, "Radiation induced strand breakage in DNA from mammalian cells. Strand separation in alkaline solution," *International Journal of Radiation Biology and Related Studies in Physics, Chemistry, and Medicine*, vol. 23, no. 3, pp. 285–289, 1973.
- [18] M. Donà, L. Ventura, A. Balestrazzi et al., "Dose-dependent reactive species accumulation and preferential double-strand breaks repair are featured in the γ -ray response in *Medicago truncatula* cells," *Plant Molecular Biology Reporter*, 2013.
- [19] W. M. Waterworth, J. Kozak, C. M. Provost, C. M. Bray, K. J. Angelis, and C. E. West, "DNA ligase 1 deficient plants display severe growth defects and delayed repair of both DNA single and double strand breaks," *BMC Plant Biology*, vol. 9, article 79, 2009.
- [20] C. Charbonnel, E. Allain, M. E. Gallego, and C. I. White, "Kinetic analysis of DNA double-strand break repair pathways in *Arabidopsis*," *DNA Repair*, vol. 10, no. 6, pp. 611–619, 2011.

RESEARCH ARTICLE

Open Access

The AtRAD21.1 and AtRAD21.3 Arabidopsis cohesins play a synergistic role in somatic DNA double strand break damage repair

José A da Costa-Nunes^{1*}, Cláudio Capitão^{2,3}, Jaroslav Kozak⁴, Pedro Costa-Nunes^{5,6}, Gloria M Ducasa⁵, Olga Pontes^{5,6} and Karel J Angelis⁴

Abstract

Background: The RAD21 cohesin plays, besides its well-recognised role in chromatid cohesion, a role in DNA double strand break (dsb) repair. In *Arabidopsis* there are three *RAD21* paralog genes (*AtRAD21.1*, *AtRAD21.2* and *AtRAD21.3*), yet only *AtRAD21.1* has been shown to be required for DNA dsb damage repair. Further investigation of the role of cohesins in DNA dsb repair was carried out and is here reported.

Results: We show for the first time that not only *AtRAD21.1* but also *AtRAD21.3* play a role in somatic DNA dsb repair. Comet data shows that the lack of either cohesins induces a similar high basal level of DNA dsb in the *nuclei* and a slower DNA dsb repair kinetics in both cohesin mutants. The observed *AtRAD21.3* transcriptional response to DNA dsb induction reinforces further the role of this cohesin in DNA dsb repair. The importance of *AtRAD21.3* in DNA dsb damage repair, after exposure to DNA dsb damage inducing agents, is notorious and recognisably evident at the phenotypical level, particularly when the *AtRAD21.1* gene is also disrupted. Data on the kinetics of DNA dsb damage repair and DNA damage sensitivity assays, of single and double *atrad21* mutants, as well as the transcription dynamics of the *AtRAD21* cohesins over a period of 48 hours after the induction of DNA dsb damage is also shown.

Conclusions: Our data demonstrates that both *Arabidopsis* cohesin (*AtRAD21.1* and *AtRAD21.3*) play a role in somatic DNA dsb repair. Furthermore, the phenotypical data from the *atrad21.1 atrad21.3* double mutant indicates that these two cohesins function synergistically in DNA dsb repair. The implications of this data are discussed.

Keywords: Arabidopsis, *AtRAD21.1*, *AtRAD21.3*, Cohesins, Comet assay, DNA damage, Gene expression

Background

RAD21 (also known as SCC1) [1,2], SMC1, SMC3 and SCC3 are the core subunits of a complex required for sister chromatid cohesion [3]. Sister chromatid cohesion in budding yeast is established during late G1 and S phase [4,5] and is abolished during the metaphase/anaphase transition, to allow the correct and timely mitotic sister chromatid segregation [6]. Sister chromatid cohesion is also established *de novo* during the G2/M diploid phases when DNA dsb are formed [5,7]. This *de novo* cohesion induced by DNA dsb occurs in budding yeast

on a genome-wide scale [7,8]. In contrast, in human cells at the G2 phase, the RAD21 cohesin is recruited and targeted specifically to the vicinity of the DNA dsb *loci* [9,10]. It has been proposed that the *de novo* cohesion establishment tethers the DNA dsb damaged strand with its identical and intact sister chromatid counterpart to promote error-free DNA repair [7].

DNA dsb can be repaired via different DNA repair pathways such as the error-free homologous recombination (HR) pathway, which requires a homologous DNA strand template for repair, or via other alternative DNA dsb repair pathways that do not require a homologous template. The latter, such as the canonical non-homologous end-joining (C-NHEJ), the single strand annealing and the micro-homology end-joining DNA repair pathways are

* Correspondence: j.dacostanunes@wolfson.oxon.org

¹Instituto de Tecnologia Química e Biológica (ITQB), Universidade Nova de Lisboa (UNL), Av. República, Apartado 127, 2781-901 Oeiras, Portugal
 Full list of author information is available at the end of the article

mostly error-prone [11,12]. In imbibed seeds, for example, DNA dsb can be repaired via different DNA dsb repair pathways. Accordingly, mutations that affect either HR or C-NHEJ have been reported to cause loss of viability, or developmental delay, in seedlings germinated from imbibed mutants seeds of *Arabidopsis thaliana* (henceforth *Arabidopsis*) and maize exposed to DNA dsb damage inducing agents [13-16].

Other than triggering *de novo* cohesion, DNA dsb damage also triggers changes in gene expression. Some of the *Arabidopsis* genes that code for proteins required at the early stages of HR repair of DNA dsb, such as *AtRAD51*, *AtBRCA1*, *AtRPA-related*, *AtGR1/COM1/CtIP* and *GMI1*, increase gene expression after DNA dsb induction [17-23]. Yet, not all *Arabidopsis* genes involved in HR, namely *AtRAD50* and *AtNBS1* (which are also involved in C-NHEJ), are transcriptionally responsive to DNA dsb damage [21,22,24,25]. DNA dsb damage also induces increase of the expression levels of the *AtWEE1*, *CycB1:1* and *AtRAD17*, genes that are involved in cell cycle arrest at G2 [21,26,27]. This DNA dsb induced G2 cell cycle arrest is detected mainly in meristems [21,22,28,29]. The observed increase of steady-state transcript levels, induced by DNA dsb, of the genes mentioned above and of *AtRAD21.1* is mediated by the ATM kinase [21,30].

Arabidopsis has three *RAD21* homologous genes; *AtRAD21.1/SYN2*, *AtRAD21.2/SYN3* and *AtRAD21.3/SYN4* [14,31]. *AtRAD21.1* transcripts are detected in low levels in most plant tissues [14,32], yet in the shoot apex and particularly in seeds (and more so in dry and imbibed seeds), higher levels of *AtRAD21.1* transcript can be found [33-35]. *AtRAD21.1* transcripts become more abundant, in an ATM dependent manner, after DNA dsb induction [14,20,21]. The detection of higher *AtRAD21.1* expression levels in seeds and the shoot apical apex is particularly interesting since these contain actively dividing meristem cells where maintenance of genomic integrity is crucial. Like *AtRAD21.1*, the *AtRAD21.2* gene is also expressed in different tissues at low levels [14,31]. Yet, and unlike *AtRAD21.1*, *AtRAD21.2* steady-state transcript levels have been shown not to increase in response to DNA dsb damage induction [14]. In contrast, the cohesin *AtRAD21.3* exhibits the highest steady-state transcript levels of all *AtRAD21* genes [14]. *AtRAD21.3* has been shown to play a role in genome stability and to be associated with replication factors [36]. Indeed, the *atrad21.3* mutant experiences genomic instability (like *atrad21.1*) and chromatid alignment defects [37], yet, unlike the *atrad21.1* mutant, the *atrad21.3* single mutant has not been reported to be associated with DNA dsb damage repair nor to exhibit a DNA dsb damage hypersensitivity phenotype [14]. However, and unexpectedly, *AtRAD21.3* is involved in DNA dsb damage repair.

Here, we report for the first time that *AtRAD21.3*, like *AtRAD21.1*, also plays a role in somatic DNA dsb repair. Both *atrad21.3* and *atrad21.1* single mutants have a higher basal level of DNA dsb, in comparison to wild-type Columbia-0 (*Col*). Additionally, the *atrad21.3* mutation also affects the kinetics of DNA dsb damage repair after the induction of DNA dsb. Furthermore, the combination of both mutations renders the imbibed seeds of the *atrad21.1 atrad21.3* double mutant more hypersensitive to DNA dsb induction than the *atrad21.1* and the *atrad21.3* single mutants.

We also show that the emergency-like *AtRAD21.1* gene expression response to DNA damage is triggered immediately and abruptly after the induction of DNA dsb.

Results

The *AtRAD21.1* complementation construct is sufficient to promote resistance to ionising radiation-induced damage in imbibed seeds

The *atrad21.1* mutation (salk_044851) renders *Arabidopsis* imbibed seeds hypersensitive to DNA dsb-inducing agents [14]. To establish that the described phenotype is caused by the *atrad21.1* mutation alone, and not derived from chromosomal rearrangement or the disruption of another gene not physically linked to the T-DNA insertion [38], *atrad21.1* mutant plants were transformed with the complementation construct.

To obtain the complementation construct, the genomic region comprising the *AtRAD21.1* gene and its 2,602 bp upstream sequence, was amplified as a single PCR product and cloned. Sequencing of the genomic complementation construct confirmed that the coding sequence in the construct is identical to the coding sequence of the *AtRAD21.1* wild-type allele. Sequencing also confirmed that the complementation construct *AtRAD21.1* gene sequence is cloned in frame with the epitope-tags *GFP-6xHis* (from the pMDC107 vector).

The transformation of *atrad21.1* homozygous plants with the complementation construct yielded, at least, nine independently transformed complementation lines (Comp). Five of these lines were further analysed and shown to rescue the *atrad21.1* mutant phenotype, exhibiting wild-type-like resistance to a dose of 150 Gy (3.25 Gy/minute; source: Cs137) of ionising radiation (Figure 1). These plants were genotyped and confirmed to carry the complementation construct and the *atrad21.1* mutant allele (data not shown). Hence, our results show that the *AtRAD21.1* gene and its upstream sequence are required and sufficient to rescue the *atrad21.1* mutant phenotype (hypersensitivity to ionising radiation) (Figure 1). Molecular characterisation of a Comp line exposed to ionising radiation also suggests a correlation between the re-established *Col*-like resistance to ionising radiation and the high amounts of *AtRAD21.1-GFP-6xHis* transcript

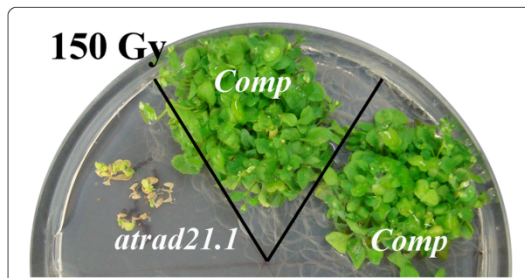


Figure 1 The genomic construct, comprising the putative *AtRAD21.1* promoter region and gene, complements the *atr21.1* mutation. The complementation lines (*Comp*) are not hypersensitive to DNA dsb damage inducing ionising radiation, unlike the *atr21.1* mutant. Plants were photographed 27 days after exposure of the imbibed seeds to ionising radiation (150 Gy; 3.25 Gy/minute; source: Cs137). Two independent complementation lines (*Comp*) (in *atr21.1* mutant background carrying the complementation construct) and the *atr21.1* mutant (with no complementation construct) are shown.

detected (Additional file 1: Figures S1a and S1c); (primer pairs: CR1 + GFPOUT and 3HOM6 + GFPOUT; Additional file 1: Table S1).

The complementation lines also demonstrate that the *atr21.1* mutant retains the ability to be transformed and integrate T-DNA into its genome and that the epitope-tag (GFP-6xHis) fused to the predicted C-terminal end of the *AtRAD21.1* protein does not affect the function of the AtRAD21.1 protein in γ -ray irradiated imbibed seeds (Figure 1). Unfortunately, we were not able to detect GFP signal using fluorescence microscopy, either in non-irradiated or in γ -ray irradiated complementation lines (data not shown), possibly due to conformational changes of the GFP tag in the context of the recombinant protein.

***AtRAD21.1* expression: an emergency-like response to DNA dsb damage induction**

It has been shown that the transcription of *AtRAD21.1* is responsive to the induction of DNA dsb damage (in an ATM dependent manner) [14,20,21], and that the *atr21.1* mutant imbibed seeds are hypersensitive to DNA dsb damage [14]. This suggests that the *AtRAD21.1* transcript content increase, induced by DNA dsb, may be required for DNA dsb damage repair.

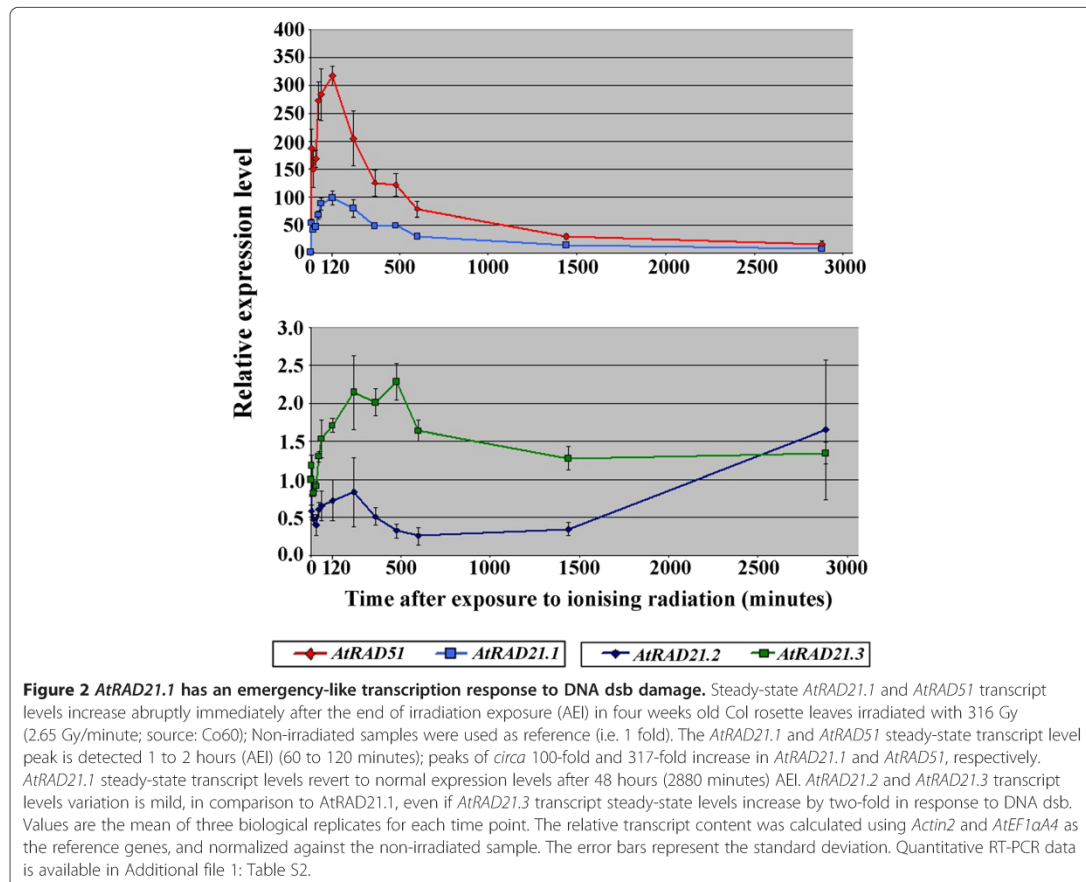
It has been reported that, 1 hour after the exposure to 100 Gy of ionising radiation, no significant change in *AtRAD21.2* and *AtRAD21.3* gene transcription is detectable in a northern blot [14]. Yet, it is not known whether transcription also remains unchanged when higher doses of ionising radiation are applied and more DNA damage is induced. The *AtRAD21.2* and *AtRAD21.3* gene transcription dynamics at different time points after the induction of DNA dsb damage are also unknown. Hence, due

to the importance of the RAD21 cohesin in DNA repair, and due to the lack of a more detailed characterisation of *Arabidopsis AtRAD21* gene expression responsiveness to DNA dsb, we monitored the dynamics of *AtRAD21.1*, *AtRAD21.2* and *AtRAD21.3* transcript content at different time points, during the first 48 hours After Exposure to Ionising radiation (AEI). The *AtRAD21* genes' transcript content variation was monitored in rosette leaves from four weeks old Col plant, using quantitative real-time PCR (qRT-PCR), after exposure to 316 Gy of ionising radiation (2.65 Gy/minute; source: Co60).

As early as 5 minutes AEI, we observed a 50-fold increase of *AtRAD21.1* transcript content in irradiated *versus* control (non-irradiated) samples (Figure 2; Additional file 1: Figures S2(A) and S2(B); Additional file 1: Table S2). The amount of transcript peaked *circa* 1 to 2 hours AEI, being almost 100-fold higher than in non-irradiated samples (Figure 2; Additional file 1: Table S2). At 4 hours AEI, the steady state levels of *AtRAD21.1* transcript progressively decrease, approaching non-irradiated levels after 48 hour AEI (Figure 2). The presented data was obtained from three independent replicates, and using two different primer pairs (Additional file 1: Table S3; primer pairs '1' and '1 m') targeting two different regions of the *AtRAD21.1* transcript (Additional file 1: Figure S1f).

AtRAD51, a gene involved in HR [17], and *AtRAD21.1* have very similar patterns of transcript steady-state content variation. This variation is, however, much more pronounced in *AtRAD51* than in *AtRAD21.1*. *AtRAD51* reaches a peak of 317-fold increase in transcript steady-state levels, 2 hours AEI (Figure 2; Additional file 1: Figures S2(A) and S2(B); Additional file 1: Table S2).

Reports on *AtRAD21.2* and *AtRAD21.3* gene expression after DNA dsb induction are limited to certain time points (i.e. 1 hour AEI and 1.5 hours AEI; northern blots and microarray data, respectively [14,21]), and suggest that the expression of these genes is not responsive to the induction of DNA dsb. Our results show that *AtRAD21.2* transcript content is diminished during most of the period of 48 hours after the induction of DNA dsb (Figure 2); The *AtATM* mRNA content variation after the induction of DNA dsb is more difficult to interpret since a decrease as well as an increase in transcription content is detected (Additional file 1: Figure S2(A)). In contrast, the qRT-PCR data shows that the steady-state *AtRAD21.3* transcript levels double after the exposure to 316 Gy of ionising radiation. *AtRAD21.3* expression, which is not as responsive as *AtRAD21.1* is to DNA dsb induction, reaches its peak between 4 and 8 hours AEI in contrast with *AtRAD21.1* transcript levels that reach their peak *circa* 1 to 2 hours AEI (Figure 2; Additional file 1: Figure S2(A)). These observations suggest that these two cohesin genes may be required for different roles in the cell since the dynamics of their RNA content



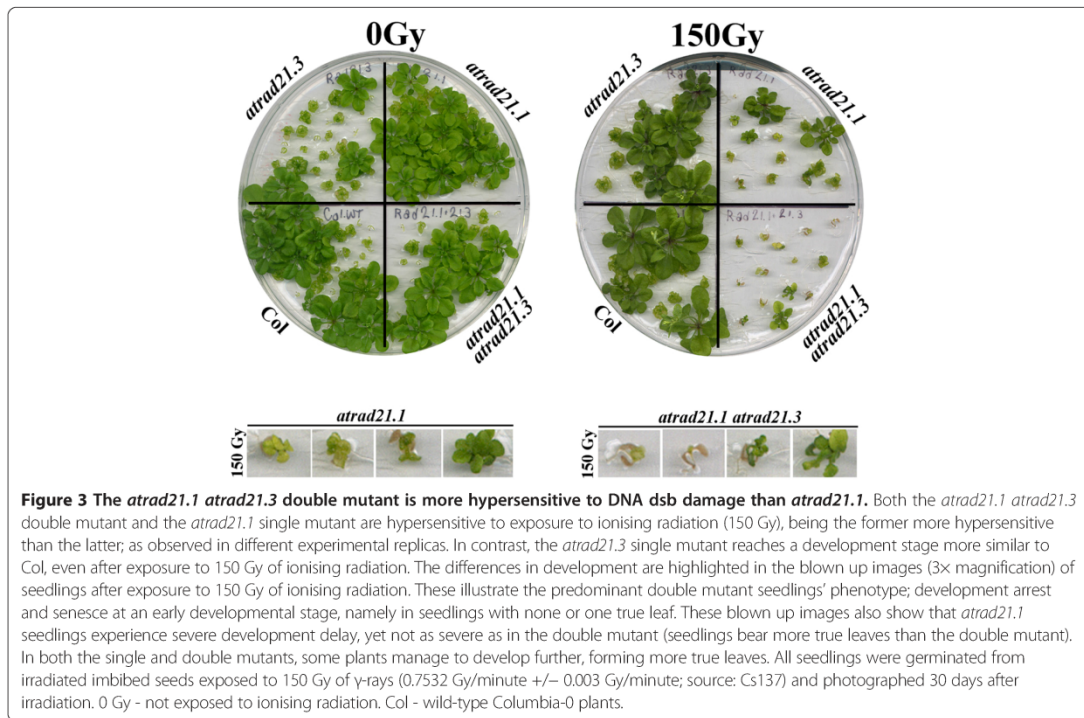
variation, after the induction of DNA dsb damage, is not identical.

***AtRAD21.3*, in association with *AtRAD21.1*, confers resistance to ionising radiation-induced damage**

Because qRT-PCR data shows that the induction of DNA dsb induces the doubling of the *AtRAD21.3* steady-state transcript content, we investigated further if *AtRAD21.3* does play a role in DNA dsb repair. Unlike *atrada21.1*, the *atrada21.3* single mutant does not exhibit clearly discernible DNA dsb damage hypersensitivity phenotypes (such as DNA damage induced lethality) [14]. Hence, we used the *atrada21.1 atrada21.3* double mutant to more easily identify and characterise the role played by *AtRAD21.3* in DNA dsb. The rationale is that any *atrada21.3* induced DNA dsb damage phenotype (that may go unnoticed in the *atrada21.3* single mutant because it is masked by the function played by *AtRAD21.1*) will be more easily detected in the double mutant. The *atrada21.1 atrada21.3* double mutant plants

are viable and fully fertile, producing a full seed set in each silique (data not shown).

30 days after irradiating (with γ -ray) imbibed seeds with 150 Gy (3.25 Gy/minute; source: Cs137), *atrada21.1 atrada21.3* seedlings exhibit a more acute hypersensitivity to γ -irradiation than the *atrada21.1* seedlings (Figure 3). The *atrada21.1 atrada21.3* γ -ray hypersensitivity phenotype, in comparison to the *atrada21.1* and *atrada21.3* single mutants, is characterised by a higher incidence of seedlings that bear only two expanded cotyledons and no true leaves (Figure 4). This is particularly evident at 100 Gy (γ -rays; 3.25 Gy/minute; source: Cs137) (Figure 4(A); Additional file 1: Table S4 and Figure S3), although a few seedlings do develop more true leaves. The higher incidence of seedlings with no true leaves in the *atrada21.1 atrada21.3* double mutant, in comparison to the *atrada21.1* single mutants and Col, is clearly reflected in the value of the medians (Figure 4(B)), modes and means (Additional file 1: Table S5 and Figure S4). Furthermore, according to the Mann-Whitney U-test analysis of the number of true



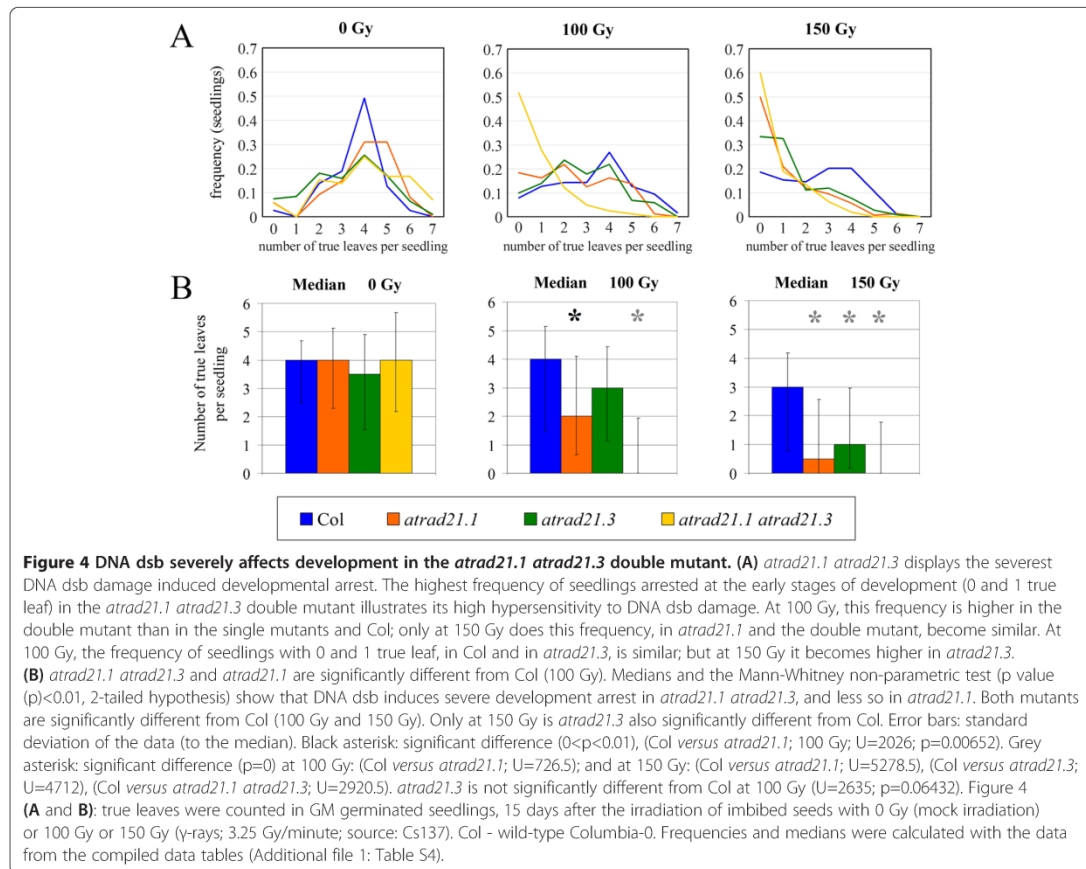
leaves data (obtained 15 days after the exposure to 100 Gy and 150 Gy (γ -rays; 3.25 Gy/minute; source: Cs137)), the *atrada21.1 atrad21.3* double mutant is significantly different (p value (p) = 0, 2-tailed hypothesis) from Col (Figure 4(B)). Comparatively to the double mutant, γ -ray hypersensitive *atrada21.1* mutant seedlings bear more true leaves. Still, *atrada21.1* is developmentally delayed in comparison to wild-type as far as the number of true leaves and the size of the leaves is concerned (Figures 3 and 4). At 100 Gy, *atrada21.1* is already significantly different from Col, albeit with a higher p value (p = 0.00652) than the double mutant (p = 0). In contrast, *atrada21.3* is not significantly different from Col at 100 Gy (p = 0.06432). Only at 150 Gy is it possible to detect a significant difference between *atrada21.3* and Col (Figure 4(B); Additional file 1: Figure S4). Ultimately, many, if not all, of the seedlings exhibiting hypersensitivity to ionising radiation (mostly the *atrada21.1* and the *atrada21.1 atrad21.3* mutants with none or few true leaves) will senesce.

The kinetics of DNA dsb damage repair is affected, and higher basal levels of DNA dsb are detected, in the *atrada21.3* mutant

To further characterise the role of AtRAD21 cohesins, we monitored repair of DNA dsb by comet assays in 10-days-old seedlings exposed to Bleomycin. We chose to

use Bleomycin, a radiomimetic cancerostatic agent that induces DNA dsb in a similar manner to ionising radiation [39], because it allowed us to compare our results with previously published data of DNA dsb repair kinetics [23,40,41]. Three different *atrada21* homozygous mutants were used in the comet assay (*atrada21.1*, *atrada21.3* and *atrada21.1 atrad21.3*). The *atrada21.2* mutant was excluded from this and other assays because, to the best of our knowledge, there are no viable *atrada21.2* homozygous mutant knockout lines available [42].

Repair kinetics observed in seedlings of wild-type Col, *atrada21.1*, *atrada21.3* and the *atrada21.1 atrad21.3* double mutant control (not exposed) and exposed to 10 μ g/ml Bleomycin are not significantly different (data not shown). However, when higher Bleomycin concentrations (30 μ g/ml) are used, which result in the induction of more DNA dsb [40], impaired DNA dsb repair becomes perceptible in the single mutants relative to wild-type. Significant differences are particularly evident between 10 to 60 minutes after DNA dsb induction (Figure 5(A)), i.e. in the transition period from the initial fast phase of dsb repair kinetics to the following slow phase of dsb repair kinetics [43,44] (Additional file 1: Figure S5; Additional file 1: Table S6). Unlike the single mutants, *atrada21.1 atrad21.3* has wild-type-like (Col-like) DNA dsb damage repair kinetics when exposed to 30 μ g/ml Bleomycin. Yet, the



double mutant as well as the *atrada21.1* and the *atrada21.3* single mutants exhibit a significantly higher content of nuclear DNA dsb (high basal level of DNA dsb) than the wild-type (Figure 5(B)), even when there is no induction of DNA dsb.

The *atrada21.1 atrada21.3* double mutant hypersensitivity to DNA dsb damage is less acute than in the *atku80 atrada21.1* double mutant and the *atku80* single mutant
 DNA dsb are repaired via different DNA repair pathways. RAD21 has been proposed to facilitate DNA dsb repair via HR by keeping the homologous DNA sequences of sister chromatids in close proximity [7]. However, in plants, DNA dsb are predominantly repaired via direct joining of double strand breaks' ends (particularly via the Canonical-Non-Homologous-End Joining – C-NHEJ), which do not require an extended homologous DNA sequence strand for repair [45]. To determine the consequences of disrupting ATRAD21 (which has been associated with HR) in a C-NHEJ DNA repair pathway mutant, we've introgressed

the *atrada21.1* mutant allele into the *atku80* mutant background [46] to produce the *atrada21.1 atku80* double mutant.

The *atku80 atrada21.1* double mutant plants were genotyped (Additional file 1: Figure S6) and shown to be viable. Under normal growth conditions (non-irradiated with ionising radiation), these plants have a normal vegetative and fertility phenotype; seed set in each silique of the double mutant is indistinguishable from that of Col plants (data not shown). When the imbibed seeds of *atku80 atrada21.1* double mutant, and the *atku80* mutant, are exposed to γ-rays (100 Gy, 3.25 Gy/minute; source: Cs137), both mutants exhibit a similar acute hypersensitivity phenotype (Figure 6; 100 Gy). No hypersensitivity to DNA dsb is detected when imbibed Col, *atku80* and *atku80 atrada21.1* mutant seeds are irradiated with 50 Gy (3.25 Gy/minute; source: Cs137) of ionising radiation (data not shown).

Comparison of hypersensitivities to DNA dsb induced by ionising radiation shows that *atku80* and *atku80*

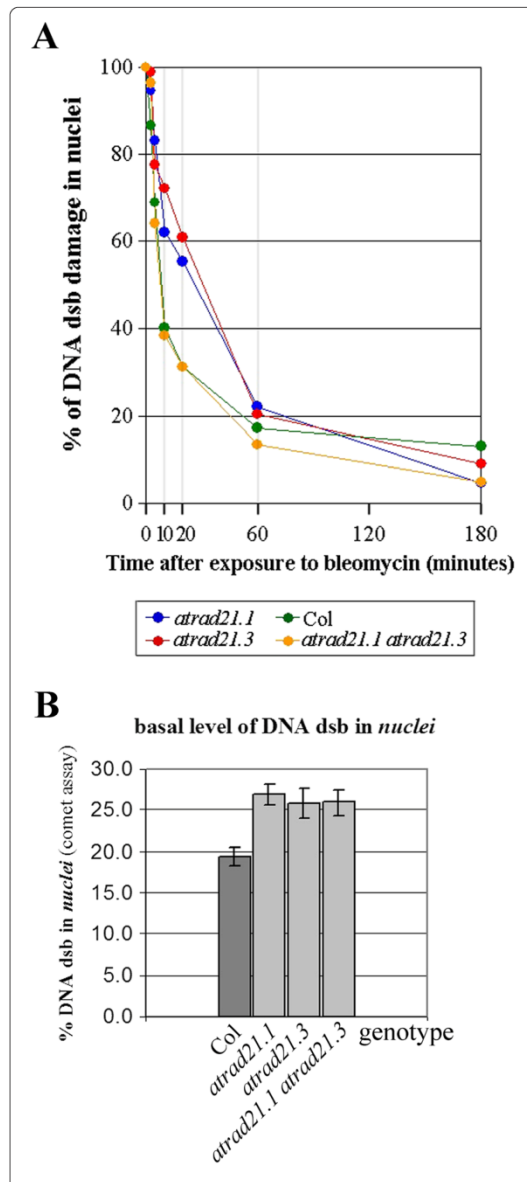


Figure 5 DNA dsb basal levels and repair kinetics are altered in the *atrada21.1* and *atrada21.3* mutants. (A) *atrada21.1* and *atrada21.3* single mutants' DNA dsb damage repair kinetics is similar. During the first 60 minutes after DNA dsb damage induction, *atrada21.1* and *atrada21.3* mutants retain more unrepaired DNA dsb than Col. This difference is more striking at 10 minutes (62.1% to 72.2% of induced DNA dsb remain unrepaired in the single mutants versus 40.2% in Col), 20 minutes (55.4% to 60.9% in the single mutant versus 31.3% in Col) and 60 minutes (20.3% to 22.1% in the single mutants versus 17.1% in Col) after DNA dsb damage induction. The *atrada21.1 atrada21.3* double mutant has a Col-like DNA dsb damage repair kinetics. DNA dsb damage quantification was carried out on nuclei from 10-days old seedlings harvested 0, 3, 5, 10, 20, 60 and 180 minutes after exposure to 30 µg/ml Bleomycin. Col - wild-type Columbia-0 plant. (B) *atrada21.1*, *atrada21.3* and *atrada21.1 atrada21.3* mutants have higher basal levels of DNA dsb than Col. The amount of DNA dsb detected, by comet assay, in nuclei obtained from seedlings not exposed to DNA dsb inducing agent, indicates that the amount of DNA dsb detected in Col is significantly lower than the amount detected in *atrada21.1*, *atrada21.3* and *atrada21.1 atrada21.3* mutants. DNA dsb damage quantification was carried out on nuclei from 10-days old seedlings that were not exposed to Bleomycin. Error bars represent the standard error. Col - wild-type Columbia-0 plant. Comet assay data is available in Additional file 1: Table S6.

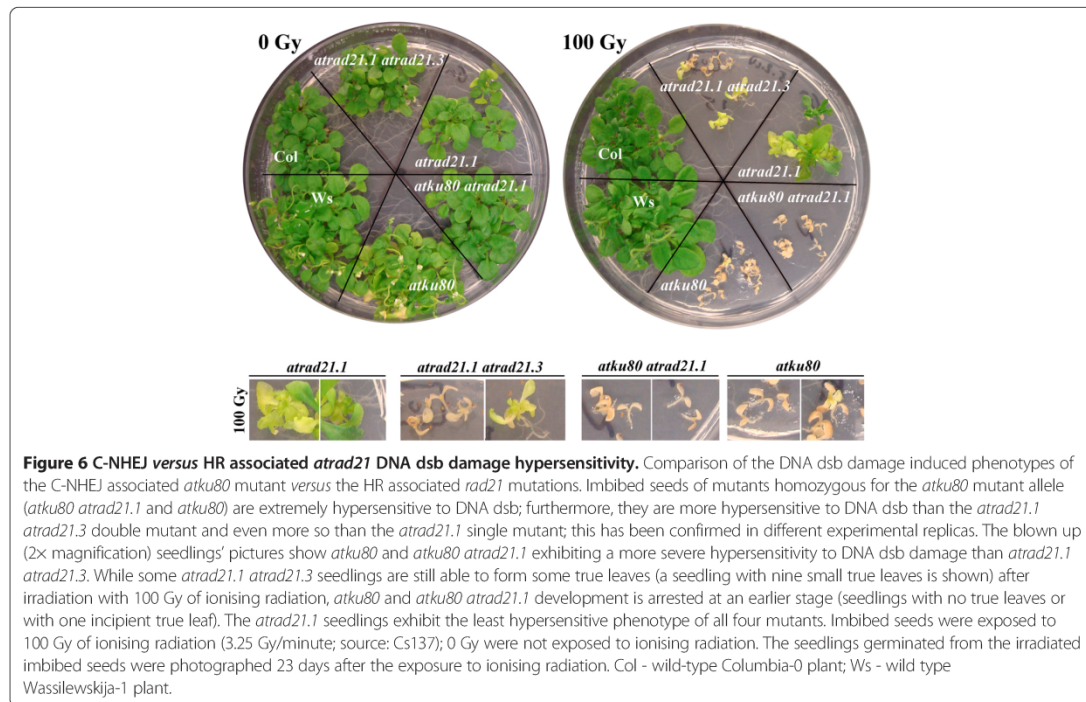
atrada21.1 mutants are clearly more hypersensitive to DNA dsb than the *atrada21.1 atrada21.3* double mutant, and even more so than the *atrada21.1* single mutant (Figure 6).

These observations indicate that even though the AtRAD21.1 and AtRAD21.3 cohesins play an important role in DNA dsb repair in imbibed seeds, the AtKu80 protein, that is associated with C-NHEJ, plays a predominant role in DNA dsb repair. This is in agreement with previous reports that show that the C-NHEJ repair pathway is the predominant repair pathway in plants [45]. Due to the severity of the *atku80* and *atku80 atrada21.1* mutant phenotypes it is not possible to determine if the DNA damage hypersensitivity phenotype observed in the *atku80 atrada21.1* double mutant is identical to that of the *atku80*, or if it is cumulative, yet masked by the severity of the *atku80* phenotype.

Discussion

AtRAD21.1 and AtRAD21.3 *Arabidopsis thaliana* cohesins' emergency response to DNA dsb damage

The increase of steady-state *AtRAD21.3* RNA levels, and more dramatically, the rapid and immediate increase of steady-state *AtRAD21.1* RNA levels after the induction of DNA dsb suggests that both cohesins play a role in an emergency response to DNA dsb damage (Figure 2; Additional file 1: Figure S2). Transcription upregulation of the *AtRAD21.1-GFP-6xHis* transgene in the complementation line plants upon exposure to ionising radiation (Additional file 1: Figure S1c) and the rescue of the *atrada21.1* DNA dsb damage hypersensitivity phenotype in these same lines (Figure 1) links the *AtRAD21.1*



emergency response to DNA dsb repair. This data suggests that the upregulation of *AtRAD21.1* transcriptional activity could be directly correlated with an increase in cohesion induced by DNA dsb (*de novo* cohesion). This hypothesis is in accordance with the reported observation that DNA damage induces in Col an increase in sister chromatid cohesion just 10 minutes after exposure to irradiation [47]. Moreover, and also 10 minutes after the induction of DNA dsb damage, the *atrad21.1* mutant experiences a striking delay in DNA dsb repair (Figure 5 (A)). Together, these observations suggest that, as observed with RAD21 homologues in other organisms, AtRAD21.1 could also be involved in DNA dsb induced *de novo* cohesion required for DNA dsb repair in Arabidopsis. Indeed, in yeast and human cells, it has been proposed that the recruitment of RAD21 cohesin to chromosomes after DNA dsb induction [7,9,10] reinforces the tethering of sister chromatids by quickly establishing DNA dsb induced *de novo* cohesion. Further experiments will be required to demonstrate if this AtRAD21.1 emergency response indeed leads to the *de novo* cohesion and the increased sister chromatid cohesion. The upregulation of *AtRAD21.3* transcription (Figure 2) and the concurrent slower DNA dsb repair detected 10 minutes after the induction of DNA dsb (Figure 5) suggest that AtRAD21.3 may also be involved in an AtRAD21.1-like DNA dsb repair emergency response.

Finally, the similar timing of *AtRAD51* and *AtRAD21.1* transcript content increase (qRT-PCR data) suggests that AtRAD21.1 might also be required during the first stages of DNA dsb repair. AtRAD51, similarly to its homologues in yeast, is thought to be involved in DNA strand invasion and homology search during the first stages of recombination [48-50]. Hence, AtRAD21.1 may play a role at the early stages of somatic recombination (DNA dsb repair) too.

Both AtRAD21.1 and AtRAD21.3 are required for DNA dsb repair

AtRAD21.1 and AtRAD21.3 are required for DNA dsb repair when numerous DNA dsb are induced (30 µg/ml Bleomycin) (Figure 5(A)), as well as when plants are not exposed to DNA dsb inducing agents (Figure 5(B)).

atrad21.1, atad21.3 single mutants, and the *atrad21.1 atad21.3* double mutant, exhibit similar and significantly higher basal level of DNA dsb when compared to Col (Figure 5(B)). This indicates that AtRAD21.1 and AtRAD21.3 are probably required for the repair (or restrict the formation) of DNA dsb induced by endogenous stresses (such as DNA replication) or naturally occurring environmental stresses.

DNA repair kinetics data from *atrad21.1* [40], *atrad21.3* (Figure 5(A)), and other Arabidopsis mutants affecting HR

in somatic tissue and with no apparent deleterious defects during meiosis, such as *atr17* [26] and *gmi1* (a SMC-Hinge Domain containing protein) [23], shows that these mutants experience a delay in DNA dsb repair when many DNA dsb are induced. This delay is evident, as early as 10 to 20 minutes after bleomycin treatment, in the *atr21.1* and *atr21.3* mutant seedlings (Figure 5(A)), as well as in the *gmi1* mutants [23]. These similarities suggest that like GMI1, AtRAD21.1 and AtRAD21.3 may also be involved in HR. The decrease in DNA dsb repair kinetics observed in the *atr21.1* and *atr21.3* single mutants has also been observed in yeast strains that contain low amounts of RAD21 protein [51]. This suggests a correlation between the amount of induced DNA dsb in the cell, and the amount of RAD21 protein required for the DNA dsb repair. Indeed, when low Bleomycin concentration (10 µg/ml) is used, inducing few DNA dsb, the observed repair kinetics between Col, the *atr21.1*, *atr21.3* and *atr21.1 atr21.3* is not significantly different (data not shown). One possible explanation for the similarity in repair kinetics being that the level of chromosome cohesion remaining in the mutant lines is sufficient to countervail the small amount of DNA dsb produced, and hence the efficiency of DNA dsb repair is not affected. Yet, when more DNA dsb are produced (30 µg/ml Bleomycin) [40], the lack of AtRAD21.1 or AtRAD21.3 in the single mutants becomes critical for DNA repair.

We hypothesise that an increasing number of DNA dsb in the cell leads to an increasing need of an abundant pool of cohesin proteins to establish *de novo* cohesion, to allow DNA dsb HR repair. Hence, a less abundant pool of cohesins in the *atr21.1* and *atr21.3* single mutants would account for the less efficient DNA repair (slower kinetics) observed during the first 10 to 20 minutes after the induction of a high incidence of DNA dsb (Figure 5(A)). The slower DNA repair kinetics observed in the *atr21.1* and *atr21.3* single mutants could also be caused by an AtRAD21-dependent DNA-damage-repair-checkpoint. Indeed, the yeast *rad21* mutation has been correlated with the disruption of DNA-damage-induced-checkpoints. Likewise, in mammalian cells, RAD21 is involved in DNA-damage-induced cell cycle progression arrest during DNA replication and at the G2/M cell cycle stages [52-54].

In the particular case of the *atr21.1 atr21.3* double mutant, which has a wild-type-like repair kinetic (Figure 5(A)), it is plausible that due to the knockout of both *AtRAD21.1* and *AtRAD21.3* genes (Additional file 1: Figure S6), an AtRAD21-dependent DNA dsb repair pathway becomes fully compromised. Consequently, we propose that in the double mutant, the DNA dsb repair is switched to an AtRAD21-non-dependent DNA dsb repair pathway with a kinetics similar to the one observed in the *atku80* mutant [40] and wild-type. AtKu80 is associated

with NHEJ DNA repair, unlike RAD21 (the AtRAD21 homologue), AtRAD17 and GMI that are associated with HR [23,26,44,53,55].

Further experiments will help validate these or other hypothesis.

Acute hypersensitivity to DNA dsb in the *atr21.1 atr21.3* double mutant

Despite the lack of AtRAD21.3 protein, which has been attributed a role in sister chromatid arm cohesion and centromere cohesion [37], the *atr21.3* single mutant morphology appears not to differ from that of Col, after exposure to ionising radiation (Figure 3). Only a more detailed characterisation (number of true leaves) of the *atr21.3* mutant indicates that only after exposure to high doses of radiation (Figure 4(B); 150 Gy) does the difference between *atr21.3* and Col becomes significant. Furthermore, the lack of AtRAD21.3 cohesin in the *atr21.1 atr21.3* mutant background results in a higher DNA dsb hypersensitivity phenotype, comparatively to the *atr21.1* single mutant's and Col's DNA dsb hypersensitivity phenotype (Figure 3; Figure 4; Figure 6). These results indicate that both AtRAD21.1 and AtRAD21.3 contribute to the plant's ability to cope with DNA dsb damage, with AtRAD21.3 having a synergistic and non-redundant effect on the AtRAD21.1 function. Other examples exist of synergistic actions on DNA dsb damage repair and genome stability, namely *AtRAD50* and *TERT*, *NBS1* and *TERT*, *NBS1* and *ATM* [25,56,57].

A shift from an AtRAD21-dependent, possibly error free HR repair, to an error-prone-AtRAD21-independent DNA dsb repair pathway could be at the origin of the increased hypersensitivity of the *atr21.1 atr21.3* double mutant to DNA dsb damage. This shift would give rise to an increased frequency of deleterious mutations resulting from the DNA dsb repair, hence inducing the enhanced hypersensitivity to DNA dsb observed in the double mutant (Figure 2). Increased frequency of genomic lesions has been observed in the moss *Physcomitrella patens ppmre11* and *pprad50* mutants [41]. These authors propose that this increased frequency of lesions is caused by a shift to an error-prone DNA repair pathway that directly joins the DNA dsb ends after processing them, and also by the disruption of the RAD50 and MRE11 role in tethering the two DNA dsb ends in close proximity.

Even though *atr21.1 atr21.3*, *atku80* and wild-type have comparable DNA dsb repair kinetics, the double mutant is not as hypersensitive to DNA dsb as the *atku80* mutant [40] (Figure 6). One can speculate that this difference is caused by the choice of different DNA dsb repair pathways in the imbibed seeds of the *atku80* and *atr21.1 atr21.3* mutants.

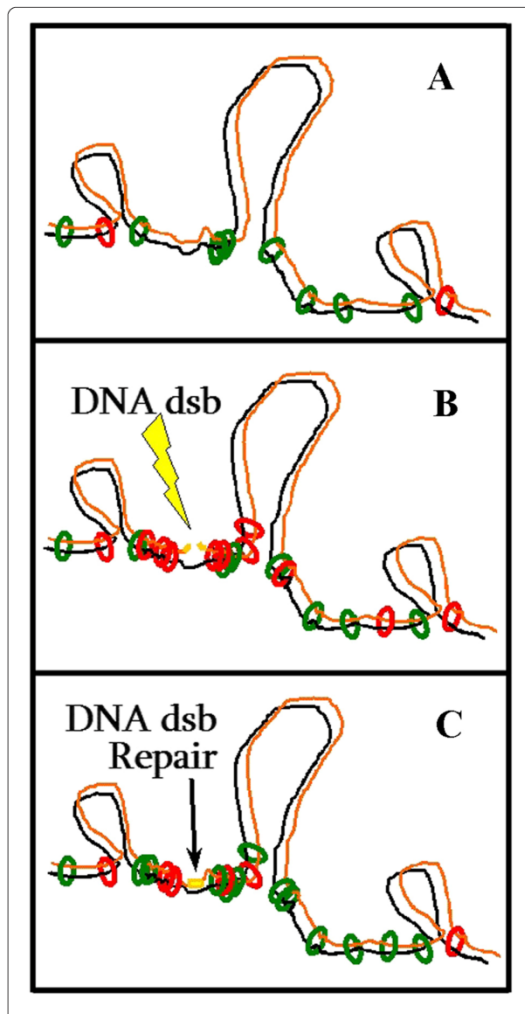


Figure 7 Proposed model: AtRAD21.1 and AtRAD21.3 before and after induction of DNA dsb damage. (A) Before the induction of DNA dsb, sister chromatid cohesion is promoted by AtRAD21.3 (green rings), and possibly also by some AtRAD21.1 (red rings) associated with DNA dsb created by endogenous factors. (B) After the induction of DNA dsb breaks (flash), *AtRAD21.1* expression is enhanced. This is expected to increase the pool of cohesin complexes containing AtRAD21.1 (red rings) in the cell, hence contributing to promote and enhance sister chromatid cohesion. (C) The DNA dsb damage induced increase of *AtRAD21.3* transcript content (that occurs after that of *AtRAD21.1*), is also expected to contribute to increase the pool cohesin complexes containing AtRAD21.3 (green rings). These cohesin complexes (green circles) may reinforce sister chromatid cohesion, or they may replace (all or some of) the AtRAD21.1 cohesin complexes (red rings) that generated the *de novo* cohesion. It has been proposed that the increased cohesion facilitates DNA dsb repair by promoting physical proximity between the chromatid with a DNA dsb (orange) and its intact sister chromatid (black). Green and red rings: cohesin complexes tethering the two sister chromatids (black and orange). Yellow lines: the site of the DNA dsb. Flash (yellow): the DNA dsb inducing agent.

Proposed role of AtRAD21.3 and AtRAD21.1 in sister chromatid cohesion and DNA repair

In this work we show that both AtRAD21.3 and AtRAD21.1 are involved in DNA dsb repair. In Figure 7 is illustrated an hypothesis that proposes that upon induction of DNA dsb, the *AtRAD21.1* emergency transcriptional response ensures an enriched pool of AtRAD21.1 that will reinforce sister chromatid cohesion after the induction of DNA dsb. This function appears to be required at the early stages of DNA dsb repair (Figure 2), and is crucial since the *atrad21.1* is hypersensitive to DNA dsb damage. *AtRAD21.3* upregulation is also proposed to contribute, but at a later stage, to the pool of AtRAD21 cohesin proteins required for DNA dsb repair after the induction of DNA dsb. However, the AtRAD21.3 primary role may be to establish chromosome cohesion and contribute to chromosome structure regardless of the presence or the absence of DNA dsb. Indeed, data from Takahashi and Quimbaya *et al.* [36] hint that AtRAD21.3 cohesion may be associated with DNA replication. Hence, the major AtRAD21.3 contribution to the repair of DNA dsb may be to provide a pre-existing chromosome scaffold and cohesion that will aid the repair of DNA dsb that arise subsequently.

The conjecture that AtRAD21.3 plays a role in chromosome structure is based on evidences that the RAD21 protein, in metazoans, is involved in chromatin structure [58,59] and associates with the nuclear matrix [60]. Interestingly, like for the *atrad21.3* mutant [14] (Additional file 1: Figure S7), it has also been reported that the mis-expression or the knocking-out of some matrix-associated proteins that contribute to chromatin remodelling, also affects flower-bolting time [61,62].

Conclusions

The identification of AtRAD21.3's involvement in DNA dsb damage repair adds another player to the group of known proteins that are involved in DNA dsb repair in Arabidopsis. A role for AtRAD21.3 in DNA dsb damage repair is clearly demonstrated by the comet assay data and the γ -ray hypersensitivity phenotype observed in the *atrad21.1 atrad21.3* double mutant. Likewise, the reduced number of true leaves in the *atrad21.3* single mutant, in comparison to Col, particularly after exposure to high dosages of radiation (150 Gy), is also an indication that AtRAD21.3 plays a role in DNA dsb damage repair. Furthermore, the different γ -ray hypersensitivity phenotypes exhibited by the *atrad21.1*, *atrad21.3* and *atrad21.1 atrad21.3* mutants, and the fact that both genes are upregulated in response to DNA dsb damage indicates that their functions in DNA dsb damage repair are not redundant. Our data reveals an increased level of complexity to the involvement of cohesins in DNA dsb damage repair that could be specific to plants.

Methods

Plant material

Arabidopsis thaliana seeds were surface sterilised, plated in germination medium, and imbibed in the dark at 4°C, for three to four days. All seedlings, except those depicted in Figure 3, were grown on germination solid medium (GM) (MS medium + Gamborg B5 vitamins, 1% sucrose; 0.8% micro-agar - Duchefa) in sterile Petri dishes or in pots containing a sterilised commercial mix of turf, soil and fertiliser; pH 5.5 - 6.5. Both GM and soil grown plants were kept in growth chambers with a light cycle of 16 hours of light at 22°C alternating with 8 hours of darkness at 19°C. In the assay depicted in Figure 3, imbibed sterilised seeds were germinated and grown for 30 days in ½MS solid medium, in a growth chamber with continuous light (24 hours) at 21°C.

Primers used for genotyping are shown in Additional file 1: Table S7, and plant material sources (Col, Ws, *atku80*, *atrad21.1*, *atrad21.3* and *atrad21.1 atrad21.3*) are described in Additional file 1: Materials and Methods. Plant genomic DNA was extracted using the method devised by Edwards *et al.* [63].

AtRAD21.1 complementation construct

The complementation construct comprises the upstream genomic region (2,602 bp) and the coding genomic sequence (containing the introns and exons) of *AtRAD21.1* (4,109 bp), excluding the translation stop codon. The genomic fragment was PCR amplified using the Pfx50 DNA polymerase enzyme (Invitrogen), following the manufacturer's protocol; the primers GP1G (CACC GCAT CTTTGCTCACCTACCTCAAACG) and GR1cDR (ACA AGCTTTTTGTGGTCTGGAAACACGCAT) were used

(Additional file 1: Figure S1f)). Genomic DNA isolated from the MHK7 P1 clone (provided by Arabidopsis Biological Resource Centre - ABRC) was used as template. The PCR product was cloned in a pENTR/D-topo vector (Invitrogen), recombined into the pMDC107 vector [64] using the LR clonase II enzyme mix reaction (Invitrogen), and sequenced.

AtRAD21.1 complementation lines

Col and *atrad21.1* homozygous mutant plants were transformed with the genomic *AtRAD21.1-GFP-6xHis* complementation construct by the floral dip method [65], using the *Agrobacterium tumefaciens* GV3101 strain carrying the plasmid pMP90RK [66]. T1 transformants were selected on hygromycin containing media, and T2 seeds harvested. T2 seeds were exposed to ionising radiation (DNA damage sensitivity assay) and those plants not displaying hypersensitivity to DNA dsb (27 days after exposure to 150 Gy of ionising radiation) were genotyped (primer pairs information is available in Additional file 1: Table S7). The expression of the *AtRAD21.1-GFP-6xHis* construct was assessed (verifying complementation) by RT-PCR using RNA extracted from samples, frozen in liquid nitrogen, 1 hour after exposure to irradiation and mock-irradiation (Additional file 1: Table S1). RNA was extracted from irradiated (150 Gy; 3.25 Gy/minute; source: Cs137) rosette leaves from a heterozygous *atrad21.1* plant, and seedlings from a complementation line (in *atrad21.1* homozygous mutant genetic background) and from non-irradiated (mock) Col rosette leaves. cDNA was synthesised (as described in Additional file 1: Materials and Methods).

Ionising radiation sensitivity assays

Four weeks old Col plants grown *in vitro* (in GM solid medium) were irradiated with 316 Gy (2.65 Gy/minute; source: Co60), in the dark. The dosage of radiation absorbed by the samples was monitored with radiation dosimeters placed under and over the irradiated samples. After irradiation, the plants were placed back in the growth chamber.

Irradiation of seeds was carried out after surface sterilising, and imbibing the seeds in sterile 0.1% agarose for 3 to 4 days at 4°C, in the dark. Seeds were irradiated inside a GammaCell 2000 with the calculated dosages of 50 Gy, 100 Gy or 150 Gy of ionising radiation (γ -rays; 3.25 Gy/minute; source: Cs137), or inside a GammaCell 40 with the calculated dosages of 150 Gy (γ -rays; 0.7532 Gy/minute \pm 0.003 Gy/minute; source: Cs137). After irradiation, seeds were plated on GM solid medium and grown in sterile conditions in the growth chamber. Imbibed seeds and four weeks-old plants, used as experimental controls, were not irradiated (0 Gy).

Statistical analysis

The number of emerging, and formed, true leaves was counted in individual seedling after 15 days after the irradiation (15 DAI), or mock-irradiation, of the seeds. The irradiated (and non-irradiated, 0 Gy) seeds were imbibed in 0.1% agarose for 3 days, in the dark at 4°C, prior to being irradiated with 100 Gy or 150 Gy (γ -rays; 3.25 Gy/minute; source Cs137). The seeds were germinated and grown in sterile petri dishes, on germination solid medium (GM), in a growth chamber (16 hours of light, 22°C; 8 hours of dark, 19°C).

Non-parametric Mann–Whitney U-test [67] ($p < 0.01$; 2-tailed hypothesis) was performed to determine if there are significant differences between the *atrad21.1*, *atrad21.3* and *atrad21.1 atrad21.3* mutants and the wild type plants Col; differences in hypersensitivity to ionising radiation exposure were estimated via the number of true leaves per seedlings. The compiled data (Additional file 1: Table S4) was used in the Mann–Whitney U-test.

RNA extraction and quantitative real-time PCR expression data acquisition and analysis

Rosette leaves from non-irradiated and irradiated four weeks old Col plants grown in GM medium were harvested 5, 15, 30 and 45 minutes, and 1, 2, 4, 6, 8, 10, 24 and 48 hours after the 316 Gy irradiation session (2.65 Gy/minute; source: Co60), and immediately frozen in liquid nitrogen and stored at -80°C . RNA was extracted from three independent biological replicas (irradiated and non-irradiated) and cDNA was synthesised. The transcript steady-state levels were quantified by Real-Time PCR. The monitored genes were: the cohesin genes being characterised (*AtRAD21.1*, *AtRAD21.2*, *AtRAD21.3*), *AtATM*, the positive control *AtRAD51* [68], and the reference genes (*Actin2* and *AtEF1 α A4*) [47,68]. Relative quantification of transcript accumulation was obtained using the Pfaffl method [69]. Primer information and further protocol information is provided in Additional file 1: Materials and Methods and Additional file 1: Table S3.

Comet assay: DNA dsb induction, data acquisition and evaluation

Nuclear DNA dsb fragmentation of 10-days-old Arabidopsis seedlings (Col and *atrad21.1*, *atrad21.3* and *atrad21.1 atrad21.3* homozygous mutant lines) was assessed with the neutral protocol for single cell gel electrophoresis (comet) assay [40,70]. Untreated seedlings, and seedlings treated with 10 $\mu\text{g/ml}$ and 30 $\mu\text{g/ml}$ Bleomycin Sulfate (cancerostatic Bleomedac Medac, Germany) for 1 hour in liquid $\frac{1}{2}\text{MS}$, were harvested and frozen in liquid nitrogen 3, 5, 10, 20, 60 and 180 minutes after the Bleomycin treatment (DNA dsb inducing agent). After processing, nuclear 'comets' were stained with SYBR Gold stain (Molecular Probes/Invitrogen), viewed in an epifluorescence Nikon

Eclipse 800 microscope and evaluated by the Comet module (LUCIA Comet Assay) of the LUCIA cytogenetics software (LIM, Czech Republic). Three independent experiments were performed and compiled. The incidence of DNA dsb was measured as the fraction of fragmented DNA that moved from the comet head to the comet tail (% tail-DNA). The calculated percentage of DNA damage remaining for each given repair time t_x is defined as:

$$K(t) = \% \text{ damage remaining}(t_x) \\ \times \frac{\text{mean \%tail-DNA}(t_x) - \text{mean \%tail-DNA}(\text{control})}{\text{mean \%tail-DNA}(t_0) - \text{mean \%tail-DNA}(\text{control})} \times 100$$

A more detailed protocol is provided in Additional file 1: Materials and Methods.

Supporting data

The data set(s) supporting the results of this article are included within the article and in its additional file.

Additional file

Additional file 1: Materials and Methods. Plant Material; qRT-PCR analysis; Comet assay. **Figure S1.** *AtRAD21.1-GFP-6xHis* transcript detection, and gene schematic representation. **Figure S2.** Relative variation of steady-state transcript levels during the 48 hours after the exposure to ionising radiation. **Figure S3.** Frequency of seedlings with different numbers of true leaves, in different genotypes, before and after exposure to ionising radiation. **Figure S4.** Mean of the number of true leaves per seedling after exposure to ionising radiation. **Figure S5.** Comet assay - significant differences. **Figure S6.** Genotyping of the homozygous mutant plants. **Figure S7.** Bolting phenotype. **Table S1.** Primers to monitor gene expression (RT-PCR). **Table S2.** Relative variation of transcript steady-state content in Col, after the induction of DNA dsb damage. **Table S3.** Primers for qRT-PCR quantification of *AtRAD21* transcript steady state levels variation after exposure to ionising radiation. **Table S4.** Number of true leaves per seedling. **Table S5.** Mean, Mode and Median (true leaves per seedling). **Table S6.** Comet assay data. **Table S7.** Primers for mutants and complementation lines genotyping.

Abbreviations

AE: After end of irradiation exposure; C-NHEJ: Canonical non-homologous end-joining DNA repair pathway; Col: Wild-type Columbia-0; Comp: Complementation lines; dsb: Double strand break; GM: Germination solid medium; HR: Homologous recombination DNA repair pathway; NHEJ: Non-homologous end-joining DNA repair pathway; qRT-PCR: Quantitative real-time PCR; RT-PCR: Reverse transcription PCR.

Competing interests

The authors declare that they have no competing interests.

Authors' contributions

JCN co-ordinated the research, and designed all the experimental work but the qRT-PCR and the comet assays. The qRT-PCR experiment was designed and carried out jointly by JCN and CC; CC processed the data. JK and KJA designed, carried out and processed the comet data. JCN and PCN, GMD and OP carried out the irradiation assays; PCN and JCN did the genotyping. The paper was written by JCN with valuable contributions from all authors. All authors read and approved the final manuscript.

Acknowledgements

JCN is thankful to Eng. Paula Matos for her valuable help in the irradiation sessions (CHIP/Instituto Tecnológico e Nuclear, Portugal). We are also thankful to the Instituto Gulbenkian de Ciência (Portugal) and CHIP/Instituto

Tecnológico e Nuclear (Portugal) and the University of New Mexico (USA) for granting access to their facilities to carry out the irradiation assays. JCN is thankful to Dr. C. West (University of Leeds, UK) for providing the *W*s landrace and the *atku80* mutant, and to Eng. Alexandre Calapez (Instituto de Sistemas e Robótica, Universidade de Lisboa, Portugal) for critical discussion on statistical data analysis. This work was supported by Fundação para a Ciência e a Tecnologia [Fellowship SFRH/BPD/30365/2006 and Research Project PTDC/BIA-BCM/64192/2006 to JCN], the Ministry of Education, Youth and Sports of the Czech Republic [project LD13006 to JK and KJA] and Czech Science Foundation [project 13_065955 to JK and KJA], and the University of New Mexico (UNM), USA. [Postbaccalaureate Research and Education Program, R25GM075149 from the NIH, to GMD, and start-up funding to PCN and OP]. CC was funded by the Fellowship [24/04/10 CPS] (under the scope of the Project IBET Project 331 'Produção em cultura de células em suspensão in vitro do princípio activo de *Thymus mastichina*'. in the lab. of Prof. Pedro FEVEREIRO, Laboratório de Biotecnologia de Células Vegetais).

Author details

¹Instituto de Tecnologia Química e Biológica (ITQB), Universidade Nova de Lisboa (UNL), Av. República, Apartado 127, 2781-901 Oeiras, Portugal. ²Laboratório de Biotecnologia de Células Vegetais, ITQB, UNL, Av. República, Apartado 127, 2781-901 Oeiras, Portugal. ³Current address: Gregor Mendel Institute of Molecular Plant Biology, Austrian Academy of Sciences, Vienna Biocenter, 1030 Vienna, Austria. ⁴Molecular Farming Lab., Institute of Experimental Botany AS CR, Na Karlovce 1, 160 00 Praha 6, Czech Republic. ⁵Department of Biology, University of New Mexico, 235 Casteretter Hall, MSC03 2020, 1 University of New Mexico, Albuquerque NM 87131-0001, New Mexico, USA. ⁶Current address: Nuclear Organization and Epigenetics Lab., Shanghai Center for Plant Stress Biology (PSC), No. 3888 Chenhua Road, Shanghai 201602, P. R. China.

Received: 12 May 2014 Accepted: 26 November 2014

Published online: 16 December 2014

References

- Birkenbihl RP, Subramani S: Cloning and characterization of *rad21* an essential gene of *Schizosaccharomyces pombe* involved in DNA double-strand-break repair. *Nucleic Acids Res* 1992, **20**(24):6605–6611.
- Michaelis C, Ciosk R, Nasmyth K: Cohesins: chromosomal proteins that prevent premature separation of sister chromatids. *Cell* 1997, **91**(1):35–45.
- Nasmyth K: Cohesin: a catenase with separate entry and exit gates? *Nat Cell Biol* 2011, **13**(10):1170–1177.
- Uhlmann F, Nasmyth K: Cohesion between sister chromatids must be established during DNA replication. *Curr Biol* 1998, **8**(20):1095–1101.
- Heidinger-Pauli JM, Únal E, Koshland D: Distinct targets of the Eco1 acetyltransferase modulate cohesion in S phase and in response to DNA damage. *Mol Cell* 2009, **34**(3):311–321.
- Uhlmann F, Lottspeich F, Nasmyth K: Sister-chromatid separation at anaphase onset is promoted by cleavage of the cohesin subunit Scc1. *Nature* 1999, **400**(6739):37–42.
- Ström L, Lindroos HB, Shirahige K, Sjögren C: Postreplicative recruitment of cohesin to double-strand breaks is required for DNA repair. *Mol Cell* 2004, **16**(6):1003–1015.
- Únal E, Heidinger-Pauli JM, Koshland D: DNA double-strand breaks trigger genome-wide sister-chromatid cohesion through Eco1 (Ctf7). *Science* 2007, **317**(5835):245–248.
- Potts PR, Porteus MH, Yu H: Human SMC5/6 complex promotes sister chromatid homologous recombination by recruiting the SMC1/3 cohesin complex to double-strand breaks. *EMBO J* 2006, **25**(14):3377–3388.
- Bauerschmidt C, Arrichiello C, Burdak-Rothkamm S, Woodcock M, Hill MA, Stevens DL, Rothkamm K: Cohesin promotes the repair of ionizing radiation-induced DNA double-strand breaks in replicated chromatin. *Nucleic Acids Res* 2010, **38**(2):477–487.
- Lord CJ, Garrett MD, Ashworth A: Targeting the double-strand dna break repair pathway as a therapeutic strategy. *Clin Cancer Res* 2006, **12**(15):4463–4468.
- Hiom K: Coping with DNA double strand breaks. *DNA Repair* 2010, **9**(12):1256–1263.
- Friesner J, Britt AB: *Ku80*- and *DNA ligase IV*-deficient plants are sensitive to ionizing radiation and defective in T-DNA integration. *Plant J* 2003, **34**(4):427–440.
- da Costa-Nunes JA, Bhatt AM, O'Shea S, West CE, Bray CM, Grossniklaus U, Dickinson HG: Characterization of the three *Arabidopsis thaliana* RAD21 cohesins reveals differential responses to ionizing radiation. *J Exp Bot* 2006, **57**(4):971–983.
- Li J, Harper LC, Golubovskaya I, Wang CR, Weber D, Meeley RB, McElver J, Bowen B, Cande WZ, Schnable PS: Functional analysis of maize RAD51 in meiosis and DSBs repair. *Genetics* 2007, **176**(3):1469–1482.
- Waterworth WM, Masnavi G, Bhardwaj RM, Jiang Q, Bray CM, West CE: A plant DNA ligase is an important determinant of seed longevity. *Plant J* 2010, **63**(5):848–860.
- Klimyuk VI, Jones JDG: *AtDMC1*, the *Arabidopsis* homologue of yeast *DMC1* gene: characterization, transposon-induced allelic variation and meiosis-associated expression. *Plant J* 1997, **11**(1):1–14.
- Deveaux Y, Alonso B, Pierrugues O, Godon C, Kazmaier M: Molecular cloning and developmental expression of *AtGR1*, a new growth-related *Arabidopsis* gene strongly induced by ionizing radiation. *Radiat Res* 2000, **154**(4):355–364.
- Lafarge S, Montané MH: Characterization of *Arabidopsis thaliana* ortholog of the human breast cancer susceptibility gene 1: *AtBRCA1*, strongly induced by gamma rays. *Nucleic Acids Res* 2003, **31**(4):1148–1155.
- West CE, Waterworth WM, Sunderland PA, Bray CM: *Arabidopsis* DNA double-strand break repair pathways. *Biochem Soc Trans* 2004, **32**(Pt 6):964–966.
- Culligan KM, Robertson CE, Foreman J, Doerner P, Britt AB: ATR and ATM play both distinct and additive roles in response to ionizing radiation. *Plant J* 2006, **48**(6):947–961.
- Ricaud L, Proux C, Renou J-P, Pichon O, Fochesato S, Ortel P, Montané M-H: ATM-mediated transcriptional and developmental responses to γ -rays in *Arabidopsis*. *PLoS One* 2007, **2**(5):e430.
- Böhmendorfer G, Schleiffer A, Brunmeir R, Ferscha S, Nizhynska V, Kozak J, Angelis KJ, Kreil DP, Schweizer D: GMI1, a structural-maintenance-of-chromosomes-hinge domain-containing protein, is involved in somatic homologous recombination in *Arabidopsis*. *Plant J* 2011, **67**(3):420–433.
- Gallego ME, Jeanneau M, Granier F, Bouchez D, Bechtold N, White CJ: Disruption of the *Arabidopsis* RAD50 gene leads to plant sterility and MMS sensitivity. *Plant J* 2001, **25**(1):31–41.
- Waterworth WM, Altun C, Armstrong SJ, Roberts N, Dean PJ, Young K, Weil CF, Bray CM, West CE: NBS1 is involved in DNA repair and plays a synergistic role with ATM in mediating meiotic homologous recombination in plants. *Plant J* 2007, **52**(1):41–52.
- Heitzberg F, Chen IP, Hartung F, Orel N, Angelis KJ, Puchta H: The *Rad17* homologue of *Arabidopsis* is involved in the regulation of DNA damage repair and homologous recombination. *Plant J* 2004, **38**(6):954–968.
- de Schutter K, Joubès J, Cools T, Verkest A, Corellou F, Babiychuk E, Van Der Schueren E, Beeckman T, Kushnir S, Inzé D, De Veylder L: *Arabidopsis* WEE1 kinase controls cell cycle arrest in response to activation of the DNA integrity checkpoint. *Plant Cell* 2007, **19**(1):211–225.
- Culligan K, Tissier A, Britt A: ATR regulates a G2-phase cell-cycle checkpoint in *Arabidopsis thaliana*. *Plant Cell* 2004, **16**(5):1091–1104.
- Hefner E, Huefner N, Britt AB: Tissue-specific regulation of cell-cycle responses to DNA damage in *Arabidopsis* seedlings. *DNA Repair* 2006, **5**(1):102–110.
- García V, Bruchet H, Camescasse D, Granier F, Bouchez D, Tissier A: AtATM is essential for meiosis and the somatic response to DNA damage in plants. *Plant Cell* 2003, **15**(1):119–132.
- Dong F, Cai X, Makaroff CA: Cloning and characterization of two *Arabidopsis* genes that belong to the RAD21/REC8 family of chromosome cohesion proteins. *Gene* 2001, **271**(1):99–108.
- Winter D, Vinegar B, Nahal H, Ammar R, Wilson GV, Provart NJ: An "Electronic Fluorescent Pictograph" browser for exploring and analyzing large-scale biological data sets. *PLoS One* 2007, **2**(8):e718.
- AtGenExpress Visualization Tool (AVT) (development). [http://jps.weigelworld.org/expviz/expviz.jsp?experiment=development&normalization=absolute&probesetscsv=At5g40840&action=Run]
- Arabidopsis* eFP Browser (Data source: Developmental Map; Primary gene ID: At5g40840). [http://bar.utoronto.ca/efp/cgi-bin/efpWeb.cgi]
- Schmid M, Davison TS, Henz SR, Pape UJ, Demar M, Vingron M, Schölkopf B, Weigel D, Lohmann JU: A gene expression map of *Arabidopsis thaliana* development. *Nat Genet* 2005, **37**(5):501–506.
- Takahashi N, Quimbaya M, Schubert V, Lammens T, Vandepoel K, Schubert I, Matsui M, Inzé D, Berr G, De Veylder L: The MCM-binding protein ETG1

- aids sister chromatid cohesion required for postreplicative homologous recombination repair. *PLoS Genet* 2010, **6**(1):e1000817.
37. Schubert V, Weißbleder A, Ali H, Fuchs J, Lermontova I, Meister A, Schubert I: Cohesin gene defects may impair sister chromatid alignment and genome stability in *Arabidopsis thaliana*. *Chromosoma* 2009, **118**(5):591–605.
 38. Tax FE, Vernon DM: T-DNA-Associated Duplication/Translocations in *Arabidopsis*. implications for mutant analysis and functional genomics. *Plant Physiol* 2001, **126**(4):1527–1538.
 39. Charles K, Povirk LF: Action of bleomycin on structural mimics of intermediates in DNA double-strand cleavage. *Chem Res Toxicol* 1998, **11**(12):1580–1585.
 40. Kozak J, West CE, White C, da Costa-Nunes JA, Angelis KJ: Rapid repair of DNA double strand breaks in *Arabidopsis thaliana* is dependent on proteins involved in chromosome structure maintenance. *DNA Repair* 2009, **8**(3):413–419.
 41. Kamisugi Y, Schaefer DG, Kozak J, Charlot F, Vrielynck N, Holá M, Angelis KJ, Cuming AC, Nogué F: MRE11 and RAD50, but not NBS1, are essential for gene targeting in the moss *Physcomitrella patens*. *Nucleic Acids Res* 2012, **40**(8):3496–3510.
 42. Jiang L, Xia M, Strittmatter LJ, Makarov CA: The *Arabidopsis* cohesin protein SYN3 localizes to the nucleolus and is essential for gametogenesis. *Plant J* 2007, **50**(6):1020–1034.
 43. Goodarzi AA, Jeggo P, Lobrich M: The influence of heterochromatin on DNA double strand break repair: getting the strong, silent type to relax. *DNA Repair* 2010, **9**(12):1273–1282.
 44. Jeggo PA, Geuting V, Löbrich M: The role of homologous recombination in radiation-induced double-strand break repair. *Radiother Oncol* 2011, **101**(1):7–12.
 45. Charbonnel C, Allain E, Gallego ME, White C: Kinetic analysis of DNA double-strand break repair pathways in *Arabidopsis*. *DNA Repair* 2011, **10**(6):611–619.
 46. West CE, Waterworth WM, Story GW, Sunderland PA, Jiang Q, Bray CM: Disruption of the *Arabidopsis AtKu80* gene demonstrates an essential role for AtKu80 protein in efficient repair of DNA double-strand breaks in vivo. *Plant J* 2002, **31**(4):517–528.
 47. Watanabe K, Pacher P, Dukowic S, Schubert V, Puchta H, Schubert I: The structural maintenance of chromosomes 5/6 complex promotes sister chromatid alignment and homologous recombination after DNA damage in *Arabidopsis thaliana*. *Plant Cell* 2009, **21**(9):2688–2699.
 48. Bleuyard JY, Gallego ME, Savigny F, White C: Differing requirements for the *Arabidopsis* Rad51 paralogs in meiosis and DNA repair. *Plant J* 2005, **41**(4):533–545.
 49. Sanchez-Moran E, Santos J-L, Jones GH, Franklin FCH: ASY1 mediates AtDMC1-dependent interhomolog recombination during meiosis in *Arabidopsis*. *Genes Dev* 2007, **21**(17):2220–2233.
 50. Pradillo M, López E, Linacero R, Romero C, Cuñado N, Sánchez-Morán E, Santos JL: Together yes, but not coupled: new insights into the roles of RAD51 and DMC1 in plant meiotic recombination. *Plant J* 2012, **69**(6):921–933.
 51. Covo S, Westmoreland JW, Gordenin DA, Resnick MA: Cohesin is limiting for the suppression of DNA damage-induced recombination between homologous chromosomes. *PLoS Genet* 2010, **6**(7):e1001006.
 52. Watrin E, Peters J-M: The cohesin complex is required for the DNA damage-induced G2/M checkpoint in mammalian cells. *EMBO J* 2009, **28**(17):2625–2635.
 53. Xu H, Balakrishnan K, Malaterre J, Beasley M, Yan Y, Essers J, Appeldoorn E, Thomaszewski JM, Vazquez M, Verschoor S, Lavin MF, Bertoncello I, Ramsay RG, McKay MJ: Rad21-cohesin haploinsufficiency impedes DNA repair and enhances gastrointestinal radiosensitivity in mice. *PLoS One* 2010, **5**(8):e12112.
 54. Xu H, Thomaszewski JM, McKay MJ: Can corruption of chromosome cohesin create a conduit to cancer? *Nat Rev Cancer* 2011, **11**(3):199–210.
 55. Gallego ME, Bleuyard JY, Daoudal-Cotterell S, Jallut N, White C: Ku80 plays a role in non-homologous recombination but is not required for T-DNA integration in *Arabidopsis*. *Plant J* 2003, **35**(5):557–565.
 56. Vannier JB, Depeiges A, White C, Gallego ME: Two roles for Rad50 in telomere maintenance. *EMBO J* 2006, **25**(19):4577–4585.
 57. Najdekrova L, Siroky J: NBS1 plays a synergistic role with telomerase in the maintenance of telomeres in *Arabidopsis thaliana*. *BMC Plant Biol* 2012, **12**:167.
 58. Bose T, Gerton JL: Cohesinopathies, gene expression, and chromatin organization. *J Cell Biol* 2010, **189**(2):201–210.
 59. Kim YJ, Cecchini KR, Kim TH: Conserved, developmentally regulated mechanism couples chromosomal looping and heterochromatin barrier activity at the homeobox gene A locus. *Proc Natl Acad Sci U S A* 2011, **108**(18):7391–7396.
 60. Sadano H, Sugimoto H, Sakai F, Nomura N, Osumi T: NXP-1, a human protein related to Rad21/Sccl1/Mcd1, is a component of the nuclear matrix. *Biochem Biophys Res Commun* 2000, **267**(1):418–422.
 61. Yun J, Kim Y-S, Jung J-H, Seo PJ, Park C-M: The AT-hook motif-containing protein AHL22 regulates flowering initiation by modifying FLOWERING LOCUS T chromatin in *Arabidopsis*. *J Biol Chem* 2012, **287**(19):15307–15316.
 62. Xu Y, Wang Y, Stroud H, Gu X, Sun B, Gan E-S, Ng K-H, Jacobsen SE, He Y, Ito T: A matrix protein silences transposons and repeats through interaction with retinoblastoma-associated proteins. *Curr Biol* 2013, **23**(4):345–350.
 63. Edwards K, Johnstone C, Thompson C: A simple and rapid method for the preparation of plant genomic DNA for PCR analysis. *Nucleic Acids Res* 1991, **19**(6):1349.
 64. Curtis M, Grossniklaus U: A Gateway™ cloning vector set for high-throughput functional analysis of genes in plants. *Plant Physiol* 2003, **133**(2):462–469.
 65. Clough SJ, Bent AF: Floral dip: a simplified method for *Agrobacterium*-mediated transformation of *Arabidopsis thaliana*. *Plant J* 1998, **16**(6):735–743.
 66. Koncz C, Schell J: The promoter of T₁-DNA gene 5 controls the tissue-specific expression of chimeric genes carried by a novel type of *Agrobacterium* binary vector. *Mol Gen Genet* 1986, **204**(3):383–396.
 67. Social Science Statistics. [http://www.socscistatistics.com/tests/mannwhitney/]
 68. Endo M, Ishikawa Y, Osakabe K, Nakayama S, Kaya H, Araki T, Shibahara K, Abe K, Ichikawa H, Valentine L, Hohn B, Toki S: Increased frequency of homologous recombination and T-DNA integration in *Arabidopsis* CAF-1 mutants. *EMBO J* 2006, **25**(23):5579–5590.
 69. Pfaffl MW: A new mathematical model for relative quantification in real-time RT-PCR. *Nucleic Acids Res* 2001, **29**(9):e45.
 70. Olive PL, Banath JP: The comet assay: a method to measure DNA damage in individual cells. *Nat Protoc* 2006, **1**(1):23–29.

doi:10.1186/s12870-014-0353-9

Cite this article as: da Costa-Nunes et al.: The ATRAD21.1 and ATRAD21.3 *Arabidopsis* cohesins play a synergistic role in somatic DNA double strand break damage repair. *BMC Plant Biology* 2014 **14**:353.

Submit your next manuscript to BioMed Central and take full advantage of:

- Convenient online submission
- Thorough peer review
- No space constraints or color figure charges
- Immediate publication on acceptance
- Inclusion in PubMed, CAS, Scopus and Google Scholar
- Research which is freely available for redistribution

Submit your manuscript at
www.biomedcentral.com/submit



5. Diskuze

Efektivní rekombinace určuje schopnost rostlin vyrovnat se s DSB. Dva oblíbené rostlinné modely reprezentující vyšší a nižší rostliny, *Arabidopsis* a *Physcomitrella*, se liší nejen ve stavbě těla, ale i koncepcí opravy DSB. Tělo zástupce krytosemenných rostlin, *Arabidopsis*, je tvořeno diploidním sporofytem. Naopak zelená část mechu *Physcomitrella* je haploidní gametofyt. I přes svůj haploidní charakter je však *Physcomitrella* vysoce efektivní v cílené integraci cizorodé DNA, která je naopak u diploidní *Arabidopsis* mizivá (Kamisugi et al. 2005; Hanin a Paszkowski 2003). Avšak schopnost integrace cizorodé DNA nevyovídá o rychlosti opravy DSB. Vybízelo se tedy porovnat kinetiku opravy DSB těchto u dvou sice příbuzných, ale evolučně vzdálených druhů. Testovanými stádii byly 10 dní starý semenáček *Arabidopsis* a 1, 7 a 14 dní stará protonema *Physcomitrella* lišící se množstvím apikálních buněk (1 den – 50 %, 7 dní – 15 % a 14 dní – 3 %).

5.1. Oprava DSB u *Arabidopsis* a *Physcomitrella*

Při monitorování opravy DSB byla použita neutrální varianta kometového testu a k indukci DSB sloužilo hodinové působení BLM. Poměrně vysoké dávky BLM (30 - 50 $\mu\text{g/ml}$) byly nezbytné pro výraznou fragmentaci genomu a vytvoření měřicího okna, v němž přibližně polovina jaderné DNA byla volná a migrovala v elektrickém poli. V kontrolních vzorcích studovaných wt *Arabidopsis* a *Physcomitrella* ohon komety obsahoval 20-25 % jaderné DNA (Kozák et al. 2009; Kamisugi et al. 2012). Tato základní hodnota vypovídala o přítomnosti jistého množství zlomů DNA, především SSB, které podle modelu formace ohonu komety umožňují rozvolnění superstuktury domén DNA a tak i migraci této části DNA v elektrickém poli. Takto formovaný ohon je spojen s hlavou komety (Collins 2004). Naopak indukce DSB se projevuje migrací fragmentů DNA, které migrací vytváří ohon, jenž není spojen s hlavou komety (Olive a Banáth 1993).

Kinetika opravy DSB měla u obou rostlinných druhů bifázický průběh, přičemž první velmi rychlá fáze byla odpovědná za odstranění většiny indukovaného poškození. U *Arabidopsis* i *Physcomitrella* bylo opraveno během prvních 20 minut více než 80 % indukovaných DSB a poločas první fáze byl kolem 5 minut (Kozák et al. 2009; Kamisugi et al. 2012). Pozorování takto rychlé opravy DSB není běžné.

U savců, stejně jako kvasinek se poločas první fáze opravy pohybuje v řádu desítek minut. Snadná příprava vzorku v rámci kometového testu sice umožnila zachytit kinetiku rychlé opravy DSB, ale na druhou stranu byl poločas první fáze stejný jako první měřený čas zkoumané kinetiky.

U savců se za klíčové faktory první, stejně jako druhé fáze opravy DSB, považují především proteiny C-NHEJ. Proteiny nezbytné pro druhou pomalejší fázi opravy jsou ATM, γ -H2AX, MRN komplex a další faktory, které hrají roli v rozvolnění DNA a signalizaci. Druhá, pomalejší fáze opravy může také reprezentovat časově náročnější opravu v heterochromatinu, nebo opravu komplexnějšího poškození DNA (Goodarzi et al. 2010; Stenerlöv et al. 2000).

V kometovém testu se k lýzi jader používá roztok o vysokém obsahu solí, který uvolní většinu proteinů z vazby na DNA. Přesto však mohla být extrémně rychlá oprava DSB výsledkem vyvázání fragmentů DNA opravnými proteiny, a tak mohlo dojít k zamaskování opravdového obnovení celistvosti DNA. K vyloučení této možnosti byla do lýzovacího roztoku přidána Proteináza K. U semenáčků, hodinové působení formaldehydem o koncentraci 10 mM, který se běžně používá k fixaci buněčných struktur, vedlo ke kompletní inhibici migrace DNA v elektrickém poli. Naopak přidavek proteinázy K obnovil úroveň migrace DNA na původní kontrolní hodnotu. Použití tohoto modifikovaného protokolu při analýze kinetiky opravy DSB vyvrátilo podezření, že by rychlá oprava byla metodologickým artefaktem (nepublikováno).

Indukce rozsáhlé fragmentace genomu nezbytné pro analýzy kinetiky opravy DSB byla v případě wt *Arabidopsis* a *Physcomitrella* stále biologicky relevantní, neboť semenáčky, stejně jako 1 den stará protonema přežívaly akutní hodinové působení BLM o koncentraci až 50 μ g/ml. Indukce DSB se projevila jen zpomalením růstu (Kamisugi et al. 2012; Kozák et al. 2009). Protože nedocházelo k bezprostřednímu odumření rostlin, musely být spojovány především sobě odpovídající konce DNA. Rychlá oprava DSB, a s ní spojená schopnost přežít vysoké akutní dávky BLM, byla srovnatelná u těchto zástupců nižších a vyšších rostlin.

V případě chronické toxicity BLM se projevil výrazný rozdíl mezi *Arabidopsis* a *Physcomitrella*. Semenáčky přežívaly 50 i 100 μ g/ml BLM (Kozák et al. 2009). Naopak pro 1 den starou protonemu byla dávka 0,2 - 1 μ g/ml BLM letální (Kamisugi

et al. 2012; Holá et al. 2013). V případě *Arabidopsis* se působilo na poměrně diferencovanou rostlinu, zatímco u *Physcomitrella* se jednalo o fragmenty protonemy, které obsahovaly až 50 % apikálních mitoticky aktivních buněk. Obecně mohla být vyšší citlivost dělicích se buněk vůči DSB zdrojem rozdílné chronické toxicity BLM. Citlivost *Arabidopsis* se výrazně zvýšila, pokud byla vystavena BLM už od semene. Budoucí semenáček se musel vyvíjet v prostředí indukujícím DSB, a tak dávka zastavující rozvoj pravých lístků byla jen 10 µg/ml BLM (nepublikováno).

Různě stará stádia protonemy *Physcomitrella* se lišila v četnosti zastoupení mitoticky aktivních buněk, a to se projevilo v kinetice opravy DSB. Oprava DSB byla nejrychlejší u 1 den staré protonemy a rostoucím stářím se prodlužoval poločas první i druhá fáze opravy. U *Physcomitrella* tak rychlá oprava DSB dominovala v mitoticky aktivních apikálních buňkách (Kamisugi et al. 2012).

5.2. Oprava DSB v mutantech C-NHEJ dráhy

Za hlavní dráhu opravy DSB v somatických buňkách vyšších rostlin se považuje C-NHEJ (Puchta 2005). Mutanti C-NHEJ jsou sice citliví vůči IR (Friesner a Britt 2003), ale na druhou stranu u nich stále probíhá fúze telomer, ligace linearizovaných plastidů i integrace cizorodé DNA (Heacock et al. 2004; van Attikum et al. 2003; Gallego et al. 2003). Tato C-NHEJ nezávislá oprava DSB (A-NHEJ) není mediována HR (Charbonnel et al. 2011; Decottignies 2013). U C-NHEJ mutantů je nehomologní spojování DSB stále aktivní a tak zůstává otázkou, do jaké míry se C-NHEJ podílí na opravě DSB.

U semenáčků mutantů C-NHEJ nebyla pozorována kumulace endogenních DSB, tedy defekt v C-NHEJ nevedl za standardních podmínek k detekovatelné fragmentaci DNA. Vzhledem k citlivému fenotypu C-NHEJ mutantů bylo překvapivé, že oprava DSB probíhala u *atku80* a *atlig4* stejně rychle, ne-li dokonce rychleji než ve wt. Na pozadí C-NHEJ se projevila další dráha opravy DSB s masivní ligační aktivitou. Na základě prvních dvou časových bodů 5 a 10 minut byly stanoveny alespoň přibližné poločasy první fáze opravy. U *atku80* a *atlig4* byla první fáze opravy DSB dokonce rychlejší než u wt (Kozák et al. 2009). Později bylo měření pro *atlig4* opakováno a analýza dat programem GraphPad Prism ukázala, že pro *atlig4* stejně jako wt je 50% DSB odstraněno během první fáze, avšak její poločas je u *atlig4* 1,3 minut a u wt 4,2 minut (nepublikováno). Podobně

u *Physcomitrella*, 1 den stará protonema *pplig4* nevykazovala ve srovnání s wt defekt v opravě DSB. Poločasy první fáze opravy pro wt a *pplig4* byly 1,5 a 2,5 minut (Holá et al. 2013).

C-NHEJ nezávislé spojování DSB u *Arabidopsis* nebylo možné připsat HR, neboť její úroveň je obecně velmi nízká (Puchta 2005), a tak se opravy DSB mohla účastnit A-NHEJ. Naopak pro *Physcomitrella* je dokumentována výrazně vyšší úroveň HR, a tak se její účast na rychlé opravě DSB nedala vyloučit (Kamisugi et al. 2005). Avšak obecný model bifazické opravy DSB počítá s HR spíše v druhé pomalejší fázi (Goodarzi et al. 2010) a kinetika opravy DSB u *prrad51AB* byla srovnatelná s wt (nepublikováno).

Physcomitrella byla v případě chronického působení BLM výrazně citlivější než *Arabidopsis*. Růst protonemy byl zcela inhibován působením BLM o koncentraci 1 µg/ml, a to u *pplig4* stejně jako u wt (Holá et al. 2013). Naopak semenáčky *atku80*, *atlig4* a wt přeživaly nejen hodinové, ale dokonce i týdenní působení BLM o koncentraci až 100 µg/ml (Kozák et al. 2009), přestože byl pro *atku80* a *atlig4* dokumentován citlivý fenotyp vůči DSB (West et al. 2002; van Attikum et al. 2003). Rozdíl v tomto chování spočíval v různě nastavených cytotoxických testech. Působením na semena anebo semenáčky jen s děložními lístky se využilo dělení buněk k zintenzivnění toxického efektu DSB u *atku80* a *atlig4*. Naopak pokud se působilo na již rozvinuté semenáčky s první rozetou pravých lístků, citlivý fenotyp C-NHEJ mutantů nebyl znatelný. Po vysazení semen na živnou půdu obsahující BLM, byl citlivý fenotyp C-NHEJ mutantů pozorován už při koncentraci 3-5 µg/ml (nepublikováno).

Rychlá, C-NHEJ nezávislá oprava DSB musela být poněkud mutabilní, neboť indukce DSB vedla k citlivému fenotypu *atku80* a *atlig4* (West et al. 2002; van Attikum et al. 2003). Přítomnost C-NHEJ u *Arabidopsis* by tak mohla inhibovat jiné rychlejší dráhy opravy DSB za účelem potlačení kumulace nevhodných mutací. Naopak u *Physcomitrella* měl *pplig4* stejný fenotyp jako wt, a to jak v toxicitě BLM, tak v kinetice opravy DSB. U *Physcomitrella* mohl být defekt v C-NHEJ do značné míry nahrazen HR, přičemž použití této bezchybné opravy DSB by mohlo vysvětlit stejnou citlivost *pplig4* a wt vůči DSB (Holá et al. 2013).

U *Arabidopsis* se kinetika opravy DSB měřená kometovým testem lišila od kinetiky získané prostřednictvím počítání ohnisek γ -HA2X. V mitotických

buňkách kořenových meristémů byl u *atku80* po indukci DSB pozorován defekt v odstraňování γ -HA2X. Srovnatelný defekt měl i *atxrcc1*, a tak na něm založená A-NHEJ nezávislá dráha nebyla v těchto buňkách jen čistě záložní (Charbonnel et al. 2010). Rozdílná kinetika opravy DSB u *atku80* mohla být důsledkem odlišného principu měření množství DSB v kometovém testu a při počítání ohnisek γ -HA2X.

V kometovém testu byly používány semenáčky, tedy především somatické buňky a vysoké dávky BLM, které vedly k rozsáhlé fragmentaci DNA, přičemž detekce DSB byla založena na obnovení celistvosti DNA (Kozák et al. 2009). Naopak v čistě mitotických buňkách *wt* vedlo 25 Gy k formaci celkem 15 samostatných signálů γ -HA2X. S rostoucí mírou defektu v opravě DSB se významně zvedala úroveň maximálního počtu γ -HA2X, a to až na dvojnásobek u mutantů všech dosud známých drah opravy DSB (Charbonnel et al. 2011). U *wt* tedy musela být část indukovaných DSB opravena dříve, než se vytvořilo dostatečně velké ohnisko umožňující fluorescenční detekci γ -HA2X, a tak část opravy DSB nebyla měřením γ -HA2X zachycena.

5.3. AtLIG1 je určující pro rychlou opravu DSB

Pozorování rychlé opravy DSB u *atlig4* a *pplig4* vedlo nutně k závěru, že jiná ligáza musela být schopná toto poškození odstranit (Kozák et al. 2009; Holá et al. 2013). V genomu *Physcomitrella* se mimo PpLIG4 nachází jen PpLIG1. Zůstává tak otázkou, zda PpLIG1 vystupuje u mechu pouze v HR, anebo je schopná HR proteiny opustit a participovat i na A-NHEJ. Vzhledem k přítomnosti rychlé opravy DSB i u mutantů PpRAD51AB (nepublikováno), PpRAD50 a PpMRE11, charakteristickým výrazným poklesem v HR se nedala účast PpLIG1 v A-NHEJ vyloučit (Markmann-Mulisch et al. 2007; Kamisugi et al. 2012).

U *Arabidopsis* se mimo AtLIG1 nachází ještě pro rostliny specifická AtLIG6, která se podílí na opravě DNA v semenech (Waterworth et al. 2010). Kinetika opravy DSB probíhala u *atlig6* srovnatelně s *wt*, a tak AtLIG6 nebyla důležitá pro první rychlou fázi opravy DSB (nepublikováno). Opravdu esenciální rostlinnou DNA ligázou je jen replikační AtLIG1 (Waterworth et al. 2010). Esenciálnost AtLIG1 v replikaci se odráží v tom, že *atlig1* není viabilní (Babiychuk et al. 1998). Ke studiu funkce AtLIG1 byla použita RNA inhibiční technologie, kterou byli připraveni dva mutantů se sníženým obsahem proteinu (Waterworth et al. 2009).

Ve srovnání s wt byl obsah AtLIG1 u *atlig1a* snížen čtyřikrát a u *atlig1b* jen dvakrát. V souladu s nižší expresí AtLIG1 bylo u mutantů pozorováno zvýšené množství buněk v S-fázi buněčného cyklu. Mutanti *atlig1a* a *atlig1b* byli zakrnělého vzrůstu a s rostoucím stářím vykazovali fenotyp podobný rostlinám, které byly vystaveny UV či IR (Waterworth et al. 2009; Jiang et al. 1997; Kovalchuk et al. 2007). Přesto byli *atlig1a* a *atlig1b* fertilní. AtLIG1 mohla být zčásti substituována jinou ligázou, anebo množství AtLIG1 přítomné v haploidních buňkách stačilo pro jejich zdárné dělení (Babiychuk et al. 1998).

Nižší množství AtLIG1 se projevovalo jako environmentální stres, avšak až po dvou, či třech týdnech růstu. U 10 dní starých semenáčků *atlig1a* a *atlig1b* nebyl pozorován za standardních podmínek výraznější mutantní fenotyp a ani kometový test neukázal kumulaci SSB a DSB. U *atlig1a* a *atlig1b* mohlo docházet k akceleraci poškození DNA až kolem tří týdnů, nebo se v tomto čase konečně projevila postupná kumulace mutací, jejichž zdrojem byla tak nízká úroveň poškození DNA, že byla pod detekčním limitem kometového testu. Rozdíly v množství AtLIG1 se naopak výrazně projevily v kinetice opravy DSB. Oprava DSB byla u *atlig1a* a *atlig1b* ve srovnání s wt pomalejší s poločasy první fáze 9,1 respektive 6,7 minut. AtLIG1 se jevila jako klíčová ligáza rychlé fáze opravy DSB (Waterworth et al. 2009).

U *atlig1a* byla patrná nízká efektivita C-NHEJ v případě rozsáhlé fragmentace genomu. Zatímco defekt v AtLIG4 (Kozák et al. 2009) anebo AtLIG6 se v kinetice opravy DSB neprojevil (nepublikováno), pokles v AtLIG1 vedl až k dvojnásobnému prodloužení první fáze opravy DSB (Waterworth et al. 2009). Za rychlou opravu DSB tak byla zodpovědná především A-NHEJ založená na AtLIG1, avšak vzhledem k její esenciálnosti nebylo možné určit její roli v plném rozsahu. U *Arabidopsis* se ve srovnání s AtLIG1 definovanou A-NHEJ jevila C-NHEJ spíše jako záložní, minimálně v případě rozsáhlé fragmentace genomu, kdy mohlo dojít k překročení opravné kapacity C-NHEJ a nutnosti povolání A-NHEJ.

5.4. Oprava SSB v rostlinách

Pro měření opravy SSB byl do neutrální varianty kometového testu zařazen krok alkalické denaturace (Menke et al. 2001). Ve srovnání s opravou DSB byla oprava SSB u *Arabidopsis* a *Physcomitrella* výrazně pomalejší (Waterworth et al. 2009; Holá et al. 2013). To však může být obecná vlastnost rostlin (Donà et al. 2014). Za standardních podmínek sice nebyla u *atlig1a* a *pplig4* pozorována

kumulace SSB, avšak u obou mutantů defekt v DNA ligáze vedl k poklesu v kinetice opravy indukovaných SSB (Waterworth et al. 2009; Holá et al. 2013).

U *atlig1a* byl patrný výrazný defekt v opravě SSB, respektive alkylačního poškození DNA, kde bylo po 6 hodinách opraveno přibližně dvakrát méně SSB než u wt. Snížená úroveň exprese AtLIG1 se také projevila zcela odlišným průběhem kinetiky opravy SSB. Během první hodiny po působení MMS byl u *atlig1a* pozorován nárůst v množství SSB, který mohl souviset s mechanismem opravy alkylačního poškození DNA, kde excizní část BER odstraňuje poškozené báze a produkuje SSB. Následná ligace byla u *atlig1a* méně efektivní než excese poškozených bází, a to se zpočátku projevilo kumulací SSB. U *Arabidopsis* byla AtLIG1 zapojena do BER, a představovala tak funkční homolog LIG3 (Waterworth et al. 2009). Podobně také nedávná studie prokázala účast AtLIG1 v BER a vyvrátila možnost zapojení AtLIG4 (Córdoba-Cañero et al. 2011).

U LIG4 se obecně počítá pouze s rolí v opravě DSB v rámci C-NHEJ (Adachi et al. 2001; Tomkinson et al. 2013), přestože v *in vitro* testech jsou všechny DNA ligázy schopné poměrně efektivně ligovat jak DSB, tak SSB (Chen et al. 2009). U *Physcomitrella pplig4* byl vůbec poprvé pozorován defekt v opravě SSB. Defekt nebyl tak výrazný jako u *atlig1a*, ale poukazoval na roli PpLIG4 v opravě modifikovaných bází, tedy na účast BER. U *Physcomitrella*, kde byl *pplig4* stejně citlivý vůči DSB jako wt a spojoval fragmenty DNA stejně rychle, se paradoxně projevilo defekt v kinetice opravy modifikovaných bází DNA. PpLIG4 opravovala SSB nezávisle na C-NHEJ, neboť v souvislosti s poruchou v BER se po indukci poškození DNA u *pplig4* projevila kumulace převážně bodových inzercí v genu pro APT. Naopak u *ppku70* byla mutabilita APT srovnatelná s wt (Holá et al. 2013). Vzhledem k tomu, že v genomu *Physcomitrella* byly identifikovány pouze dvě DNA ligázy, PpLIG1 a PpLIG4, mohlo by být nepraktické omezit funkci PpLIG4 pouze na opravu DSB. Na rozdíl od *Physcomitrella* se u *Arabidopsis* AtLIG4 na BER nepodílí (Córdoba-Cañero et al. 2011).

5.5. MRN komplex v opravě DSB u *Physcomitrella*

Physcomitrella vykazuje až 100 % účinnost cílené integrace cizorodé DNA, a tak se HR jeví jako hlavní mechanismus opravy DSB (Kamisugi et al. 2005; Reski 1998). Jistá frakce integrací probíhá také za účasti C-NHEJ (Kamisugi et al. 2006). Naopak měření kinetiky opravy DSB ukázalo, že C-NHEJ a ani HR nebyly samy

o sobě klíčové pro rychlou a efektivní opravu DSB (Holá et al. 2013; nepublikováno). Mimo Ku70/Ku80 heterodimer se za další senzor DSB považuje MRN komplex, který svou činností ovlivňuje HR, C- i A-NHEJ (De Jager et al. 2001; Lamarche et al. 2010; Rass et al. 2009; So et al. 2009). Proto byl u Pp zkoumán vliv defektu MRN komplexu na opravu DSB.

Fenotyp *pprad50* a *ppmre11* se za standardních podmínek projevoval neschopností produkce lístků a sporofytu. Naopak *ppnbs1* byl nerozlišitelný od *wt* a neměl evidentní problém s meiózou a produkcí spor, a tak pouze centrální proteiny MRN komplexu, PpRAD50 a PpMRE11, byly nezbytné pro dokončení vývojového programu mechu (Kamisugi et al. 2012).

Defekt v PpRAD50 a PpMRE11 se projevoval citlivým fenotypem vůči akutnímu poškození DNA. Toxicita byla určena z počtu regenerovaných protoplastů izolovaných z protonemy, která byla vystavena rostoucím dávkám BLM a UV záření. V případě BLM stačilo k dosažení poloviční viability *pprad50* a *ppmre11* přibližně 50 ng/ml, avšak u *ppnbs1* a *wt* to bylo až 500 ng/ml. Pokud se k určení toxicity BLM použila 1 den stará protonema, *wt* přežíval i 50 µg/ml. Naopak u *pprad50* a *ppmre11* už 5 µg/ml vedlo k zastavení růstu (Kamisugi et al. 2012). Důvodem výrazného rozdílu v toxicitě BLM u protoplastů a protonemy mohl být dodatečný stres způsobený izolací a regenerací protoplastů.

V případě chronické toxicity BLM byli *pprad50* a *ppmre11* dokonce citlivější než *pprad51AB* (Markmann-Mulisch et al. 2007). Letální pro ně bylo už 8 ng/ml BLM (Kamisugi et al. 2012). Pokus byl následně opakován společně s *pplig4* a *pprad51AB*, kde se však podařilo zreprodukovat citlivý fenotyp jen pro *pprad50*. Důvod ztráty fenotypu u *ppmre11* byl neznámý (Holá et al. 2013).

V souladu s funkcí MRN komplexu v HR byl u *pprad50* a *ppmre11* pozorován řádový pokles v úrovni cílené integrace cizorodé DNA a jen dvojnásobný nárůst integrace nahodilé (Kamisugi et al. 2012). Pro srovnání, v případě *pprad51AB* byla cílená integrace zcela zrušena, a naopak došlo k výraznému navýšení integrace nahodilé (Markmann-Mulisch et al. 2007; Schaefer et al. 2010). Funkční PpRAD50 a PpMRE11 sice umožňovaly vysoce efektivní cílenou integraci, ale nebyly zcela nezbytné, neboť v jejich nepřítomnosti HR stále probíhala, avšak s účinností jen kolem 10 %. Naopak u *ppnbs1* byla HR stále plně funkční, a tak se PpNBS1 nepodílel na resekci 3'-jednovláknových konců DNA (Kamisugi et al. 2012).

U savců MRN komplex povolává ATM do oblastí s DSB, usnadňuje její aktivaci a řídí opravu směrem k HR, nebo C-NHEJ (So et al. 2009; Lamarche et al. 2010). MRN komplex interaguje prostřednictvím NBS1 s ATM, která následně NBS1 fosforyluje v doméně konzervované i u *Arabidopsis* a *Physcomitrella* (Falck et al. 2005; Garcia et al. 2003). Defekt v PpNBS1 však nevedl k retardovanému růstu, problémům v meióze, změnám v cílené integraci DNA a ani k citlivému fenotypu vůči DSB (Kamisugi et al. 2012). Fenotyp *ppnbs1* vyvrátil účast PpNBS1 na aktivaci PpATM, anebo při vyřazení PpATM signalizace mohlo dojít ke spouštění HR podobně jako u kvasinek pomocí ATR a nezávisle na ATM (Dubrana et al. 2007; Mantiero et al. 2007). Také u *Arabidopsis* byl *atnbs1* srovnatelný s wt a *atrads50* a *atmre11* vykazovali defekt v růstu, plodnosti a odpovědi na indukci poškození DNA. Avšak kombinace defektu v AtNBS1 a AtATM měla aditivní negativní vliv na růst a plodnost, což poukazovalo na jejich poněkud odlišné úlohy v aktivaci DDR a opravě DSB (Waterworth et al. 2007).

U 1 den staré protonemy mutantů MRN komplexu byla kinetika opravy DSB srovnatelná s wt. V rámci první fáze bylo opraveno přibližně 60-90 % indukovaných DSB, a to s poločasem 1-4 minuty. Bez ohledu na jisté rozdíly v poločasech, mutanti MRN komplexu byli srovnatelně efektivní v opravě rozsáhle fragmentovaného genomu jako wt (Kamisugi et al. 2012), a to i přes fakt, že se jedná o obecně významnou součást opravy DSB zahrnující HR, C- a A-NHEJ (Lamarche et al. 2010; Rass et al. 2009; So et al. 2009).

Základem mnoha funkcí MRN komplexu je schopnost tvorby dimerů prostřednictvím RAD50 (Hohl et al. 2011), a tak pro studium závislosti kinetiky opravy DSB na stáří protonemy byl vybrán *pprad50*. S růstem protonemy klesalo zastoupení mitoticky aktivních buněk, což se u wt projevilo prodloužením první i druhé fáze opravy DSB. Naopak u *pprad50* se sice rychlost první fáze opravy se stářím neměnila, avšak klesala její účast na celkové opravě ze 70 % na 45 %. To se nakonec projevilo v odlišných kinetických profilech opravy DSB u 14 dní staré protonemy wt a *pprad50*. S rostoucím stářím mizela část rychlé opravy DSB řízená PpRAD50 a potažmo celým MRN komplexem (Kamisugi et al. 2012).

Kinetika opravy DSB u 1 den staré protonemy *pprad50* a *ppmre11* nemohla být důvodem jejich extrémně citlivého fenotypu vůči DSB. Ten mohl souviset s poklesem v HR a možnou kumulací mutací vedoucích k zastavení růstu a buněčné

smrti. Například u kvasinek byl v souvislosti s defektem v HR pozorován zvýšený výskyt mutací (Seong et al. 1997). Samotný defekt v PpRAD50 a PpMRE11 se za standardních podmínek nevedl k výraznějšímu nárůstu v mutabilitě *PpAPT*, přirozeného selekčního genu (Kamisugi et al. 2012). Naopak u mutantu PpMSH2, součást dráhy opravy chybného párování bází, byl pozorován až 100 násobný nárůst v mutabilitě, který souvisel s kumulací především bodových mutací (Trouiller et al. 2006; Kamisugi et al. 2012). Ztráta funkce MRN komplexu nevedla za standardních podmínek ke kumulaci mutací, a tak se defekt v PpRAD50 a PpMRE11 neprojevil v kvalitě opravy endogenního poškození DNA.

Po indukci DSB se mutabilita *PpAPT* zvýšila, a to jak u *pprad50*, tak wt. K získání *PpAPT* mutantů wt bylo nezbytné použít BLM o koncentraci 50 µg/ml po 2 hodiny na rozdíl od *pprad50*, kde stačilo jen hodinové působení o koncentraci 0,1 µg/ml. Na základě uvedených koncentrací BLM se u *pprad50* projevil defekt v kvalitě opravy DSB přinejmenším řádovým navýšením mutability *PpAPT*. Sekvence selektovaných *PpAPT* mutantů wt vyjevila přítomnost pouze bodových mutací. Naopak u 3 ze 7 *ppapt/pprad50* byly pozorovány rozsáhlé delece o délce 10 až 747 bází (Kamisugi et al. 2012). I přes nízký počet sekvenovaných *ppapt* se ukázalo, že ztráta části strukturální podpory v místě DSB, realizované PpRAD50, vedla ke kumulaci výrazných změn v sekvenci DNA, zejména delecí.

Mutabilita *PpAPT* byla dále stanovena pro *ppmre11*, *ppnbs1*, *pplig4* a *ppku80*. Počet získaných *ppapt* na jednotlivých genetických pozadích byl přepočítán na 1 µg/ml BLM a gram suché protonemy. Takto normalizovaná data ukázala až o dva řády vyšší mutabilitu *PpAPT* u *pprad50*, avšak pouze násobné navýšení bylo pozorováno u *ppmre11* a *ppnbs1* a *pplig4*. PpRAD50 měl tedy zásadní vliv na potlačení kumulace změn v genomu *Physcomitrella*. Sekvence ukázala, že mimo *pprad50* a *ppmre11*, inaktivaci *PpAPT* genu způsobily především bodové mutace (substituce, inserce a delece) v kódujících oblastech, především v exonu 4, který byl anotován jako oblast kódující enzymovou aktivitu. Překvapivě u 4 mutantů *PpAPT* na různých genetických pozadích byly detekovány mutace pouze v nekódujících oblastech, a tak se povahu ztráty *PpAPT* aktivity zatím nepodařilo vysvětlit (Holá et al. 2013).

Zdrojem bodových mutací může být C- a nebo A-NHEJ, ale je pravděpodobnější, že vznikají v souvislosti s opravou oxidačního poškození bází

DNA. Naopak delší delece bylo možné připsat C-NHEJ anebo A-NHEJ, neboť až na jednu relativně krátkou deleci nalezenou u wt se všechny ostatní detekované delece nacházeli pouze u *ppmre11* a *pprad50* (Kamisugi et al. 2012; Holá et al. 2013).

Defekt v MRN komplexu vedl i bez indukce DSB k akumulaci transkriptů proteinů podílejících se na opravě DNA. Zejména u *ppmre11* a *pprad50* byla patrná zvýšená exprese *PpRAD51-1*, *PpRAD51-2*, *PpPARP-1*, *PpPARP-2*, *PpKu80* a *PpKu70* (Kamisugi et al. 2012). I když byla u mutantů MRN komplexu pozorována výrazná indukce *PpRAD51-1* a stále u nich probíhala v omezené míře cílená integrace, je celkem nepravděpodobné, že by HR odpovídala za rychlou opravu DSB v *pprad50* a *ppmre11*. Navýšení mutability poukazovalo spíše na mechanismy založené na rekombinaci nehomologní.

5.6. Role AtSMC6b, AtRAD21 a AtGMI1 v opravě DSB

Pro mutanty proteinů AtSMC6b (AtMIM), AtRAD21 a AtGMI1, které participují na organizaci struktury chromozomů, byl pozorován citlivý fenotyp vůči poškození DNA. Zatímco role SMC6 a RAD21 byla u *Arabidopsis* a jiných organismů delší dobu zkoumána, funkce SMCHD proteinu AtGMI1 byla zcela neznámá. Analýza kinetiky opravy DSB u výše uvedených mutantů ukázala různě intenzivní defekt v jejich opravě (Kozák et al. 2009; da Costa-Nunes et al. 2014; Böhmdorfer et al. 2011), přestože je HR považována za minoritní dráhu opravy DSB u *Arabidopsis* (Puchta 2005; Britt a May 2003). Možnou účast HR na rychlé opravě DSB by bylo vhodné podrobit dalšímu studiu například analýzou jejich opravy u vícečetných mutantů jednotlivých opravných drah.

5.6.1. AtSMC6b a rychlá oprava DSB

Vliv defektu v proteinech AtSMC6b a AtRAD21.1 na kinetiku opravy DSB byl analyzován v sérii experimentů společně s mutanty C-NHEJ. Největší defekt v opravě DSB byl pozorován u *atsmc6b*, kde v souladu s předchozími studii oprava DSB probíhala monofazicky s poločasem kolem 1 hodiny (Kozák et al. 2009; Takeda et al. 2004). V případě indukce poškození DNA u semen byl *atsmc6b* citlivý vůči UV, IR a MMC (Mengiste et al. 1999). I když *atsmc6b* vykazoval značný defekt v kinetice opravy DSB, semenáčky *atsmc6b* nebyly ve srovnání s wt znatelně citlivější vůči akutnímu, ani chronickému působení BLM. Navzdory stále funkční C-NHEJ nebyla u *atsmc6b* pozorována počáteční rychlá fáze opravy DSB. V případě

rozsáhlé fragmentace genomu nezávisela rychlá fáze opravy DSB na C-NHEJ, ale byla zcela odkázána na procesy spojené s AtSMC6b (Kozák et al. 2009).

Pro AtSMC5/6 komplex byla navržena obdobná funkce jako u jiných organismů, tj. stabilizace sesterských chromatid, tedy funkce v HR během S a G₂ fáze buněčného cyklu (Watanabe et al. 2009). V souladu s tím *atsmc6b* vykazoval výrazně nižší úroveň intrachromozomální rekombinace (Watanabe et al. 2009; Mengiste et al. 1999; Hanin et al. 2000). Avšak defekt v kinetice opravy DSB u *atsmc6b* se nedal vysvětlit pouze vyřazením HR z funkce. Znamenalo by to, že za rychlou fázi opravy DSB by byla zcela odpovědná HR, což se však poněkud vylučuje s minoritní rolí HR v opravě DSB u *Arabidopsis* (Puchta 2005; Britt a May 2003).

Průběh kinetiky opravy DSB u *atsmc6b* spíše poukazoval na obecnější roli AtSMC6b v opravě DSB. Na základě dat byl navržen model, ve kterém AtSMC6b přispívá k opravě DSB nejen skrze stabilizaci struktury DNA organizací sesterských chromatid, ale také překlenutím zlomu podobně jako Ku70/Ku80 heterodimer, nebo MRN komplex, a tak by mohl participovat nejen na HR, ale i A- a C-NHEJ (Kozák et al. 2009). Mutační analýza u kvasinek ukázala oddělitelnost funkcí SMC6 v opravě DSB a strukturní organizaci genomu (Fousteri a Lehmann 2000). AtSMC6b by tak mimo strukturní roli mohl fungovat také jako mediátor, neboť celý SMC5/6 komplex je tvořen dalšími proteiny s potenciálně zajímavými enzymatickými aktivitami, ubikvitinací a sumoylací (obr. 3) (Potts a Yu 2005; Doyle et al. 2010).

5.6.2. Podjednotka kohezinů AtRAD21 v opravě DSB

Napřed byla kinetika opravy DSB určena jen pro *atrada21.1* a to ve stejném panelu experimentů společně s *atsmc6b* a mutanty C-NHEJ. Vyřazení AtRAD21.1 vedlo k defektu v kinetice opravy DSB, kde sice zůstal zachován bifazický průběh, avšak došlo k prodloužení první fáze jejich opravy. Stejně jako u *atsmc6b*, semenáčky *atrada21.1* nevykazovaly citlivý fenotyp vůči akutnímu, nebo chronickému působení BLM (Kozák et al. 2009).

Ve druhé studii byly ze tří existujících homologů AtRAD21 analyzováni pouze *atrada21.1* a *atrada21.3*, neboť homozygotní mutant AtRAD21.2 nebyl k dispozici (Jiang et al. 2007). Při nižších dávkách IR vykazoval citlivý fenotyp pouze *atrada21.1* (da Costa-Nunes et al. 2006). Zvýšení dávky ze 100 Gy na 150 Gy vedlo k projevu citlivého fenotypu i u *atrada21.3*. U dvojitého mutantu AtRAD21.1/AtRAD21.3

se ukázal synergistický a neredundantní efekt AtRAD21.3 na roli AtRAD21.1 (da Costa-Nunes et al. 2014). Dávka 100 Gy zvyšovala expresi pouze *AtRAD21.1* (da Costa-Nunes et al. 2006). Třikrát vyšší dávka IR vedla k indukci exprese i *AtRAD21.3*. Avšak v rámci DDR hrál výraznější roli *AtRAD21.1*, neboť jeho exprese se po indukci poškození DNA zvýšila až o dva řády, naopak pro *AtRAD21.3* se exprese zvedla pouze dvakrát (da Costa-Nunes et al. 2014).

U *atrad21.1* a *atrad21.3* byl pozorován defekt v kinetice opravy DSB, přičemž zpomalení opravy bylo nejvíce patrné v rozmezí 10 až 20 minut po působení BLM, tedy na rozmezí mezi rychlou a pomalou fází opravy DSB. Přestože *atrad21.1/atrad21.3* byl více citlivý vůči indukci DSB než jednotliví mutanti, kinetika opravy DSB u dvojitého mutanta byla srovnatelná s wt (da Costa-Nunes et al. 2014). U *atrad21.1/atrad21.3* mohlo dojít ke kompletnímu zrušení AtRAD21 dependentní opravy DSB, přičemž oprava pak byla směřována k drahám, které vedly ke kinetice srovnatelné s wt. RAD21 je spojován s funkcí v HR a tak posun od AtRAD21 dependentní, pravděpodobně bezchybné HR opravy DSB, k více chybovému AtRAD21 nezávislému procesu vedl k větší citlivosti *atrad21.1/atrad21.3* vůči BLM.

U *atrad21.1* a *atrad21.3* nebyl zaznamenán defekt v opravě DSB, pokud se k jejich indukci použilo BLM o koncentraci 10 ug/ml. Defekt v kinetice opravy DSB se u mutantů projevil až při třikrát vyšší dávce (nepublikováno). Větší množství DSB mohlo vyvázat více AtRAD21 proteinu na zajištění *de novo* koheze v místech poškození DNA, a proto se snížení celkové zásoby AtRAD21 u *atrad21.1* a *atrad21.3* projevilo poklesem efektivity opravy DSB (da Costa-Nunes et al. 2014). Zpomalení opravy DSB u *atrad21.1* a *atrad21.3* mohlo také souviset s poruchou v DDR. U savců byl totiž po indukci DSB u mutanta RAD21 pozorován defekt v některých kontrolních bodech buněčného cyklu (Watrin a Peters 2009; Yazdi et al. 2002).

Na základě získaných dat byl navržen model funkce AtRAD21 v opravě DSB, který je založen na stabilizaci struktury chromozomů a využití sesterské chromatidy. V nepřítomnosti DSB je koheze dána především AtRAD21.3, neboť po indukci DSB docházelo k minimálnímu navýšení jeho exprese (da Costa-Nunes et al. 2014). Navíc by tento protein mohl být asociován s replikací (Takahashi et al. 2010). Hlavní příspěvek AtRAD21.3 k opravě DSB je v předem připravené kohezi sesterských

chromatid. Naopak masivní indukce AtRAD21.1 po působení IR vede k navýšení zásoby proteinu, pravděpodobně na pokrytí *de novo* koheze v místech poškození DNA (da Costa-Nunes et al. 2014). Oba proteiny by tak mohli vystupovat v opravě DSB synergisticky a neredundantně.

5.6.2. SMCHD protein AtGMI1 v opravě DSB

Mimo skupinu SMC proteinů existují také proteiny obsahující minimálně SMC dimerizační doménu a vytváří novou skupinu SMCHD proteinů (Blewitt et al. 2005; Kanno et al. 2008). V genomu *Arabidopsis* se nachází mimo AtDMS3 další dvě sekvence, které vykazovaly výraznou shodu s SMCHD1 a to dosud neidentifikovaný AtGMI1 a jeho pseudogen, ve kterém byla ATPázová doména přerušena transpozómem (Böhmdorfer et al. 2011).

Pro studium role AtGMI1 v opravě DSB byli připraveni čtyři mutanti s označením *atgmi1-1* až *atgmi1-4*. Název GMI1 byl odvozen z pozorování výrazné indukce exprese *AtGMII* po působení IR a MMC. Naopak exprese *AtDMS3* se neměnila. Expresní profil *AtGMII* se po indukci DSB poněkud lišil od *AtRAD51* a *AtBRCA1*. Exprese *AtGMII* dosahovala maxima později a zároveň přetrvávala déle než exprese *AtRAD51* a *AtBRCA1*. K indukované expresi AtGMI1 docházelo především v rozvíjejících se pravých lístcích a apikálních meristémech (Böhmdorfer et al. 2011).

Transkripční odpověď po indukci DSB je u *Arabidopsis* řízena AtATM a AtATR (Culligan et al. 2006; Ricaud et al. 2007). Analýza indukované exprese *AtGMII* u *atatm*, *atatr*, *weel* a wt ukázala absolutní závislost na AtATM. Vyšší citlivost *atgmi1-2/atatr* vůči DSB ve srovnání s *atgmi1-2* a *atatr* poukázala na defekt v části AtATM řízené DRR u *atgmi1-2* (Böhmdorfer et al. 2011). AtGMI1 tak mohl být zapojen do mediace DDR, neboť pro SMCHD1 i AtDMS3 byla pozorována účast na regulaci transkripce (Kanno et al. 2008; Blewitt et al. 2008). Avšak expresní profily wt a *atgmi1-1* po indukci DSB byly srovnatelné, a tak se AtGMI1 na rozdíl od AtSOG1 nepodílel na řízení exprese opravných proteinů (Böhmdorfer et al. 2011). Naopak, po indukci poškození DNA AtSOG1 řídil expresi mnoha genů, včetně *AtGMII* (Yoshiyama et al. 2009).

Kinetika opravy DSB u mutantů AtGMI1 vykazovala defekt, který byl stejně jako u mutantů AtRAD21 nejvíce patrný v čase 10 až 20 minut po působení BLM. AtGMI1 by mohl být mediátor HR, neboť u mutantů AtGMI1 byla po indukci

poškození DNA pozorována poloviční úroveň HR ve srovnání s wt (Böhmdorfer et al. 2011). Pokles v HR byl sice méně výrazný než u *atrad51c*, avšak srovnatelný s *atsmc6b* (Mengiste et al. 1999; Abe et al. 2005).

AtGMI1 je vůbec první člen skupiny SMCHD proteinů, pro kterého byla dokumentována role v opravě DNA. AtGMI1 strukturou připomíná SMC proteiny. Mimo dimerizační doménu obsahuje také dosud neurčený spojník a hlavně ATPázovou doménu (Böhmdorfer et al. 2011). SMC1/3 a SMC5/6 se jako dimery účastní opravy DSB, kde usnadňují HR prostřednictvím prostorové organizace sesterských chromatid (Chiu et al. 2004; De Piccoli et al. 2006; Heidinger-Pauli et al. 2008). Mutanti AtGMI1 postrádali dimerizační doménu, a tak snížená úroveň HR i defekt v kinetice opravy DSB poukazoval na důležitost této domény a tedy i dimerizace ve funkci AtGMI1. V navrhovaném modelu se AtGMI1 účastní opravy DSB jako dimer, který stabilizuje sesterské chromatidy podobně jako AtSMC1/3 a AtSMC5/6 komplexy a tím napomáhá HR (Böhmdorfer et al. 2011).

6. Závěr

V předkládaných publikacích jsou prezentovány výsledky, které do jisté míry mění pohled na opravu DNA u rostlin. U *Arabidopsis* i *Physcomitrella* je oprava DSB rychlá a účinná s poločasem první fáze opravy okolo 5 minut. Většina DSB je z rozsáhle fragmentovaného genomu odstraněna poměrně kvalitním způsobem, neboť *Arabidopsis* i *Physcomitrella* indukci DSB přežívají. U *Physcomitrella* rychlá oprava DSB dominuje v mitoticky aktivních buňkách.

U *Arabidopsis* není rychlá oprava DSB závislá na C-NHEJ. Naopak je pro ni zcela esenciální SMC protein AtSMC6b, který se může stabilizací DNA účastnit HR, a pravděpodobně je také obecnějším faktorem opravy DSB. AtSMC6b by také mohl společně s AtLIG1 definovat novou A-NHEJ, neboť ze všech dostupných DNA ligáz má AtLIG1 jako jediná signifikantní vliv na rychlou opravu DSB. AtLIG1 se podílí také na opravě alkylačního poškození DNA a tak představuje rostlinný homolog LIG3.

Podobnou roli v opravě DSB mají AtRAD21 a AtGMI1. Pro funkci AtRAD21.1 a AtRAD21.3 byl navržen model, ve kterém jimi předem připravená koheze sesterských chromatid přispívá k opravě DSB pomocí HR. S indukcí DSB se výrazně navyšuje množství AtRAD21.1, který pak umožňuje *de novo* kohezi v místech poškození DNA. AtGMI1 je vůbec první člen SMCHD skupiny proteinů s prokázanou rolí v opravě DNA. AtGMI1 podobně jako SMC proteiny může fungovat jako dimer. Indukce DSB vede v závislosti na AtATM k jeho expresi a tak se podobně jako AtRAD21 může podílet na kohezi anebo *de novo* kohezi, a tím usnadňovat HR.

Stejně jako u *Arabidopsis*, ani u *Physcomitrella* není PpLIG4, a tedy celá C-NHEJ, esenciální pro rychlou opravu DSB. Překvapivě se PpLIG4 v rozporu se svou obecnou funkcí v C-NHEJ účastní BER a chrání tak před kumulací bodových mutací. Vůbec poprvé byla pozorována C-NHEJ nezávislá úloha LIG4 v opravě DNA.

U *Physcomitrella* se pouze PpMRE11 a PpRAD50 jeví jako esenciální pro funkce MRN komplexu. Oba dva proteiny jsou klíčové pro dokončení vývojového programu mechu stejně jako pro efektivní cílenou integraci cizorodé DNA. Extrémně citlivý fenotyp *ppmre11* a *pprad50* vůči BLM nesouvisí s kinetikou

opravy DSB, ale s kumulací mutací. Pro ochranu genomu je zásadní strukturní funkce PpRAD50, neboť v jeho nepřítomnosti se mutabilita *PpAPT* zvyšuje až o dva řády.

7. Seznam literatury

- Abdalla, F.H. a Roberts, E.H., 1969. The effects of temperature and moisture on genetic changes in seeds of barley, broad beans and peas during storage. *Annals of Botany*, (33), pp.153–167.
- Abe, K. et al., 2005. Arabidopsis RAD51C gene is important for homologous recombination in meiosis and mitosis. *Plant physiology*, 139(2), pp.896–908.
- Adachi, N. et al., 2001. DNA ligase IV-deficient cells are more resistant to ionizing radiation in the absence of Ku70: Implications for DNA double-strand break repair. *Proceedings of the National Academy of Sciences of the United States of America*, 98, pp.12109–12113.
- Adachi, S. et al., 2011. Programmed induction of endoreduplication by DNA double-strand breaks in Arabidopsis. *Proceedings of the National Academy of Sciences of the United States of America*, 108, pp.10004–10009.
- Ames, B.N., Shigenaga, M.K. a Hagen, T.M., 1993. Oxidants, antioxidants, and the degenerative diseases of aging. *Proceedings of the National Academy of Sciences of the United States of America*, 90, pp.7915–7922.
- Amiard, S. et al., 2010. Distinct roles of the ATR kinase and the Mre11-Rad50-Nbs1 complex in the maintenance of chromosomal stability in Arabidopsis. *The Plant cell*, 22, pp.3020–3033.
- Amiard, S., Gallego, M.E. a White, C.I., 2013. Signaling of double strand breaks and deprotected telomeres in Arabidopsis. *Frontiers in plant science*, 4(October), p.405.
- Angelis, K.J. et al., 2000. Adaptation to alkylation damage in DNA measured by the comet assay. *Environmental and molecular mutagenesis*, 36(2), pp.146–150.
- Angelis, K.J. et al., 1999. Single cell gel electrophoresis: detection of DNA damage at different levels of sensitivity. *Electrophoresis*, 20(10), pp.2133–2138.
- Assenmacher, N. a Hopfner, K.P., 2004. MRE11/RAD50/NBS1: Complex activities. *Chromosoma*, 113, pp.157–166.
- Atienza, J.M. et al., 2005. Suppression of RAD21 gene expression decreases cell growth and enhances cytotoxicity of etoposide and bleomycin in human breast cancer cells. *Molecular cancer therapeutics*, 4(3), pp.361–368.
- van Attikum, H. et al., 2003. The Arabidopsis AtLIG4 gene is required for the repair of DNA damage, but not for the integration of Agrobacterium T-DNA. *Nucleic Acids Research*, 31(14), pp.4247–4255.

- van Attikum, H. a Gasser, S.M., 2005. The histone code at DNA breaks: a guide to repair? *Nature reviews. Molecular cell biology*, 6, pp.757–765.
- Audebert, M. et al., 2008. Effect of double-strand break DNA sequence on the PARP-1 NHEJ pathway. *Biochemical and Biophysical Research Communications*, 369, pp.982–988.
- Audebert, M. et al., 2004. Involvement of poly(ADP-ribose) polymerase-1 and XRCC1/DNA ligase III in an alternative route for DNA double-strand breaks rejoining. *Journal of Biological Chemistry*, 279, pp.55117–55126.
- Babiychuk, E. et al., 1998. Higher plants possess two structurally different poly(ADP-ribose) polymerases. *Plant Journal*, 15(5), pp.635–645.
- Bakkenist, C.J. a Kastan, M.B., 2003. DNA damage activates ATM through intermolecular autophosphorylation and dimer dissociation. *Nature*, 421, pp.499–506.
- Ban ath, J.P. et al., 2004. Radiation sensitivity, H2AX phosphorylation, and kinetics of repair of DNA strand breaks in irradiated cervical cancer cell lines. *Cancer Research*, 64(19), pp.7144–7149.
- Barlev, N.A. et al., 1998. Repression of GCN5 histone acetyltransferase activity via bromodomain-mediated binding and phosphorylation by the Ku-DNA-dependent protein kinase complex. *Molecular and cellular biology*, 18, pp.1349–1358.
- Bennett, C.B. et al., 1996. A Double-Strand Break within a Yeast Artificial Chromosome (YAC) Containing Human DNA Can Result in YAC Loss , Deletion , or Cell Lethality. , 16(8), pp.4414–4425.
- Bertrand, P. et al., 2004. p53’s double life: Transactivation-independent repression of homologous recombination. *Trends in Genetics*, 20, pp.235–243.
- B ertermier, M. et al., 2014. Is Non-Homologous End-Joining Really an Inherently Error-Prone Process? *PLoS Genetics*, 10(1).
- Birkenbihl, R.P. a Subramani, S., 1992. Cloning and characterization of rad21 an essential gene of *Schizosaccharomyces pombe* involved in DNA double-strand-break repair. *Nucleic acids research*, 20(24), pp.6605–6611.
- Blewitt, M.E. et al., 2005. An N-ethyl-N-nitrosourea screen for genes involved in variegation in the mouse. *Proceedings of the National Academy of Sciences of the United States of America*, 102(21), pp.7629–7634.
- Blewitt, M.E. et al., 2008. SmcHD1, containing a structural-maintenance-of-chromosomes hinge domain, has a critical role in X inactivation. *Nature genetics*, 40(5), pp.663–669.

- Blier, P.R. et al., 1993. Binding of Ku protein to DNA: Measurement of affinity for ends and demonstration of binding to nicks. *Journal of Biological Chemistry*, 268, pp.7594–7601.
- Boboila, C. et al., 2010. Alternative end-joining catalyzes robust IgH locus deletions and translocations in the combined absence of ligase 4 and Ku70. *Proceedings of the National Academy of Sciences of the United States of America*, 107, pp.3034–3039.
- Böhmdorfer, G. et al., 2011. GMI1, a structural-maintenance-of-chromosomes-hinge domain-containing protein, is involved in somatic homologous recombination in Arabidopsis. *Plant Journal*, 67(3), pp.420–433.
- Boubriak, I. et al., 1997. The requirement for DNA repair in desiccation tolerance of germinating embryos. *Seed Science Research*, 7.
- Boubriak, I.I. et al., 2008. Adaptation and impairment of DNA repair function in pollen of *Betula verrucosa* and seeds of *Oenothera biennis* from differently radionuclide- contaminated sites of Chernobyl. *Annals of Botany*, 101, pp.267–276.
- Boyko, A. a Kovalchuk, I., 2011. Genome instability and epigenetic modification- heritable responses to environmental stress? *Current Opinion in Plant Biology*, 14, pp.260–266.
- Brand, M. et al., 2001. UV-damaged DNA-binding protein in the TFIIIC complex links DNA damage recognition to nucleosome acetylation. *EMBO Journal*, 20, pp.3187–3196.
- Britt, A.B. a May, G.D., 2003. Re-engineering plant gene targeting. *Trends in Plant Science*, 8(2), pp.90–95.
- Cappelli, E. et al., 1997. Involvement of XRCC1 and DNA ligase III gene products in DNA base excision repair. *Journal of Biological Chemistry*, 272(38), pp.23970–23975.
- Ciccia, A. a Elledge, S.J., 2010. The DNA Damage Response: Making It Safe to Play with Knives. *Molecular Cell*, 40, pp.179–204.
- Cimprich, K.A. a Cortez, D., 2008. ATR: an essential regulator of genome integrity. *Nature reviews. Molecular cell biology*, 9, pp.616–627.
- Collins, A.R., 2004. The comet assay for DNA damage and repair: principles, applications, and limitations. *Molecular Biotechnology*, 26(3), pp.249–261.
- Collins, A.R. et al., 1997. The comet assay: What can it really tell us? *Mutation Research - Fundamental and Molecular Mechanisms of Mutagenesis*, 375(2), pp.183–193.

- Córdoba-Cañero, D. et al., 2011. Arabidopsis ARP endonuclease functions in a branched base excision DNA repair pathway completed by LIG1. *Plant Journal*, 68(4), pp.693–702.
- da Costa-Nunes, J.A. et al., 2006. Characterization of the three Arabidopsis thaliana RAD21 cohesins reveals differential responses to ionizing radiation. *J Exp Bot*, 57(4), pp.971–983.
- da Costa-Nunes, J.A. et al., 2014. The AtRAD21.1 and AtRAD21.3 Arabidopsis cohesins play a synergistic role in somatic DNA double strand break damage repair. *BMC plant biology*, 14, p.353.
- Covo, S. et al., 2010. Cohesin is limiting for the suppression of DNA damage-induced recombination between homologous chromosomes. *PLoS Genetics*, 6(7), pp.1–16.
- Culligan, K.M. et al., 2004. ATR regulates a G2-phase cell-cycle checkpoint in Arabidopsis thaliana. *The Plant cell*, 16, pp.1091–1104.
- Culligan, K.M. et al., 2006. ATR and ATM play both distinct and additive roles in response to ionizing radiation. *Plant Journal*, 48(6), pp.947–961.
- Culligan, K.M. a Britt, A.B., 2008. Both ATM and ATR promote the efficient and accurate processing of programmed meiotic double-strand breaks. *Plant Journal*, 55, pp.629–638.
- D’Silva, I. et al., 1999. Relative affinities of poly(ADP-ribose) polymerase and DNA-dependent protein kinase for DNA strand interruptions. *Biochimica et Biophysica Acta - Protein Structure and Molecular Enzymology*, 1430, pp.119–126.
- Dandoy, E. et al., 1987. Appearance and repair of apurinic/apyrimidinic sites in DNA during early germination of Zea mays. *Mutation Research*, 181, pp.57–60.
- Decottignies, A., 2013. Alternative end-joining mechanisms: A historical perspective. *Frontiers in Genetics*, 4.
- Delacôte, F. a Lopez, B.S., 2008. Importance of the cell cycle phase for the choice of the appropriate DSB repair pathway, for genome stability maintenance: The trans-S double-strand break repair model. *Cell Cycle*, 7, pp.33–38.
- DiBiase, S.J. et al., 2000. DNA-dependent protein kinase stimulates an independently active, nonhomologous, end-joining apparatus. *Cancer Research*, 60, pp.1245–1253.
- Donà, M. et al., 2014. Dose-Dependent Reactive Species Accumulation and Preferential Double-Strand Breaks Repair are Featured in the γ -ray Response in Medicago truncatula Cells. *Plant Molecular Biology Reporter*, 32(1), pp.129–141.

- Downs, J.A. et al., 2003. Suppression of homologous recombination by the *Saccharomyces cerevisiae* linker histone. *Molecular Cell*, 11, pp.1685–1692.
- Doyle, J.M. et al., 2010. MAGE-RING protein complexes comprise a family of E3 ubiquitin ligases. *Molecular Cell*, 39(6), pp.963–974.
- Dubrana, K. et al., 2007. The processing of double-strand breaks and binding of single-strand-binding proteins RPA and Rad51 modulate the formation of ATR-kinase foci in yeast. *Journal of cell science*, 120(Pt 23), pp.4209–4220.
- Van Dyck, E. et al., 1999. Binding of double-strand breaks in DNA by human Rad52 protein. *Nature*, 398, pp.728–731.
- Eccles, L.J. et al., 2009. Hierarchy of lesion processing governs the repair, double-strand break formation and mutability of three-lesion clustered DNA damage. *Nucleic Acids Research*, 38, pp.1123–1134.
- Falck, J. et al., 2005. Conserved modes of recruitment of ATM, ATR and DNA-PKcs to sites of DNA damage. *Nature*, 434, pp.605–611.
- Fattah, F.J. et al., 2008. Ku70, an essential gene, modulates the frequency of rAAV-mediated gene targeting in human somatic cells. *Proceedings of the National Academy of Sciences of the United States of America*, 105, pp.8703–8708.
- Ferguson, D.O. et al., 2000. The nonhomologous end-joining pathway of DNA repair is required for genomic stability and the suppression of translocations. *Proceedings of the National Academy of Sciences of the United States of America*, 97, pp.6630–6633.
- Flores, M.J. et al., 1998. Protection provided by exogenous DNA ligase in G0 human lymphocytes treated with restriction enzyme MspI or bleomycin as shown by the comet assay. *Environmental and Molecular Mutagenesis*, 32(4), pp.336–343.
- Foster, M.I. a Lehmann, A.R., 2000. A novel SMC protein complex in *Schizosaccharomyces pombe* contains the Rad18 DNA repair protein. *The EMBO journal*, 19(7), pp.1691–1702.
- Friedberg, E.C. et al., 2006. *DNA Repair and Mutagenesis*, Washington, D.C.: ASM Press.
- Friesner, J. a Britt, A.B., 2003. Ku80- and DNA ligase IV-deficient plants are sensitive to ionizing radiation and defective in T-DNA integration. *Plant Journal*, 34(4), pp.427–440.
- Friesner, J.D. et al., 2005. Ionizing radiation-dependent gamma-H2AX focus formation requires ataxia telangiectasia mutated and ataxia telangiectasia mutated and Rad3-related. *Molecular biology of the cell*, 16, pp.2566–2576.

- Fulcher, N. a Sablowski, R., 2009. Hypersensitivity to DNA damage in plant stem cell niches. *Proceedings of the National Academy of Sciences of the United States of America*, 106, pp.20984–20988.
- Furukawa, T. et al., 2015. Arabidopsis DNA polymerase lambda mutant is mildly sensitive to DNA double strand breaks but defective in integration of a transgene. *Frontiers in plant science*, 6, p.357.
- Gallego, M.E. et al., 2003. Ku80 plays a role in non-homologous recombination but is not required for T-DNA integration in Arabidopsis. *Plant Journal*, 35(5), pp.557–565.
- Garcia, V. et al., 2003. AtATM is essential for meiosis and the somatic response to DNA damage in plants. *The Plant cell*, 15(1), pp.119–132.
- Gauss, G.H. a Lieber, M.R., 1996. Mechanistic constraints on diversity in human V(D)J recombination. *Molecular and cellular biology*, 16, pp.258–269.
- Gerstein, R.M. a Lieber, M.R., 1993. Extent to which homology can constrain coding exon junctional diversity in V(D)J recombination. *Nature*, 363, pp.625–627.
- Girard, P.M. et al., 2002. Nbs1 promotes ATM dependent phosphorylation events including those required for G1/S arrest. *Oncogene*, 21, pp.4191–4199.
- Gladyshev, E. a Meselson, M., 2008. Extreme resistance of bdelloid rotifers to ionizing radiation. *Proceedings of the National Academy of Sciences of the United States of America*, 105, pp.5139–5144.
- Goodarzi, A.A. et al., 2008. ATM Signaling Facilitates Repair of DNA Double-Strand Breaks Associated with Heterochromatin. *Molecular Cell*, 31, pp.167–177.
- Goodarzi, A.A. et al., 2010. The influence of heterochromatin on DNA double strand break repair: Getting the strong, silent type to relax. *DNA Repair*, 9(12), pp.1273–1282.
- Grabarz, A. et al., 2012. Initiation of DNA double strand break repair : signaling and single-stranded resection dictate the choice between homologous recombination , non-homologous end-joining and alternative end-joining. , 2(3), pp.249–268.
- Gu, J. et al., 2007. XRCC4:DNA ligase IV can ligate incompatible DNA ends and can ligate across gaps. *The EMBO journal*, 26, pp.1010–1023.
- Guirouilh-Barbat, J.K. et al., 2010. AKT1/BRCA1 in the control of homologous recombination and genetic stability: the missing link between hereditary and sporadic breast cancers. *Oncotarget*, 1, pp.691–699.
- Haber, J.E., 1999. DNA recombination: The replication connection. *Trends in Biochemical Sciences*, 24, pp.271–275.

- Haering, C.H. et al., 2002. Molecular architecture of SMC proteins and the yeast cohesin complex. *Molecular Cell*, 9(4), pp.773–788.
- Haince, J.F. et al., 2008. PARP1-dependent kinetics of recruitment of MRE11 and NBS1 proteins to multiple DNA damage sites. *Journal of Biological Chemistry*, 283, pp.1197–1208.
- Han, L. a Yu, K., 2008. Altered kinetics of nonhomologous end joining and class switch recombination in ligase IV-deficient B cells. *The Journal of experimental medicine*, 205, pp.2745–2753.
- Hanin, M. et al., 2000. Elevated levels of intrachromosomal homologous recombination in Arabidopsis overexpressing the MIM gene. *Plant Journal*, 24(2), pp.183–189.
- Hanin, M. a Paszkowski, J., 2003. Plant genome modification by homologous recombination. *Current Opinion in Plant Biology*, 6(2), pp.157–162.
- Hays, J.B., 2002. Arabidopsis thaliana, a versatile model system for study of eukaryotic genome-maintenance functions. *DNA Repair*, 1, pp.579–600.
- He, J. et al., 2012. Rad50 zinc hook is important for the Mre11 complex to bind chromosomal DNA double-stranded breaks and initiate various DNA damage responses. *Journal of Biological Chemistry*, 287, pp.31747–31756.
- Heacock, M. et al., 2004. Molecular analysis of telomere fusions in Arabidopsis: multiple pathways for chromosome end-joining. *The EMBO journal*, 23, pp.2304–2313.
- Heidinger-Pauli, J.M. et al., 2008. The Kleisin Subunit of Cohesin Dictates Damage-Induced Cohesion. *Molecular Cell*, 31(1), pp.47–56.
- Helton, E.S. a Chen, X., 2007. p53 modulation of the DNA damage response. *Journal of Cellular Biochemistry*, 100, pp.883–896.
- Herschleb, J. et al., 2007. Pulsed-field gel electrophoresis. *Nature protocols*, 2(3), pp.677–684.
- Hirano, T., 2006. At the heart of the chromosome: SMC proteins in action. *Nature reviews. Molecular cell biology*, 7(5), pp.311–322.
- Hoeberichts, F.A. a Woltering, E.J., 2003. Multiple mediators of plant programmed cell death: Interplay of conserved cell death mechanisms and plant-specific regulators. *BioEssays*, 25, pp.47–57.
- Hohl, M. et al., 2011. The Rad50 coiled-coil domain is indispensable for Mre11 complex functions. *Nature Structural & Molecular Biology*, 18(10), pp.1124–1131.

- Holá, M. et al., 2013. Genotoxin induced mutagenesis in the model plant *Physcomitrella patens*. *BioMed Research International*, 2013.
- Hühn, D. et al., 2013. Targeting DNA double-strand break signalling and repair: recent advances in cancer therapy. *Swiss medical weekly*, 143.
- Chance, B. et al., 1979. Hydroperoxide metabolism in mammalian organs. *Physiological reviews*, 59, pp.527–605.
- Chapman, J.R. a Jackson, S.P., 2008. Phospho-dependent interactions between NBS1 and MDC1 mediate chromatin retention of the MRN complex at sites of DNA damage. *EMBO reports*, 9, pp.795–801.
- Charbonnel, C. et al., 2011. Kinetic analysis of DNA double-strand break repair pathways in *Arabidopsis*. *DNA Repair*, 10, pp.611–619.
- Charbonnel, C. et al., 2010. Xrcc1-dependent and Ku-dependent DNA double-strand break repair kinetics in *Arabidopsis* plants. *Plant Journal*, 64, pp.280–290.
- Chen, X. et al., 2009. Distinct kinetics of human DNA ligases I, III α , III β , and IV reveal direct DNA sensing ability and differential physiological functions in DNA repair. *DNA Repair*, 8(8), pp.961–968.
- Chiu, A. et al., 2004. DNA interaction and dimerization of eukaryotic SMC hinge domains. *Journal of Biological Chemistry*, 279(25), pp.26233–26242.
- Chowdhury, D. et al., 2005. gamma-H2AX dephosphorylation by protein phosphatase 2A facilitates DNA double-strand break repair. *Molecular cell*, 20(5), pp.801–809.
- Jackson, S.P. a Bartek, J., 2010. The DNA-damage response in human biology and disease. *Nature*, 461, pp.1071–1078.
- De Jager, M. et al., 2001. Human Rad50/Mre11 is a flexible complex that can tether DNA ends. *Molecular Cell*, 8, pp.1129–1135.
- Jang, E.R. et al., 2010. ATM modulates transcription in response to histone deacetylase inhibition as part of its DNA damage response. *Experimental a molecular medicine*, 42, pp.195–204.
- Jazayeri, A. et al., 2006. ATM- and cell cycle-dependent regulation of ATR in response to DNA double-strand breaks. *Nature cell biology*, 8, pp.37–45.
- Jazayeri, A. et al., S.P., 2004. *Saccharomyces cerevisiae* Sin3p facilitates DNA double-strand break repair. *Proceedings of the National Academy of Sciences of the United States of America*, 101, pp.1644–1649.
- Jiang, C.Z. et al., 1997. UV- and gamma-radiation sensitive mutants of *Arabidopsis thaliana*. *Genetics*, 147(3), pp.1401–1409.

- Jiang, L. et al., 2007. The Arabidopsis cohesin protein SYN3 localizes to the nucleolus and is essential for gametogenesis. *Plant Journal*, 50(6), pp.1020–1034.
- Johnston, L.H., 1979. The DNA repair capability of *cdc9*, the *Saccharomyces cerevisiae* mutant defective in DNA ligase. *Molecular a general genetics : MGG*, 170(1), pp.89–92.
- Kabotyanski, E.B. et al., 1998. Double-strand break repair in Ku86- and XRCC4-deficient cells. *Nucleic acids research*, 26, pp.5333–5342.
- Kamisugi, Y. et al., 2012. MRE11 and RAD50, but not NBS1, are essential for gene targeting in the moss *Physcomitrella patens*. *Nucleic Acids Research*, 40(8), pp.3496–3510.
- Kamisugi, Y. et al., 2006. The mechanism of gene targeting in *Physcomitrella patens*: homologous recombination, concatenation and multiple integration. *Nucleic acids research*, 34(21), pp.6205–14.
- Kamisugi, Y. et al., 2005. Parameters determining the efficiency of gene targeting in the moss *Physcomitrella patens*. *Nucleic Acids Research*, 33(19), pp.1–10.
- Kanno, T. et al., 2008. A structural-maintenance-of-chromosomes hinge domain-containing protein is required for RNA-directed DNA methylation. *Nature genetics*, 40(5), pp.670–675.
- Karanjawala, Z.E. et al., 2002. The embryonic lethality in DNA ligase IV-deficient mice is rescued by deletion of Ku: Implications for unifying the heterogeneous phenotypes of NHEJ mutants. *DNA Repair*, 1, pp.1017–1026.
- Keogh, M.C. et al., 2006. A phosphatase complex that dephosphorylates gammaH2AX regulates DNA damage checkpoint recovery. *Nature*, 439(7075), pp.497–501.
- Killion, D.D. a Constantin, M.J., 1972. Gamma irradiation of corn plants: Effects of exposure, exposure rate, and developmental stage on survival, height, and grain yield of two cultivars. *Radiation Botany*, 12(3), pp.159–164.
- Kim, J.H. et al., 2009. Characterization of metabolic disturbances closely linked to the delayed senescence of Arabidopsis leaves after γ irradiation. *Environmental and Experimental Botany*, 67, pp.363–371.
- Kim, J.S. et al., 2002. Specific recruitment of human cohesin to laser-induced DNA damage. *Journal of Biological Chemistry*, 277(47), pp.45149–45153.
- Kinner, A. et al., 2008. Gamma-H2AX in recognition and signaling of DNA double-strand breaks in the context of chromatin. *Nucleic acids research*, 36(17), pp.5678–94.

- Kirik, A. et al., 2000. Species-specific double-strand break repair and genome evolution in plants. *The EMBO journal*, 19, pp.5562–5566.
- Klekowski, E., 1997. Somatic mutation theory of clonality. In H. DeKroon a J. van Groenendael, eds. *Ecology and Evolutionary Biology of Clonal Plants*. Leyden: Backbuys Publishers, pp. 1–15.
- Kovalchuk, I. et al., 2004. Molecular aspects of plant adaptation to life in the Chernobyl zone. *Plant physiology*, 135, pp.357–363.
- Kovalchuk, I. et al., 2007. Transcriptome analysis reveals fundamental differences in plant response to acute and chronic exposure to ionizing radiation. *Mutation Research-Fundamental and Molecular Mechanisms of Mutagenesis*, 624(1-2), pp.101–113.
- Kozák, J. et al., 2009. Rapid repair of DNA double strand breaks in *Arabidopsis thaliana* is dependent on proteins involved in chromosome structure maintenance. *DNA Repair*, 8(3), pp.413–419.
- Kranner, I. et al., 2010. What is stress? Concepts, definitions and applications in seed science. *New Phytologist*, 188(3), pp.655–673.
- Krogh, B.O. a Symington, L.S., 2004. Recombination proteins in yeast. *Annual review of genetics*, 38, pp.233–271.
- Kuhfittig-Kulle, S. et al., 2007. The mutagenic potential of non-homologous end joining in the absence of the NHEJ core factors Ku70/80, DNA-PKcs and XRCC4-LigIV. *Mutagenesis*, 22, pp.217–233.
- Kun, E. et al., 2002. Coenzymatic activity of randomly broken or intact double-stranded DNAs in auto and histone H1 trans-poly(ADP-ribosylation), catalyzed by poly(ADP-ribose) polymerase (PARP I). *Journal of Biological Chemistry*, 277, pp.39066–39069.
- Kuzminov, A., 2001. Single-strand interruptions in replicating chromosomes cause double-strand breaks. *Proceedings of the National Academy of Sciences of the United States of America*, 98(15), pp.8241–8246.
- Lamarche, B. et al., 2010. The MRN complex in double-strand break repair and telomere maintenance. *FEBS letters*, 584(17), pp.3682–3695.
- Lammens, K. et al., 2011. The Mre11:Rad50 structure shows an ATP-dependent molecular clamp in DNA double-strand break repair. *Cell*, 145(1), pp.54–66.
- Lang, J. et al., 2012. Plant γ H2AX foci are required for proper DNA DSB repair responses and colocalize with E2F factors. *New Phytologist*, 194, pp.353–363.

- Langerak, P. et al., 2011. Release of Ku and MRN from DNA ends by Mre11 nuclease activity and Ctp1 is required for homologous recombination repair of double-strand breaks. *PLoS Genetics*, 7.
- Lehmann, A.R. et al., 1995. The rad18 gene of *Schizosaccharomyces pombe* defines a new subgroup of the SMC superfamily involved in DNA repair. *Molecular and cellular biology*, 15(12), pp.7067–7080.
- Lewis, T.G. a Nydorf, E.D., 2006. Intralesional bleomycin for warts: a review. *Journal of drugs in dermatology : JDD*, 5, pp.499–504.
- Li, X. a Heyer, W.D., 2008. Homologous recombination in DNA repair and DNA damage tolerance. *Cell research*, 18, pp.99–113.
- Liang, L. et al., 2008. Human DNA ligases I and III, but not ligase IV, are required for microhomology-mediated end joining of DNA double-strand breaks. *Nucleic Acids Research*, 36(10), pp.3297–3310.
- Lieber, M.R., 2010a. NHEJ and its backup pathways in chromosomal translocations. *Nature structural & molecular biology*, 17(4), pp.393–395.
- Lieber, M.R., 2010b. The mechanism of double-strand DNA break repair by the nonhomologous DNA end-joining pathway. *Annual review of biochemistry*, 79, pp.181–211.
- Lieber, M.R. et al., 1997. Tying loose ends: Roles of Ku and DNA-dependent protein kinase in the repair of double-strand breaks. *Current Opinion in Genetics and Development*, 7, pp.99–104.
- Lindahl, T. a Wood, R.D., 1999. Quality control by DNA repair. *Science*, 286(5446), pp.1897–1905.
- Lok, B.H. a Powell, S.N., 2012. Molecular pathways: Understanding the role of Rad52 in homologous recombination for therapeutic advancement. *Clinical Cancer Research*, 18, pp.6400–6406.
- Lukas, J. et al., 2004. Mammalian cell cycle checkpoints: Signalling pathways and their organization in space and time. *DNA Repair*, 3, pp.997–1007.
- Ma, J.L. et al., 2003. Yeast Mre11 and Rad1 proteins define a Ku-independent mechanism to repair double-strand breaks lacking overlapping end sequences. *Molecular and cellular biology*, 23(23), pp.8820–8828.
- Mansour, W.Y. et al., 2010. The alternative end-joining pathway for repair of DNA double-strand breaks requires PARP1 but is not dependent upon microhomologies. *Nucleic Acids Research*, 38, pp.6065–6077.
- Mantiero, D. et al., 2007. Dual role for *Saccharomyces cerevisiae* Tel1 in the checkpoint response to double-strand breaks. *EMBO reports*, 8(4), pp.380–387.

- Markmann-Mulisch, U. et al., 2007. Differential requirements for RAD51 in *Physcomitrella patens* and *Arabidopsis thaliana* development and DNA damage repair. *The Plant cell*, 19(10), pp.3080–3089.
- McVey, M. a Lee, S.E., 2008. MMEJ repair of double-strand breaks (director's cut): deleted sequences and alternative endings. *Trends in Genetics*, 24, pp.529–538.
- Meek, K. et al., 2004. The DNA-dependent protein kinase: The director at the end. *Immunological Reviews*, 200, pp.132–141.
- Mengiste, T. et al., 1999. An SMC-like protein is required for efficient homologous recombination in *Arabidopsis*. *EMBO Journal*, 18(16), pp.4505–4512.
- Menke, M. et al., 2001. DNA damage and repair in *Arabidopsis thaliana* as measured by the comet assay after treatment with different classes of genotoxins. *Mutation research*, 493(1-2), pp.87–93.
- Miller, K.M. et al., 2010. Human HDAC1 and HDAC2 function in the DNA-damage response to promote DNA nonhomologous end-joining. *Nature structural & molecular biology*, 17, pp.1144–1151.
- Mimitou, E.P. a Symington, L.S., 2008. Sae2, Exo1 and Sgs1 collaborate in DNA double-strand break processing. *Nature*, 455, pp.770–774.
- Molinier, J. et al., 2006. Transgeneration memory of stress in plants. *Nature*, 442, pp.1046–1049.
- Mortusewicz, O. et al., 2008. Spatiotemporal dynamics of regulatory protein recruitment at DNA damage sites. *Journal of Cellular Biochemistry*, 104, pp.1562–1569.
- Murray, J.M. a Carr, A.M., 2008. Smc5/6: a link between DNA repair and unidirectional replication? *Nature reviews. Molecular cell biology*, 9(2), pp.177–182.
- Nabetani, A. a Ishikawa, F., 2011. Alternative lengthening of telomeres pathway: Recombination-mediated telomere maintenance mechanism in human cells. *Journal of Biochemistry*, 149, pp.5–14.
- Nagata, T. et al., 1999. Gamma-radiation induces leaf trichome formation in *Arabidopsis*. *Plant physiology*, 120, pp.113–120.
- Nasmyth, K. a Haering, C.H., 2005. The structure and function of SMC and kleisin complexes. *Annual review of biochemistry*, 74, pp.595–648.
- Nimonkar, A. V. et al., 2011. BLM-DNA2-RPA-MRN and EXO1-BLM-RPA-MRN constitute two DNA end resection machineries for human DNA break repair. *Genes and Development*, 25, pp.350–362.

- O'Driscoll, M. a Jeggo, P.A., 2006. The role of double-strand break repair - insights from human genetics. *Nature reviews. Genetics*, 7, pp.45–54.
- Olive, P.L. a Banáth, J.P., 1993. Detection of DNA double-strand breaks through the cell cycle after exposure to X-rays, bleomycin, etoposide and 125IdUrd. *International journal of radiation biology*, 64(Charlton 1986), pp.349–358.
- Osborne, D. et al., 1984. DNA repair in plant cells. An essential event of early embryo germination in seeds. *Folia Biologica*, 30(Spec No), pp.155–169.
- Osley, M.A. et al., 2007. ATP-dependent chromatin remodeling factors and DNA damage repair. *Mutation Research - Fundamental and Molecular Mechanisms of Mutagenesis*, 618, pp.65–80.
- Ostling, O. a Johanson, K.J., 1984. Microelectrophoretic study of radiation-induced DNA damages in individual mammalian cells. *Biochemical and biophysical research communications*, 123(1), pp.291–298.
- Park, J.H. et al., 2006. Mammalian SWI/SNF complexes facilitate DNA double-strand break repair by promoting gamma-H2AX induction. *The EMBO journal*, 25, pp.3986–3997.
- Pelczar, P. et al., 2003. Different genome maintenance strategies in human and tobacco cells. *Journal of Molecular Biology*, 331, pp.771–779.
- Petrini, J.H. et al., 1995. DNA ligase I mediates essential functions in mammalian cells. *Molecular and cellular biology*, 15(8), pp.4303–4308.
- Petrini, J.H.J. a Stracker, T.H., 2003. The cellular response to DNA double-strand breaks: Defining the sensors and mediators. *Trends in Cell Biology*, 13, pp.458–462.
- Pfeiffer, P. et al., 2004. Pathways of DNA double-strand break repair and their impact on the prevention and formation of chromosomal aberrations. In *Cytogenetic and Genome Research*. pp. 7–13.
- Phillips, E.R. a McKinnon, P.J., 2007. DNA double-strand break repair and development. *Oncogene*, 26(56), pp.7799–808.
- De Piccoli, G. et al., 2006. Smc5-Smc6 mediate DNA double-strand-break repair by promoting sister-chromatid recombination. *Nature cell biology*, 8(9), pp.1032–1034.
- Pitcher, R.S. et al., 2007. NHEJ protects mycobacteria in stationary phase against the harmful effects of desiccation. *DNA Repair*, 6, pp.1271–1276.
- Polo, S. a Jackson, S., 2011. Dynamics of DNA damage response proteins at DNA breaks: a focus on protein modifications. *Genes a development*, pp.409–433.

- Potts, P.R. et al., 2006. Human SMC5/6 complex promotes sister chromatid homologous recombination by recruiting the SMC1/3 cohesin complex to double-strand breaks. *The EMBO journal*, 25(14), pp.3377–3388.
- Potts, P.R. a Yu, H., 2005. Human MMS21/NSE2 is a SUMO ligase required for DNA repair. *Molecular and cellular biology*, 25(16), pp.7021–7032.
- Povirk, L.F. et al., 1977. Dna double-strand breaks and alkali-labile bonds produced by bleomycin. *Nucleic Acids Research*, 4, pp.3573–3580.
- Povirk, L.F., 2012. Processing of Damaged DNA Ends for Double-Strand Break Repair in Mammalian Cells. *ISRN Molecular Biology*, 2012, pp.1–16.
- Puchta, H., 2005. The repair of double-strand breaks in plants: Mechanisms and consequences for genome evolution. *Journal of Experimental Botany*, 56, pp.1–14.
- Puchta, H. a Fauser, F., 2013. Gene targeting in plants: 25 years later. *The International journal of developmental biology*, 57(6-8), pp.629–37.
- Qi, Y. et al., 2013. Increasing frequencies of site-specific mutagenesis and gene targeting in Arabidopsis by manipulating DNA repair pathways. *Genome Research*, 23, pp.547–554.
- Qin, S. a Parthun, M.R., 2002. Histone H3 and the histone acetyltransferase Hat1p contribute to DNA double-strand break repair. *Molecular and cellular biology*, 22, pp.8353–8365.
- Rass, E. et al., 2009. Role of Mre11 in chromosomal nonhomologous end joining in mammalian cells. *Nature structural & molecular biology*, 16, pp.819–824.
- Raven, J.A., 2012. Protein turnover and plant RNA and phosphorus requirements in relation to nitrogen fixation. *Plant Science*, 188-189, pp.25–35.
- Reski, R., 1998. Physcomitrella and Arabidopsis: the David and Goliath of reverse genetics. *Trends in Plant Science*, 3(6), pp.209–210.
- Ricaud, L. et al., 2007. ATM-mediated transcriptional and developmental responses to γ -rays in Arabidopsis. *PLoS ONE*, 2(5).
- Ries, G. et al., 2000. Elevated UV-B radiation reduces genome stability in plants. *Nature*, 406, pp.98–101.
- Richardson, C. et al., 1998. Double-strand break repair by interchromosomal recombination: Suppression of chromosomal translocations. *Genes and Development*, 12, pp.3831–3842.
- Rogakou, E.P. et al., 1999. Megabase chromatin domains involved in DNA double-strand breaks in vivo. *Journal of Cell Biology*, 146, pp.905–915.

- Rosidi, B. et al., 2008. Histone H1 functions as a stimulatory factor in backup pathways of NHEJ. *Nucleic Acids Research*, 36, pp.1610–1623.
- Rubnitz, J. a Subramani, S., 1984. The minimum amount of homology required for homologous recombination in mammalian cells. *Molecular and cellular biology*, 4, pp.2253–2258.
- Saleh-Gohari, N. a Helleday, T., 2004. Conservative homologous recombination preferentially repairs DNA double-strand breaks in the S phase of the cell cycle in human cells. *Nucleic acids research*, 32, pp.3683–3688.
- Sallon, S. et al., 2008. Germination, genetics, and growth of an ancient date seed. *Science (New York, N.Y.)*, 320, p.1464.
- Seong, K.Y. et al., 1997. Cloning of an E. coli RecA and yeast RAD51 homolog, radA, an allele of the uvsC in *Aspergillus nidulans* and its mutator effects. *Molecules and cells*, 7(2), pp.284–289.
- Shaw, P. a Moore, G., 1998. Meiosis: vive la difference! *Current opinion in plant biology*, 1, pp.458–462.
- Shibata, A. et al., 2011. Factors determining DNA double-strand break repair pathway choice in G2 phase. *EMBO J*, 30, pp.1079–1092.
- Shieh, S.Y. et al., 1997. DNA damage-induced phosphorylation of p53 alleviates inhibition by MDM2. *Cell*, 91, pp.325–334.
- Shrivastav, M. et al., 2008. Regulation of DNA double-strand break repair pathway choice.
- Shuman, S. a Glickman, M.S., 2007. Bacterial DNA repair by non-homologous end joining. *Nature reviews. Microbiology*, 5, pp.852–861.
- Schaefer, D.G. et al., 2010. RAD51 loss of function abolishes gene targeting and de-represses illegitimate integration in the moss *Physcomitrella patens*. *DNA Repair*, 9(5), pp.526–533.
- Schipler, A. a Iliakis, G., 2013. DNA double-strand-break complexity levels and their possible contributions to the probability for error-prone processing and repair pathway choice. *Nucleic Acids Research*, 41, pp.7589–7605.
- Schwacha, A. a Kleckner, N., 1995. Identification of double Holliday junctions as intermediates in meiotic recombination. *Cell*, 83, pp.783–791.
- Simsek, D. et al., 2011. DNA ligase III promotes alternative nonhomologous end-joining during chromosomal translocation formation. *PLoS Genetics*, 7.
- Simsek, D. a Jasin, M., 2010. Alternative end-joining is suppressed by the canonical NHEJ component Xrcc4-ligase IV during chromosomal translocation formation. *Nature structural & molecular biology*, 17, pp.410–416.

- Sirbu, B.M. a Cortez, D., 2013. DNA damage response: three levels of DNA repair regulation. *Cold Spring Harbor perspectives in biology*, 5.
- Siu, W.Y. et al., 2004. Topoisomerase poisons differentially activate DNA damage checkpoints through ataxia-telangiectasia mutated-dependent and -independent mechanisms. *Molecular cancer therapeutics*, 3, pp.621–632.
- Sjögren, C. a Nasmyth, K., 2001. Sister chromatid cohesion is required for postreplicative double-strand break repair in *Saccharomyces cerevisiae*. *Current biology : CB*, 11(12), pp.991–995.
- So, S. et al., 2009. Autophosphorylation at serine 1981 stabilizes ATM at DNA damage sites. *The Journal of cell biology*, 187(7), pp.977–90.
- Stenerlöv, B. et al., 2000. Rejoining of DNA fragments produced by radiations of different linear energy transfer. *International journal of radiation biology*, 76(4), pp.549–557.
- Strekowski, L. et al., 1988. A biphasic nature of the bleomycin-mediated degradation of DNA. *FEBS letters*, 241, pp.24–28.
- Ström, L. et al., 2004. Postreplicative recruitment of cohesin to double-strand breaks is required for DNA repair. *Molecular Cell*, 16(6), pp.1003–1015.
- Stucki, M. et al., 2005. MDC1 directly binds phosphorylated histone H2AX to regulate cellular responses to DNA double-strand breaks. *Cell*, 123, pp.1213–1226.
- Sweeney, P.R. et al., 2009. The Arabidopsis ATRIP ortholog is required for a programmed response to replication inhibitors. *Plant Journal*, 60, pp.518–526.
- Symington, L.S., 2002. Role of RAD52 epistasis group genes in homologous recombination and double-strand break repair. *Microbiology and molecular biology reviews : MMBR*, 66, pp.630–670, table of contents.
- Takahashi, N. et al., 2010. The MCM-binding protein ETG1 aids sister chromatid cohesion required for postreplicative homologous recombination repair. *PLoS Genetics*, 6(1).
- Takata, M. et al., 2001. Chromosome instability and defective recombinational repair in knockout mutants of the five Rad51 paralogs. *Molecular and cellular biology*, 21, pp.2858–2866.
- Takeda, S. et al., 2004. BRU1, a novel link between responses to DNA damage and epigenetic gene silencing in Arabidopsis. *Genes and Development*, 18(7), pp.782–793.

- Tamburini, B.A. a Tyler, J.K., 2005. Localized histone acetylation and deacetylation triggered by the homologous recombination pathway of double-strand DNA repair. *Molecular and cellular biology*, 25, pp.4903–4913.
- Tice, R.R. a Setlow, R.B., 1985. *Handbook of the Biology of Aging* E. L. Finch, E.E. and Schneider, ed., New York: Van Nostrand Reinhold.
- Tomkinson, A.E. et al., 2013. DNA ligases as therapeutic targets. *Translational cancer research*, 2(3), pp.203–214.
- Triantaphylidès, C. a Havaux, M., 2009. Singlet oxygen in plants: production, detoxification and signaling. *Trends in Plant Science*, 14, pp.219–228.
- Trouiller, B. et al., 2007. Comparison of gene targeting efficiencies in two mosses suggests that it is a conserved feature of Bryophyte transformation. *Biotechnology Letters*, 29(10), pp.1591–1598.
- Trouiller, B. et al., 2006. MSH2 is essential for the preservation of genome integrity and prevents homeologous recombination in the moss *Physcomitrella patens*. *Nucleic Acids Research*, 34(1), pp.232–242.
- Vernoux, T. et al., 2000. Developmental control of cell division patterns in the shoot apex. *Plant Mol Biol*, 43, pp.569–81.
- Virsik-Köpp, P. et al., 2003. Role of DNA-PK in the process of aberration formation as studied in irradiated human glioblastoma cell lines M059K and M059J. *International journal of radiation biology*, 79, pp.61–68.
- Wada, H. et al., 1998. Involvement of peroxidase in differential sensitivity to γ -radiation in seedlings of two *Nicotiana* species. *Plant Science*, 132, pp.109–119.
- Wang, H. et al., 2001. Efficient rejoining of radiation-induced DNA double-strand breaks in vertebrate cells deficient in genes of the RAD52 epistasis group. *Oncogene*, 20, pp.2212–2224.
- Wang, J.H. et al., 2008. Oncogenic transformation in the absence of Xrcc4 targets peripheral B cells that have undergone editing and switching. *The Journal of experimental medicine*, 205, pp.3079–3090.
- Wang, M. et al., 2006. PARP-1 and Ku compete for repair of DNA double strand breaks by distinct NHEJ pathways. *Nucleic Acids Research*, 34, pp.6170–6182.
- Ward, J.F., 1990. The yield of DNA double-strand breaks produced intracellularly by ionizing radiation: a review. *International journal of radiation biology*, 57, pp.1141–1150.
- Warmerdam, D.O. a Kanaar, R., 2010. Dealing with DNA damage: Relationships between checkpoint and repair pathways. *Mutation Research - Reviews in Mutation Research*, 704, pp.2–11.

- Watanabe, K. et al., 2009. The STRUCTURAL MAINTENANCE OF CHROMOSOMES 5/6 complex promotes sister chromatid alignment and homologous recombination after DNA damage in *Arabidopsis thaliana*. *The Plant cell*, 21(9), pp.2688–2699.
- Waterworth, W.M. et al., 2010. A plant DNA ligase is an important determinant of seed longevity. *Plant Journal*, 63, pp.848–860.
- Waterworth, W.M. et al., 2009. DNA ligase 1 deficient plants display severe growth defects and delayed repair of both DNA single and double strand breaks. *BMC plant biology*, 9, p.79.
- Waterworth, W.M. et al., 2007. NBS1 is involved in DNA repair and plays a synergistic role with ATM in mediating meiotic homologous recombination in plants. *Plant Journal*, 52(1), pp.41–52.
- Watrin, E. a Peters, J.M., 2009. The cohesin complex is required for the DNA damage-induced G2/M checkpoint in mammalian cells. *The EMBO journal*, 28(17), pp.2625–2635.
- Weinstock, D.M. et al., 2007. Formation of NHEJ-derived reciprocal chromosomal translocations does not require Ku70. *Nature cell biology*, 9, pp.978–981.
- West, C.E. et al., 2002. Disruption of the *Arabidopsis* AtKu80 gene demonstrates an essential role for AtKu80 protein in efficient repair of DNA double-strand breaks in vivo. *Plant Journal*, 31(4), pp.517–528.
- Wu, D. et al., 2008. Recruitment and Dissociation of Nonhomologous End Joining Proteins at a DNA Double-Strand Break in *Saccharomyces cerevisiae*. *Genetics*, 178(3), pp.1237–1249.
- Wu, N. a Yu, H., 2012. The Smc complexes in DNA damage response. *Cell a Bioscience*, 2(1), p.5.
- Wyman, C. a Kanaar, R., 2006. DNA double-strand break repair: all's well that ends well. *Annual review of genetics*, 40, pp.363–383.
- Yajima, H. et al., 2013. The complexity of DNA double strand breaks is a critical factor enhancing end-resection. *DNA Repair*, 12, pp.936–946.
- Yazdi, P.T. et al., 2002. SMC1 is a downstream effector in the ATM/NBS1 branch of the human S-phase checkpoint. *Genes and Development*, 16(5), pp.571–582.
- Yoo, S. et al., 1999. Photocross-linking of an oriented DNA repair complex: Ku bound at a single DNA end. *Journal of Biological Chemistry*, 274, pp.20034–20039.

- Yoshiyama, K. et al., 2009. Suppressor of gamma response 1 (SOG1) encodes a putative transcription factor governing multiple responses to DNA damage. *Proceedings of the National Academy of Sciences of the United States of America*, 106, pp.12843–12848.
- Yoshiyama, K. et al., 2013a. DNA damage response in plants: conserved and variable response compared to animals. *Biology*, 2(4), pp.1338–56.
- Yoshiyama, K. et al., 2013b. ATM-mediated phosphorylation of SOG1 is essential for the DNA damage response in Arabidopsis. *EMBO reports*, 14, pp.817–22.
- Zahradka, K. et al., 2006. Reassembly of shattered chromosomes in *Deinococcus radiodurans*. *Nature*, 443, pp.569–573.
- van Zanten, M. et al., 2011. Seed maturation in *Arabidopsis thaliana* is characterized by nuclear size reduction and increased chromatin condensation. *Proceedings of the National Academy of Sciences*, 108, pp.20219–20224.